

RECEIVED BY OSTI

AUG 27 1985

DOE/ET/27019--1

GEOLOGIC, GEOPHYSICAL, AND GEOCHEMICAL ASPECTS  
OF SITE-SPECIFIC STUDIES  
OF THE GEOPRESSURED-GEOTHERMAL ENERGY RESOURCE  
OF SOUTHERN LOUISIANA

FINAL REPORT

DOE/ET/27019--1

DE85 016911

DOE CONTRACT NUMBER DE-AC08-79ET27019

EDITED BY

REX H. PILGER, JR.

PROJECT DIRECTOR

**MASTER**

DEPARTMENT OF GEOLOGY  
LOUISIANA STATE UNIVERSITY

---

**DISCLAIMER**

This report was prepared as an account of work sponsored by an agency of the United States Government. Neither the United States Government nor any agency thereof, nor any of their employees, makes any warranty, express or implied, or assumes any legal liability or responsibility for the accuracy, completeness, or usefulness of any information, apparatus, product, or process disclosed, or represents that its use would not infringe privately owned rights. Reference herein to any specific commercial product, process, or service by trade name, trademark, manufacturer, or otherwise does not necessarily constitute or imply its endorsement, recommendation, or favoring by the United States Government or any agency thereof. The views and opinions of authors expressed herein do not necessarily state or reflect those of the United States Government or any agency thereof.

## **DISCLAIMER**

**This report was prepared as an account of work sponsored by an agency of the United States Government. Neither the United States Government nor any agency Thereof, nor any of their employees, makes any warranty, express or implied, or assumes any legal liability or responsibility for the accuracy, completeness, or usefulness of any information, apparatus, product, or process disclosed, or represents that its use would not infringe privately owned rights. Reference herein to any specific commercial product, process, or service by trade name, trademark, manufacturer, or otherwise does not necessarily constitute or imply its endorsement, recommendation, or favoring by the United States Government or any agency thereof. The views and opinions of authors expressed herein do not necessarily state or reflect those of the United States Government or any agency thereof.**

## **DISCLAIMER**

**Portions of this document may be illegible in electronic image products. Images are produced from the best available original document.**

## CONTENTS

Foreword . . . . .	3
Introduction . . . . .	3
LaFourche Crossing Prospect (Snyder and Pilger) . . . . .	5
LaFourche Crossing Seismic Survey (Pilger) . . . . .	111
Lirette Field Area (Flournoy and Ferrell). . . . .	116
Computer Prospecting (Kupfer) . . . . .	135

## FOREWORD

This report consists of four sections dealing with progress in evaluating geologic geochemical, and geophysical aspects of geopressured-geothermal energy resources in South Louisiana under U. S. Department of Energy contract with Louisiana State University number DE-AC08-79ET27019. At the end of the contract work was transferred to contract number DE-AS05-78ET2702, so that this report is actually an interim report on Louisiana State University investigations of the energy resource.

Rex H. Pilger, Jr.

Project Director

## INTRODUCTION

As part of previous work on Geopressured-Geothermal Energy resources in Louisiana, the Louisiana State University Petroleum Engineering Department, under contract to the Department of Energy, identified a number of prospects in Louisiana, based on various empirical criteria, (Bassiouni,, 1978). Based on these selections, personnel of the LSU Geology Department (under contract number DE-AC08-79ET27019) selected several of the prospects for in-depth analysis. These prospects included LaFourche Crossing, Atchafalaya Bay, Southeast Pecan Island, and Kaplan. The in-depth site-specific analysis was to include detailed subsurface geology (structure, stratigraphy, lithology) and the fluid environment (temperature, pressure, salinity), using all available well logs and accessible seismic reflection data. Additional work outlined for the project included (1) analysis of a data bank of subsurface parameters in an effort to evaluate computergraphics approaches to prospect selection and (2) geochemical-petrographic analysis of diagenesis of geopressured reservoir sandstones.

Under the original contract, work was begun on LaFourche Crossing, Atchafalaya Bay, and Southeast Pecan Island prospects; computer-graphics analysis; and the geochemical-diagenesis work. Work was completed on the initial study of LaFourche Crossing prospect by Franklin Snyder, as part of his master's thesis in geology at LSU, and Leigh Anne Flournoy completed a study of the diagenesis of geopressured reservoir sands in Lirette oil field as part of her master's thesis. Dr. Donald Kupfer completed his study of computer-graphics mapping as well. At the request of the Department of Energy, continuation and completion of work on the other projects was shifted to an umbrella contract of DOE with LSU through the Energy Programs Office (EPO) and Louisiana Geological Survey (LGS) (contract number DE-AC08-81NV10174). Under the first contract it was decided that adequate data were not available for detailed evaluation of Atchafalaya Bay prospect, so the individual involved was shifted to the analysis of Kaplan prospect. Work on Southeast Pecan Island and Kaplan prospects was then shifted to the EPO-LGS contract.

As a byproduct of the LaFourche Crossing prospect study, it became desirable to undertake more detailed analysis by running new seismic lines over the prospect, since considerable interest in the area as a potential design test well site had been generated. Work on acquisition of the data was undertaken under an extension of the original Department of Geology contract, while interpretation was to be completed under the EPO-LSU contract.

This report consists of three sections dealing with completed work. They include (1) site-specific studies, LaFourche Crossing Prospect; (2) computergraphics approach to geopressured-geothermal prospecting, and (3) Diagenesis of geopressured reservoirs, Lirette Field.

## SITE-SPECIFIC STUDIES:

LaFourche Crossing Prospect

by

FRANKLIN C. SNYDER

REX H. PILGER, JR.

## INTRODUCTION

The purpose of this study was to evaluate various subsurface parameters in northern LaFourche and Terrebonne Parishes, Louisiana, in order to evaluate the geopressured-geothermal potential and to delineate potential fluid migration routes in the area. Relationships between these fluid migration routes and hydrocarbon migration in the northern Gulf Coast Basin as it relates to both geopressured-geothermal resources as well as oil and gas accumulations.

The subsurface parameters which were evaluated include structure, stratigraphy, temperature, water salinity, and fluid pressure. These parameters normally vary systematically within the basin depending upon depth and stratigraphy. Therefore, water which has moved within the basin should have maintained characteristics of its points of origin over some period of time. The geologic controls on these parameters, if identifiable, will assist in geopressured-geothermal resource evaluation.

## GENERAL GEOLOGIC BACKGROUND

Location and Regional Miocene Stratigraphy

The area of study is in northern LaFourche and Terrebonne Parishes of Southeast Louisiana (Fig. 1). The sediments studied are composed of a

predominantly regressive fluvio-deltaic sequence of Tertiary Miocene clastic sediments (McClellan, 1957). Seaward from this is an interbedded sandstone-shale sequence containing neritic to inner-neritic sandstones interbedded with interdistributary bay deposits and marine shales. Continual switching of individual deltaic depocenters produced a complex intermixing of these various deposits. The most seaward lithofacies contains marine outer neritic to bathyal clays and silts, intermixed with limited massive sandstones, attributable to up-dip slumping and possible turbidity currents (Coleman & Prior, 1980). Due to continual subsidence and progradation of the deltaic complexes during the deposition of the Miocene of South Louisiana, the lithofacies are usually deposited in an off-lap sequence from basal massive shales to upper massive sandstones.

#### Structural Elements

The Miocene of South Louisiana is dominated by three basic structural elements; these include 1) growth faulting, 2) deep seated domal structures and associated faulting, and 3) piercement salt domes and associated faulting. All of these structural features have contributed to the development of the study area. The growth faults, particularly define the limits of potential geopressured-geothermal reservoir.

#### Abnormal pressures

Intimately related to the structure, stratigraphy, and occurrence of economic petroleum accumulations in the Gulf Coast Miocene has been attributed to (1) rapid deposition with limited fluid escape after burial due to low hydraulic conductivity of the sediments (Dickinson, 1953), (2) aquithermal pressuring of a confined fluid volume (Barker,

1972), (3) the formation of a high density, clay 'seal', (4) clay dewatering associated with a diagenetic alteration of smectite to illite (Powers, 1967; Burst, 1969), and (5) from the generation of hydrocarbons, especially methane, within the source rocks.

Within the abnormally pressured zone a distinct increase in porosity occurs, a higher geothermal temperature gradient exists, and lower salinities within the abnormally pressured sandstones are observed (Schmidt, 1973).

#### METHODS

The data used in this study were obtained from available wireline surveys run in wells drilled in the area, scout reports, and seismic surveys. Primarily, spontaneous potential-induction electric logs run in the bore holes were used (Appendix A). Other wireline well surveys incorporated to a limited extent were sonic logs, density logs, and dipmeter logs. Scouting reports were used as sources for reservoir production data such as pressures, oil/gas ratios, and production zones.

#### Structure and Stratigraphy

Interpretation of the structure and stratigraphy was made through correlations of spontaneous potential and resistivity patterns on electric logs between each bore hole. Confidential interpretations from selected wells were used to aid in correlations where significant stratigraphic variations occurred, particularly across major growth faults. These data were integrated with interpretations of available processed seismic data through use of downhole velocity surveys obtained for several wells. Structure maps (Plates 4-8) and cross sections (Plates 9, 11-20) were then constructed for selected horizons using all these data.

Expansion indices (Thorsen, 1963) were calculated for the major growth faults and domal uplifts within the area. All the stratigraphic intervals chosen were of approximately the same thickness, within the upthrown block. The same method was used to delineate domal growth by using off-structure and on-structure thicknesses. The growth indices were then used to interpret the periods of maximum growth movement and uplift for the various structural features.

### Temperature

Maximum temperatures recorded at the bottom of logging runs (BHT) were used to construct maps of selected isotherms. The empirical relationship of Kehle (1971) was used to estimate the equilibrium BHT (Fig,2). Assuming a surface temperature of 75°F, linear interpolation between the corrected BHT data was used to calculate the depths to the 200, 250, and 300° isotherms for each well. Extrapolations, not exceeding 15°F, were used to estimate the depths to various isotherms when those temperatures were not reached in the bore hole. Each isotherm was usually calculated from different BHT data points within each well, so that each isotherm surface is semi-independent.

Maps were constructed for the 200 and 250° isotherm surfaces (Plates 1 and 22). Not enough data points were available to construct a 300°F map so these depth points were displayed only on the cross sections.

### Salinities

Estimated salinities were calculated using a computer program of the Schlumberger method of salinity determination from spontaneous potential (SP) and mud filtrate resistivity (Rmf) measurements (Schlumberger, 1972a, 1972b). Salinities were calculated for all non-producing sandstone aquifers over 20 feet in thickness, below the Texularia stapperi horizon, in which the SP deflection appeared to reach a maximum static potential and were then used to construct regional salinity variation maps (Plates 23 and 24). The UL-5 and McCulla marker sandstones were used for these maps since they exhibited the best developed SP sandstone character in their depositional areas.

Variations in the calculated salinity values are felt to adequately portray differences between the actual salinities within the sandstone aquifers. However, comparison of calculated SP salinity values with more accurate salinity determinations using density and sonic logs showed that the SP salinity values are usually lower than these other salinity determinations (D. G. Bebout, personal communication, 1980).

### Pressure

An evaluation of shale resistivity patterns in the area was undertaken prior to attempting construction of regional isopleth maps (Appendix B). It showed that short-normal shale resistivities were not constant, reliable values from which absolute pressure gradients could be estimated using various empirical relationships.

Because the shale resistivity-depth plots for adjacent wells do follow similar trends, these plots can be used to approximate the present tops of 'seals' across which there are dramatic pressure changes. Such a seal is seen in the Mosbacher Ledet #2 well at approximately 12,900 feet where the shale resistivity abruptly decreases from 1.4 OHM-M/M to .7 OHM-M/M (Fig. 3). Regionally these 'seals' appear to follow specific stratigraphic intervals within different fault blocks. Based on available shut in bottom hole pressures (S-I-BHP) from drill-stem tests in productive sands above and below these 'seals', these pressure barriers correspond to an abrupt pressure increase from near hydrostatic (.465 psi/ft) to approximately .7 psi/ft. Shale resistivity plots for each individual well along with the available S I BHP data were used to approximate the top of the 'hard' abnormal pressure (.7 psi/ft). These data are displayed on the cross sections. A transition pressure zone (.466 psi/ft to .69 psi/ft) usually exists between the hydro-pressured zone and 'hard' abnormally pressured zone. However, this transition zone is variable in thickness and difficult to precisely define using the shale resistivity method of pressure gradient estimation discussed in Appendix B. Therefore, no specific reference is made to the transition zone in this study.

## GEOLOGY OF THE STUDY AREA

Stratigraphy

The stratigraphically deepest well in the area (Hassie Hunt Trusts #1 Bilello-Martinez, T15S, R17E Section 61) penetrated Lower Miocene Cristellaria 'A' (Robulus chambersi) to possible Marginulina ascencionesis age sediments. This interval consists of massive marine shales and was not extensively studied due to the limited well control. The main sequence of sediments studied extend from the upper Lower Miocene Operculinoides (Camerina) section upward to the lower Upper Miocene Textularia stapperi horizon (Plate 2 and 3). The Operculinoides to Bigenerina humblei sequence consists of alternating sandstones and shales deposited primarily by prograding deltaic sequences interbedded with more marine shales. The sequence above Bigenerina humblei consists of massive upper alluvial plain sandstones interrupted by thin, regionally extensive marine transgressive shales, such as the Textularia stapperi and Bigenerina '2' intervals.

Numerous stratigraphic variations occur throughout the study area in relationship to structural movements. Sandstone intervals above the UL-8 horizon are regionally developed across the entire study area. Although variations in thickness of individual sandstone bodies occur, discrete sandstone intervals constituting depositional packages do not significantly vary across the area. Sandstone intervals below and including UL-8 horizon were strongly affected by structural development in the area during their deposition. In particular the UL-8 sand,

Barnhart sand, McCulla sands, and Robulus (43) L shale exhibit radical facies changes over relatively short distances (3,000-5,000 feet) which were primarily controlled by contemporaneous growth faulting and domal uplifts. The Operculinoides Ridgefield sands were also highly affected by structural development. However, except in the most southerly areas, these sandstones do appear to have been deposited throughout the study area.

#### Structural Development

The study area is bounded on the north and south by two long-lived south-dipping regional growth faults (Plate 4). The northern fault (T) extends from the northeast flank of the Chacahoula salt dome eastward in an arcuate trend across the northern flanks of Thibodaux, Rousseau, and Melodia fields. It dips to the south at 37 within the drilled section and has a throw greater than 1800 feet at the Regional Operculinoides marker horizon in Melodia field. Hydrocarbon entrapment in the three fields is controlled extensively by this fault. Growth indices (Fig. 4) constructed along the length of this fault show that growth, already active in the upper Lower Miocene Operculinoides section, reached a maximum during Robulus (43) L time. Since then growth and movement continued at an ever slowing rate until approximately Textularia stapperi time when movement ceased. Fault L, forming the southern boundary, extends west-southwest from the Lake Boeuf field to LaFourche Crossing where it bifurcates. One branch of the fault extends south-southwest from LaFourche Crossing while the larger, second segment extends west-

ward into the East Donner field area. Fault L dips to the south at 40° in the drilled section and has a throw that probably exceeds 2000 feet at the Regional Operculinoides Marker horizon. Maximum growth occurred during the deposition of the Barnhart Sand and Cibicides opima intervals (Fig. 8) which was at a later time than the northern bounding Fault T.

Fault L also underwent rapid growth, similar to Fault T, in the south-southeast portion of T15S, R17E. This area and farther to the south was probably a small Operculinoides and Robulus (43) L slope-graben basin bounded on the north by fault L and on the south by a down-to-the-north growth fault of similar magnitude. The north-dipping Fault O cuts the Humble LL&E EE-1 well in T16S, R17E, Section 77 (Plate 20). Fault L also extends farther upsection into the massive sandstones (above Bigenerina '2') than the north-bounding fault.

The structural development of the study area bounded by the two regional growth faults (T and L), is dominated by deep-seated domal uplifts and extensive regional growth faulting. The area had three distinct episodes of growth faulting and structural readjustment within the drilled portion of the sediment column. These structural episodes correspond to the deposition of the Plater sands, upper Robulus (43) L sands, and the UL-8 Cibicides opima sands (plate 3). Each of these sandstone packages constituted a distinct depositional pulse which prograded the shelf edge farther south into the Gulf of Mexico. A fourth minor deposition package in this area was the UL-to-UL-3 Cristellaria T sands.

The major structural features produced were the Rousseau anticline, the Southwest LAKE Boeuf dome, and the Thibodaux dome (Fig.1). The Rousseau feature is the most pronounced of these uplifts as can be seen on the shallower UL-3 and UL-8 structure maps (Plates 4 and 5). The Southwest Lake Boeuf dome can be divided into an eastern and western segment. The western segment is located in the east central one-third of T15S, R17E, while the eastern segment is centered in Sections 24 and 46 of T15S, R18E (Plate 7). The Melodia high is most likely a northern extension of the Southwest Lake Boeuf uplift. The Thibodaux dome is centered to the south of Fault T in Sections 35 and 36 of T15S, R16E. Neither the Thibodaux nor the Southwest Lake Boeuf feature extends a significant distance above the abnormally pressured zone.

During deposition of the Ridgefield and Plater sands, growth faulting appears to have been very active throughout the area. All of the long lived faults (T, L, Q, B, and R) offset this interval, as do numerous other smaller displacement faults. Structure maps (Plates 8 and 7) of the Regional Opeculinoides I sand (Operc) show extensive faulting during these intervals. Maximum growth and sandstone development within this interval appears to have occurred across the large, north-bounding fault in Thibodaux field, along fault Q in the southern portion of Rousseau field, and in a probable rim syncline of the east-northeast flank of the Chacahoula Salt Dome. These expansions are reflected in the growth indices for Faults Q and T (Fig. 4 and 6), in the north-south cross sections for the Thibodaux and Rousseau fields

(Plates 11 and 12), and in the Chacahoula strike section (Plate 19). The Plater and Ridgefield sands mainly developed on the downthrown block of Fault Q; they did not, however, develop as well to the south and east of the Rousseau anticline. This is confirmed both by SP log responses from available well control and the loss of coherent events in a dip seismic line (Plate 10) located on the flank of the dome. Paleobathymetric interpretations indicate that, within this area, the Plater and Ridgefield sands were probably deposited in local basin on the upper continental slope. The most likely process of deposition could have been slumping of material from an up-dip position. As previously stated, noticeable growth also appears to have occurred along Fault L in an area south of the Southwest Lake Boeuf field as seen in the Melodia dip cross section (Plate 14). The effect of Fault L upon this interval in other portions of the study area, however, is vague due to very limited well control in the downthrown fault block at these depths. Uplift was also active in the Rousseau and Southwest Lake Boeuf structures as shown by the development of graben features in both areas (Plates 11, 13, 15, and 16).

The deposition of the Operculinoides I sand interval marked the end of the first major phase of structural development within the area. Many of the smaller faults existing in the Operculinoides section ceased movement shortly after the deposition of the Operculinoides I sands. All of the graben faulting on the Southwest Lake Boeuf anticline stopped during this interval (Plates 15 and 16). This sandstone is regionally

well developed and showed some effects of growth-fault movement. The very uniform electric-log character and thickness of the interval from above the Operculinoides I sand to just below the Bourgeois sand indicates that the shelf area was very 'stable' during deposition. Movement on the major northern faults (R, T, and B) was continuing but at a much slower rate (Fig. 7 and 9). Movement on Faults M and Q along the southern edge of the Rousseau anticline was extensive. This is shown by the expanded section in the Texas Pacific Coal and Oil #1 Martinez well in the Rousseau dip cross section (Plate 11) and by the growth index for Fault Q (Fig. 9). This growth was compounded since the southern nose of Rousseau dome had probably been very near the shelf edge of hinge line since Operculinoides deposition. This hinge line is suggested by the upper slope paleobathymetry of the Ridgefield shale faunas (Fig. 6), change in dip of these beds across this area (Plated 11 and 12), rapid thickening of the interval since Ridgefield sand deposition, and the marked 'shale out' of most of the Operculinoides sandstone bodies to the south of the anticline.

During the deposition of the Robulus (43) L and McCulla sand-McCulla marker intervals, substantial movement on faults T and R to the north was coupled with accelerated uplift of all the domal features (Rousseau, Southwest Lake Boeuf, and Chacahoula). This structural episode was by far the most pronounced in the area. Uplift on a broader-based Chacahoula Dome produced an erosional unconformity with a maximum relief of 600 feet extending from the east flank of the current dome, approximately four miles to the east, as now seen in the

Chacahoula strike cross section (Plate 19). This ridge appears to merge with a concurrently developed uplift in southern Thibodaux Field. Growth indices on Fault B (Fig. 6) indicate substantial thinning in the Robulus (43) L interval. Hintze (1967b) concluded that since the domal structure of the deep Plater and Ridgefield Sand intervals coincided with a gravity anomaly minimum, these structures were formed by a deep-seated salt uplift in Thibodaux field. Extensive uplift also occurred on Rousseau and Southwest LAKE Boeuf anticlinings producing substantial thinning and a probable unconformity at Rousseau. Domal growth indices for these two areas show this substantial thinning (Fig. 7). Movement of these two uplifts slowed before Chacahoula dome movement.

Deposition of Bourgeois and Robulus I sand intervals was primarily confined to an east-west trough existing north of the domal structures and south of Fault T. As previously noted, maximum growth occurred along Fault T during this interval. Thinning across these uplifts can be seen in all the north-south cross sections but it is most pronounced in the two Thibodaux dip sections (Plated 12 and 17) and the Southwest Lake Boeuf dip cross section (Plate 15). The Thibodaux cross sections show rapid thinning and decreasing sandstone percentages in the Robulus (43) L interval to the south across the Thibodaux Field towards the Chacahoula ridge. Well developed sandstones also exist on the crest of Rousseau anticline due to continued growth within the central graben.

The Alliance Robichaux #1 (T15S R17E Section 11§0 in the Rousseau strike cross section (Plate 13) shows extensive Robulus I and Bourgeois sand development while the wells flanking the dome exhibit a probable unconformity in this interval.

McCulla sand and McCulla marker deposition prograded farther to the south but was also deposited in a trough, south of Faults T, B, and R. Both sandstones shaled out very rapidly to the south of these faults. Movement on Faults Q (Fig.9), Q', M, and N all ceased during this interval or shortly thereafter. Fault C, which had developed on the Thibodaux uplift during Operculinoides time, also died out. Growth of Rousseau and Southwest Lake Boeuf anticlines slowed dramatically after McCulla sand deposition. During this interval, radial faulting appears to have started on Chacahoula dome. The fault patterns at Chacahoula were different than those existing prior to the Robulus (43) L unconformity. This marked the end of the second major phase of structural development within the area.

The Barnhart sand to Cibicides opima depocenters moved much farther to the south. Deposition was primarily controlled by Fault L which exhibited its maximum growth during this interval. The Barnhart and UL-8 intervals developed into thick sandstones downthrown to this fault (Plates 11 and 12). North of Fault L, the section exhibits a uniform electric-log character indicating stable conditions between Fault L and north bounding Fault T. Movement on all the northern faults (T, R, and B) slowed markedly (Fig. 4 and 7). In the area of northern Rousseau,

Fault R appears to have completely died out but movement continued along it to the west for sometime.

The outer continental shelf and upper slope had most likely shifted southward to the Houma embayment area by Cibicides opima time (Sloan, 1966). As previously noted, the Hollywood sands within the Houma embayment underwent rapid development at the end of Cibicid opima time. Paleobathymetric data in the northern Rousseau area indicated a shallowing of deposition there to a middle shelf environment. Southwest Lake Boeuf domal movement had ceased by Barnhart sand deposition time while uplift in the Chacahoula and Rousseau areas continued at a slower rate (Fig. 10). Radial faulting and stratigraphic thinning occurred within this interval adjacent to Chacahoula uplift (Plate 19).

Following UL-8 deposition, the Cibicides opima transgression resulted in the deposition of a thick (600 to 700 feet) shale section in the area. This shale section was interrupted only by a thin (20 to 40 feet thick) blanket UL-7 sand. Directly below the UL-7 sand, however, a well-developed sandstone was deposited west of the Thibodaux field area and east of Chacahoula dome. Movement on the remaining northern faults (T, B, and the western end of R) continued at a slow rate. Rapid Growth was still occurring along fault L to the south. Growth of Rousseau anticline appears to have accelerated slightly during deposition of the lower portion of the Cibicides opima interval (Fig. 7). Substantial thinning and radial faulting continue to occur adjacent to the dome at Chacahoula as the salt stock became more centralized.

Rapid deltaic deposition again began with the deposition of UL-5 to UL-3 sands and has continued since then except for thin, regionally well developed transgressions such as Cristellaria T, Bigenerina humblei, and Textularia stapperi. Maximum development and growth within the Cristellaria T to Bigenerian humblei stratigraphic interval was centered within the Houma embayment, to the south. After the Textularia stapperi transgression, only upper deltaic plain massive sandstones were deposited within the area. Paleobathymetric data indicate that the Textularia stapperi interval was deposited in an upper-shelf position (Fig. 3).

Movement on the two bounding Faults L and T showed a minor increase in growth while movement on Faults B and R died out during UL-5 to UL-3 deposition (Fig. 9). Fault T ceased movement by the Textularia stapperi transgression (Fig. 7) while fault L, to the south, continued movement farther upsection (Fig. 5).

Significant 'rollover' was produced in LaFourche Crossing and Thibodaux fields during the Cibicides opima to Textularia stapperi deposition. Radial faulting which was initialized during McCulla Sand deposition at Chacahoula Dome continued movement throughout this interval. During and following the UL-5 deposition a large salt overhang developed on the east-northeast flank of Chacahoula dome (Plate 19). The two large salt withdrawal faults (H and H1) on the northeast flank of Chacahoula continued to move long after the deposition of Middle Miocene sandstones ended (Plate 18). One of these faults extends to within 2500 feet of the surface.

## Hydrocarbon Accumulations

Hydrocarbons within the study area can be divided into groups depending upon their composition and mode of structural entrapment. Hydrocarbons within the 'hard' abnormally pressured section consist entirely of gas and gas condensate. The most prolific producing horizons are the Plater and Ridgefield sands. Condensate production from the abnormally pressured intervals is much higher than the hydrostatically pressured section which consists of condensate-poor gas and heavy oil (A PI Gravity 32 to 37). The only reservoirs producing oil from this zone are in the LaFourche Crossing and Chacahoula fields. These liquid oil reservoirs usually have a discrete gas cap. Discussion of the hydrocarbons contained within the different fields will help to delineate these relationships further.

### Southwest Lake Boeuf Field

Most of the accumulations within Southwest Lake Boeuf field (Plate 1) are confined to the abnormally pressured section (.72 to .92 psi/ft) below the top of the Robulus (43) L paleozone. The abnormally pressured accumulations consist of gas and condensate trapped in the Plater, Ridgefield, and Robulus (43) #3 Sands (Plates 15 and 16). Condensate production of A PI Gravity 47 to 52 oils within these intervals is extremely high with gas/oil (G/O) ratios ranging from 2000/1 to 9000/1. The Robulus (43) #3 accumulation is in a combined structural-

stratigraphic trap within a small anticlinal closure above the dome. The lower Plater Sand and Ridgefield sand accumulations are primarily structural traps associated with the Operculinoides graben-faulting over the uplift. No structural closure is seen above the Robulus (43) L zone in which hydrocarbons could be trapped. Southeast of the main Lake Boeuf uplift in T15S, R18E, Section 46 three Bradco wells also produce from the gas and condensate (Ridgefield and Plater) trapped on the south flank of a north dipping fault which developed over the eastern portion of the Southwest Lake Boeuf uplift. The only hydrostatically pressured hydrocarbons in the area are contained by a 'rollover' structure along fault L, within the UL-8 sand (T15S, R18E, Sections 48 and 49 ) (Plate 5).

#### Melodia Field

Accumulations in the Melodia field (Plate 1) occur in the northern end of Southwest Lake Boeuf uplift and are trapped by the north bounding fault T. Gas and gas condensate occurs within all the sandstones below the Bourgeois sand interval. The structural trap is a reverse-dip closure on the northern upthrown side of Fault T (Plate 7). These accumulations occur both above and below the top of the 'hard' abnormal pressure, but hydrocarbons within the 'hard' pressure zone contain appreciably more condensate. As in Southwest Lake Boeuf field, no significant closure occurs in higher stratigraphic intervals, as is apparent on the (Plate 6).

### LaFourche Crossing

All accumulations in LaFourche Crossing field (Plate 1) are trapped in a simple 'rollover' closure on the south side of faults L and L', which cut the southern nose of the Rousseau anticline (Plate 20). The structural closures developed during the accelerated movement of these faults from Cibicides opima to Bigenerina humblei time. Hydrocarbon reservoirs include the UL-4 to UL-2 sands and some Textularia stapperi sands. No accumulations have been found in the UL-8 to UL-5 sands despite good sandstone development and 'rollover' closure. These hydrocarbons all occur within the hydro-statically pressured section having fluid pressures of .43 to .45 psi/ft. They consist exclusively of dry gas with minor condensate in the UL-4 to UL-2 sands and heavier oil accumulation in the Textularia stapperi sands.

### Rousseau Field

The Rousseau field (Plate 1) area may be divided into northern and southern structures. The northern structures are dominated by the regionally developed growth Faults T, B, and R. Hydrocarbons are primarily trapped in abnormally pressured reverse dip structures on the north flank of Fault T within Operculinoides I, Plater, and Ridgefield sands (Plate 11). Significant accumulations also exist in the normally pressured McCulla sands in both reverse dip and 'rollover' traps along Faults T and R.

The structure in southern Rousseau, above the Barnhart sand is a simple unfaulted anticline whose axis extends north-northwest to south-southeast across the western edge of T15S, R17E. The structural axis shifts to the northeast in successively stratigraphically shallower sections. Shallow hydro pressured hydrocarbons, as in LaFourche Crossing, are trapped in the UL-5 to UL-2 Cristellaria T sands. A significant reservoir also exists in the UL-8 sand (Plate 11). These reservoirs contain only gas with minor condensate.

Deep hydrocarbons in southern Rousseau are trapped by a complex graben fault system below the top of the abnormal pressure zone within Robulus (43) L and older deposits. These deeper accumulations are trapped in Plater and Ridgefield sand reverse dip closures on the northern flank of the graben, upthrown to Faults Q and R. One south flank accumulation exists in the Operculinoides I (1300 foot) sand south of Fault Q in the Alliance #1 Robichaux well.

Recovery from the normally pressured UL-2 to UL-8 sands averages 1.65 million cubic feet per acre foot (MMCF/acre ft) with 20 barrels (BBL) of condensate per MMCF gas (Hintze, 1967a). Here difference in the hydrocarbons produced above and below the top of the abnormally pressured zone.

#### Northeast Chacahoula Field

Chacahoula dome is a mature piercement salt stock extending to within 2000 feet of the surface. Nearly all the sandstones abutting the

salt below Bigennerina humblei contain hydrocarbons in commercial quantities. The primary shallow, normally pressured reservoirs are the UL-5 (Pure), UL-7 (Lyric), and UL-8 (Mire) sands (Plates 18 and 19). The UL-7 and UL-8 reservoirs contain heavy oil (A PI Gravity 32-37) with a significant gas cap while the UL-5 sand contains gas and condensate. All these wedge-shaped reservoirs are bounded on two sides by radial faults with an updip sandstone pinchout as the seal. Above Bingennerina humblei additional gas and oil reservoirs occur in the massive sandstones especially on the southern flanks of the dome. The top of the 'hard' abnormal pressure varies greatly across stratigraphic intervals on the east flank of the dome (Plate 18). In Section 69 the high pressure is encountered just below the McCulla sand zone but becomes increasingly stratigraphically deeper to the north. Upthrown to the two large salt withdrawal faults, the abnormal pressure is encountered just above the Regional Operculinoides marker. The abnormal pressure is not reached in the downthrown blocks within the withdrawal basin. Below the erosional unconformity, significant gas condensate is trapped in the remaining Robulus (43) L Sand. These accumulations extend some distance to the northwest of the current dome and are trapped in apparent structural highs. Additional gas condensate production is found in the Plater and Ridgefield Sands within extremely complex fault segments.

## SALINITY AND TEMPERATURE PATTERNS

Temperatures

Examination of the regional isotherm maps (Plates 21 and 22) for the 250°F and 200°F surfaces indicate significant variations within the area. Depth-temperature plots of the corrected BHT for numerous wells in the different fields are shown in figures 10 through 12. The corrected BHT data points are overlain by gradient lines depicting the average of the temperature gradients within the hydro pressured and abnormally pressured zones for the individual wells plotted. Averaged of the temperature gradients for the hydrostatically pressured section range from 1.16°F/100 ft to 1.24°F/100 ft. These values agree with values calculated by Moses (1961). Averages of the temperature gradients within the upper abnormally pressured section vary from 2.25°F/100 ft for Southwest Lake Boeuf (Fig. 11) to 2.98°F/100 ft for Thibodaux field (Fig. 12). Since heat transfer by water migration during compaction has been limited within the abnormally pressured zone these higher gradients should be expected. These very high temperature gradients, however, appear to decrease after an indeterminate distance below the top of the 'hard' abnormally pressured zone. The resulting dog-leg temperature gradient, which can be seen in numerous wells in the area, is illustrated by the Stanolind #1 Ridgefield sand Unit 3 in Thibodaux field (Fig. 12). Considering the BHT data for this well,

points A and B were used to determine the temperature gradient in the hydro pressured zone while points C, D, and E delineate the very high temperature gradient in the upper abnormally pressured zone. A decrease in the abnormally pressured gradient is delineated by points C, F, and G which fall below this high temperature gradient. The exact value of the very deep temperature gradients is difficult to determine because of limited BHT data. The numerous BHT values that fall below the vary high temperature gradient in the abnormally pressured temperature zone reflect the dog-leg effect.

The 200°F isothermal surface map (Plate 21) shows a maximum relief of approximately 4500 feet. The shallowest occurrence of this temperature is around 7000 feet in LaFourche Crossing and northeast Chacahoula fields, while the deepest occurrence is approximately 11,500 feet in numerous other locations.

For aid in describing the anomalies in the 200°F isothermal map, areas in which this temperature was reached above 900 feet are shaded on the map (Plate 21). This 9000 foot depth, indicating a relief of 2500 feet for the isotherm, is felt to adequately describe anomalously shallow occurrences of 200°F isothermal surface considering the expected error in BHT measurements. Using this criterium nine anomalies are displayed on the 200°F isothermal surface map.

The 250°F isothermal surface map (Plate 22) indicates a relief of 5000 feet on this surface, ranging from a high of 10,000 feet to a low of approximately 15,000 feet. Depths shallower than 12,000 feet, showing 3000 feet of relief, were used to indicate anomalies on this surface. Several other areas, extending to shallow depths may also be anomalies but are not indicated in the map using this criterium. Consequently, only four anomalies are shown on the 250F isothermal surface map.

For easier reference, anomalies on both the 200°F and 250°F isothermal surface maps are distinguished by the same letter designation where they occur in the same general location. Further, the number of wells delineating each anomaly is shown in Table 1.

TABLE 1.  
Well Delineation Of Various Anomalies.  
Thermal Anomalies

<u>Designation</u>	<u># Wells Delineating 200°F (9500')</u>	<u># Wells Delineating 250°F (12,500')</u>
A	2	0
B	1	3
C	1	3
D	10	7
E	3	0
F	2	0
G	1	0
H	5	2
I	2	2

UL - 5 Sand Salinity Anomalies

<u>Anomals</u>	<u># Wells Delineating (80,000 ppm)</u>
A	1
B	1
C	2
D	1
E	2
F	2

McMulla Marker Sand Salinity Anomalies

<u>Designation</u>	<u># Wells Delineating (55,000 ppm)</u>
A	1
B	7
C	4
D	5
E	3
F	1

Several isothermal anomalies appear along the trace of the southern bounding Fault L. Three anomalies (A, B, and C) occurring in the eastern part of the area in T15S, R18E are shown on the 200°F map (Plate 21). Anomaly B is delineated in the Southwest Lake Boeuf dip cross section (Plate 15) by the sharp rise in the 200 and 250° isothermal surfaces south of Fault L. Lack of well control at the depth of the 250° isotherm makes a verification of the A anomaly at this level impossible

(Plate 22). These anomalies are elongated within a general high extending in an east-west direction along Fault L. The LaFourche Crossing cross section just comes to the edge of the anomaly (Plate 20). The bifurcation of Fault L can be seen on the UL-3, UL-5, and McCulla sands structure maps (Plates 4, 5, and 6 respectively). Anomaly D is the best documented and most extensively developed anomaly in the area. Farther to the west, in T15S, R16E, Section 74, a single well marks the occurrence of anomaly G on the 200°F map along this same fault. Again, lack of deep well control prevents a 250°F verification.

Several anomalies also extend along the regionally developed growth Fault R south of Thibodaux and in the northern area of Rousseau field. Anomaly E is located on the north flank of the southern Rousseau anticline while anomaly F extends north-northeast to south-southwest along Fault R in Sections 81, 93, and 142 of T15S, R16E (Plate 21). Anomalies E and F are only shown as anomalies on the 200°F map but distinct highs in the same areas also exist on the 150°F map. Although not shown as anomalies, thermal highs exist in northern Rousseau near the junction of Faults B and R with the north bounding Fault T (Plates 21 and 22). These highs extend the anomalies of E and F farther to the northeast along the same trend.

Two anomalies (H and I) are developed on both isothermal surface maps adjacent to Chacahoula salt stock. These two anomalies show very extensive relief similar to that seen in the LaFourche Crossing area. Very extensive faulting of the flank of the dome combined with the high thermal conductivity of the salt makes analysis of these areas difficult. The occurrence of thermal troughs (lows) on both isothermal surface maps to the east of these highs is similar to temperature

patterns observed by Oden (1980). This pattern may result from the salt stock conducting heat from deeper flank sediments to the upper portion of the sedimentary column adjacent to the salt due to the high thermal conductivity of the salt, or from fluid movement up the flanks of the dome through fault zones. Both anomalies H and I occur adjacent to the actual salt stock.

Salinity maps for the UL-5 and McCulla Marker sand horizons were used to illustrate salinity variations within the study area (plates 23 and 24). As previously noted, these two sandstones were chosen because they exhibit limited stratigraphic variation within their depositional areas and contain negligible hydrocarbon accumulations. Zones containing hydrocarbons or poorly developed sandstones within each of these intervals are noted on the perspective maps. The UL-5 sand occurs entirely within the hydrostatically pressured section throughout the study area while the equivalent to the McCulla Marker sand (shale section) is abnormally pressured south of fault L. Calculated salinity values within the UL-5 sandstones vary from a maximum of approximately 175,000 parts per million (ppm) to a low of approximately 50,000 ppm. For visual display, areas exhibiting salinities less than 75,000 were considered anomalous (Plate 23). Hydrocarbon production from this interval in Chacahoula and southern Rousseau prohibited calculations of salinities in these two areas as shown. Also, this sandstone was not well developed in an elongated zone south of the southern bounding Fault L in T16S, R16 & 17E.

The UL-5 sandstone thus exhibits six significant salinity anomalies (Plate 23). Salinity anomalies A and B in T15S, R18E correspond with the thermal anomalies A and C and Extend north-northwest to

east-southeast along the trace of Fault L. To the southeast of salinity anomaly B, two other zones exhibit salinities with less than 100,000 ppm and correspond to the thermal anomaly B. Salinity anomaly C occurs in the LaFourche Crossing Field in the same location as thermal anomaly D. A zone of less than 100,000 ppm extends to the east and southwest along faults L and L' respectively. Lower salinities do not, however, appear to the west of the bifurcation. Salinity anomalies D, in the northwestern part of Thibodeaux field, and E, in northeast Chacahoula field, do not correspond to previously noted thermal anomalies. However, anomaly D occurs very close to the north bounding Thibodaux Fault T. Anomaly E is significant in that it is surrounded by an extensive 100,000 ppm salinity zone which is verified by six wells and does not seem to correspond to any fault offsetting This interval. Anomaly F occurs on the northeast flank of the Chacahoula dome downdip from significant oil and gas production in the Mire sand. It closely corresponds to the thermal anomaly H. Two zones of salinities less than 100,000 ppm along R in T15S, R16E, Sections 77 and 39 correspond with the E and F thermal anomalies.

The McCulla marker sand salinity map only covers the upper half of the study area (Plate 24). McCulla marker and McCulla sand deposition was controlled by growth faulting along Faults T, B, and R and all the domal uplifts. These sandstone intervals rapidly change to shale south of the faults and the Chacahoula Dome as indicated on the McCulla Marker salinity map (Plate 24). Salinity changes in this horizon range from approximately 160,000 ppm to 45,000 ppm. Areas showing water salinities less than 50,000 were considered anomalies and designated on the map.

Seven zones are shown as anomalies on the McCulla Marker salinity

map (Plate 24). Anomalies A and B located in the eastern portion of the study area both occur along the north bounding Fault T but also adjacent to the zone in which the McCulla marker 'shales out'. Anomaly C occurs in the northern area of Rousseau field, south of Fault T, near the junction with Fault R. Anomaly D extends over a broad zone between Faults B and R along the north boundary between T15E, R16 & 17E. This anomaly may be two separate low salinity zones existing along each fault, but the lack of well control prohibits adequate resolution. Farther to the southwest in Sections 77 and 80, anomaly F also occurs between the two faults. Salinity anomalies C, D, and F are probably related to thermal anomalies E and F extending along Fault R. Directly over the central portion of Rousseau dome is anomaly E. This anomaly, as well as anomalies A, B, and G, occurs very close to the depositional edge of the McCulla marker sand.

Salinity profiles for several wells in the LaFourche Crossing and Thibodaux areas (Figures 13 and 14) illustrate the salinity variations which can occur in the shallow hydro pressured sandstones. Wells used for comparison in these profiles were chosen based on the similarity of sandstone development and maximum deviation in the salinity values. The Thibodaux profile (Fig. 13) corresponds to the McCulla marker sand salinity anomaly D while the LaFourche Crossing profile (Figure 14) corresponds to the UL-5 sand salinity anomaly C. The calculated salinities within the hydro pressured sandstones vary by as much as 75,000 ppm while the deeper abnormally pressured sandstones have essentially the same salinity values.

### Water Migration

Comparison of the anomaly patterns for temperatures and salinities on the selected mapping horizons has shown that these two parameters bear definite relationships to each other. Low salinity and high temperature anomalies usually occur along major regional growth faults in the same locations (Fig. 15.). Further, all the faults (T, R, B, and L) along which these anomalies occur had the longest growth histories in the area and extend a significant distance above the 'hard' abnormally pressured zone. These relationships suggest that the anomalies resulted from the movement of hot, low-salinity (approximately 50,000 ppm) waters from the abnormally pressured zone up permeable zones along the faults to hydro pressured aquifer systems containing cooler, high-salinity (approximately 150,000 ppm) waters. Numerous authors, including Jones (1975) and Weber et al. (1978), reached similar conclusions concerning fluid migration routes from abnormally pressured zones. Further, similar studies in south Louisiana conducted at Louisiana State University by Gatenby (1979), Harrison (1979), and others reach the same conclusion.

The permeability of growth faults during migration seems probable, since many fault zones contain a significant gouge zone composed of formational debris assimilated during fault movement. Smith (1980) discussed several published examples of gouge zones existing in Gulf Coast growth faults. Further, in studying hydrocarbon reservoir characteristics, Smith also concluded that many Gulf Coast growth faults are not necessarily barriers to lateral fluid migrations. The fluid conduction properties of a growth fault would be best developed in the abnormally pressured zone where fault movement has been the greatest and

higher pressures tend to 'prop open' the faults (Hubbert & Rubey, 1959). All the faults within the study area, along which fluids migrated, have throws in excess of 400 feet at depth. The more limited fault movement within the upper hydropressure zone is less likely to have produced a substantial gouge zone.

Examination of a hypothetical model for salinity anomalies within the hydro pressured zone (see Appendix C) indicates that the low salinities produced by a migration of abnormally pressured water could remain for significant periods of geological time. The uncertainty of sodium chloride (NaCl) diffusion rates used in the model make the absolute time needed to reach a salinity equilibrium uncertain. Since many of the calculated salinity values within the upper hydro pressured sandstones are in the range of 40,000-50,000 ppm, the water movements necessary to produce these salinity contrasts must have recurred over an extended period of time. Several of these anomalies, most particularly LaFourche Crossing, must have had some flushing in the last few million years. Temperature anomalies in the hydro pressure zone probably would also be relatively short-lived due to continual convective water movement caused by compaction.

Several salinity anomalies such as E, occurring in the UL-5 sandstone, between Thibodaux and northeast Chacahoula fields (Plate 23) do not correspond to fault trends or thermal highs. Due to the nature of the salinity and temperature data sets, anomalies for each parameter may not coincide in a planar map view. Figure 16 shows a situation where the thermal anomalies produced by the flow of hot, low-salinity waters along a fault zone are substantially offset from the salinity anomalies within a sandstone of the hydro pressured zone. The specific

migration routes of water within the fault and aquifer systems are much too complex to delineate adequately with the methods used here. However, it can be said that significant vertical movements of water have occurred along Faults R, T, and L, as noted by the coexistence of salinity and temperature anomalies. The most pronounced of these anomalies occurs in LaFourche Crossing.

Several of the salinity anomalies on both maps may be due to causes other than extended vertical fluid migration. Salinity anomalies A, B, E, and G, adjacent to the 'shale out' on the McCulla marker sand map (Plate 24), may be due to a lateral migration of less saline shale pore waters within the same stratigraphic interval into the updip sandstone aquifers (Schmidt, 1973). Depth salinity plots for several wells in Rousseau Field (Fig. 17), which did not exhibit salinity values indicating flushes, suggest that the zone below the UL-5 sand is undergoing the second stage of smectite dehydration as proposed by Burst (1969). Temperatures within this stratigraphic interval fall well within the temperatures needed to initiate this dehydration (180 to 230F). It should be noted that this zone of smectite to illite conversion is occurring approximately 1,500 feet above the top of the 'hard' abnormal pressure.

#### Hydrocarbon Migration

Significant, shallow, hydro pressured, hydrocarbon accumulations of oil and dry gas described previously for the individual fields, occur in conjunction with the areas of proposed vertical fluid migration. The most notable of these are the LaFourche Crossing UL-2 to UL-4 and Textularia stapperi accumulations, the shallow Rousseau dome UL-2 to

UL-8 accumulations, the UL-8 'rollover' accumulation in T15S, R18E, Sections 48 and 49, and the abundant oil and gas accumulations on Chacahoula dome. Several noticeable exceptions to this apparent relationship are the hydropressured Barnhart and McCulla sand accumulations in Thibodaux and the lack of hydrocarbon accumulations occurring in conjunction with thermal anomalies A and B. If hydrocarbon migration is related to vertical water movement from the abnormally pressured section, then later migration of hydrocarbons up dip within the reservoirs due to buoyancy could account for the offsets of current accumulations from zones of vertical flush. The elongation of temperature anomaly D in LaFourche Crossing to the north-northwest over southern Rousseau anticline might indicate such a lateral fluid movement. It should also be noted that most of the deep, abnormally pressured, condensate-rich gas accumulations within the Operulinoides and Ridgefield Sand horizons have no significant temperature anomalies associated with them. One exception to this in the accumulation southwest of Lake Boeuf in T15S, R18E Section 46 (Plate 15).

#### Fluid-Structural Relationships

Since a noticeable number of the proposed areas of vertical water movement are located along growth faults where 'rollover' structures have developed, a relationship between the structural development and water migration may exist. 'Rollover' structures have developed only along Fault L in LaFourche Crossing and south of Lake Boeuf where vertical water migration has occurred. Both of these structures also occur where Fault L bifurcates, as seen in the UL-3 and UL-8 structure maps (Plates 4 and 5). This occurrence possibly represents a condi-

tion where vertical fluid movements, along a structurally weak zone of the fault, produced additional downthrown subsidence due to compaction resulting from the water escape at depth. This could lead to the development of a local depositional pod and structural 'rollover'. Fluid migration could thus enhance structural development and fault movement which could, in turn, be favorable for further fluid movement up the permeable fault may also exist in Thibodaux field and the northern area of Rousseau field, although, the salinity and temperature anomalies are not as well developed in these fields. The northern area of Rousseau field has both temperature and salinity anomalies which coincide but Thibodaux field lacks evidence of such relationships. These poorly delineated relationships were probably produced by several factors including 1) limited availability of data, 2) timing of fluid migration, and 3) complexity of migration paths.

Chacahoula salt dome might also fit a model of structural development occurring in conjunction with vertical fluid migrations. Adjacent to the prominent salt overhang of northeast Chacahoula dome substantial salinity and thermal anomalies are apparent (Plates 18 and 19). The structures adjacent to the dome were obviously produced by the salt uplift but fluid migration around the dome may have had a 'lubricating' effect upon the salt-sediment interaction. As previously produced by the salt uplift but fluid migrations around the dome may have had a 'lubricating' effect upon the salt-sediment interaction. As previously stated, however, these anomalies may be due to the heat conduction properties of the salt stock or fluid movement up the flanks of the dome.

## DISCUSSION

Conclusions as to the exact mechanisms by which hydrocarbons migrate within the basin are very speculative considering the data used within the study. However, several relevant observations may be made as to the nature of the migration. First, the current hydrocarbon profile within the sediment column, as discussed within the hydrocarbon section, conforms to the stratification expected during the normal maturation staged of kerogen with increasing temperatures (Fig. 18; Hart, 1980). The temperature used in this chart are the maximum temperatures that the source rock has been subjected too and thus cannot necessarily be applied to temperature gradients currently existing in the geologic section. But with increasing temperature, petroleum generated from source rocks consists first of heavier weight liquid hydrocarbons from approximately 150°F to 250°F, followed by condensate rich gas from approximately 225°F to 300°F, and finally dry gas from 250°F to 350°F. It should be noted that these temperature zones delineating the generation of different hydrocarbons are overlapping. Further, the type of hydrocarbon generated is highly dependent upon the nature of the original organic material. Liquid hydrocarbons formed at shallow depths having lower temperatures would be progressively broken down into lighter hydrocarbons with increased burial to depths having higher temperatures (Tissot et al., 1974; Rice, 1980)

Second, the most commonly proposed mechanism for significant vertical hydrocarbon migration, which consists of a true solution in water, has several inadequacies which would indicate that it is not an important primary migration mechanism. Price (1976) indicated that significant hydrocarbons could be dissolved in fresh waters at tempera-

tures higher than 180C (356F) to account for molecular-solution as a primary petroleum migration mechanism. However, the paleo-temperature ranges for hydrocarbon maturation (Fig. 18; Hart, 1980), indicate that at temperatures greater than 356°F, no liquid hydrocarbons would be left in the source beds to be moved by this mechanism. Jones (1980) stated that at temperatures above 200°C (392°F), there is usually a drastic drop in the ratio of the weight percent bitumen to the total organic carbon (TOC) found in potential source rocks. Thus, the available butumens in the rocks at temperatures greater than 200°C are probably not significant enough to produce significant enough to produce commercial oil accumulations. Also studies of liquid hydrocarbon accumulations indicate that variations in the solubilities of different molecular weights and types of liquid hydrocarbons are not reflected in these crude oil compositions (McAuliffe, 1979). Further, by modeling fluid migrations, Bonham (1980) concluded that insufficient water had moved up permeable fault systems to account for the origin of known oil accumulations within the hydro pressured zones of the Gulf Coast; therefore, liquid hydrocarbon accumulations, such as in LaFourche Crossing and northeast Chacahoula fields, could not have come from the very deep abnormally pressured shale sections with temperatures in excess of 356°F which occur below the base of the drilled section in the study area.<sup>2</sup> The reported solubilities of lighter hydrocarbons (Price, 1976) and methane (Bonham, 1980) appear high enough to account for their migration from the deep abnormally pressured zone in solutions. Secondary migration up the permeable fault zones would have to be accomplished, in part, as a separate hydrocarbon phase due to the drop in temperatures and pressures with decreasing depth. But even then gas and

condensate accumulations within the 'hard' abnormally pressured section of the study area are still difficult to explain using Price's solution migration.

Third, the total organic carbon (TOC) content of the shale source rocks in tertiary delta systems is substantially below the values for most other known source rocks. TOC in the Niger and Mississippi delta systems range from only .3 to 1.0 weight percent. Most other source rocks from other parts of the world contain TOC ranges from 2.5 weight percent to over 10 weight percent (Jones, 1980). With the exception of the Tertiary delta systems, such as in the Gulf Coast, rocks with low TOC are not the sources of major oil accumulations. Jones concluded that the low TOC in the Gulf Coast sediments made primary migration of oil in a continuous phase highly unlikely.

#### Conclusions

Due to the occurrences of probable vertical water migration from the 'hard' abnormally pressured section as delineated by thermal and salinity anomalies, it seems likely that petroleum accumulation and structural development were facilitated by the water movements. A deep, long distance transport of most of the hydrocarbons in solution, along permeable fault zones as proposed by Price (1976) seems unlikely. But substantial redistribution of hydrocarbons, particularly gases, from the 'hard' abnormally pressured zone during times of vertical water flushes is probable. These hydrocarbons would have moved as a separate phase within the water in response to buoyancy. Hydrocarbons within the 'hard' abnormally pressured section, which occur throughout the study area, probably also moved in response to water leaving this zone but

were not transported over extensive distances. Abnormally pressured fields such as a Southwest Lake Boeuf may have experienced negligible vertical hydrocarbon migration and significant lateral migration. Shallow, normally pressured hydrocarbon accumulations such as those in LaFourche Crossing and northeast Chacahoula fields are most likely related to migration from the 'hard' abnormally pressured zones. The shallow accumulations in southern Rousseau are probably related to vertical fluid migration in LaFourche Crossing to the south and along Fault R to the north of the anticline. Absence of salinity and thermal anomalies over the Rousseau Dome indicate that the shallow accumulations did not come from the extensive graben system developed in the abnormally pressured zone. This is easily understood, since none of the graben faults (Fault Q, Q', N, or P) continued movement for a significant time after the current top of the 'hard' abnormally pressured zone (Robulus (43) L) was deposited.

It must be remembered that the sediment deposition, structural development, and fluid migration within the Miocene of the study area constitute a dynamic and continually changing system. The changes in sedimentation and structural development as described in this study can be readily documented since they leave a permanent record within the drilled stratigraphic column. Fluid movements, on the other hand, must be short-lived events which may persist in the same location over a significant geologic time. A record of these fluid movements is neither simple nor permanent. Later structural movements and fluid migrations may completely destroy the evidence of past hydrocarbon accumulations or vertical fluid migrations. The hydrocarbons ultimately found in reservoirs may thus have had a long history of secondary migration and may

have been generated in innumerable source rocks within the basin.

#### Recommendations

Due to the quantity and quality of data used, a study of this nature can only give a generalized picture of fluid migration within a basin. The parameters of salinity, temperature, and pressure were all derived through indirect measuring methods involving numerous assumptions. A much more precise model of fluid migration could be developed if direct measurements could be obtained. Such data would consist of 1) temperature, sonic, and density logs, 2) detailed reservoir production data, 3) cores, and 4) fluid samples. Such data could give precise values for temperatures, pressures, porosities, rock matrices, and fluid composition within the basin. If a significant amount of data of this could be obtained, then a more detailed model of fluid migration could be developed. This model could combine methods such as those used by Bonham (1980) and Bredehoeft and Hanshaw (1968). Problems such as mechanisms of primary and secondary migration, development and maintenance of abnormal pressures, and volumes of water moved could then be properly evaluated. Such a model would have to involve substantial computer techniques.

Significant planning and background research would be involved in locating an appropriate study area. Such an area would have to be 1) structurally simple, 2) not actively under hydrocarbon exploration, and 3) data-rich as described above.

## References Cited

- Amery, G.B., 1978, Structure of Continental Slope, Northern Gulf of Framework, Facies, and Oil-Trapping Characteristics of the Upper Continental Margin, A.H. Bouma, et al., eds.: Am. Assoc. Petrol. Geol. Studies in Geology #7, Tulsa, Oklahoma, p. 141-153.
- Baird, J.A., 1977, Unconformities-neglected oil finders' tools: Trans. Gulf Coast. Geol. Soc., v. 27, p. 1-5.
- Barker, C., 1972, Aquathermal pressuring - role of temperature in development of abnormal-pressure zones: Am. Asso. Petrol. Bull., v. 56, no. 10, p. 2068-2071.
- Berg, R.R., 1975, Capillary pressures in stratigraphic traps: Am. Assoc. Petrol. Geol. Bull., v. 59 no. 6, 9. 939-956.
- Bishop, R.S., 1979, Calculated compaction states of thick abnormally pressured shales: Am. Assoc. Petrol. Geol. Bull., v. 63, no 6, p. 918-933.
- Bonham, L.C., 1980, Migration of hydrocarbons in compacting basins: Am. Assoc. Petrol. Geol. Bull., v. 64, no. 4, p. 549-567.
- Bredehoeft, J.D. and B.B. Hanshaw, 1968, On the maintenance of anomalous fluid pressures; I. thick sedimentary sequences: Geol. Soc. Am. Bull., v. 79, p. 1097-1106.
- Bruce, C.H., 1973, Pressured shale and related sediment deformation: a mechanism for development of regional contemporaneous faults: Am. Assoc. Petrol. Geol. Bull., v. 57, p. 878-886.
- Burst, J.F., 1969, Diagenesis of Gulf Coast clayey sediments and its possible relation to petroleum migration: Am. Assoc. Petrol. Geol. Bull., v. 53, no. 1, p. 73-93.
- Chapman, R.E., 1972, Clays with abnormal interstitial fluid pressures: Am. Assoc. Petrol. Geol. Bull., v. 56, no. 4, p. 790-795.
- Coleman, J.M., and D.B. Prior, 1980, Deltaic sand bodies: Am. Assoc. Petrol. Geol. Continuing education course note series #15, Tulsa, Oklahoma, 171 pages.
- Currie, J.B., 1956, Role of concurrent deposition and deformation of sediments in development of salt-dome graben structures: Am. Assoc. Petrol. Geol. Bull., v. 40, no 1, p. 1-16.
- Dickinson, G., 1953, Geological aspects of abnormal reservoir pressures in Gulf Coast Louisiana: Am. Assoc. Petrol. Geol. Bull., v. 37, no. 2, p. 410-432.
- Fallow, W.C., 1973, Grabens on anticlines in Gulf Coastal Plain, and thinning of sedimentary section in downthrown fault block: Am. Assoc. Petrol. Geol. Bull., v. 57, no. 1, p. 198-203.

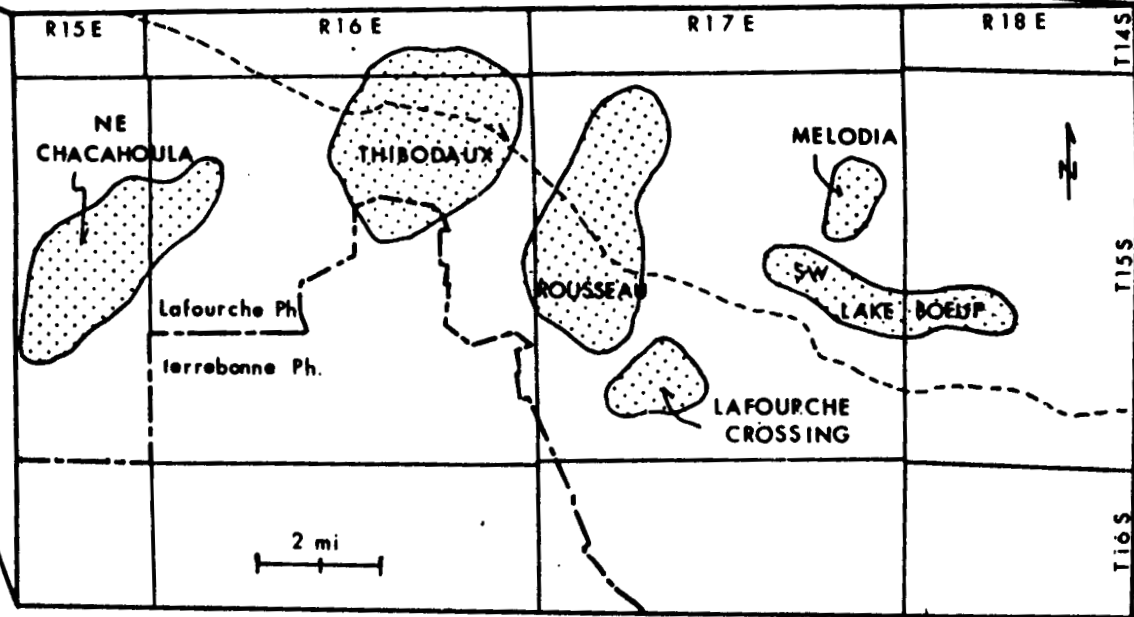
- Fertl, W.H., and D.J. Timko, 1971, How abnormal-pressure-detection techniques are applied: Oil and Gas Jour., v. 68, no. 2, p. 62-71.
- George, R., 1959, Approximate formation pressure from resistivity logs in south Louisiana: Schlumberger Well Surveying Corp., New Orleans, Louisiana (Log Interpretation Chart).
- Gatenby, G.M., 1979, Subsurface fluid migrations in the Borgne-Valentine area of southeastern Louisiana: Master's Thesis, Louisiana State University, Baton Rouge, Louisiana, 107 pages.
- Hammack, G.W., and W.H. Fertl, 1974, How well logs can be misinterpreted: World Oil, v. 179, p. 69-73.
- Hardin, F.R. and G.C. Hardin, Jr., 1961, Contemporaneous normal faults of Gulf Coast and their relation to flexures: Am. Assoc. Petrol. Geol. Bull., v. 45, no. 2, p. 238-248.
- Harrison, F.W., 1979, The role of pressure, temperature, salinity, lithology and structure in hydrocarbon accumulation in Constance Bayou, Deep Lake, and Southeast Little Pecan Lake Fields, Cameron Parish, Louisiana: Master's Thesis, Louisiana State University, Baton Rouge, Louisiana, 124 pages.
- Hart, G.F., 1980, Maceral analysis and its application in petroleum exploration, Maceral analysis techniques paper #2: Unpublished duplicate report, Hartax International, Baton Rouge, La., 20 pages.
- Hedberg, H.D., 1980, Methane generation and petroleum migration, in Problems of Petroleum Migration, Roberts III, W.H., and R.J. Cordell eds.: Am. Assoc. Petrol. Geol. Studies in Geology #10, p. 179-206.
- Hintze, W.H., 1967a, Rousseau field, in Oil and Gas Fields in Southeast La.: New Orleans Geol. Soc., v.2, p. 137-142.
- \_\_\_\_\_, 1967b, Thibodaux field, in Oil and Gas Fields in Southeast La.: New Orleans Geo. Soc., v. 2, p. 149-155.
- Hubbert, M.K. and W.W. Rubey, 1959, Role of fluid pressure in mechanics of overthrusting faulting: Geol. Soc. Am. Bull., v. 70, no. 2, p. 115-166.
- Humphries, Jr., C.C., 1976, Salt movement on continental slope northern Gulf of Mexico: Am. Assoc. Petrol. Geol. Bull., v. 63, no. 5, p. 782-798.
- Jam, P.L., P.A. Dickey, and E. Tryggvason, 1969, Subsurface temperature in south Louisiana: Am. Assoc. Petrol. Geol. Bull., v. 53, no. 10, p. 2141-2149.
- Johnson, H.A., and D.H. Bredeson, 1971, Structural development of some salt domes in Louisiana Miocene productive belt: Am. Assoc. Petrol. Geol. Bull., v. 55, no. 2, p. 204-226.

- Jones, P.H., 1975, Geothermal and hydrocarbon regimes, northern Gulf of Mexico basin, in Proc. First Geop. Geothermal Energy Conf., M.H. Dorfman and R.W. Deller, eds.: University of Texas at Austin, p. 15-89.
- Jones, R.W., 1980, Some mass balance and geological constraints on migration mechanisms, in Problems of Petroleum Migration, W.H. Roberts, III and R.J. Cordell, eds.: Am. Assoc. Petrol. Geol. Studies in Geology #10, p. 47-68.
- Kehle, R.C., 1971, Geothermal survey of North America, 1971, Annual progress reports: Unpublished duplicate report, Research Comm., Am. Assoc. Petrol. Geol., Tulsa, Okla., 31 pages.
- Krom, M.D., and R.A. Berner, 1980, The diffusion coefficients of sulfate, ammonium, and phosphate ions in anoxic marine sediments: Limnol. Océogr. v. 25, no.2, p.327-337.
- Kharaka, Y.K., and F.A.F. Berry, 1973, Simultaneous flow of water and soluted through geological membranes-I. Experimental investigation: Geochim. Cosmochim. Acta, v. 37, p. 2577-2603.
- Lerman, A., 1979, Geochemical Processes Water and Sediment Environments: John Wiley & Sons Pub., New York, N.Y., 212 pages.
- Magara, K., 1975, Re-evaluation of Montmorillonite dehydration as cause of abnormal pressure and hydrocarbon migration: Am. Assoc. Petrol. Geol. Bull., v. 52, no. 2, p. 292-302.
- Martin, R.G., and A.H. Bouma, 1978, Physiography of Gulf of Mexico, in Framework, Facies, and Oil-Trapping Characteristics of the Upper Continental Margin, A.H. Bouma, et al., eds., Am. Assoc. Petrol. Geol. Studies in Geology #7, p. 21-42.
- McAuliffe, C.D., 1979, Oil and gas migration - chemical and physical constraints: Am. Assoc. Petrol. Bull., v. 64, no. 4, p. 549-567.
- McClellan, C.M., 1957, Miocene geology of southeastern Louisiana: Trans. Gulf Coast Assoc. Geol. Soc., v 7, p. 241-246.
- Moses, P.L., 1961, Geothermal gradients: World Oil, v. 152, no. 6, p. 79-82.
- Ocanb, R., 1961, Growth faults of South Louisiana: Trans. Gulf Coast Assoc. Geol. Soc., v. 11, p. 139-173.
- Oden, S.L., 1980, Natural temperature distribution around salt domes: Master's Thesis, Louisiana State University, Baton Rouge, Louisiana, 111 pages.
- O'Neill III, C.A., 1973, Evolution of Belle Isle salt dome, Louisiana: Trans. Gulf Coast Assoc. Geol. Soc., E. 23, p. 115-135.

- Pope, D.E., personal communication 1980: La. Geol. Survey, Baton Rouge, La.
- Powers, M.C., 1967, Fluid-release mechanisms in compacting marine mudrocks and their importance in oil exploration: Am. Assoc. Petrol. Geol. Bull., v. 60, no. 2, p. 213-244.
- Price, L.C., 1976, Aqueous solubility of petroleum as applied to its origin and primary migration: Am. Assoc. Petrol. Geol. Bull., v. 60, no. 2, p. 213-244.
- Rice, D.D., 1980, Chemical and isotopic evidence of the origins of natural gases in offshore Gulf of Mexico, Trans. Gulf Coast Assoc. Geol. Soc., p. 203-213.
- Schlumberger Ltd., 1972a, Schlumberger Log Interpretation Charts Booklet, 92 pages.
- \_\_\_\_\_, 1972b, Schlumberger Log Interpretation Principles Booklet, v. 1, 113 pages.
- Schmidt, G.W., 1973, International water composition and geochemistry of deep Gulf Coast Shales and sands: Am. Asso. Petrol. Bull., v. 57, p. 321-337.
- Segland, J.A., 1974, Collapse fault systems of the Louisiana Gulf coast: Trans. Gulf Coast Assoc. Geol. Soc., v. 24, p. 1-3.
- Sloane, B.J., 1966, The structural history of the Houma embayment: Trans. Gulf Coast Assoc. Geol. Soc., b. 16, p. 249-260.
- Smith, D.A., 1980, Sealing and non-sealing faults in the Gulf Coast Salt Basin: Am. Assoc. Petrol. Geol. Bull., v. 64, no.2, p. 145-172.
- Thorsen, C.E., 1963, Age of growth faulting in southeast Louisiana: Trans. Gulf Coast Assoc. Geol. Soc., v. 13, p. 103-110.
- Tipsword, A.L., F.M. Setzer, and F.L. Smith, Jr., 1966, Interpretation of depositional environment in Gulf Coast petroleum exploration from paleoecology and related stratigraphy: Trans. Gulf Coast Assoc. Geol. Soc., v. 16, p. 119-130.
- Tissot, B., et al., 1974, Influence of mature and diagenesis of organic matter in formation of petroleum: Am. Assoc. Petrol. Geol. Bull., v. 58, no. 3, p. 499-506.
- Wallace, W.W., 1944, Structure of South La. Deep-seated domes: Am. Assoc. Petrol. Geol. Bull., v. 28, no. 9, p. 1249-1312.
- Waples, D.W., 1980, Time and temperature in petroleum formation: Application of Lopatin's method to petroleum exploration: Am. Assoc. Petrol. Geol. Bull., v. 64, no. 6, p. 916-926.



Fig. 1 - Location map of the study area in northern Lafourche and Terrebonne Parishes, Louisiana.



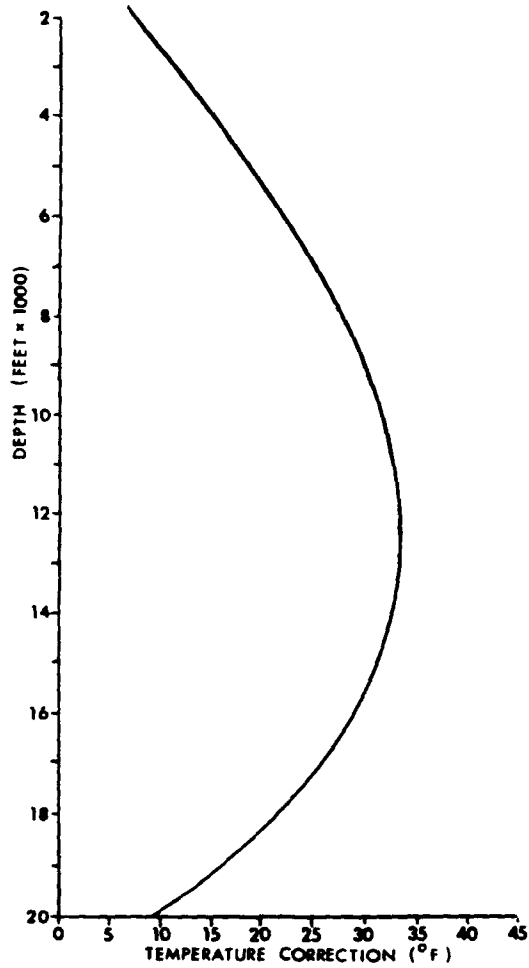


Fig. 2 - Empirically derived bottom temperature (BHT) correction curve used to approximate equilibrium temperature. Temperature indicated is added to the observed BHT at the bottomhole depth (after Kehle, 1971).

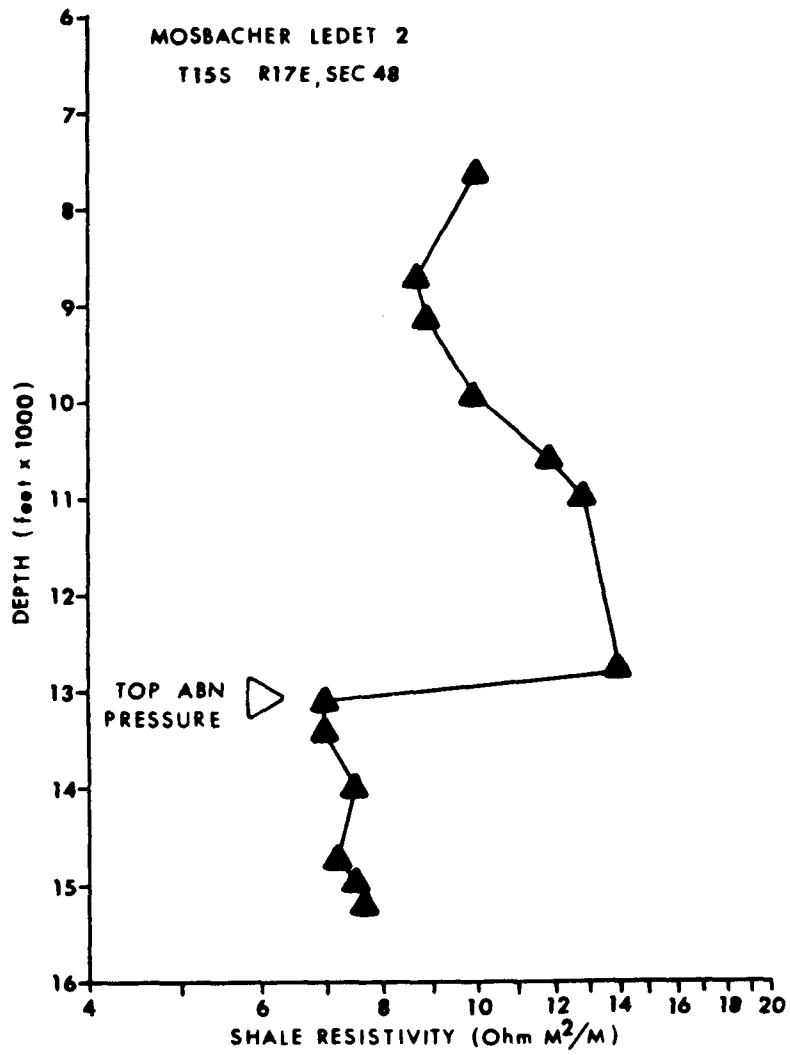


Fig. 3 - Plot of short-normal resistivity measurements versus depth showing the typical abrupt resistivity drop occurring across the 'seal' at the top of the 'hard' abnormally pressured zone (.7 psi/ft).

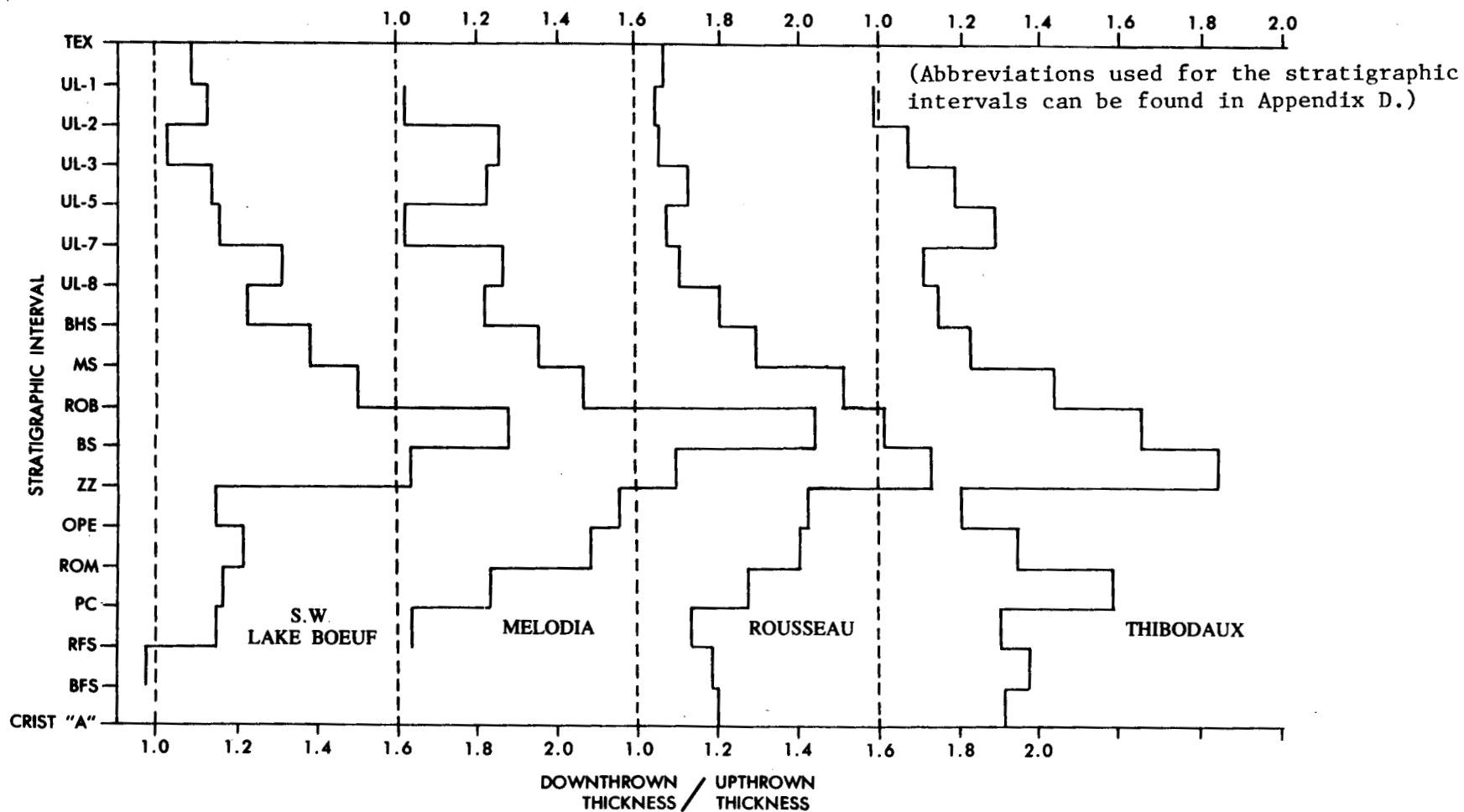


Fig. 4 - Growth indices (Thorsen, 1963) on four parts of the northern regional fault T, from west (right) to east (left). Note that the largest growth period occurred during the Robulus I (ROB) to Bourgeois Sand (BS) deposition. Names refer to fields in which the measurements were taken (see location map, Plate 1).

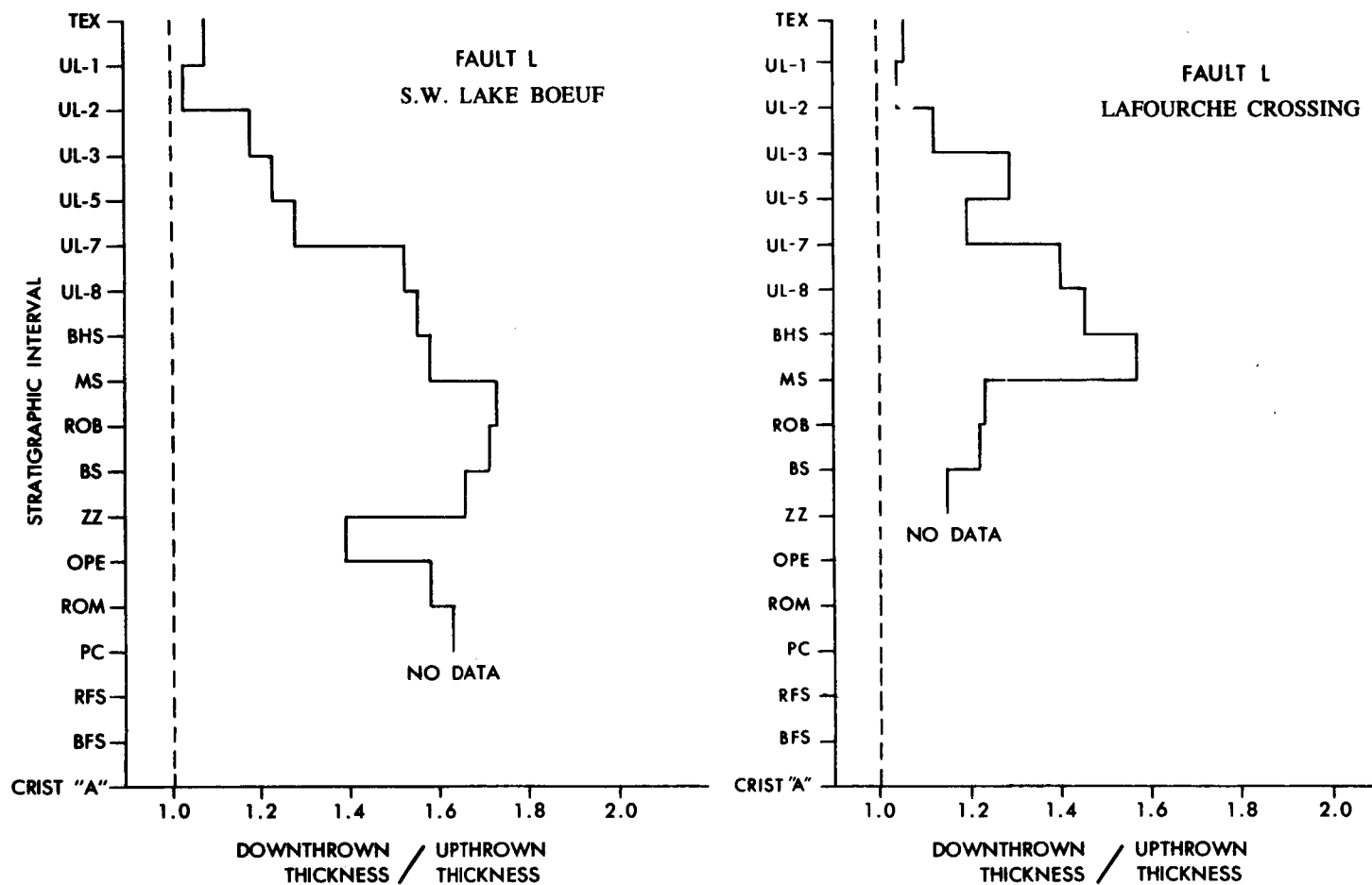


Fig. 5 - Growth indices (Thorsen, 1963) on the southern regional fault L in the Lafourche Crossing and Southwest Lake Boeuf areas. (See Plate 1 for field locations.) Note that the largest growth period occurred during the Robulus I (ROB) to UL-7 sand (UL-7) deposition.

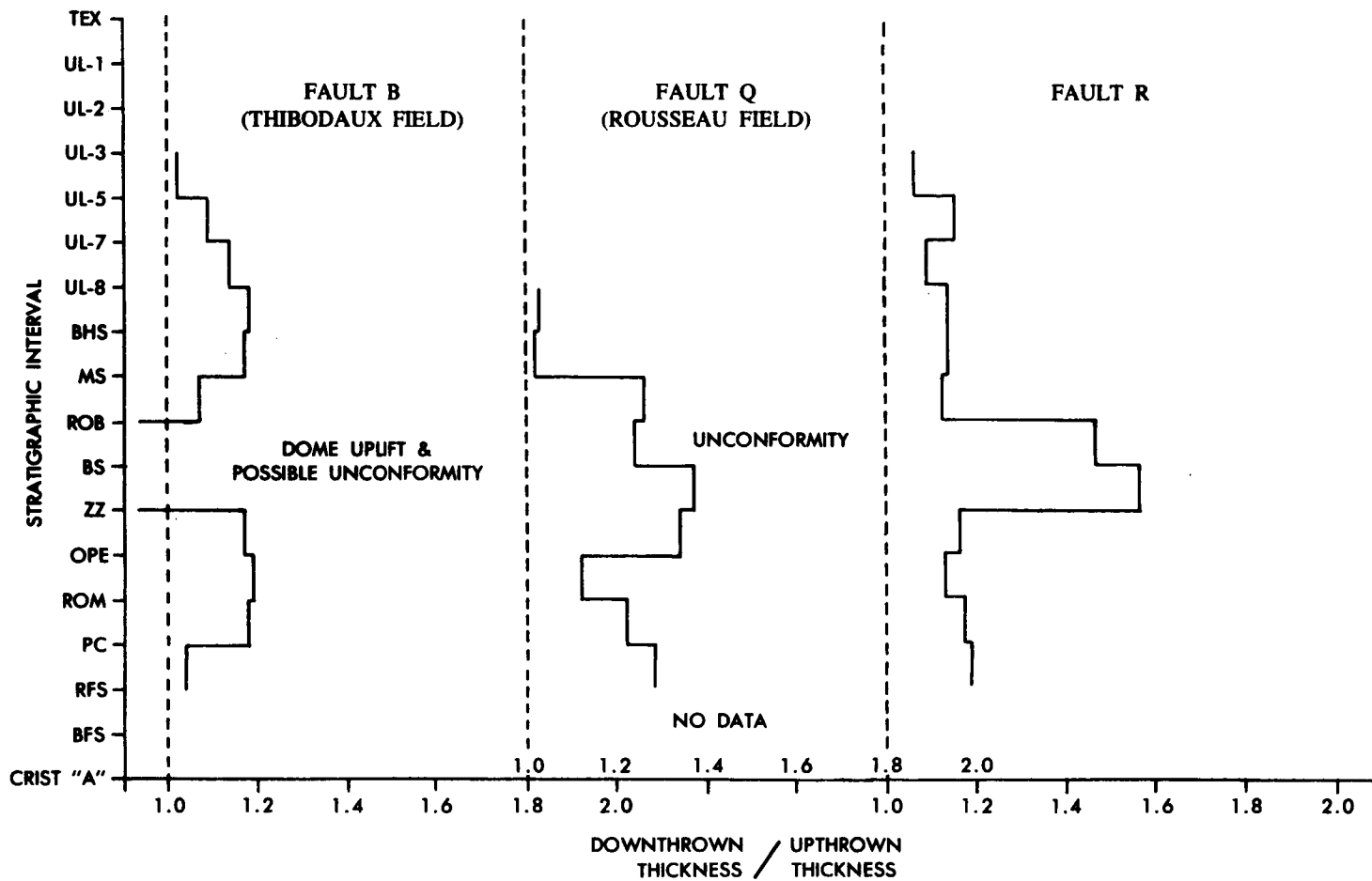


Fig. 6 - Growth indices (Thorsen, 1963) for three, long-lived, south-dipping growth faults in the study area. Faults Q and R were most active from the deposition of ZZ to the Robulus I (ROB) sand. Growth indices for Fault B are complicated by a domal uplift Robulus deposition, across which the fault extended.

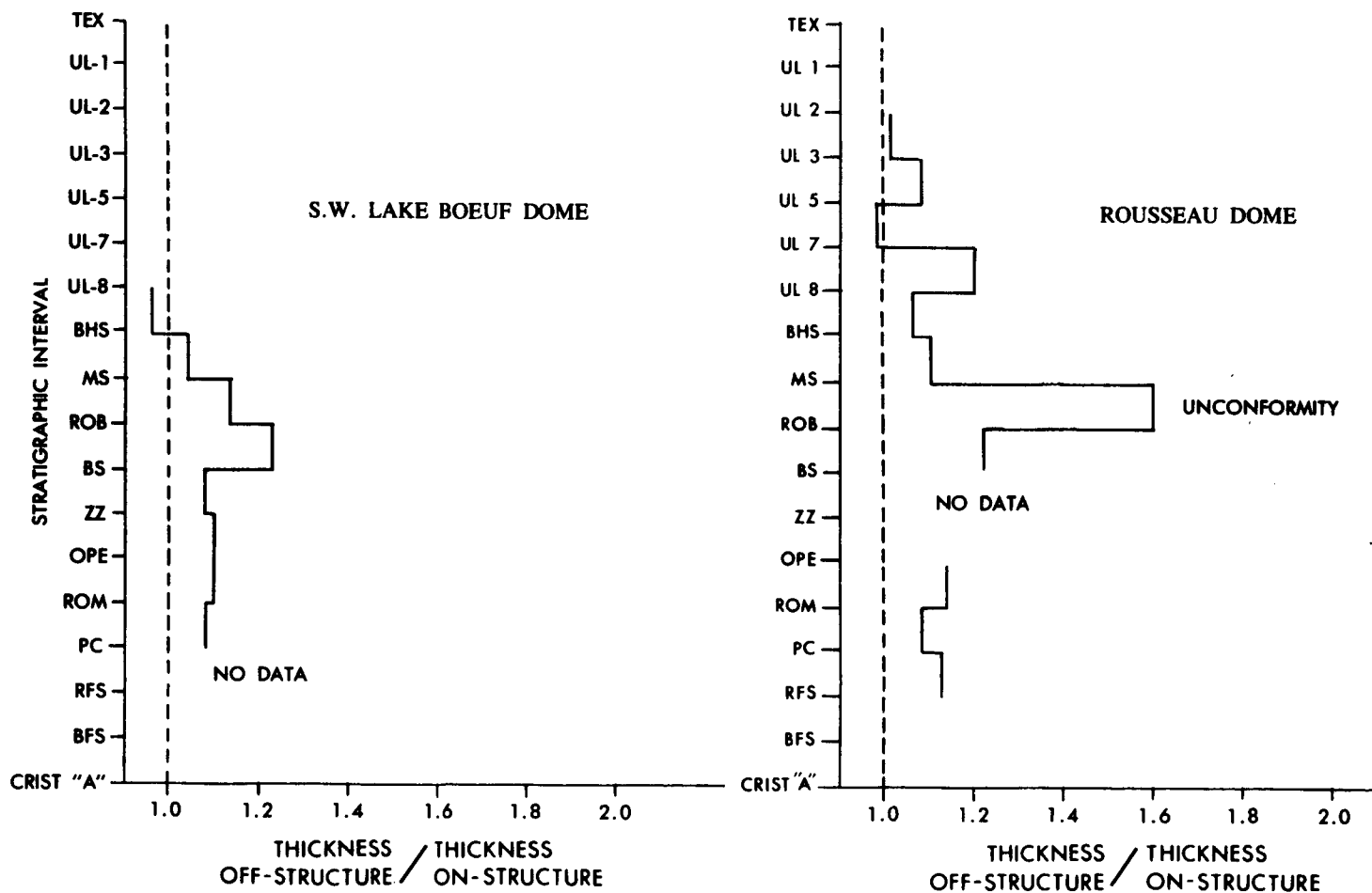


Fig. 7 - Growth indices (Thorsen, 1963) for the Rousseau and Southwest Lake Boeuf domes. Note that accelerated growth occurred on both domes during Robulus I sand (ROB) deposition and that movement on the Rousseau domes continued much longer than at Southwest Lake Boeuf.

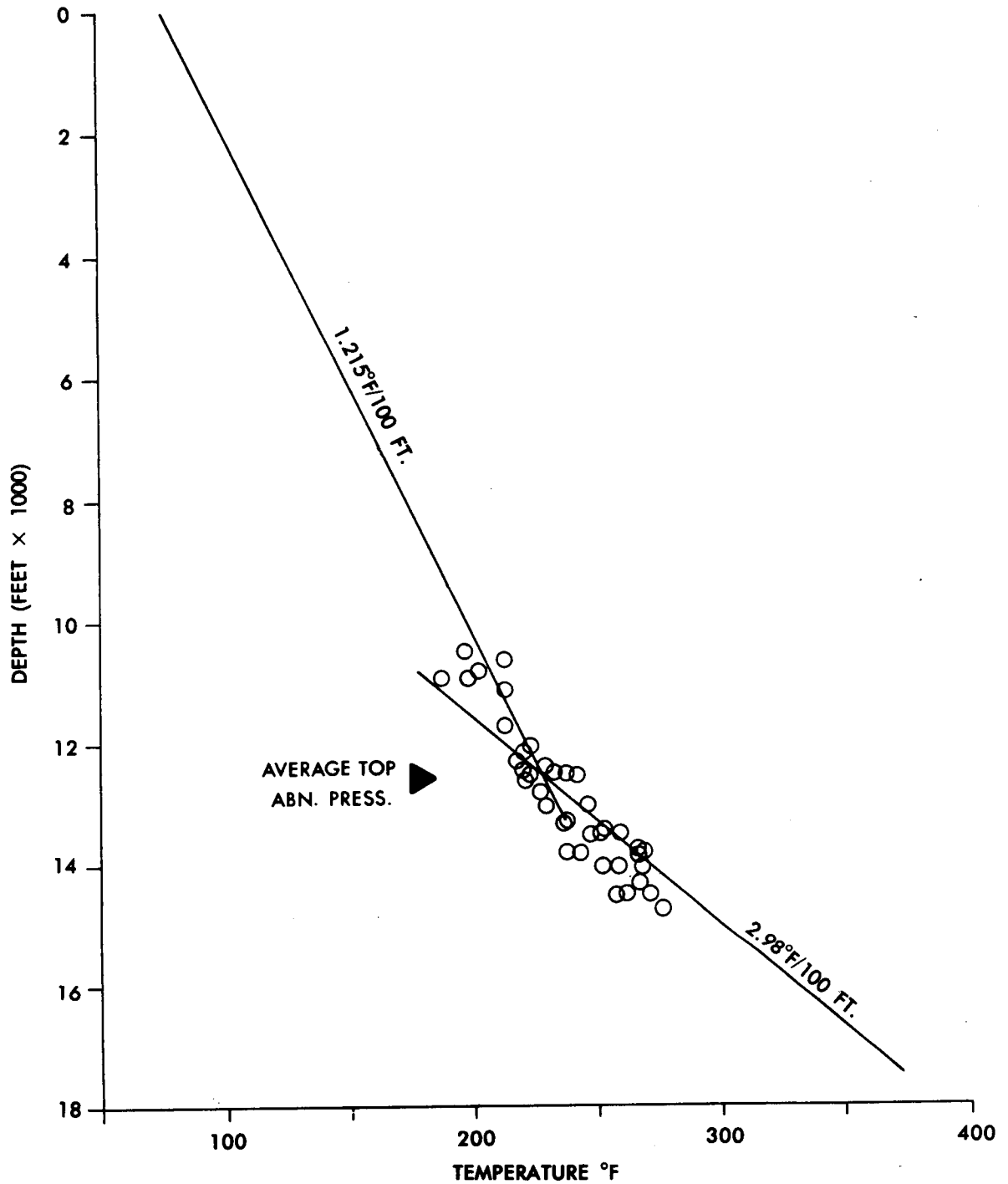


Fig. 8 - Plot of corrected bottom hole temperatures (BHT) (Kehle, 1971) from fourteen wells in the Thibodaux field. Data is overlain by the average of the temperature gradients, in the abnormally pressured and hydrostatically pressured zone, from the individual wells.

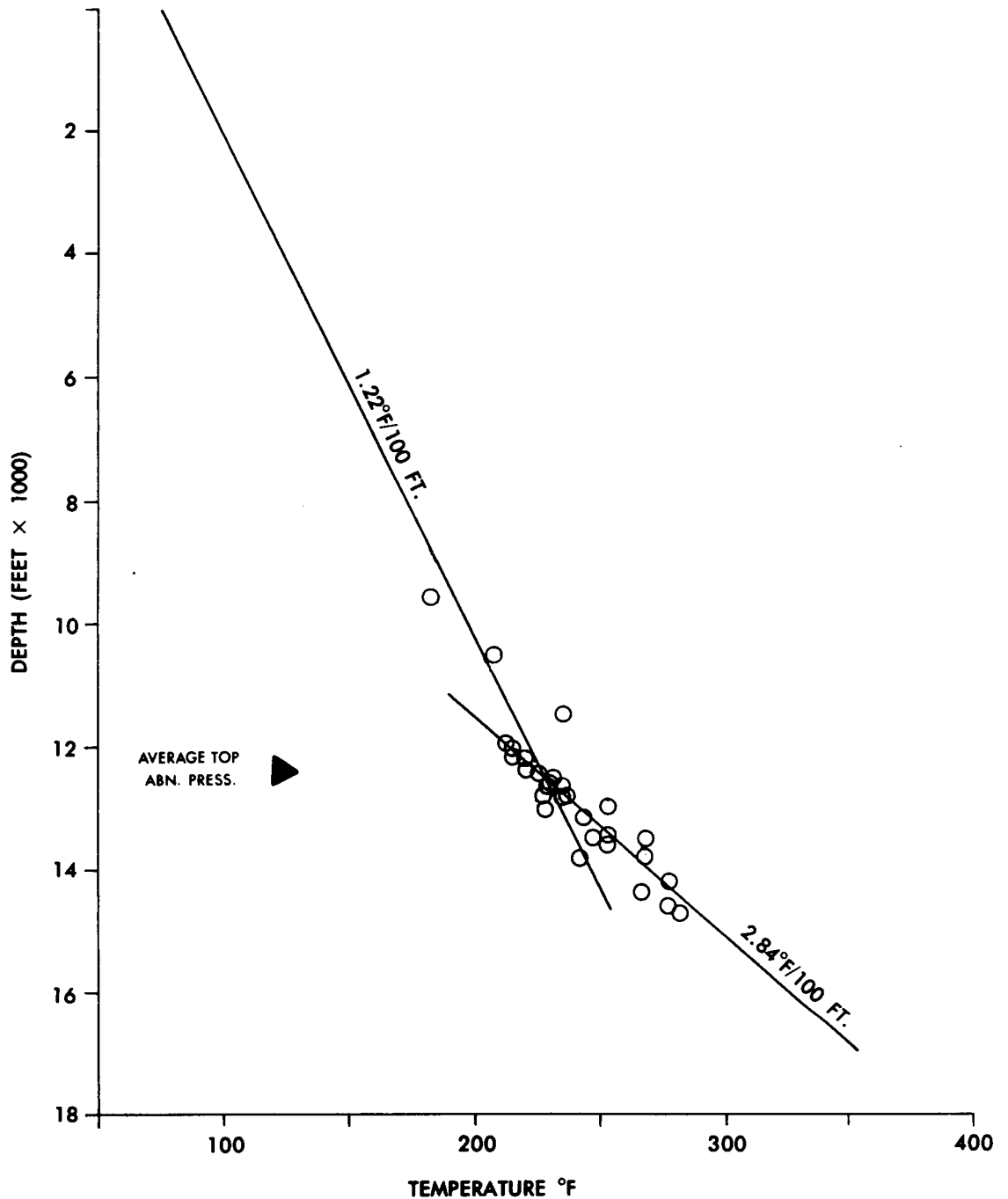


Fig. 9 - Plot of corrected bottom hole temperatures (BHT) (Kehle, 1971) from seven wells in the northern area of Rousseau field. Data is overalin by the average of the temperature gradients, in the abnormally pressured and hydrostatically pressured zone, from the individual wells.

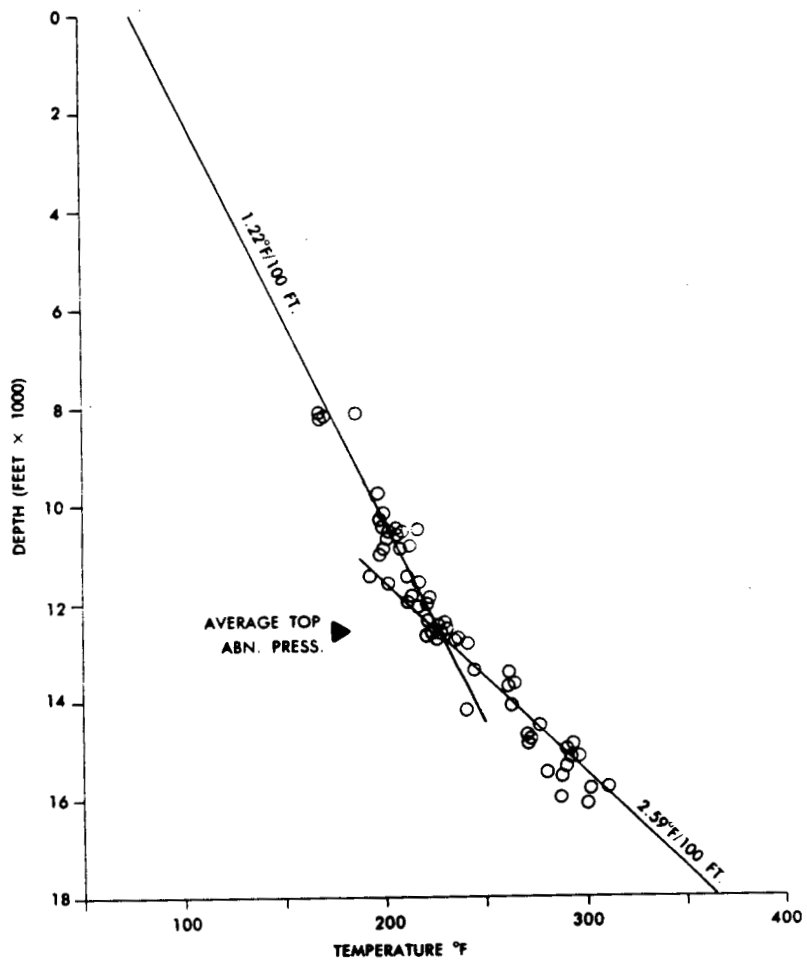


Fig. 10 - Plot of corrected bottom hole temperatures (BHT) (Kehle, 1971) from sixteen wells in the southern area of Rousseau field. Data is overlain by the average of the temperature gradients, in the abnormally pressured and hydrostatically pressured zone, from the individual wells.

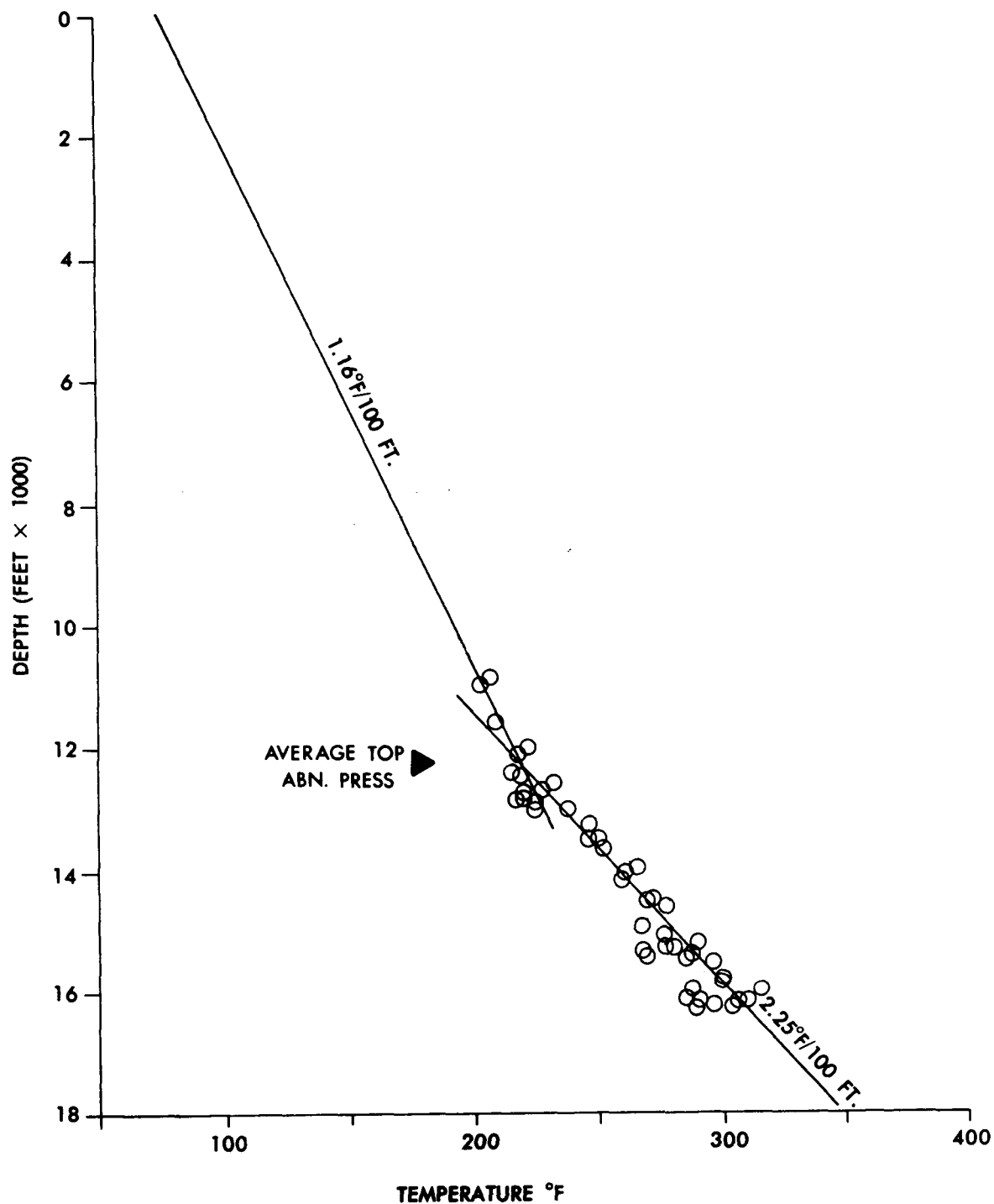


Fig. 11 - Plot of corrected bottom hole temperatures (BHT) (Kehle, 1971) from thirteen wells in the Southwest Lake Boeuf field. Data is overlain by the average of the temperature gradients, in the abnormally pressured and hydrostatically pressured zone, from the individual wells.

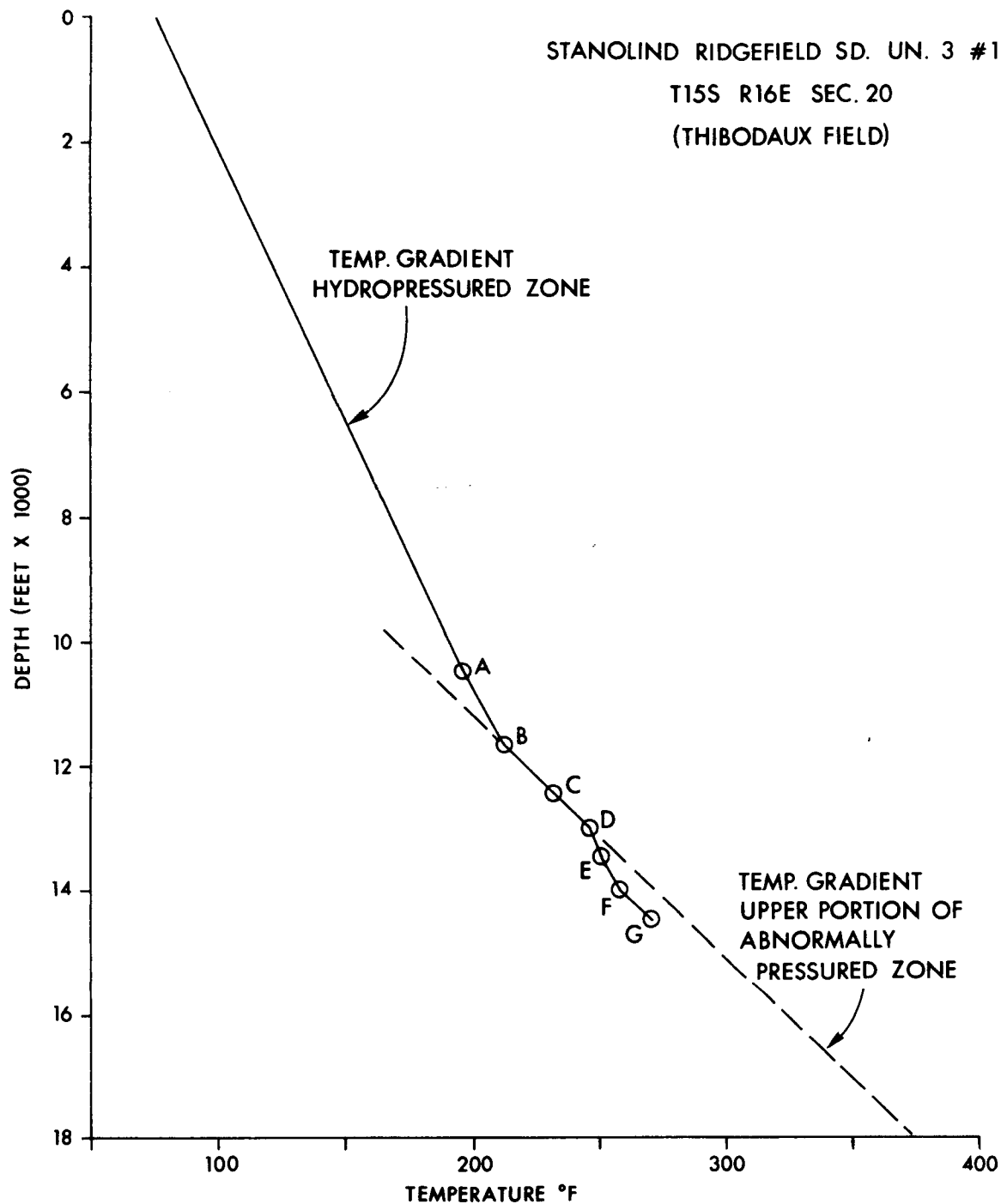


Fig. 12 - Plot of corrected BHT data for a well in Thibodaux Field showing the typical dog-leg temperature gradients. The temperature gradient is initially very high in the upper portion of the abnormal zone (B, C, D), but decreases deeper in this zone below 13,000 feet (point D).

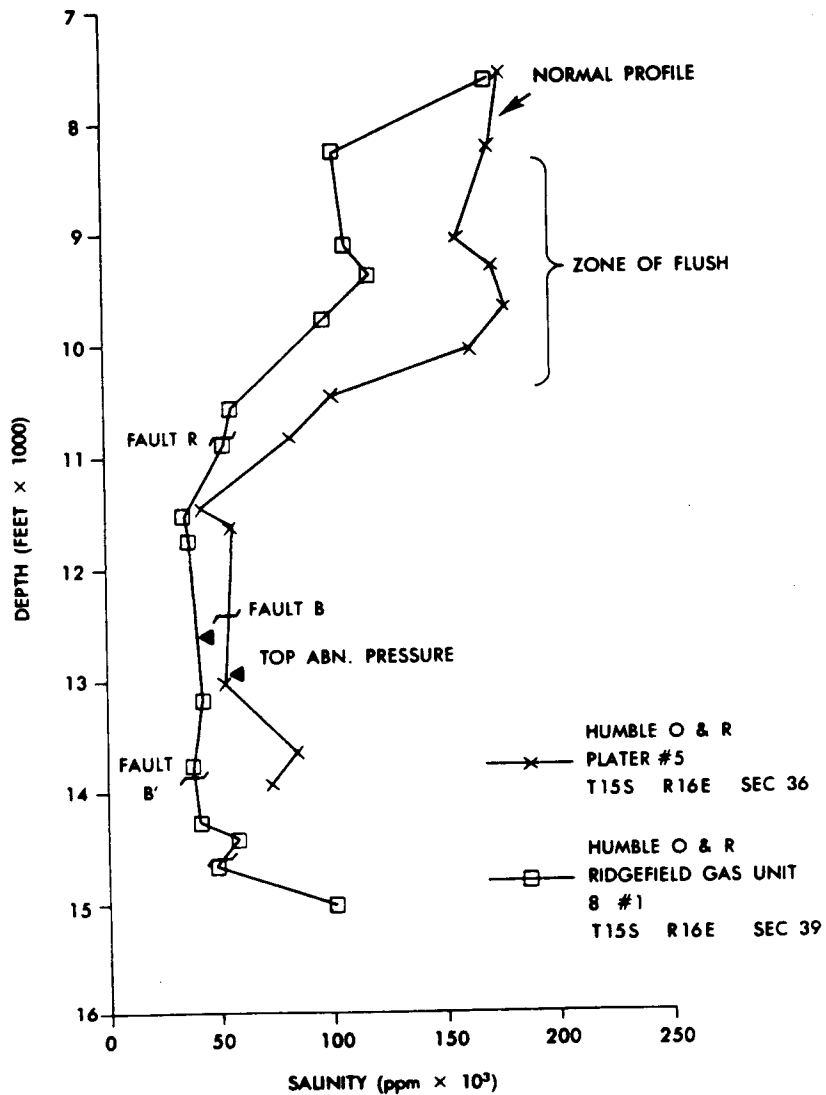


Fig. 13- Sandstone water salinity profile for two wells in the Thibodaux field area. The Humble O & R, #1 Ridgefield Gas Unit 8 well shows a zone of abnormally low salinity water between 10,500 to 8,500 feet indicating an invasion of water from the abnormally pressured zone. Both fault R and B could have proved the avenue for vertical fluid movement.

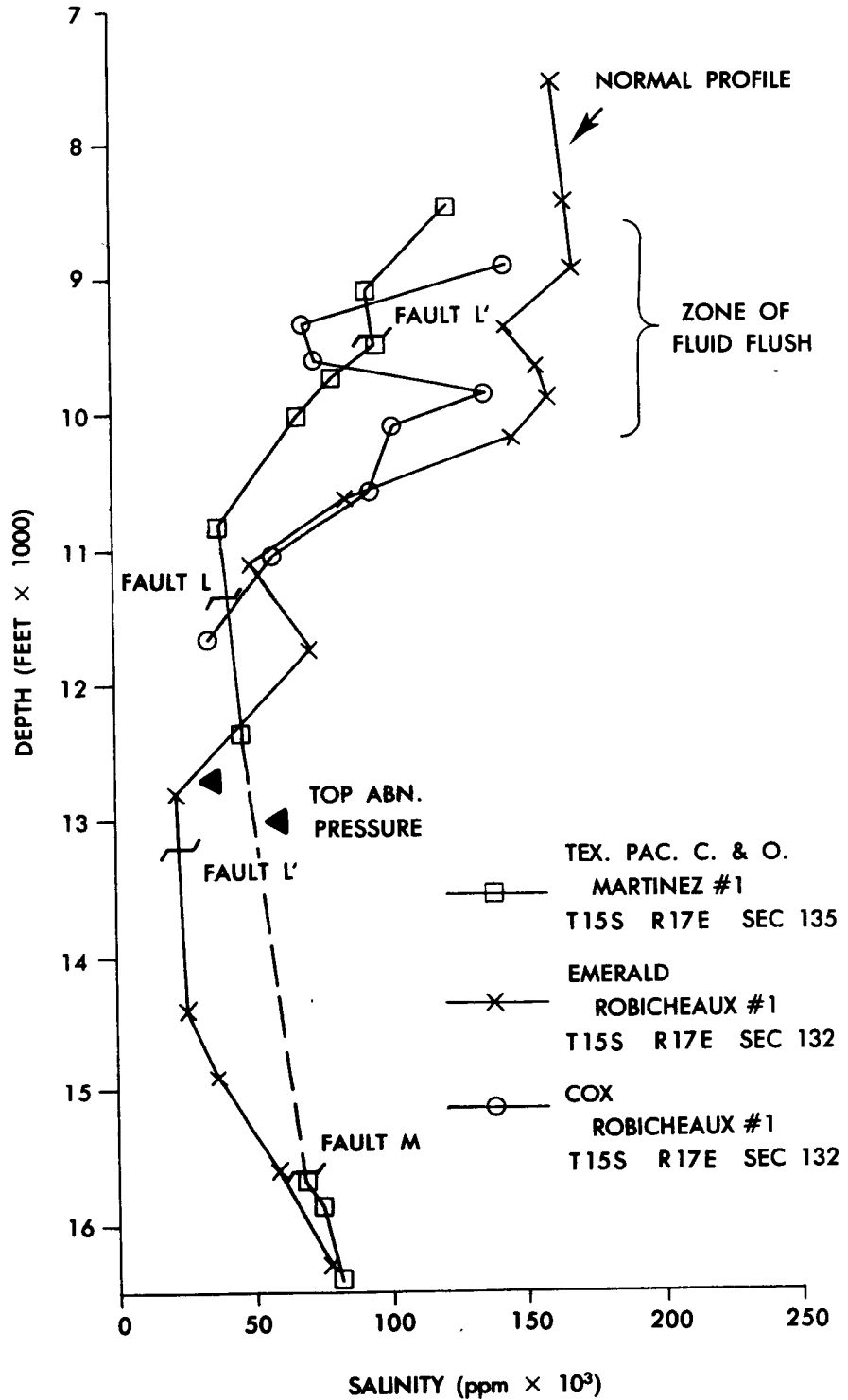


Fig. 14 - Sandstone salinity profiles for three wells in the Lafourche Crossing Field, indicating an anomalous zone between 9,000 and 10,000 feet which received low salinity waters from the abnormally pressured zone below approximately 13,000 feet. The Emerald Robicieux #1 well is a normal profile showing limited fluid invasion. Both Faults L and L' could have provided an avenue of fluid migration.

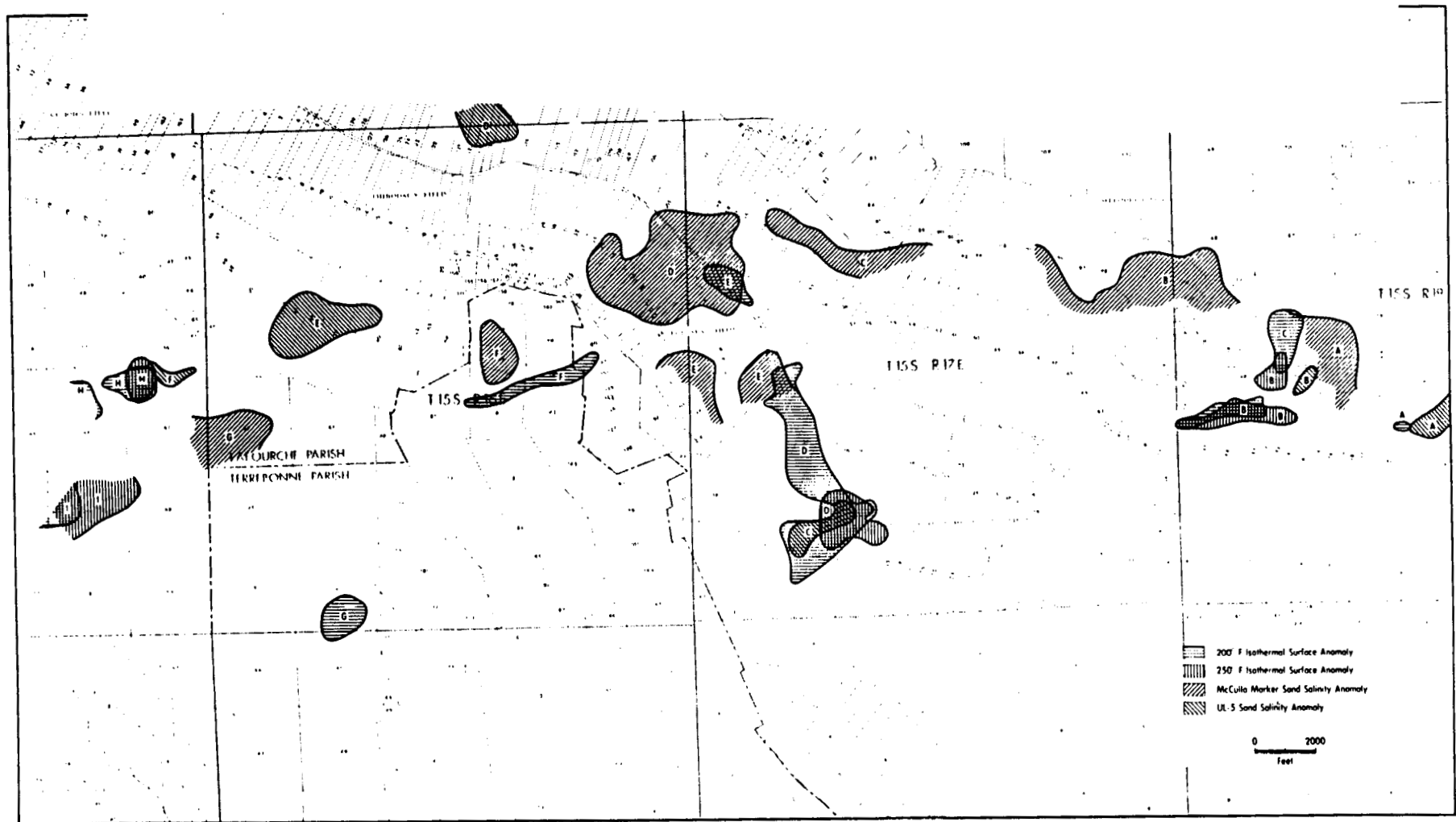


Fig. 15 - Summary of sandstone salinities and thermal anomalies.

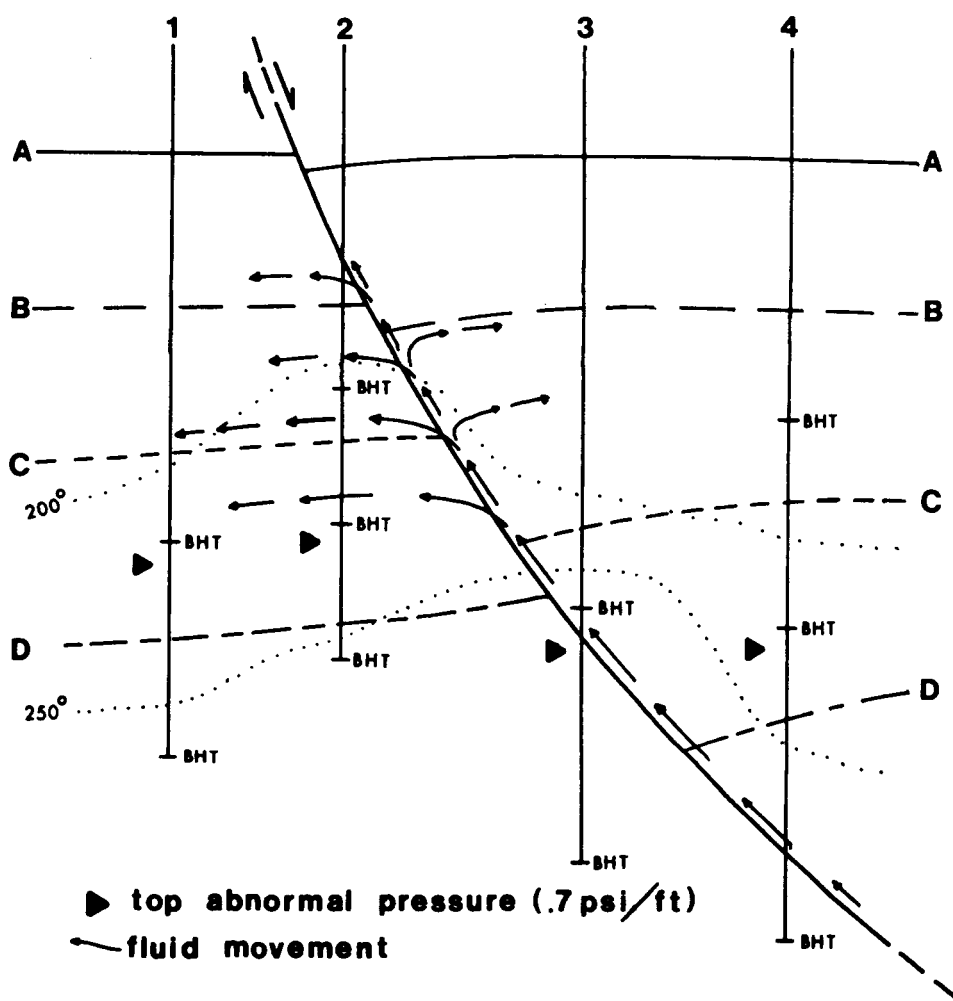
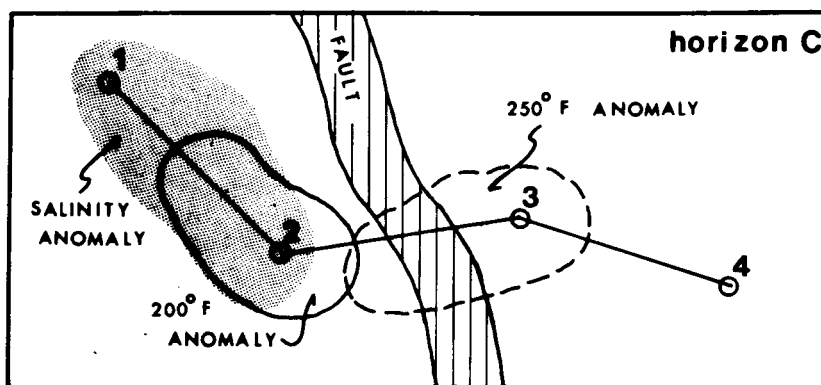


Fig. 16 - Hypothetical cross section and anomaly map illustrating the effect that the distribution of available BHT and salinity measurements can have on the temperature and salinity anomaly patterns. Temperature and salinity anomalies for horizon C are shown in the situation. Anomalies are observed only where well measurements occur in zones receiving hot, low salinity water from below the abnormally pressured zone.

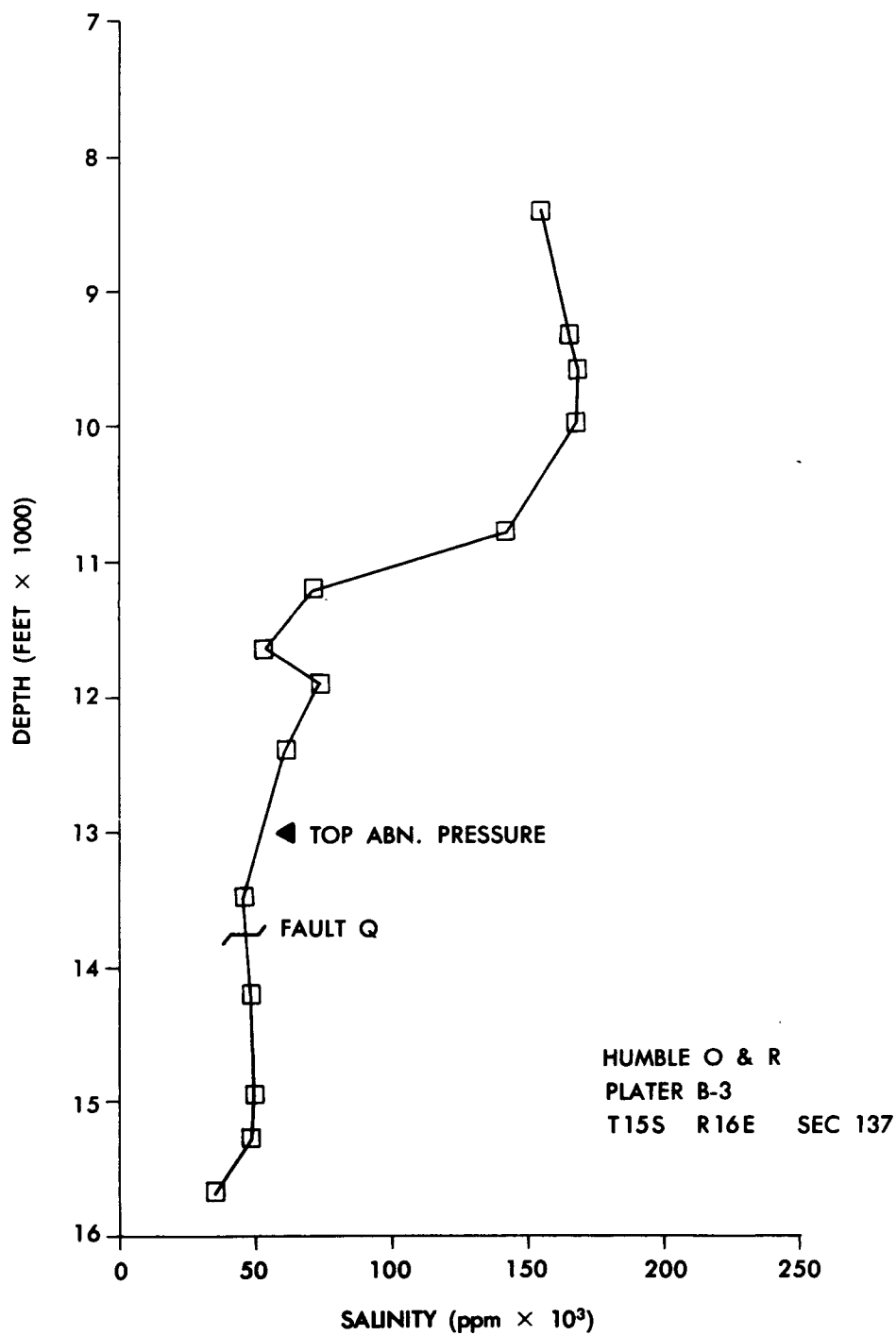


Fig. 17 - Typical sandstone salinity profile for a well in the study area. Note the abrupt change in salinity from approximately 50,000 ppm to 175,000 ppm between 11,700 to 10,500 feet. This change occurs above the top of the 'hard' abnormal pressure zone (.7 psi/ft) and may indicate diagenetic alteration of clays from smectite to illite.

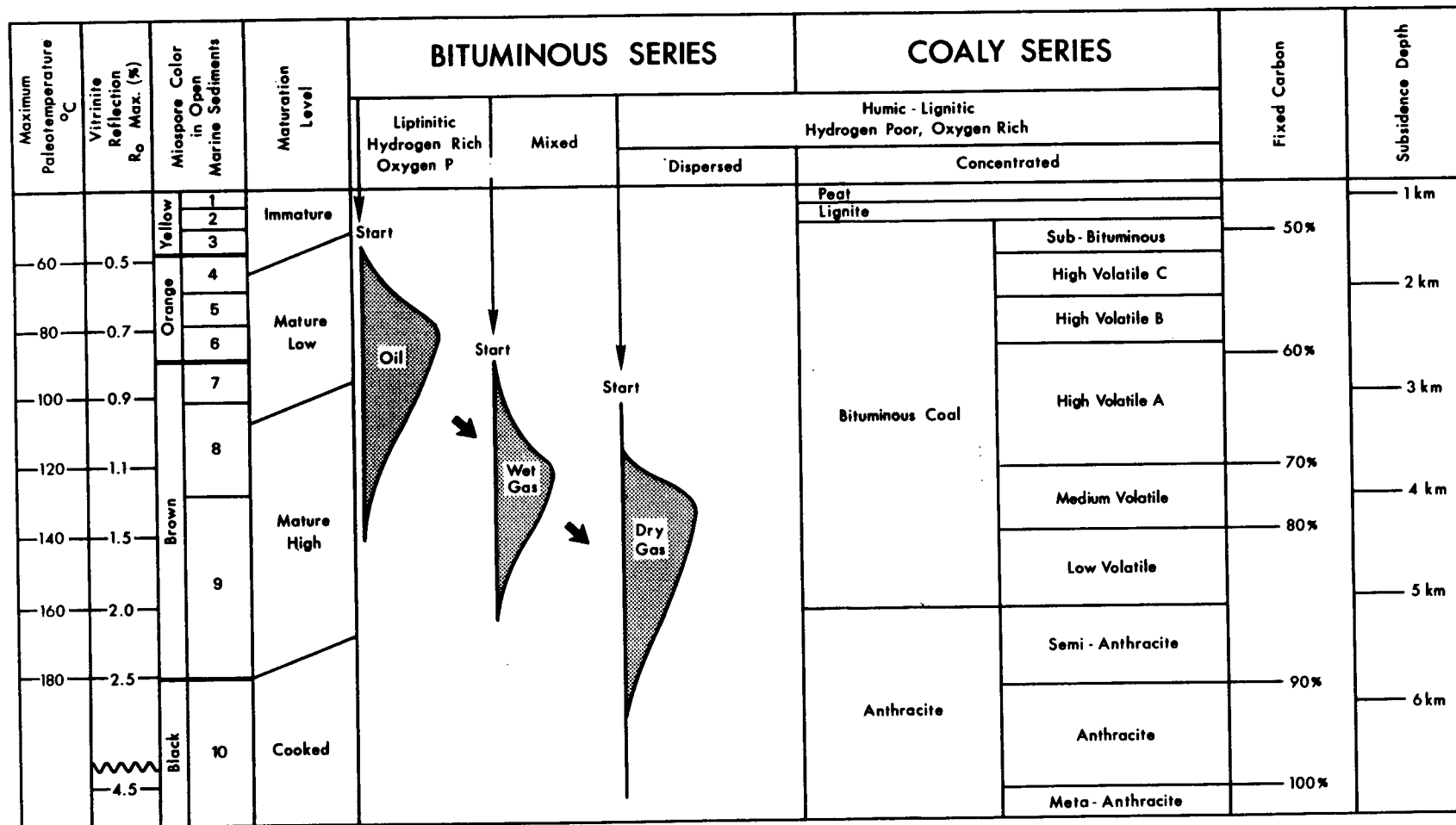


Fig. 18 - Hydrocarbon formation window as delineated by various maturation indices (after Hart, 1979).

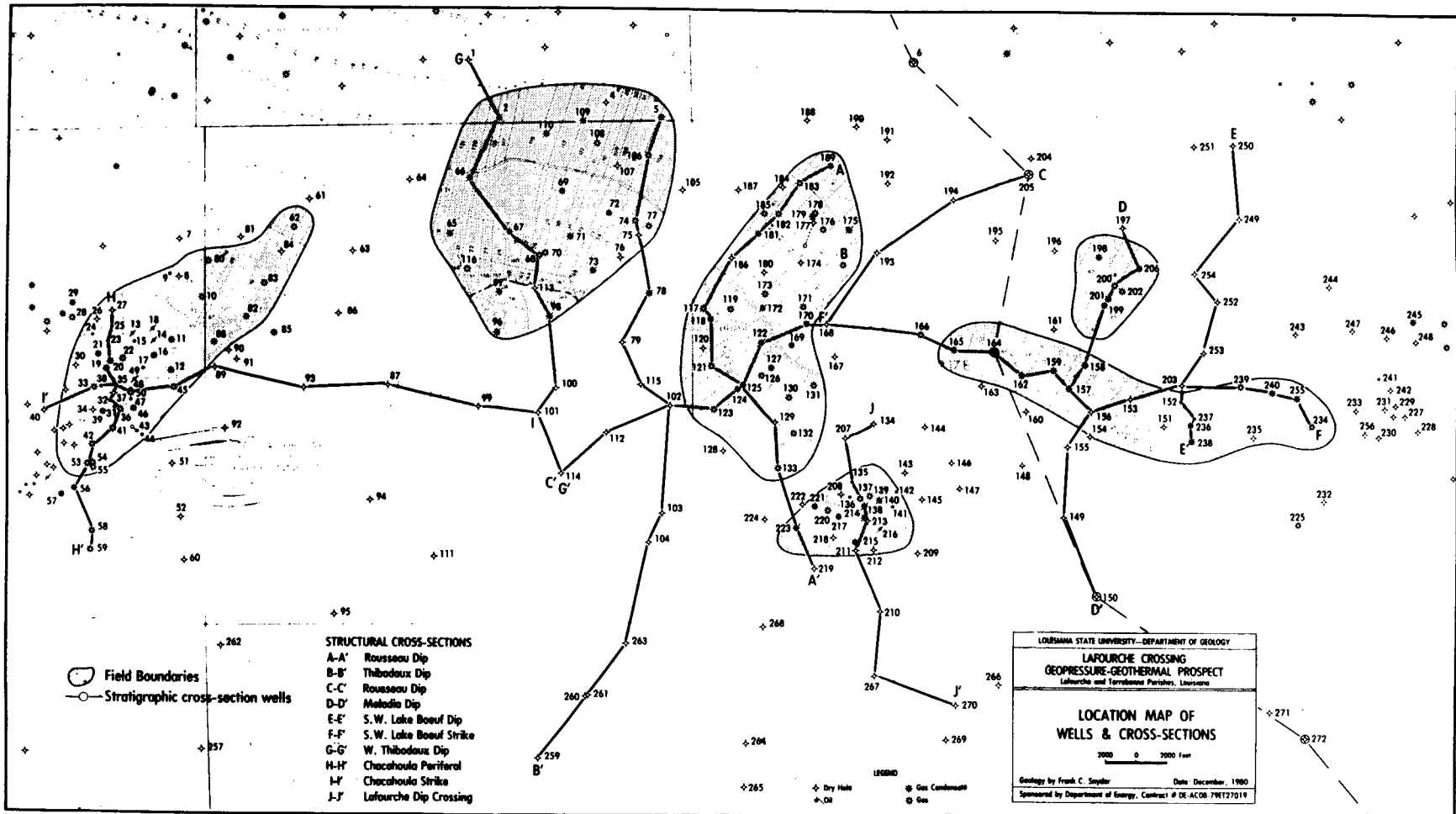
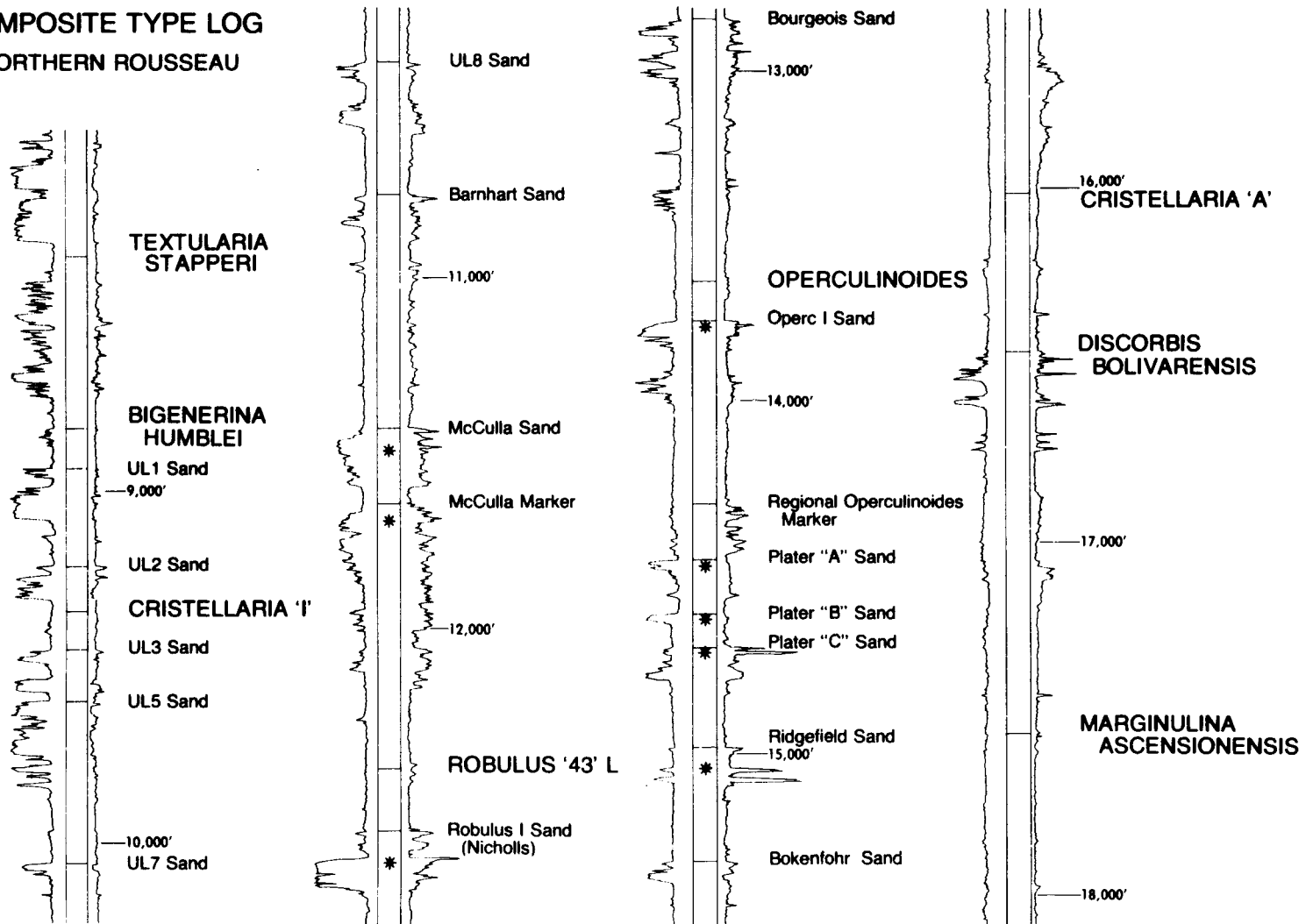


PLATE 1

**COMPOSITE TYPE LOG  
NORTHERN ROUSSEAU**

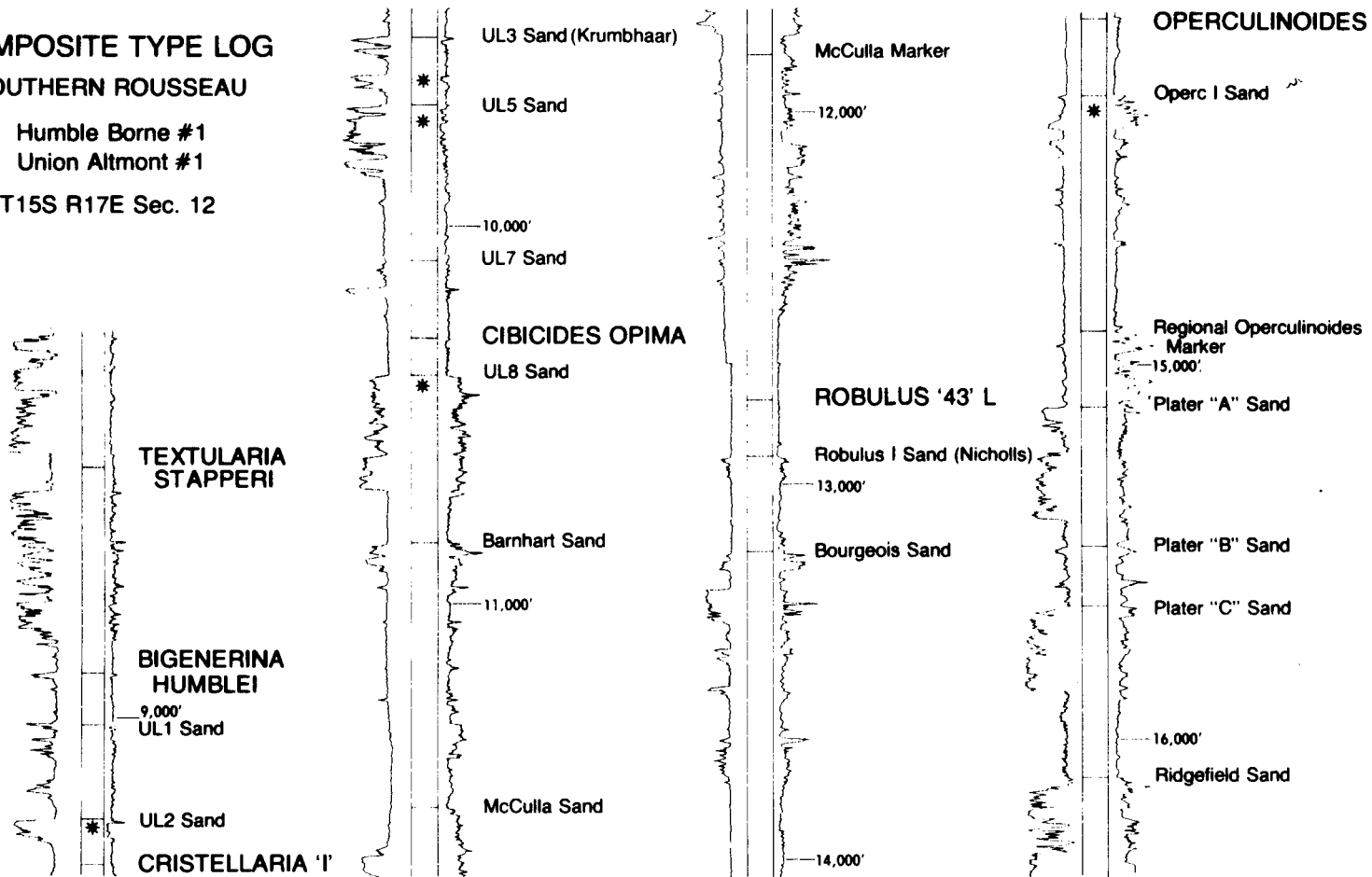


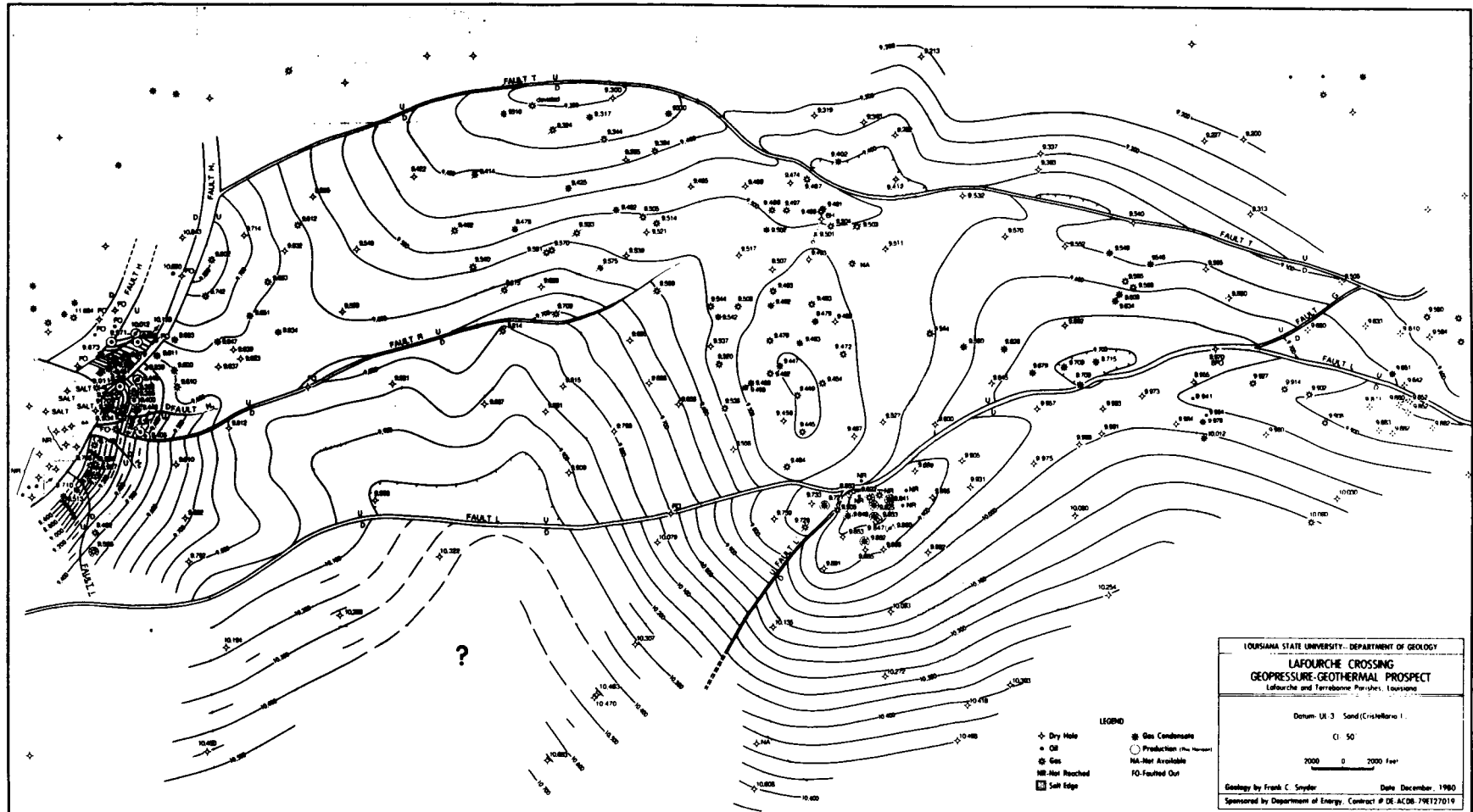
# COMPOSITE TYPE LOG

## SOUTHERN ROUSSEAU

Humble Borne #1  
Union Altmont #1

T15S R17E Sec. 12





LOUISIANA STATE UNIVERSITY - DEPARTMENT OF GEOLOGY

**LAFOURCHE CROSSING  
GEOPRESSURE-GEOTHERMAL PROSPECT**  
Lafourche and Terrebonne Parishes, Louisiana

Datum: U.S. Standard (Crestedmark I.)

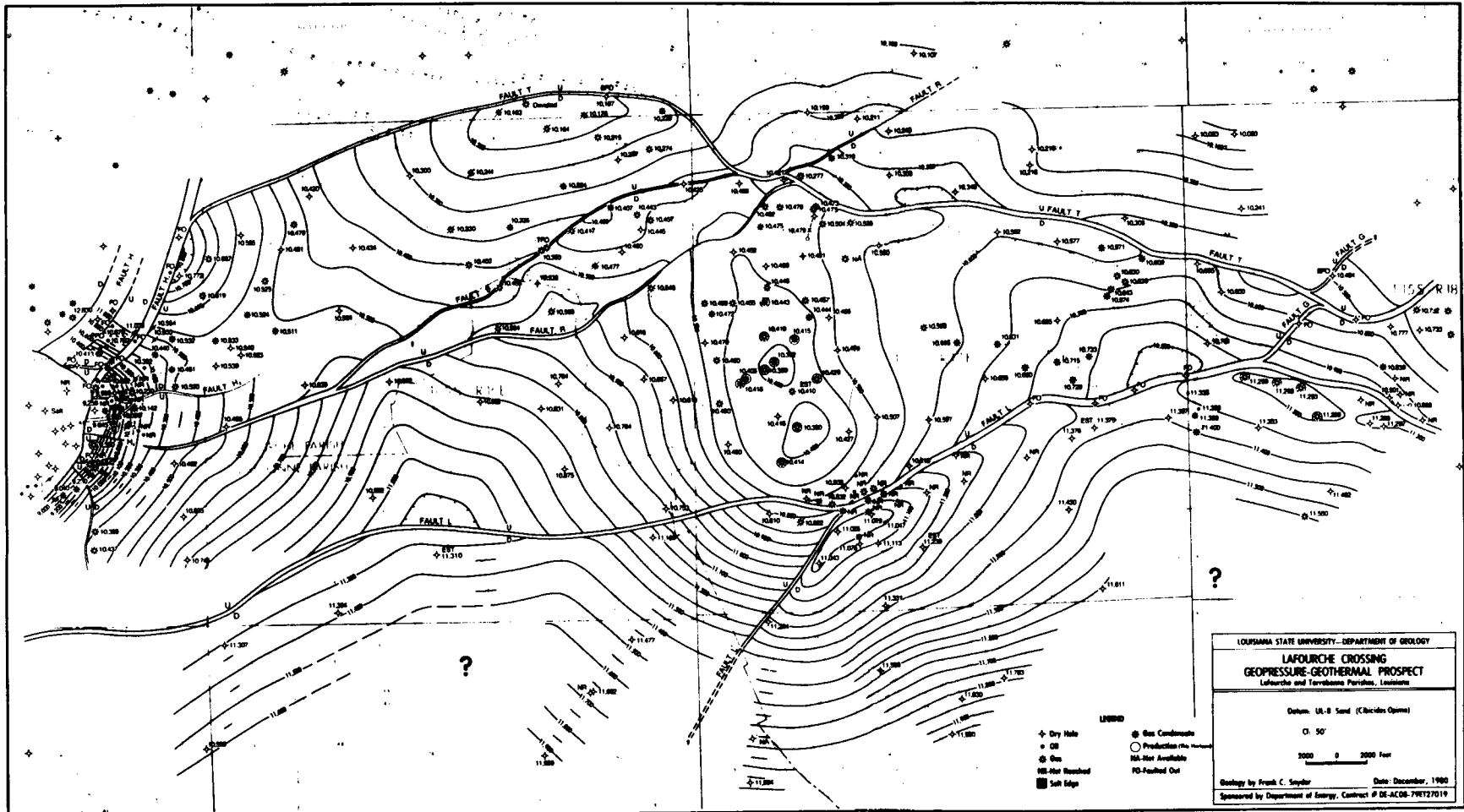
1:50

2000 0 2000 Feet

Geology by Frank C. Snyder Date December, 1980

Sponsored by Department of Energy, Contract # DE-AC06-79ET27019

PLATE 4



LOUISIANA STATE UNIVERSITY—DEPARTMENT OF GEOLOGY

**LAFOURCHE CROSSING  
GEOPRESSURE-GEOTHERMAL PROSPECT**  
Terrebonne and Iberville Parishes, Louisiana

Datum: US-B Sea Level (Circulus Optimus)  
CI: 50'  
0 2000 Feet

Geology by Frank C. Snyder Date: December, 1980  
Sponsored by Department of Energy, Contract # DE-AC08-79RT27019

PLATE 5

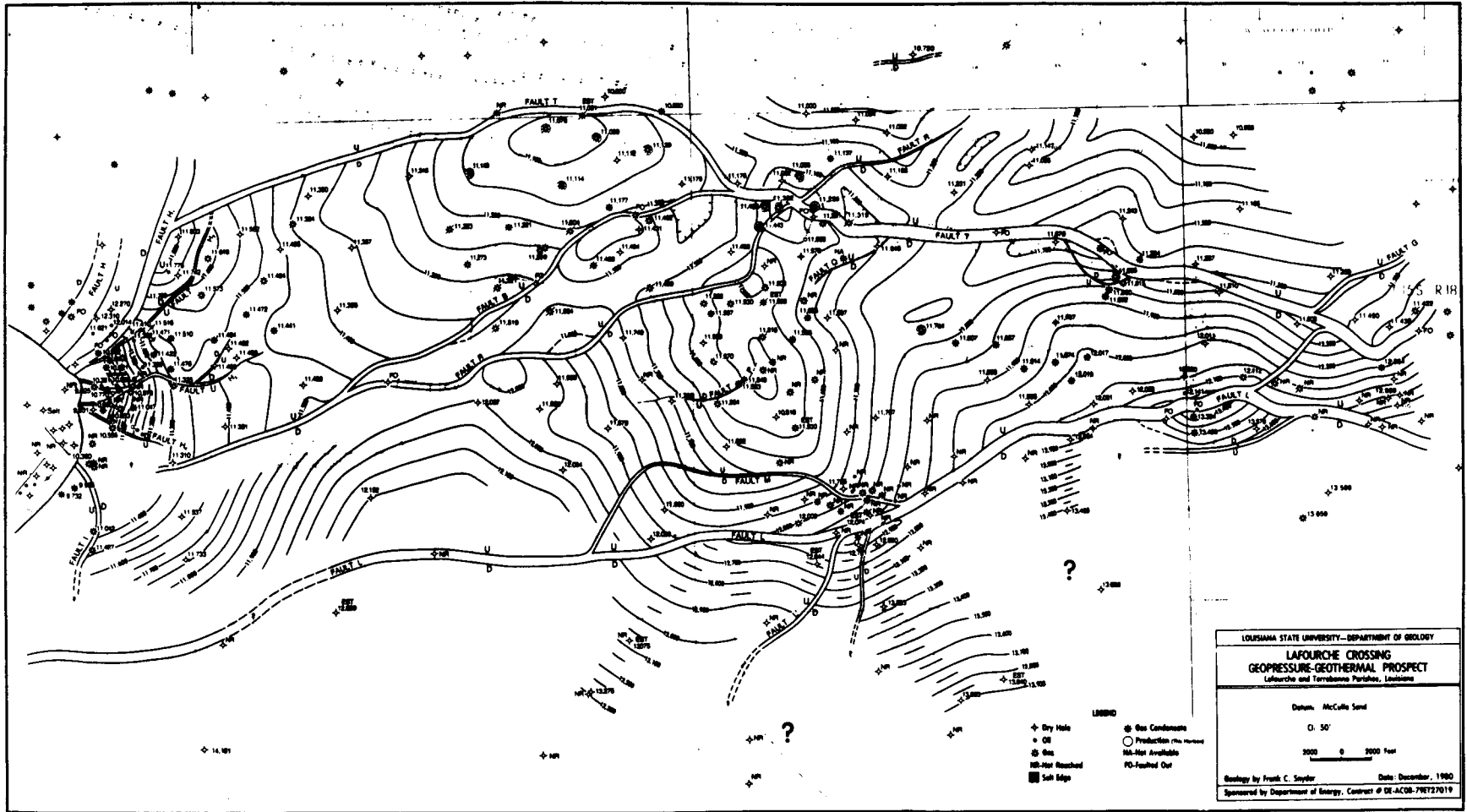


PLATE 6

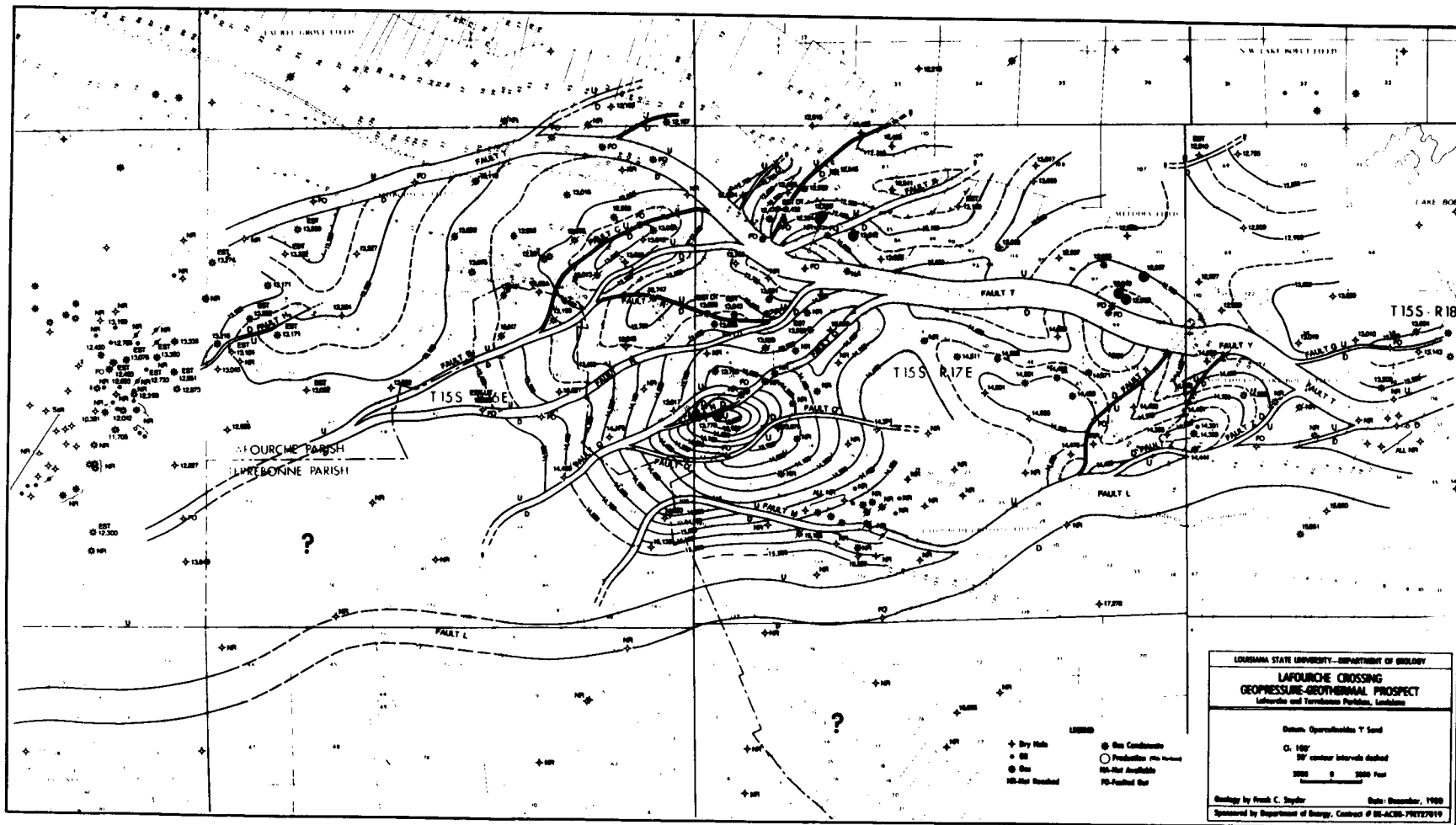
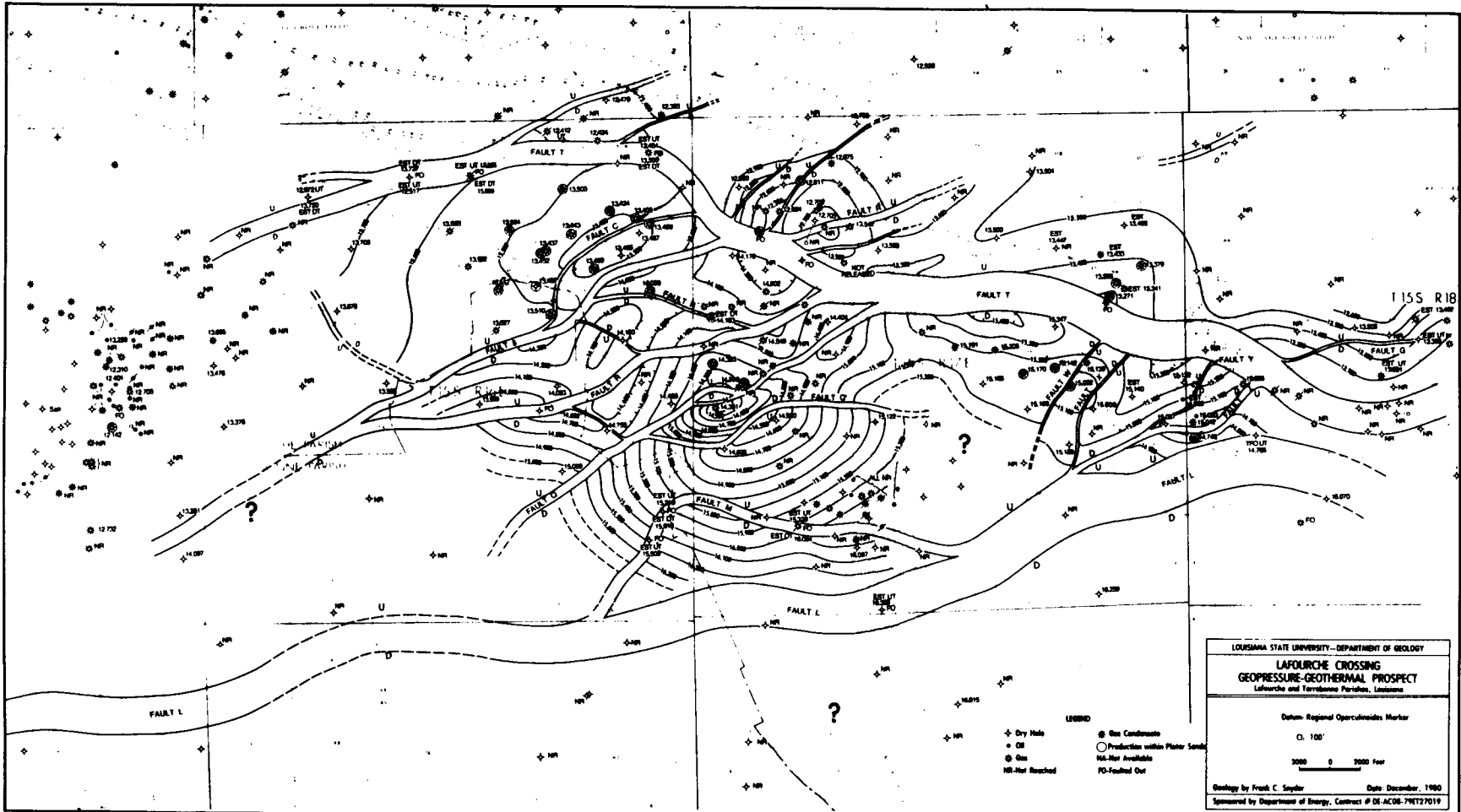


PLATE 7





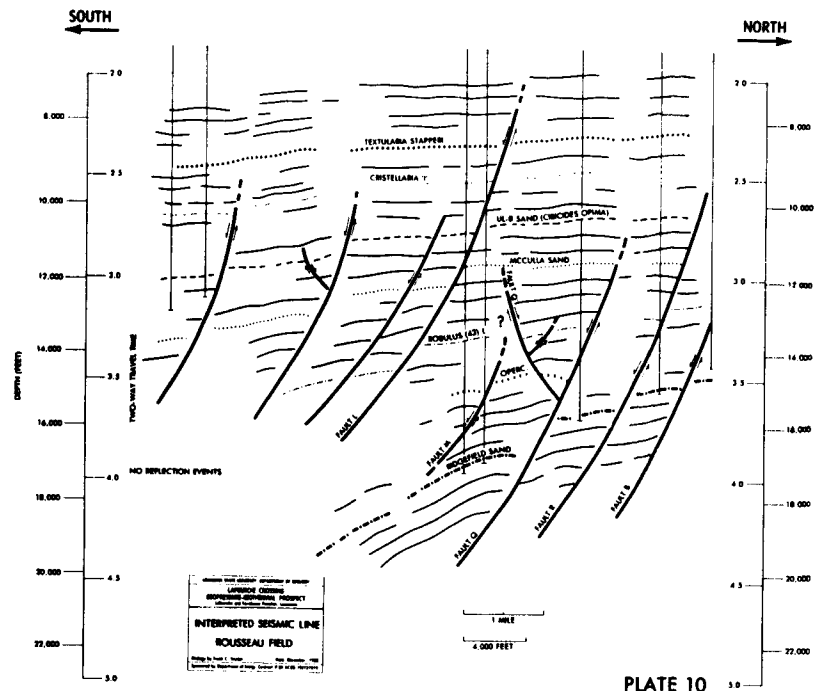


PLATE 10







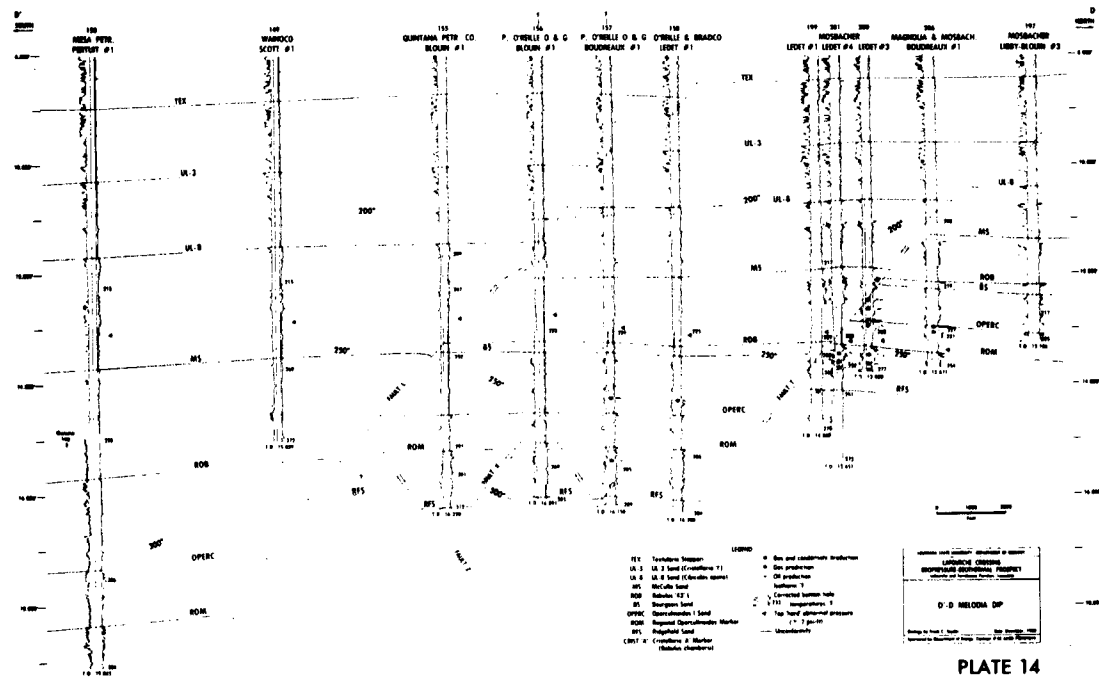
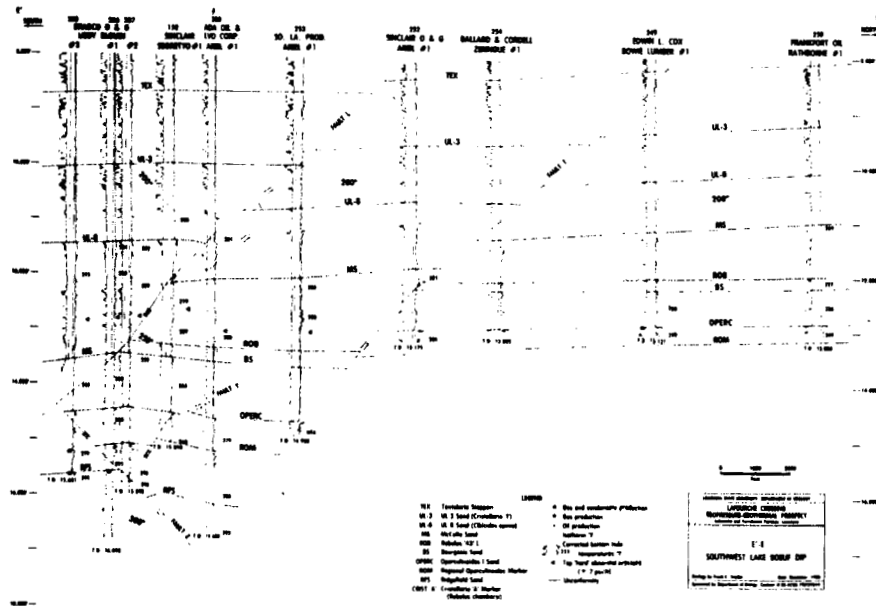


PLATE 14



- LEGEND**
- W-1 Conductor (Shallow)
  - W-2 W-3 Sand (Crescent #1)
  - W-3 W-4 Sand (Crescent #2)
  - W-4 W-5 Sand (Crescent #3)
  - W-5 W-6 Sand (Crescent #4)
  - W-6 W-7 Sand (Crescent #5)
  - W-7 W-8 Sand (Crescent #6)
  - W-8 W-9 Sand (Crescent #7)
  - W-9 W-10 Sand (Crescent #8)
  - W-10 W-11 Sand (Crescent #9)
  - W-11 W-12 Sand (Crescent #10)
  - W-12 W-13 Sand (Crescent #11)
  - W-13 W-14 Sand (Crescent #12)
  - W-14 W-15 Sand (Crescent #13)
  - W-15 W-16 Sand (Crescent #14)
  - W-16 W-17 Sand (Crescent #15)
  - W-17 W-18 Sand (Crescent #16)
  - W-18 W-19 Sand (Crescent #17)
  - W-19 W-20 Sand (Crescent #18)
  - W-20 W-21 Sand (Crescent #19)
  - W-21 W-22 Sand (Crescent #20)
  - W-22 W-23 Sand (Crescent #21)
  - W-23 W-24 Sand (Crescent #22)
  - W-24 W-25 Sand (Crescent #23)
  - W-25 W-26 Sand (Crescent #24)
  - W-26 W-27 Sand (Crescent #25)
  - W-27 W-28 Sand (Crescent #26)
  - W-28 W-29 Sand (Crescent #27)
  - W-29 W-30 Sand (Crescent #28)
  - W-30 W-31 Sand (Crescent #29)
  - W-31 W-32 Sand (Crescent #30)
  - W-32 W-33 Sand (Crescent #31)
  - W-33 W-34 Sand (Crescent #32)
  - W-34 W-35 Sand (Crescent #33)
  - W-35 W-36 Sand (Crescent #34)
  - W-36 W-37 Sand (Crescent #35)
  - W-37 W-38 Sand (Crescent #36)
  - W-38 W-39 Sand (Crescent #37)
  - W-39 W-40 Sand (Crescent #38)
  - W-40 W-41 Sand (Crescent #39)
  - W-41 W-42 Sand (Crescent #40)
  - W-42 W-43 Sand (Crescent #41)
  - W-43 W-44 Sand (Crescent #42)
  - W-44 W-45 Sand (Crescent #43)
  - W-45 W-46 Sand (Crescent #44)
  - W-46 W-47 Sand (Crescent #45)
  - W-47 W-48 Sand (Crescent #46)
  - W-48 W-49 Sand (Crescent #47)
  - W-49 W-50 Sand (Crescent #48)
  - W-50 W-51 Sand (Crescent #49)
  - W-51 W-52 Sand (Crescent #50)
  - W-52 W-53 Sand (Crescent #51)
  - W-53 W-54 Sand (Crescent #52)
  - W-54 W-55 Sand (Crescent #53)
  - W-55 W-56 Sand (Crescent #54)
  - W-56 W-57 Sand (Crescent #55)
  - W-57 W-58 Sand (Crescent #56)
  - W-58 W-59 Sand (Crescent #57)
  - W-59 W-60 Sand (Crescent #58)
  - W-60 W-61 Sand (Crescent #59)
  - W-61 W-62 Sand (Crescent #60)
  - W-62 W-63 Sand (Crescent #61)
  - W-63 W-64 Sand (Crescent #62)
  - W-64 W-65 Sand (Crescent #63)
  - W-65 W-66 Sand (Crescent #64)
  - W-66 W-67 Sand (Crescent #65)
  - W-67 W-68 Sand (Crescent #66)
  - W-68 W-69 Sand (Crescent #67)
  - W-69 W-70 Sand (Crescent #68)
  - W-70 W-71 Sand (Crescent #69)
  - W-71 W-72 Sand (Crescent #70)
  - W-72 W-73 Sand (Crescent #71)
  - W-73 W-74 Sand (Crescent #72)
  - W-74 W-75 Sand (Crescent #73)
  - W-75 W-76 Sand (Crescent #74)
  - W-76 W-77 Sand (Crescent #75)
  - W-77 W-78 Sand (Crescent #76)
  - W-78 W-79 Sand (Crescent #77)
  - W-79 W-80 Sand (Crescent #78)
  - W-80 W-81 Sand (Crescent #79)
  - W-81 W-82 Sand (Crescent #80)
  - W-82 W-83 Sand (Crescent #81)
  - W-83 W-84 Sand (Crescent #82)
  - W-84 W-85 Sand (Crescent #83)
  - W-85 W-86 Sand (Crescent #84)
  - W-86 W-87 Sand (Crescent #85)
  - W-87 W-88 Sand (Crescent #86)
  - W-88 W-89 Sand (Crescent #87)
  - W-89 W-90 Sand (Crescent #88)
  - W-90 W-91 Sand (Crescent #89)
  - W-91 W-92 Sand (Crescent #90)
  - W-92 W-93 Sand (Crescent #91)
  - W-93 W-94 Sand (Crescent #92)
  - W-94 W-95 Sand (Crescent #93)
  - W-95 W-96 Sand (Crescent #94)
  - W-96 W-97 Sand (Crescent #95)
  - W-97 W-98 Sand (Crescent #96)
  - W-98 W-99 Sand (Crescent #97)
  - W-99 W-100 Sand (Crescent #98)

SWITCHED TO SOUTHWEST CASE SOLE PIP

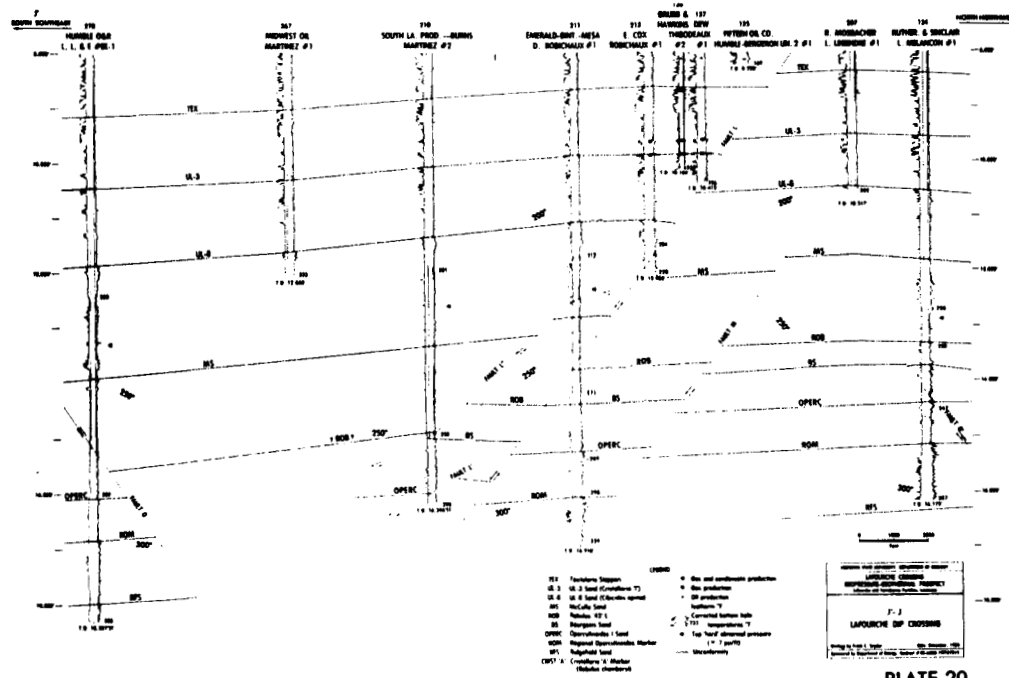
PLATE 15











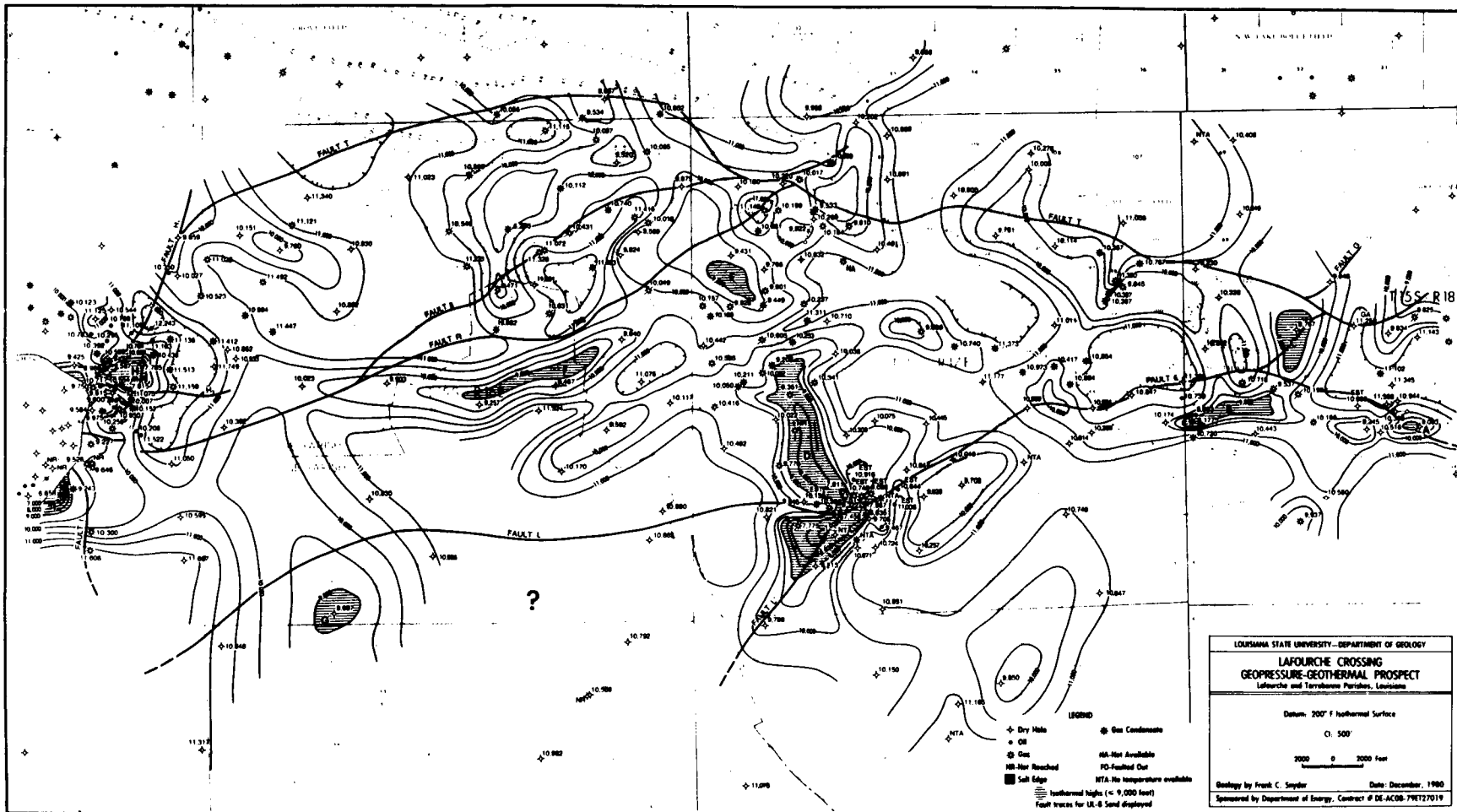
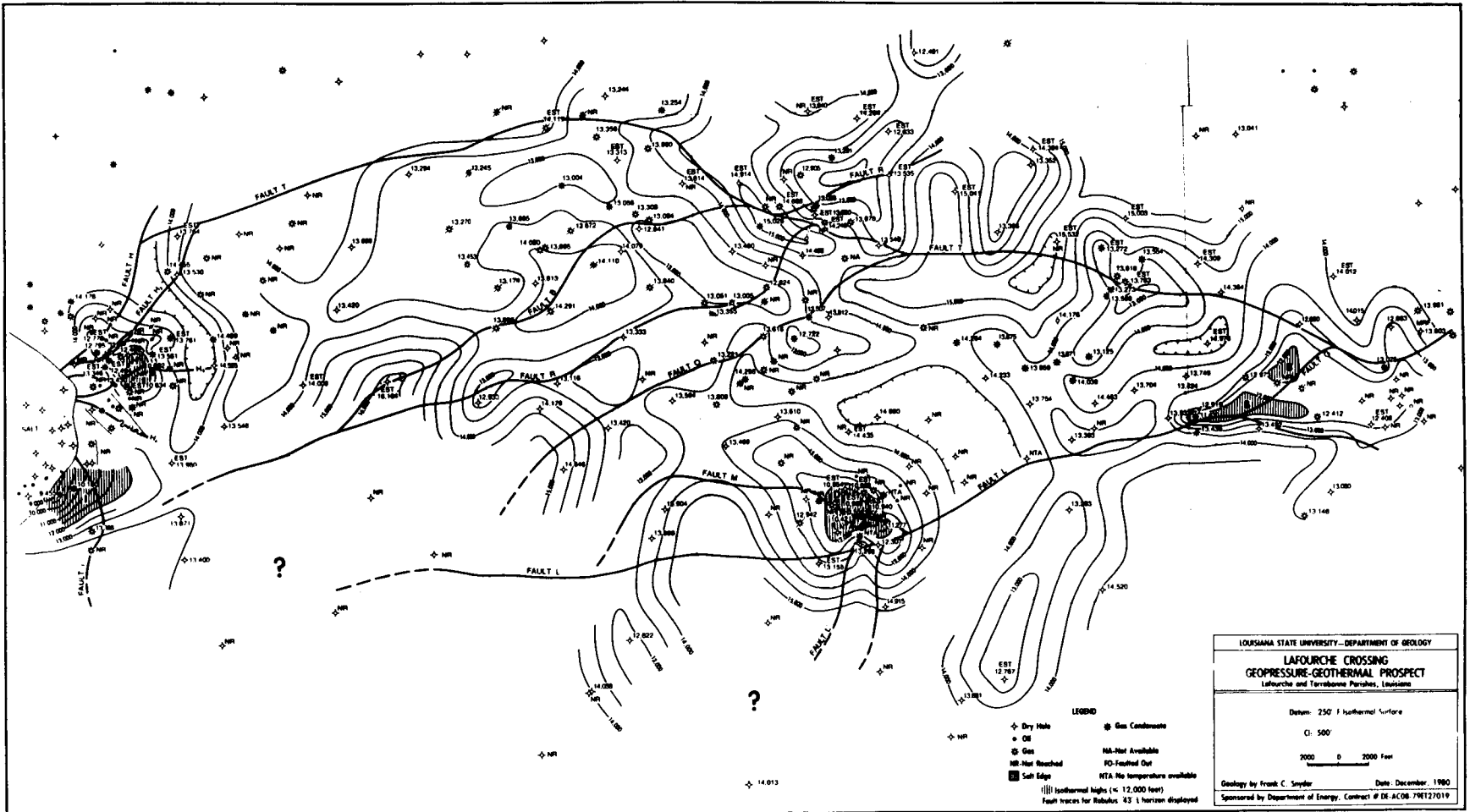


PLATE 21

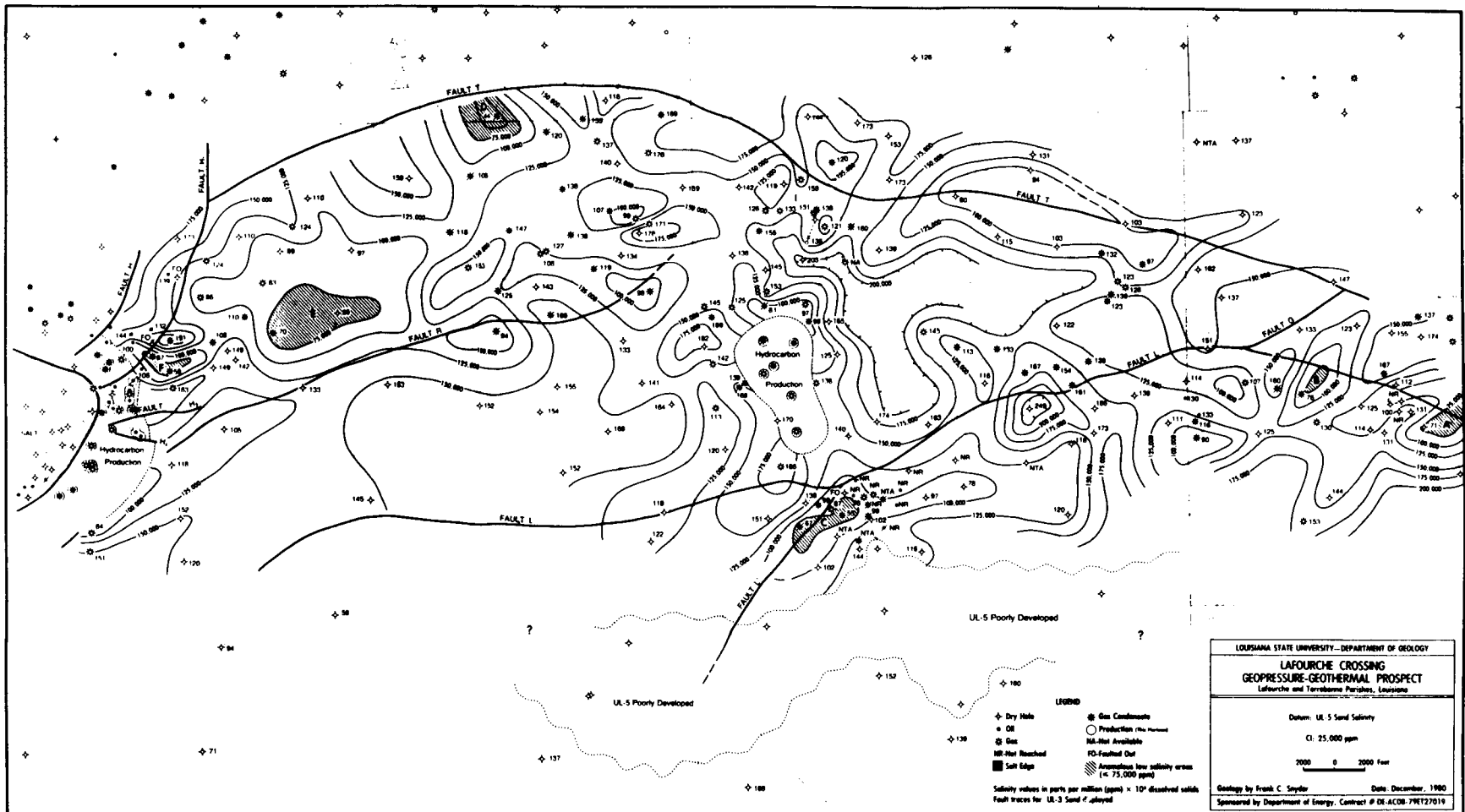


LOUISIANA STATE UNIVERSITY - DEPARTMENT OF GEOLOGY  
**LAFOURCHE CROSSING  
 GEOPRESSURE-GEOTHERMAL PROSPECT**  
 Lafourche and Terrebonne Parishes, Louisiana

Datum: 250 f isothermal surface  
 CI: 500  
 2000 0 2000 Feet

Geology by Frank C. Snyder Date: December, 1980  
 Sponsored by Department of Energy, Contract # DE-AC06-79ET27019

PLATE 22



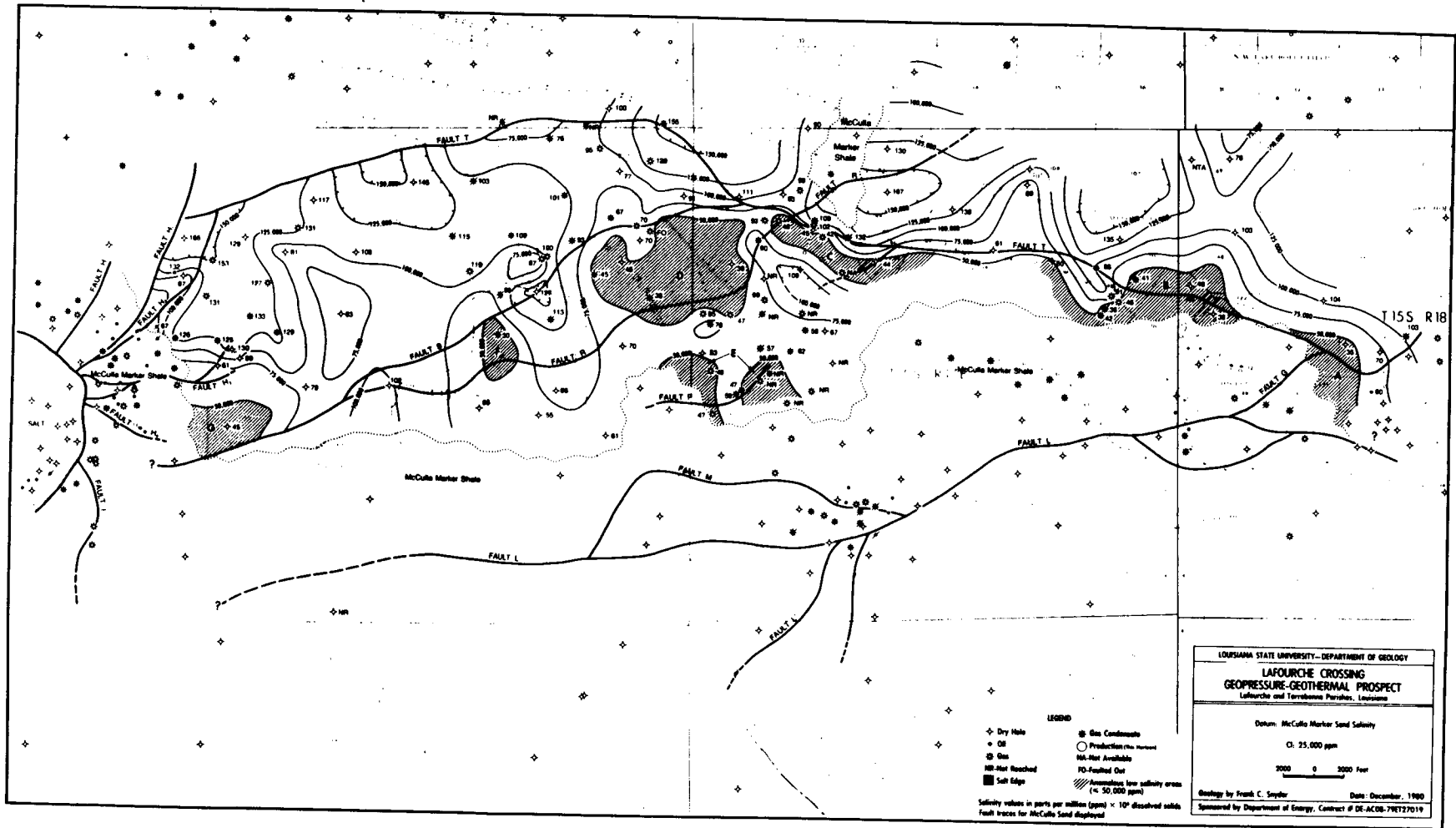


PLATE 24

69/78



APPENDIX A  
List of Wells

T14S,R16E

No.	Sec.	Operator	Lease	T.D.
1	37	McCulloch	Leche et al. #1	13,560
2	41	Davis Oil Co.	Caldwell et al #1	10,587
3	44	Pruet Pord. Co.	J. B. Levert Land #1	10,760dev
4	47	Pan-Am. Petr.	R. Hurd #1	14,405
5	90	Barnhart	C. Bourgeois #1	13,572

T14S,R17E

No.	Sec.	Operator	Lease	T.D.
275	6	Texas Pacific	Bowie Lumber 6 #1A	13,215
276	20	P. R. Bass	Laurel Valley Plant. #1	12,187
6	33	Aztec O & G	Laurel Valley #1	13,343

T15S,R15E

No.	Sec.	Operator	Lease	T.D.
7	42	Humble O & R	Rob 1 Sd. Un. 2 #1	13,000
8	43	Humble O & R	Mire #1	12,841
9	43	Birdwell & Brady	A. Guillot #1	12,784
10	45	Texas Gas Explor.	Chac. Gas Un. #2	12,777
11	56	The Texas Co.	R. B. Howell #1	13,444
12	56	The Texas Co.	R. B. Howell #2	12,930
13	56	Humble O & R	A. G. Frost et al. #1	13,225ST
14	56	Humble O & R	C. J. Coulon et al. #5	12,757
15	56	Humble O & R	C. J. Coulon et al. #6	12,750
16	56	Humble O & R	C. J. Coulon et al. #7	13,122
17	56	Humble O & R	C. J. Coulon et al. #8	12,543
18	56	Humble O & R	Humble Un. 9 #1	12,742
19	57	Humble O & R	Chac. Oil Un. 10 #1	22,717
20	57	Humble O & R	Adams st al. #3	12,717ST
21	57	Glasswell	Rogers #1	13,230
22	57	Humble O & R	Coulon #10	12,656
23	57	Humble O & R	C. Adams et al. B-1	13,360
24	57	Sun & Humble	Robers Un. Well #1	12,914ST
25	57	Humble O & R	Adams et al. Un. #1	13,314
26	57	Markley	Guillot #1	13,022
27	57	Humble O & R	A. G. Frost et at. B-1	13,133
28	57	Sun Oil	Levert Land A-1	13,714
29	57	Magna Oil Co.	Levert Lank C-1	16,214
30	57	Markley	Mire #1	11,414
31	66	Sun Oil Co.	Lyric Rlty. & Park. #1	11,131
32	66	Sun Oil Co.	Lyric Rlty. & Park. #2	10,213
33	66	Sun Oil Co.	Lyric Rlty. & Park. #5	11,133
34	66	Sun Oil Co.	Lyric Rlty. & Park. #6	12,005



35	66	Sun Oil Co.	Rob. 3 Sd. Un. 4 & #9	13,010
36	66	Sun Oil Co.	Rob. 3 Sd. 4 #9	13,010
37	66	Sun Oil Co.	Lyric Rlty. Park. #10	11,800
38	66	Sun Oil Co.	Lyric Rlty. & Park. #11	10,500
39	66	Sun Oil Co.	Lyric Rlty. & Park. #12	9,515
40	66	Sun Oil Co.	Lyric Drexler #1	12,000
41	66	Pure Oil Co.	Pure Fee #1	12,642
42	66	Union Oil Co.	Lyric Rlty. Park. #1	9,705
43	67	Sun Oil Co.	Lyric Tlty. & Park. #3	
9,699ST				
44	67	Sun Oil Co.	Lyric RLty. & Park. #4	9,707
45	67	Sun Oil Co.	Lyric Rlty. & Park. #8	12,873
46	67	Humble O & R	C. J. Coulon #1	11,409
47	67	Humble O & R	C. J. Coulon #2	10,519
48	67	Humble O & R	C. J. Coulon #3	10,045
49	67	Humble O & R	C. J. Coulon #4	9,669
50	67	Humble O & R	C. J. Coulon #9	13,100
51	68	Sun Oil Co.	Polmer #2	13,030
52	68	Union Oil Co.	Ducros Plantation #1	15,040
53	69	Union Oil Co.	Pure Fee #2	10,300
54	69	Pure Oil Co.	Pure Fee #2	9,128
55	69	Magna Oil	Pure Oil #3	9,940
56	69	Sun Oil Co.	J. L. Pool #1	10,442
57	69	Sun Oil Co.	O. J. Mire et al. #1	10,025
58	69	Magna Oil	Pure Oil Fee #1	14,050
59	78	Sun Oil Co.	Dibert C-1	11,514
60	79	Sun Oil Co.	Polmer #1	14,750ST
T15S,R16E				
No.	Sec.	Operator	Lease	T.D.
61	9	Howell, Hol.& How.	Energy Rlty. B-2	13,095
62	9	Howell, Hol.& How.	Energy Rlty. B-1	13,068
63	14	Howell, Hol.& How.	Tregre #1	14,566
64	16	Stanolind O & G	Knight #1	14,300
65	20	Stanolind O & G	Ridgefield #1	12,535
66	21	Stanolind O & G	Nicholls #11	
4,250ST				
67	25	Pan-Am Petr. Co.	Ridgefield Sd. Un. 2, #1	14,500
68	29	Humble O & R	Ridgefield Sd. Un. 4, #1	14,350ST
69	30	Stanolind O & G	Ridgefield St. Un. 3, #1	14,552
70	30	Pan-Am. Petr. Co.	Plater B SU C:McCulla #1	13,800
71	31&32	Humble O & R	Plater #3	15,800
72	34	Pan-Am. Petr. Co.	Plater A SU C:Plater #1	13,880
73	35	Humble O & R	Plater #1	14,880
74	36	Humble O & R	Plater #2	14,275
75	36	Humble O & R	Plater #5	14,095
76	36	E. L. Cox	Plater #1	14,292
77	37	Humble O & R	Plater #4	14,242
78	39	Humble O & R	Ridgefield Sd. GU 8-1	15,250
79	42	Sick & Mott	Plater #1	15,020
80	47	Texas Gas Expl. Co.	Chaco. GU #1	12,806
81	48	Texas Gas Expl. Co.	DeGravelles #1	12,800
82	50	Howell, Hol.& How.	Energy Rlty. #4	12,720
83	50	Howell, Hol.& How.	Energy Rlty. #5	12,703

84	50	Howell, Hol.& How.	Energy Rlty. #6	12,945
85	55	Howell, Hol.& How.	Energy Rlty. #2	12,717

86	58	Stanolind O & G	M. Tegre #1	14,836
87	61	Pan-Am. Petr. Co.	H. R. Aaron #1	14,436
88	65	Howell, Hol.& How.	Energy Rlty. E1	14,148
89	65	Howell. Hol.& How.	Energy Rlty. #3	15,944ST
90	65	Nortcott Expl&Czar	Energy Rlty. #1	12,700
91	65	Spooner Petr. Co.	Energy Rlty. #1	12,663
92	66	Am. Quasar Petr.	Energy Rlty. #1	14,522
93	67	Geol-Geoph. Assoc.	F. LeJune #1	13,050
94	70	Howell, Hol.& How.	Diebert, Stark, & Brown #1	13,328
95	74	Birthright Oil Co.	A. Eustis #1	12,405
96	77	Placid Oil Co.	H. Daigle Un. B-1	14,473
97	78	Placid Oil Co.	Roth #1	14,700
98	79	Placid Oil Co.	E. Boudreaux #1	14,464
99	81	Wainoco	Polmer #1	15,114
100	93	Patrick Petr. Co.	Plomer Bros. E1	15,068
101	93	Placid Oil Co.	Ducros Plantation	15,500
102	96	Humble O & RR.	C. Plater B-1	16,100
103	101	H. L. Hunt	R. C. Plater #1	16,814ST
104	101	Fla. Gas Expl.	H. Bernard #1	17,126ST
105	105	Pan-Am. Patr. Co.	Laurel Valley Plant. #1	12,500
106	106	Paul Barnhart	Bokenfohr SU 2, #1	14,700
107	108	NFC Petr. Co.	E. Nicholls Gas SU 1	12,500
108	111	Paul Barnhart	J. Bokenfohr A-1	13,384
109	112	Paul Barnhart	Barnhart Sand Comb Un #1	10,645
110	115	Paul Barnhart	J. Levert #1	13,028
111	131	Lea Expl. Inc.	E. Corbin #1	11,100
112	137	Humble O & R	Plater B #3	15,900
113	141	Placid Oil Co.	Ridgefield; Williams #1A	14,350ST
114	143	Exchange O & G	Polmer Bros. #1	16,300
115	152	C. Glasscock	R. Plater #1	11,010
116	155	Placid Oil Co.	Ridgefield #1	14,479ST

## T15S,R17E

No.	Sec.	Operator	Lease	T.D.
117	6	Bradco O & G	A. Boudreaux #1	13,440
118	7	Humble O & R	J. Aucoin #1	15,800
119	7	Bradco O & G	C. Toups #1	13,436
120	7	Pure Oil Co.	Bouterie #1	12,105
121	9	Bradco O & G	Richard #1	15,630
122	10	Cox & Anache Oil	N. Verdin #1	15,184
123	11	Alliance Expl. Co.	D. Robichaux #1	15,945
124	11	Humble O & R	D. Robichaux #1	11,911
125	11	Humble O & R	D. Robichaux #2	16,050
126	11	Humble O & R	Lefort A-2	10,600
127	11	Humble O & R(Hunt)	Rousseau Un. 2, #1	10,500
128	12	Union Oil Co.	Altmont #1	16,148
129	12	Humble O & R	Borne #1	16,000
130	12	Humble O & R	Borne #2	9,800
131	13	Humble O & R	Rousseau GU 1, #1	10,560
132	13	Humble O & S	B. Teriot #1	11,501
133	13	Callery Inc.	E. Bouvier #1; UL-8 SU #4	10,584
134	16	Ruther, & Sinclair	L. Melancon #1	16,175
135	16	Fifteen Oil Co.	Humble-Bergeron Un2, #1	8,220

136	16	Fifteen Oil Co.	Humble-Bergeron #1	8,225
137	16	Drew O & G	J. Thibodeaux #1	10,415
138	17	Grubb & Hawkins	Thibodeaux #2	10,184
139	17	Carter-Stern	Thibodeaux #1	8,154
140	17	Mikton Oil Co.	Ledet #1	10,347
141	17	Mikton & Mosbacher	Boudreaux-Thibodeaux #1	8,214
142	17	Mikton Oil Co.	Boudreaux #2	8,140
143	16	McClain Forman	L. Boudreaux #1	10,705
144	19	Sohio Petr.	Lafourche GU 1, #1	10,926
145	20	Humble O & R	Lafourche GU 1	10,504
146	22	Callery	J. Bourgeois #1	10,225
147	23	Birdwell & Brady	J. Bourgeois #1	10,528
148	25	Stick.-Hawk&Signal	Lagrade #1	10,302
149	30	Wainoco	Scott #1	15,039
150	32	Mesa Petr. Co.	L. Pertuit #1	19,045
151	38	P Oreille U Mosbach	E. Zeringue #1	
5,875ST				
152	38	Sinclair O & G	Salvadore SEgratto #1	15,010
153	42	Mosbach.-Hurt&Benin	H. Templet #1	14,727
154	43	R. Mosbacher	A. Lorio #1	10,823
155	44	Quintana Petr. Co.	J. Blouin #1	6,220
156	45	Pend Oreille O & G	J. Blouin #1	16,091
157	45	Pend Oreille O & G	Boudreaux #1	16,150
158	45	P. Oreille & Bradco	E. Ledet #1	16,300
159	46	P. Oreille & Bradco	P. Zeringue #1	16,232ST
160	47	R. Mosbacher	Ledet #2	15,530
161	47	Enterprise Oil Co.	L. Richard #1	16,010
162	48	Pend Oreille O & G	St. Charles Cath. Ch. #1	16,231
163	49	Forman Expl. Co.	Libby & Blouin #1	16,305
164	49	R. L. Burns Co.	Libby & Blouin #1	16,020
165	51	R. L. Burns Co.	Laurel Valley Plant. #1	16,055
166	54	Entex Inc.	L. Devillier #1	12,470
167	57	Hassie Hunt Trust	E. Bouvier #1	10,563
168	58	Goldking Prod. Co.	E. Binnings #1	14,840
169	59	Hassie Hunt Trust	E. Binnings #1	12,869
170	59	Hassie Hunt Trust	Marcello #1	13,202
171	60	H. Brown	Marcello	10,510
172	61	Hassie Hunt Trust	M. Moore #1	10,880
173	61	Bintliff & McCormic	Billello #1	14,850
174	61	Hassie Hunt Trust	Billelle-Martinez #1	16,514
175	61	Solio Petr. Co.	M. Moore #1	14,400
176	62	Alliance Expl. Co.	Caudet #1	12,715
177	62	McMoran Expl. Co.	P. Martinez #1	12,800dev
178	62	Sohio Petr. Co.	D. Martinez #1	13,672
179	62	Alliance Expl. Co.	Martinez #1	13,505
180	62	Emerald Petr. Co.	P. Martinez #1	10,600
181	64	Hassie Hunt Trust	Verdin Parro Unl; #1-A	14,618
182	64	Hassie Hunt Trust	T. Verdin #1	12,693
183	64	Sohio Petr. Co.	T. Verdin #2	13,524
184	65	Birthright Oil Co.	R Parro #1	12,587
185	65	Alliance Expl. Co.	R. Parr #1	12,564
186	65	Hassie Hunt Trust	R. Parro #1	15,415
187	69	Hassie Hunt Trust	A. Angellette Unl; #1	13,802

188	78	Sohio Petr. Co.	B. Marcello #1	12,750
189	81	Circle Drilling Co.	Verdin #1; Un. #1	13,675

190	81	Solatex Petr. Co.	E. Verdin #1	13,450
191	83	Kelsey Petr. Co.	Martinez #1	12,600
192	84	J. M. Huber Co.	Billello #1	12,742
193	86	Bradco O & G	Binnings #1	14,841
194	89	Pacer O & G	Blanchard #1	13,060
195	94	Anson Corp.	Libby-Blouin #1A	14,700
196	95	Mobil & Mosbacher	Libby-Blouin #2	13,092
197	97	R. Mosbacher	Libby-Blouin #3	13,106
198	97	Mosbach & Continen	Libby-Blouin #1	13,048ST
199	98	R. Mosbacher	L. Ledet #1	14,860
200	98	R. Mosbacher	L. Ledet #3	13,830
201	98	R. Mosbacher	L. Ledet #4	15,451
202	99	R. Mosbacher	A. Boudreaux #2	13,060
203	106	Ada Oil & LVO Co.	Ariel #1	16,600
204	108	Solotex Petr. Co.	Laurel Valley Plant. #1	13,185
205	108	Edwin Cox	Laurel Valley Plant. #1	13,210
206	108	Sick & Mott	Laurel Valley PLant. #1	14,316
207	111	Magnolia & MOsbach.	A. Boudreaux #1	13,671
208	116	R. Mosbacher	L. Legendre #1	10,517
209	116	Graubb & Hawkins	Gaubert #1	12,055
210	127	Texaw Pacific C & O	L. Martinez #3	10,820
211	129	South La.Prol-Burns	L. Martinez #2	16,346ST
212	132	Emerald-Bint.-Mesa	D. Robichaux #1	16,910
213	132	Phillips Petr. Co.	Martinez #1	14,258
214	132	Edwin Cox	D. Robichaux #1	12,035
215	132	Mikton Oil Co.	Martinez #1	10,511
216	132	Mikton Oil Co.	Martinez #2	11,000
217	132	Mikton Oil Co.	Martinez #4	11,472ST
218	133	Mikton Oil Co.	Martinez #5	10,707
219	133	Mikton Oil Co.	Martinez #3	10,160
220	134	Offshore Expl.	D. Robicheaux #1	12,207
221	134	Goldking Prol.	D. Robicheaux #1	10,571
222	135	Goldking Prod.	L. Martinez #1	10,156
223	135	Texas Pacific C&O	L. Martinez #2	10,520
224	135	Texas Pacific C&O	L. Martinez #1	17,200
225	136	Mikton Oil Co.	Martinez #6	11,080

## T15S,R18E

No.	Sec.	Operator	Lease	T.D.
226	3	Watson	A. Theriot #1	18,529
227	32	McMoran Expl.	T. B. Ayo #1	16,118
228	36	Southern Prod.	Godchaux Sugars #1	11,494
228	26	Bruner	Godchaux Sugars #1	10,012ST
229	36	Southern Prod.	Godchaux Sugars #3	10,354
230	37	Pioneer O & G	Gulf States Land #1	9,969
231	37	Southern Prod	Godchaux Sugars #4	11,632
232	38	Miss. River Fuel	Gulf States Land	13,700ST
233	39	Franks Petr.	Peltier Farms #1	16,891
234	39	Southern Prod.	Peltier Farms #1	10,289
235	41	Emerald Petr.	A. Foret #1	12,529
236	44	Bradco O & G	R. Knobloch #1	16,440ST
237	46	Bradco O & G	Libby & Blouin #1	16,893
238	46	Bradco O & G	Libby & Blouin #2	15,850

239	46	Bradco O & G	Libby & Blouin #3	15,651
240	48	Coastal States	Libby & Blouin #1	16,650
241	49	Davis Oil	Libby & Blouin #1	11,604
242	50	Miss. River Fuel	Gulf States Land #2	13,455
243	50	Southern Prod.	Godchaux Sugars #2	10,013
244	58	Lacal Petr & Cyprus	Libby & Blouin	13,239ST
245	58	Calco	Libby & Blouin #1	13,200
246	59	Texaco	Gulf States Land #1	13,154
247	59	Pan-Amer. Oil	Gulf States Land #1	13,250
248	59	General Amer. Oil	Gulf States Land #1	15,030
249	59	Miss. River Fuel	Gulf States Land #1	14,171
250	68	Cox	Bowie Lumber Co. #1	13,121
251	69	Frankfort Oil	J. Rathborne #1	13,020
252	69	Gulf	Bowie Lumber Co. 1-B	12,512
253	79	Sinclair O & G	Ariel #1	13,175
254	106	So. La. Prod.	Ariel #1	14,920
255	110	Ballard & Cordell	Zeringue Estate #1	13,085
256	177	Davis Oil Co.	Knobloch #1	11,600
257	199	Emerald Petr.	Gulf States Lank #1	11,450

## T16S,R15E

No.	Sec.	Operator	Lease	T.D.
-----	------	----------	-------	------

258	71	Kern Land Co.	E. W. Brown et at. #1	16,463
-----	----	---------------	-----------------------	--------

## T16S,R16E

No.	Sec.	Operator	Lease	T.D.
-----	------	----------	-------	------

259	5	Placid Oil Co.	R. Robichaux #1	15,503
260	9	Caroline Hunt Sands	Caldwell #1	12,081
261	9	Bering Oil Co.	W. Land #1	10,522
262	9	Placid Oil Co.	Prentice O & G	18,682
263	46	Eason Oil Co.	C. B. Pennington #1	11,720
264	77	Andar Oil Co.	R. C. Plater #1	12,524

## T16S,R17E

No.	Sec.	Operator	Lease	T.D.
-----	------	----------	-------	------

265	4	Pengo Petr.	R. Robichaux #1	12,500
266	6	Texaco	P. Prejean #1	12,788
267	72	Austral Oil	E. Kahn	12,531
268	73	Midwest Oil	Martinez #1	12,040
269	75	McCormick O & G	D. Robichaux #1	11,525
270	77	La. Prospect Co.	L, L, U E #A-1	12,513
271	77	Humble O & R	L, L, & #EE-1	18,327ST

## T16,R18E

No.	Sec.	Operator	Lease	T.D.
-----	------	----------	-------	------

272	8	Forest Oil Co.	Waterford #1	13,535
273	8	Forest Oil Co.	Waterford #2	18,092
274	28	Amerada Petr.	Waterford #3	16,300

## T17S,R18E

No.	Sec.	Operator	Lease	T.D.
-----	------	----------	-------	------

275 37

Cit. Ser & Forest Guidry 7-p3

17,275

APPENDIX B  
EVALUATION OF A SHALE-RESISTIVITY METHOD  
OF PRESSURE DETERMINATION

Using one inch SP-resistivity electric logs, short-normal resistivity measurements taken in clean shales (20' minimum thicknesses) were plotted against the log depths for various wells in Rousseau and Thibodaux fields. Comparison of these plots were made between very closely spaced wells and between original hole and side track log runs for the same wells. These plots (Fig. B-1 to B-3) show good similarity between the overall trend of shale resistivity and depth, but differ significantly in the actual measured resistivity values for specific depth-stratigraphic shale intervals. Variations of as much as .40 Ohms meter square per meter (OHM-M/M) were observed in the Humble Ridgefield Unit 4 and Pan American Plater 'B' wells in Thibodaux field (Fig. B-2. Further, the difference between the resistivity values for specific depth-stratigraphic intervals does not remain constant with depth as can be seen in Fig. B-1.

Variations in the observed shale resistivities may be due to several factors. First, minor lithologic changes between the bore holes such as porosity, cementation, clay composition, and fluid content may give different resistivities in the same stratigraphic interval. By using closely spaced drill holes for comparisons it was hoped to minimize these effects. Second, changes in the shale fluid composition and/or pressures between the time the two holes were drilled may have an effect (Fertl and Timko, 1971). Of the wells compared, only the Placid Ridgefield #1 side tracked original hole (Fig. B-3) show no significant changes in measured shale resistivity for correlative horizons. These two holes were both drilled in the Fall of 1956 whereas all the other

holes compared were drilled several years apart. Pressure and fluid changes observed in the later wells may have been brought about by production of hydrocarbons from the first well drilled. Third, differences in measured shale resistivities may be affected by the conditions in the drill hole during logging operations. The primary factors, applicable to shale intervals, would be the type of drilling mud in the hole, hole size, and bed thickness (Hammack and Fertl, 1974). After correction for temperature, significant differences in mud resistivities existed between holes used for comparison. An exception was Placid Williams #1 and Pan Am Williams #1 (Fig. B-3) which had mud resistivities of .90 OHM-M/M and .86 OHM-M/M at 75°F respectively. It is not clear whether hole conditions or fluid-pressure changes are the main causes of differences in measured shale resistivity. Detailed analysis is needed for more clarification.

These observations thus make the usage of shale resistivities to calculate an absolute measure of the pressure gradient (psi/ft) (George, 1959) speculative. The differences in the calculated pressure gradients are noted on the shale resistivity graphs. These calculated pressure gradients varied as much as .25 psi/ft for specific shale intervals (Fig. B-2).

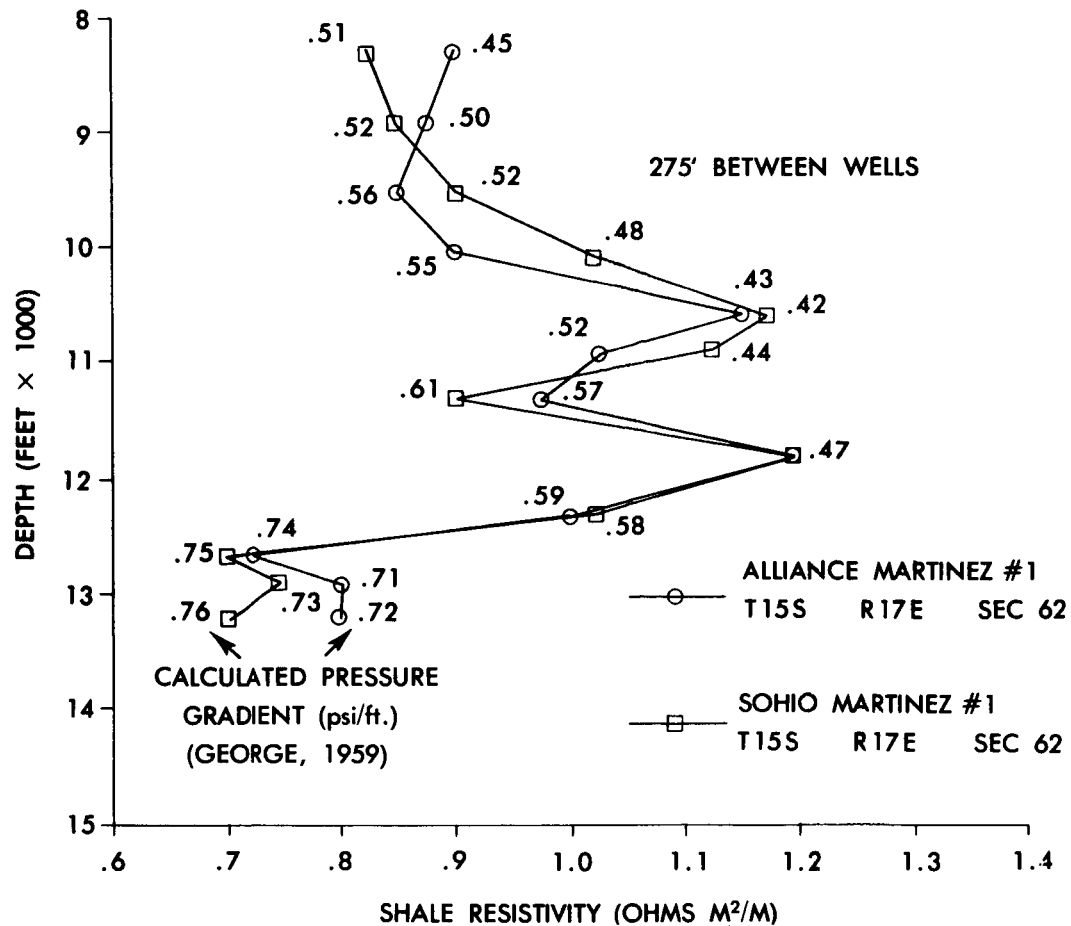


Fig. B-1 - Comparison of short-normal resistivity measurements in shales and calculated pressure gradients for two closely spaced wells in the northern portion of Rousseau Field. Note that the shale resistivities within the same stratigraphic interval vary resulting in different calculated pressure gradients.

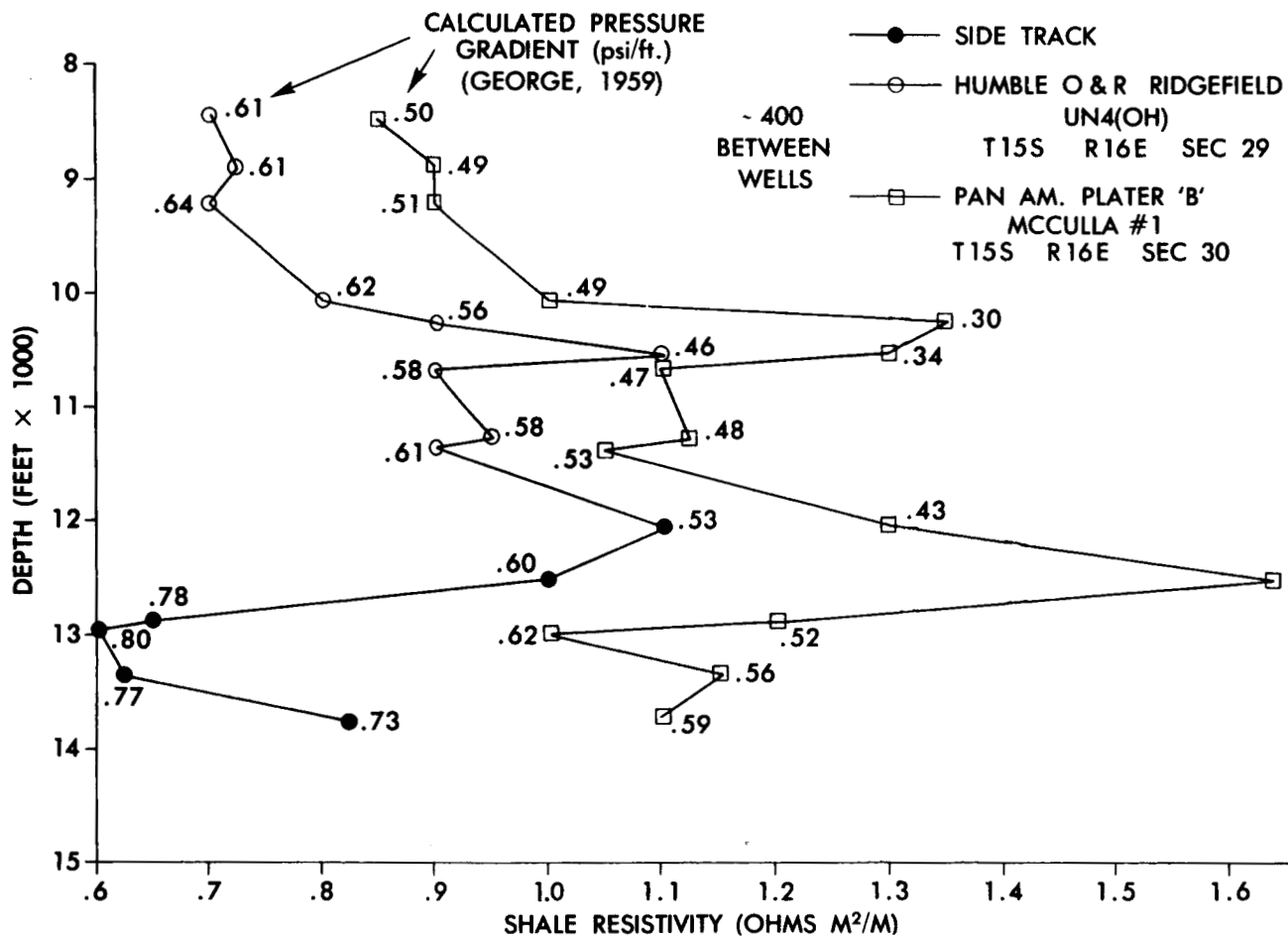


Fig. B-2 - Comparison of short-normal resistivity measurements in shales and calculated pressure gradients for two closely spaced wells in the northern portion of Thibodaux Field. Note that the shale resistivity within the same stratigraphic interval vary significantly resulting in radically different calculated pressure gradients.

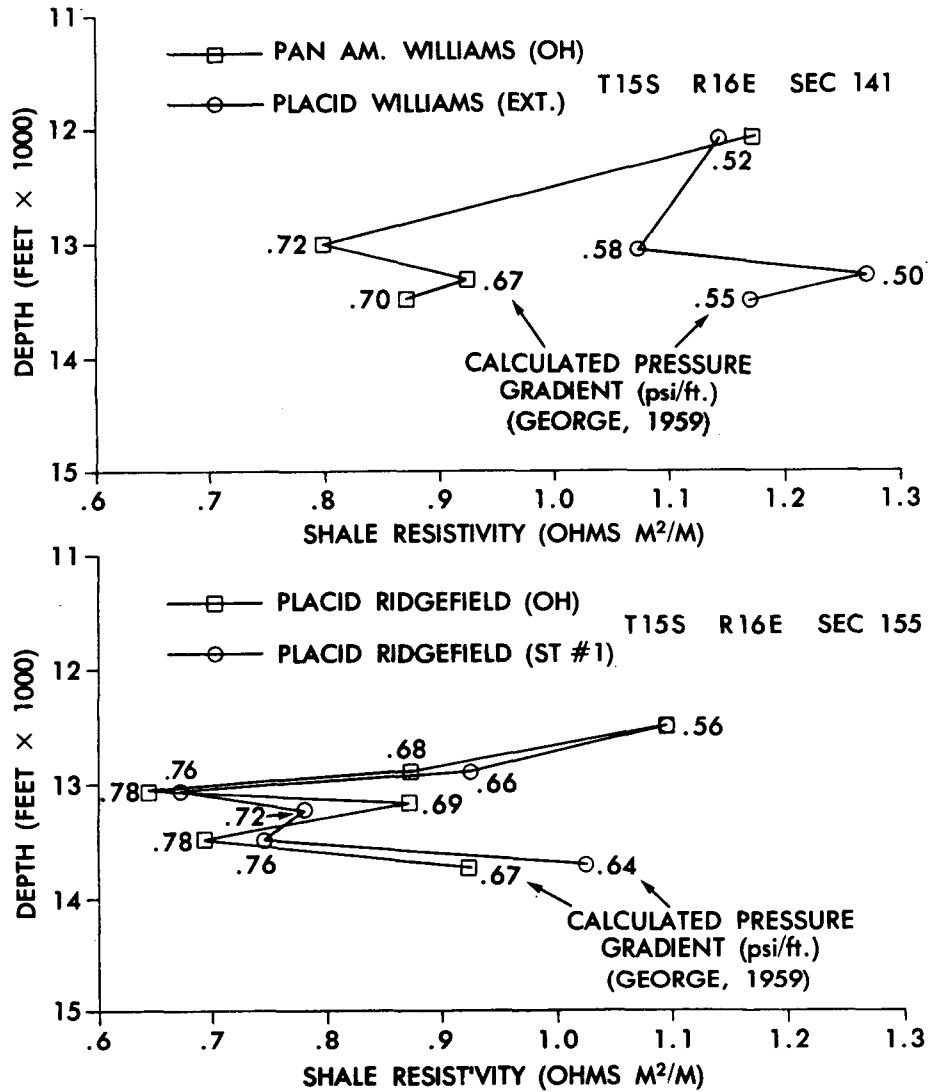


Fig. B-3 - Two graphs comparing short-normal resistivity measurements in shales and calculated pressure gradient for original and side-track holes in shale resistivities and calculated pressure gradients for both holes are nearly equal while in the upper graph little similarity is seen in the resistivity measurements.

APPENDIX C  
SALINITY DIFFUSION MODEL

Figure C-1 illustrates the result of a simplistic model derived to estimate diffusion rates for NaCl solutions in aquifer systems. The model is a one dimensional diffusion problem based on a procedure used by Krom and Berner (1980) to estimate diffusion rates of sulfate, ammonium, and phosphate ions in marine sediments. Their laboratory procedure simulated the condition seen in Figure C-2 where  $C_1$  and  $C$  are initial concentrations of the ions across a permeable interface at time zero.  $C$  is the concentration at some distance  $x$  away from the initial interface after a period of time  $t$ , and  $D_s$  the diffusion coefficient for the solute in the sediment. A measured bulk diffusion coefficient for a two molal sodium chloride (NaCl) solution at 30°C was used for one model.

The diffusion rate at a more realistic temperature of 100°C was extrapolated from available measurements for use in another model. The diffusion coefficient  $D_s$  in a sediment is a function of the sediment porosity and the tortuosity of the diffusion path. Tortuosity depends ultimately upon the sediment porosity. Experimental data have shown that the diffusion coefficient  $D_s$  for NaCl within the sediment can be estimated by

$$D_s = D_o^2 (\text{cm}^2 \text{sec}^{-1})$$

where  $D_s$  is the diffusion coefficient in a bulk solution (Lerman, 1979). Porosities calculated from available density and

sonic logs indicated porosity values ranging from 20-25% in the shallow hydro pressured UL-3 to UL-5 deltaic sandstones. A value of 25% was used to calculate  $D_{zs}$ . Values for  $D_{zs}$  vary by almost an order of magnitude for a NaCl solution at 25C and 100C.

This model ignores diffusion due to temperature differences (Soret effect) and segregation of solutions with different concentrations due to density differences. The Soret effect would act to diffuse cations in a direction opposite to that shown in the model since the higher temperature solution would have the lowest concentration. This effect would thus oppose an equilibrium condition and prolong the concentration differences.

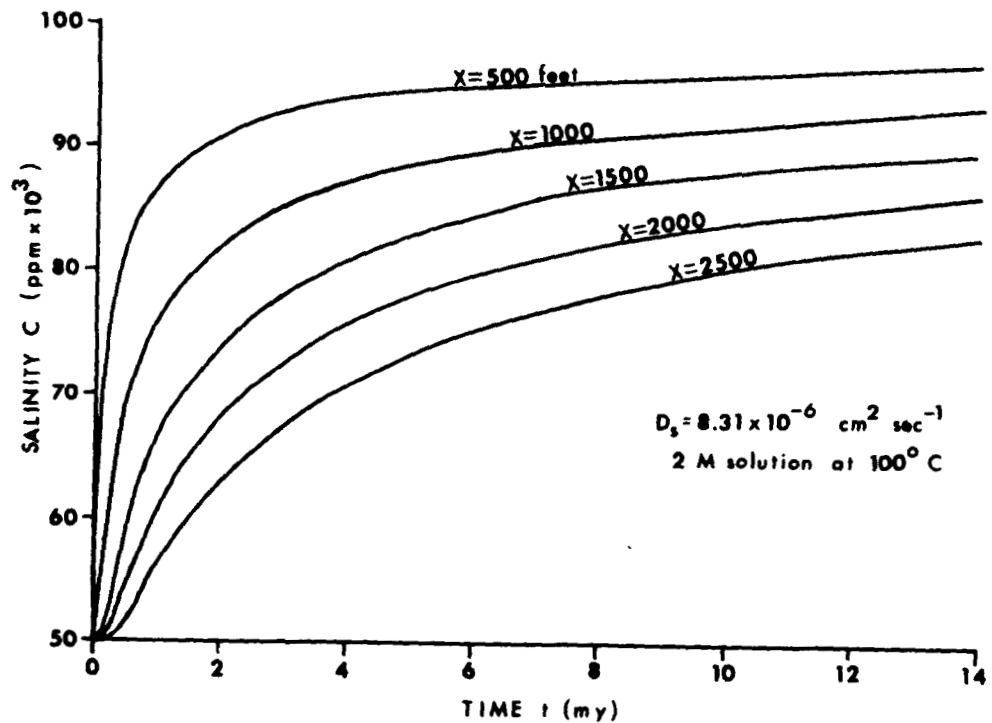
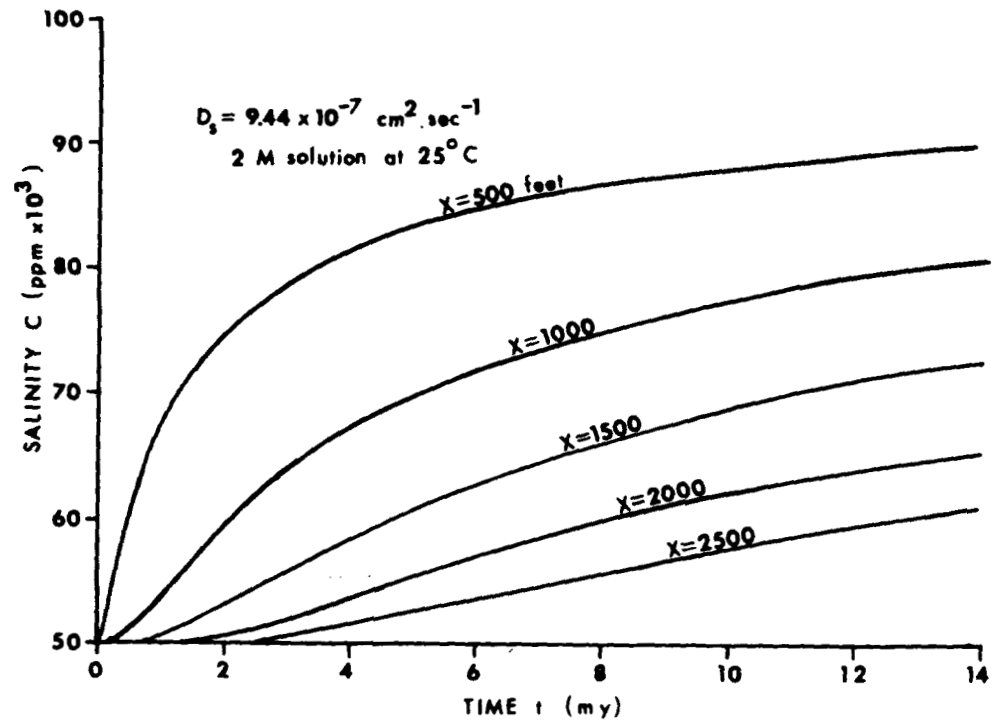
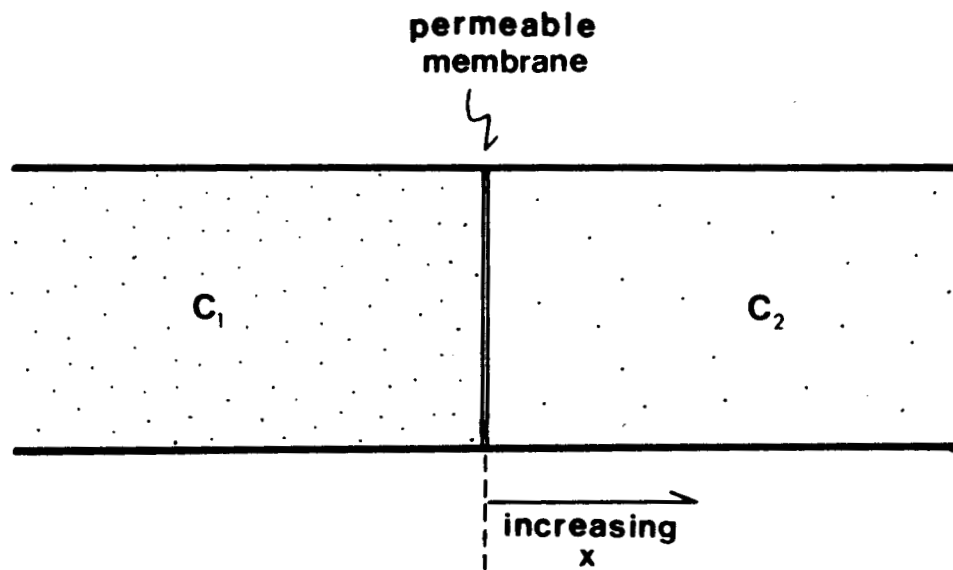


Fig. C-1 - Graphs showing salinity changes (C), with time (t), at varying distances (x) away from an initial interface between two solutions having concentrations of 150,000 ppm and 50,000 ppm sodium chloride (NaCl). A different diffusion coefficient (D) for (NaCl) solutions was assumed for each graph. Note that the salinity within the 50,000 ppm solution (shown in graphs) changes very rapidly until 2 my, where the rate of change decreases.



$$C = C_2 + \frac{1}{2}(C_1 - C_2) \operatorname{erf} \left[ \frac{x}{\sqrt{4D_s t}} \right]$$

Fig.C-2 - Diffusion model used to estimate the length of time a salinity contrast could exist within a sandstone aquifer. Concentration (C), after time (t), at a distance (x) away from the initial interface between two solutions of concentration ( $C_1$  and  $C_2$ ) is given by the equation.  $D_s$  is the diffusion coefficient for a sodium chloride (NaCl) solution.

## APPENDIX D

## List of Abbreviations

Big 2	<u>Bigenerina '2'</u>
Tex W	<u>Tuxtulariaa Stapperi</u>
Big H	<u>Bigenerina humblei</u>
UL-1	UL-1 Sand
UL-2	UL-2 Sand
Crist I	<u>Cristellaria T</u>
UL-3	UL-3 Sand
UL-5	UL-5 Sand
UL-7	UL-7 Sand
Cib Op	<u>Cibicides opima</u>
UL-8	UL-8 Sand
BHS	Barnhart Sand
MS	McCulla Sand
MM	McCulla Marker
ROB	Robulus I Sand
BS	Bourgeois Sand
ZZ	(distinctive resistivity marker)
OPE	<u>Operculinoides I Sand</u>
ROM	Regional <u>Operculinoides</u> Marker
PC	Plater C Sand
RFS	Ridgefield Sand
BFS	Bokenfohr Sand
CRIST 'A'	<u>Cristellaria 'A'</u>

## LAFOURCHE CROSSING SEISMIC SURVEY DESCRIPTION

BY

Rex. H. Pilger, Jr.

## INTRODUCTION

The Department of Geology at Louisiana State University has been conducting a detailed study of the LaFourche Crossing geopressured-geothermal prospect under contract to the U.S. Department of Energy. The earlier study by Snyder and Pilger (this report) used all available well log information and limited seismic data to define the subsurface relationships present in this area. To further define these relationships, LSU contracted for three twenty-four-fold common depth point reflection seismic lines in August of 1981 over the LaFourche crossing prospect in LaFourche and Terrebonne Parishes. These lines, labeled B, C, and D, are shown on the accompanying shotpoint map (Plate 1). Interpretation of these lines is reported by Beckman and Pilger in the final report for DOE contract number DE-AS05-78ET2702 with LSU.

## SHOOTING AND RECORDING SPECIFICATIONS

1. Paladin Geophysical Corp. Contractor
2. Vibroseis energy source used a sweep length of 20 secs and a 3. Frequency band of 10 - 40 Hz
4. Split spread geophone arrangement:  
8580 ft - 990 ft "0 - 990 ft - 8580 ft  
Both the geophone group interval and shotpoint interval were 330 ft
5. MDS 10 48 channel recorder
6. Record length of 6 secs
7. Sample rate of 4 msec

## PROCESSING SPECIFICATIONS

All line types followed this initial sequence of steps:

1. Demultiplex
2. CDP gather assuming a weathering layer velocity of 5500  
ft/sec
3. Deconvolution
4. Filter using a low cut of 10/12 Hz and a high cut of 40/42  
Hz
5. Velocity analysis - constant velocity stack
6. Normal movement corrections
7. Mute
8. Automatic residual\_dual statics - 11 trace pilot over  
window of 0.6000 - 3.6000 secs
9. Stack
10. Filter using a low cut of 10/12 Hz and a high cut of 36/40  
Hz

From this point in the processing sequence, six different processing sequences were followed, creating six different displays.

- |                           |                         |
|---------------------------|-------------------------|
| (1) Relative amplitude    | (4) AGC 500 msec window |
| (2) Relative amplitude    | Depth conversion        |
| Depth conversion          | (5) AGC 500 msec window |
| (3) AGC # 500 msec window | Wave equation migration |
|                           | (6) AGC 500 msec window |
|                           | Depth Conversion        |

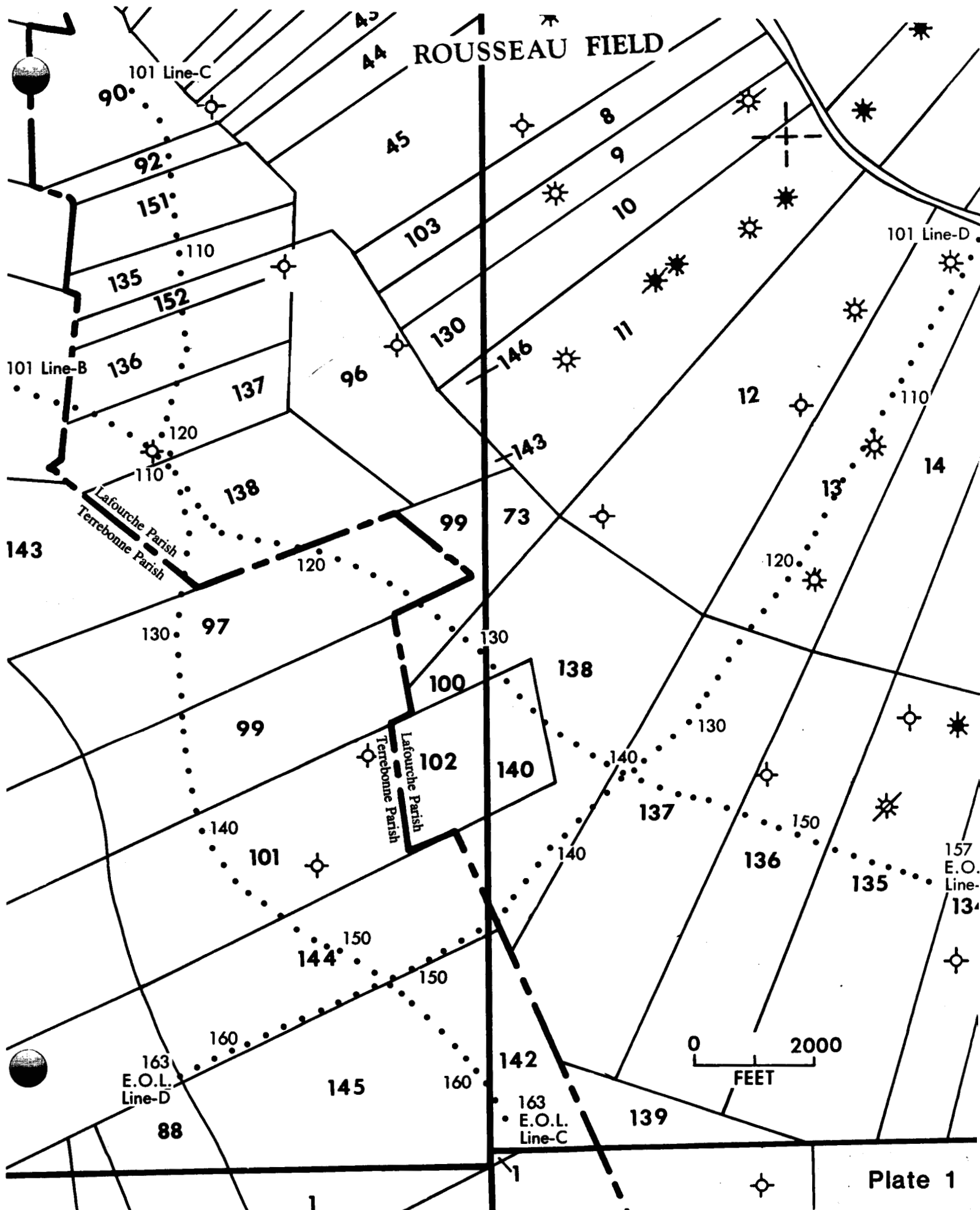
## LAFOURCHE CROSSING REFLECTION SEISMIC SURVEY, 1981

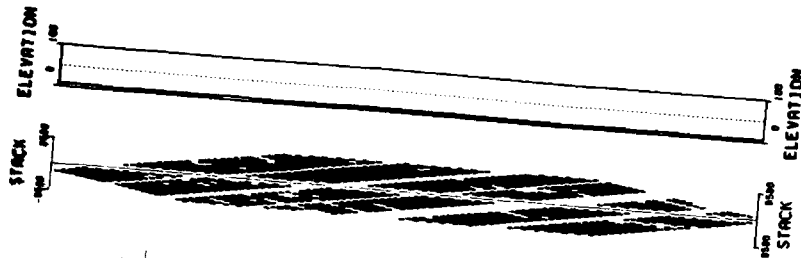
## PLATES

1. Shot Point Location Map
2. Line B:
  - a. Relative amplitude
  - b. Relative amplitude, depth conversion
  - c. AGC
  - d. AGD, depth conversion
  - e. AGC, wave-equation migration
  - f. AGC, wave-equation migration, depth conversion
3. Line C:
  - a. Relative amplitude
  - b. Relative amplitude, depth conversion
  - c. AGC
  - d. AGC, depth conversion
  - e. AGC, wave-equation migration
  - f. AGC, wave-equation migration, depth conversion
4. Line D:
  - a. Relative amplitude
  - b. Relative amplitude, depth conversion
  - c. AGC
  - d. AGC, depth conversion
  - e. AGC, wave-equation migration
  - f. AGC, wave-equation migration, depth conversion

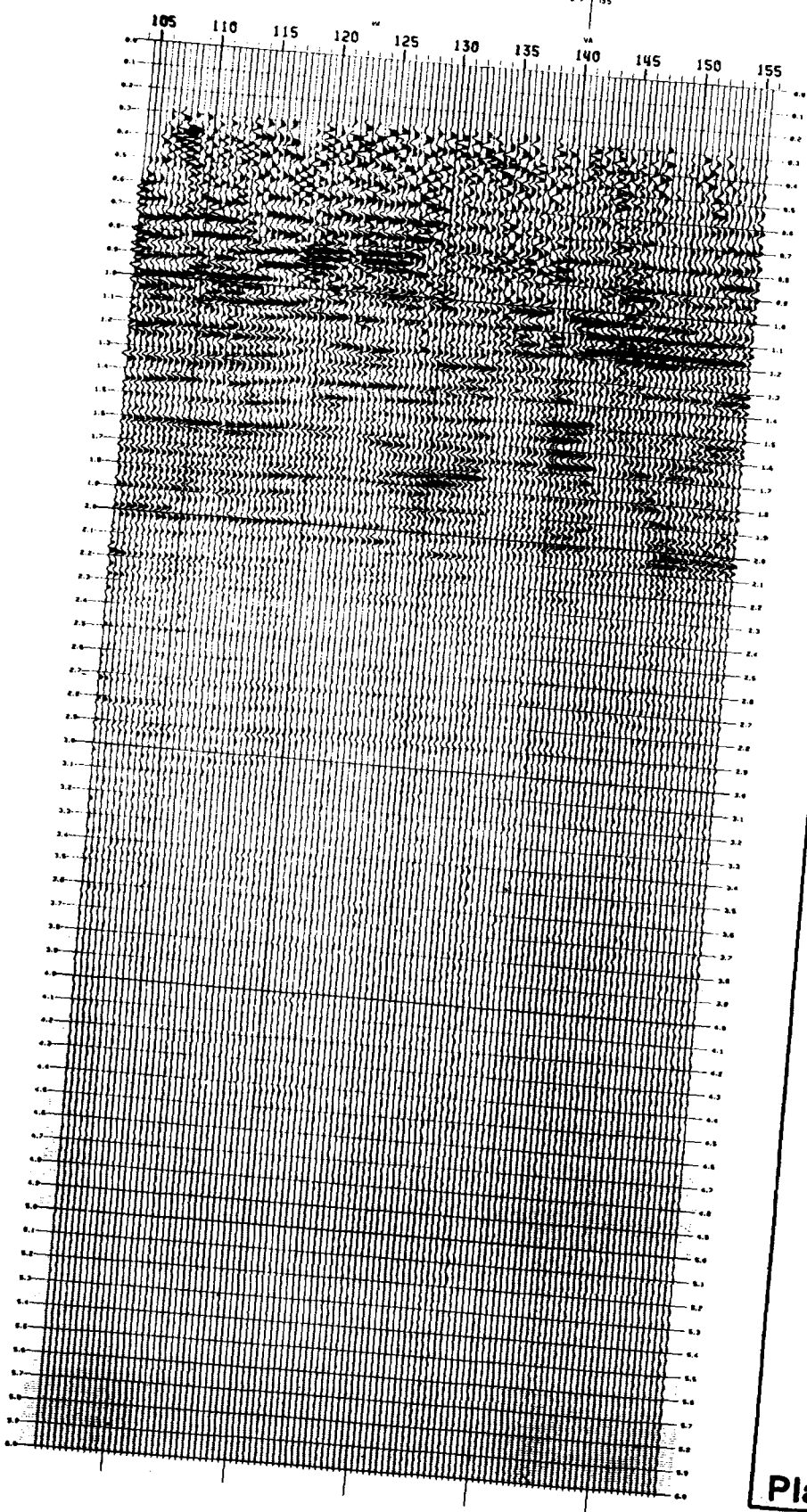
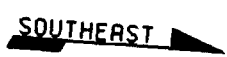
# SHOT POINT MAP, LAFOURCHE CROSSING

SEISMIC SURVEY, 1981. 114





115a



**LINE B  
LAFORCHE CROSSING**

LAFORCHE PARISH, LOUISIANA  
AND  
TERREBOUNE PARISH, LOUISIANA  
24-FOLD VIBROSEIS  
S.P. 104 NM

**L.S.U.**

**RECORDING INFORMATION**

SHOT BY: PALDIN GEOPHYSICS, CORP.  
SHEEP LENGTH: 20 SEC.  
PULS. FREQUENCY: 10-HZ. PZ.  
GROUP INTERVAL: 330 FT.  
S.P. INTERVAL: 330 FT.  
SPREAD: 800-1000-0-800-800 FT.  
INSTRUMENTS: 105-10 40-CHANNEL  
RECORD LENGTH: 6 SEC.  
SAMPLE RATE: 4 MS.  
DATE RECORDED: AUGUST, 1981

**PROCESSING INFORMATION**

1. DEMULTIPLIED
2. CORRECTED DEPTH POINT CENTER  
DEPTH: SEA LEVEL  
CORR. VELOCITY: 5500 FT./SEC.
3. DECONVOLUTION: 200 MS. OPERATOR  
TAPERED WINDOW: 1-150-3,000 SEC.
4. FILTER: 10/12-40/40 HZ.
5. VELOCITY ANALYSIS  
CONSTANT VELOCITY STACK
6. NORMAL MOVEOUT CORRECTIONS  
DATE
7. AUTOMATIC RESIDUAL STATISTICS  
II TRACE PLOT  
MINIMUM: 0.000-3.000 SEC.
8. STACK
10. FILTER: 10/12-35/40 HZ.

**VELOCITY FUNCTIONS**

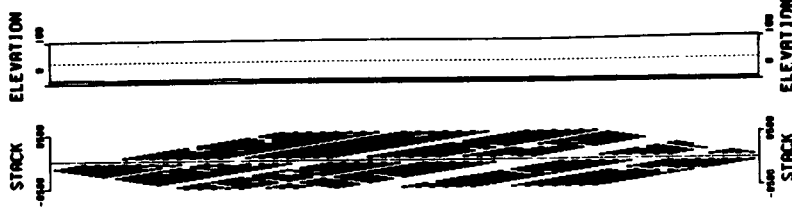
SP 123	TIME	VELOCITY	TIME	VELOCITY
	0.000	5500	0.000	5500
	0.700	8050	0.700	8050
	1.200	8650	1.050	8700
	1.600	8900	1.200	8700
	1.700	7100	1.400	8500
	2.025	7400	1.750	8500
	2.300	7700	2.050	7250
	2.700	8050	2.000	7700
	3.000	8250	3.200	8150
	4.000	8600	4.200	8600
	6.000	9000	6.000	9500

**PHOTOGRAPHY**

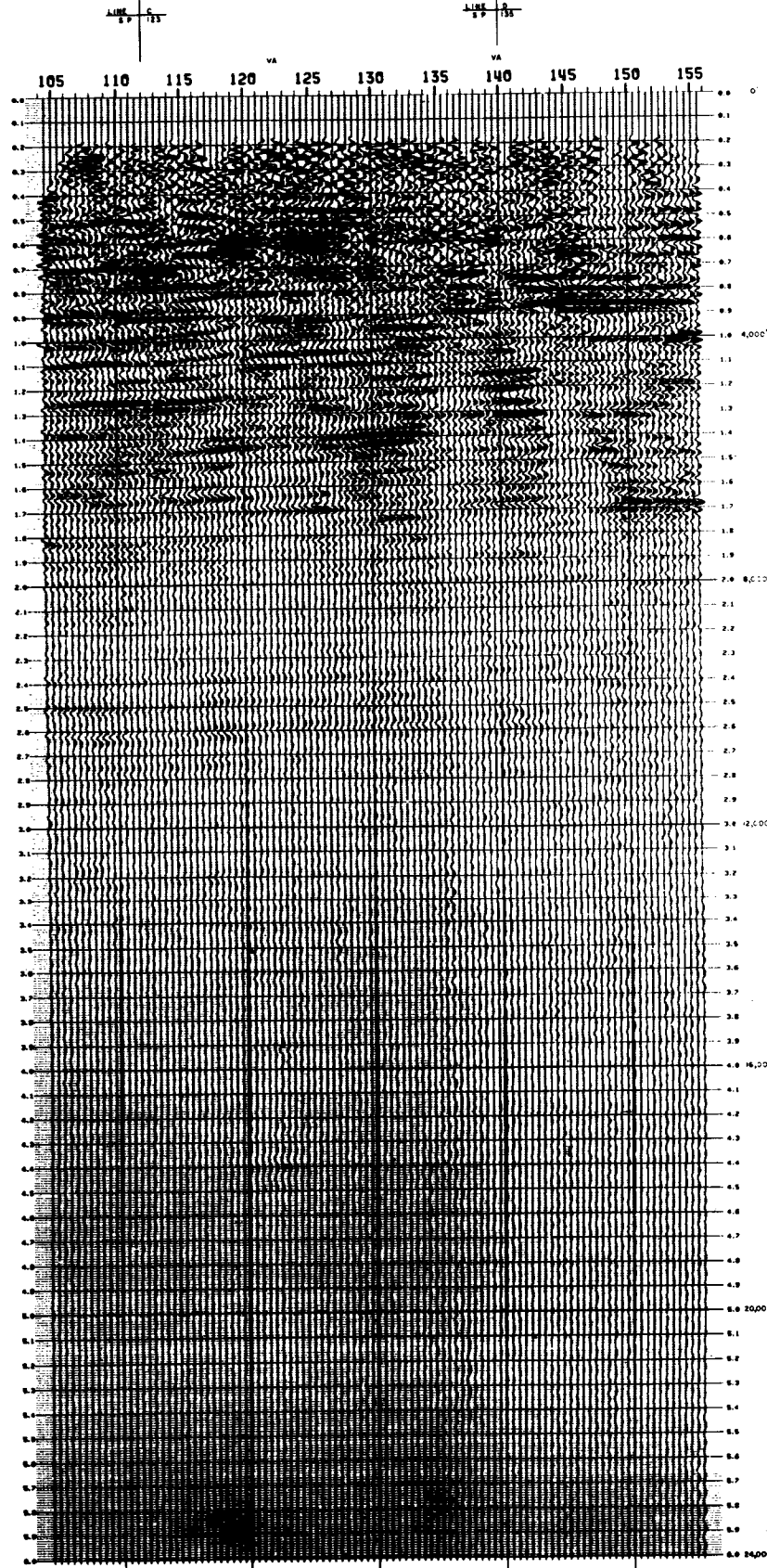
8 TRACES/INCH  
CLIENT NO. 136  
OCTOBER, 1981  
QUALITY CONTROLLED BY: RJJ

3 INCHES/SECOND  
REEL NO. 2 180N  
POLARITY: NORMAL  
PROFESSIONAL GEOPHYSICS, INC.  
NEW ORLEANS, LOUISIANA





**SOUTHEAST**



**LINE B**  
**LAFORCHE CROSSING**

LAFORCHE PARISH, LOUISIANA  
 TERREBORE PARISH, LOUISIANA  
 24-FOLD VIBROSEIS  
 S.P. 104 NW S.P. 100 SE

**L.S.U.**

**RECORDING INFORMATION**  
 SHOT BY: PALMCOIN GEOPHYSICAL CORP.  
 SHEEP LENGTH: 20 SEC.  
 PILOT FREQUENCY: 10-40 HZ.  
 GROUP INTERVAL: 330 FT.  
 S.P. INTERVAL: 330 FT.  
 SPREAD: 6000-900-0-900-6000 FT.  
 INSTRUMENTS: HSS-10 40-CANAL  
 RECORD LENGTH: 8 SEC.  
 SAMPLE RATE: 4 MS.  
 DATE RECORDED: AUGUST, 1981

**PROCESSING INFORMATION**

1. DEMULTIPLY
2. COMMON DEPTH POINT GATHER  
 ORIGIN: SEA LEVEL  
 CORR. VELOCITY: 8000 FT./SEC.
3. DECONVOLUTION: 200 MS. OPERATOR  
 TAPERED WINDOW: 1.150-3.000 SEC.
4. FILTER: 10/12-30/40 HZ.
5. VELOCITY ANALYSIS  
 CONSTANT VELOCITY STACK
6. NORMAL MOVEOUT CORRECTIONS
7. MUTE
8. AUTOMATIC RESIDUAL STACK  
 11 TRACE PILOT
9. STACK  
 WINDOW: 0.600-3.000 SEC.
10. FILTER: 10/12-30/40 HZ.
11. DEPTH CONVERSION

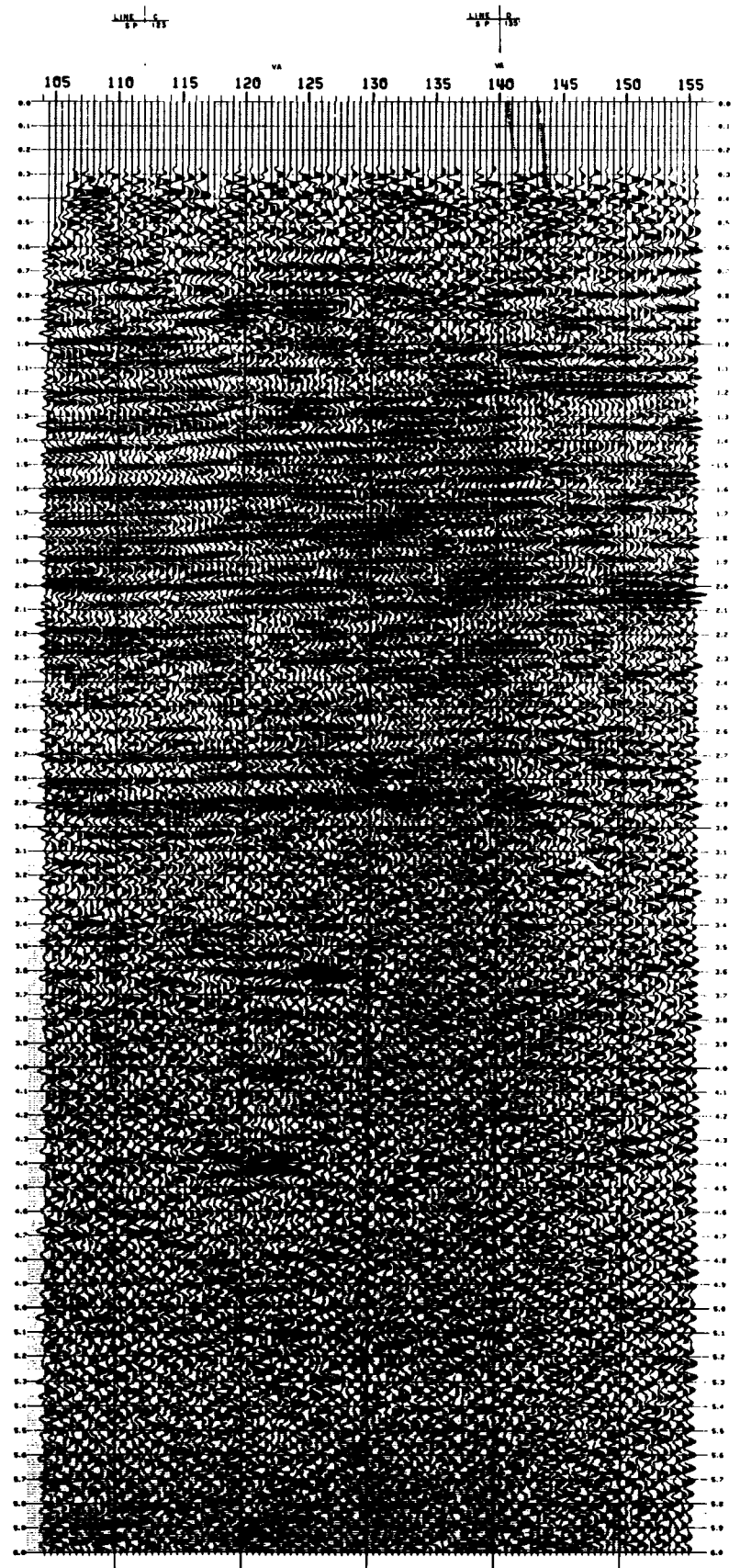
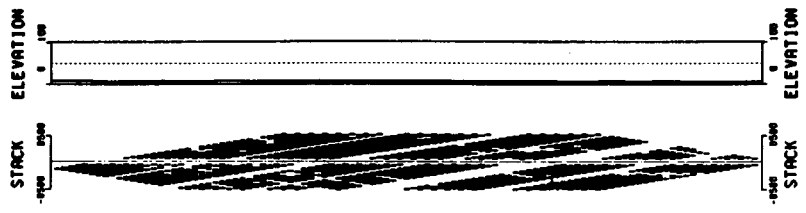
**VELOCITY FUNCTION**

TIME	VELOCITY
0.000	5500
0.500	6000
1.000	6375
1.500	6700
2.000	7000
2.500	7400
3.000	7750
3.500	8000
4.000	8250
4.500	8500
5.000	8700

**PHOTOGRAPHY**  
 8 TRACES/INCH 5 INCHES/SECOND  
 CLIENT NO. 136 REEL NO. 8 1330  
 SEPTEMBER, 1981 POS. QUALITY: NORMAL  
 QUALITY CONTROLLED BY: RJD

**PROFESSIONAL GEOPHYSICS, INC.**  
 NEW ORLEANS, LOUISIANA

**Plate 2b**



**LINE B**  
**LAFORCHE CROSSING**

LAFORCHE PARISH, LOUISIANA  
TERREBOONE PARISH, LOUISIANA  
24-FOLD VIBROSEIS  
S.P. 104 NW S.P. 106 SE

**L. S. U.**

**RECORDING INFORMATION**

SHOT BY: PALDIN GEOPHYSICAL CORP.  
SHEET LENGTH: 40 SEC.  
PILOT FREQUENCY: 10-40 HZ.  
GROUP INTERVAL: 330 FT.  
S.P. INTERVAL: 330 FT.  
SPREAD: 8500-9900-0-9900-8500 FT.  
INSTRUMENTS: MDS-10 WIG-CORREL  
RECORD LENGTH: 8 SEC.  
SAMPLE RATE: 4 MS.  
DATE RECORDED: AUGUST, 1981

**PROCESSING INFORMATION**

1. DATA FILES
2. COMMON DEPTH POINT GATHER  
ORTHO: SEA LEVEL  
CORP. VELOCITY: 5500 FT./SEC.
3. DECONVOLUTION: 200 MS. OPERATOR  
TAPERED WINDOW: 1.150-3.000 SEC.
4. FILTER: 10/12-96/42 HZ.
5. VELOCITY ANALYSIS  
CONSTANT VELOCITY STACK
6. NORMAL MOVEOUT CORRECTIONS
7. MUTE
8. AUTOMATIC RESIDUAL STATISTICS  
II. RANGE: 100 FT.  
WINDOW: 0.500-3.000 SEC.
9. STACK
10. FILTER: 10/12-96/42 HZ
11. GCI: 900 MS. WINDOW

**VELOCITY FUNCTION**

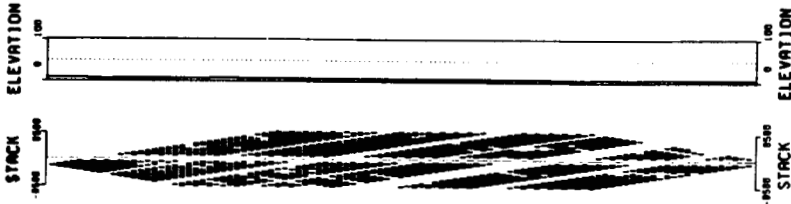
TIME	VELOCITY
0.000	5500
0.550	6000
1.000	6375
1.500	6700
1.625	7000
2.000	7200
2.550	7600
3.150	8250
3.750	8600
4.350	8950
6.000	9700

**PHOTOGRAPHY**

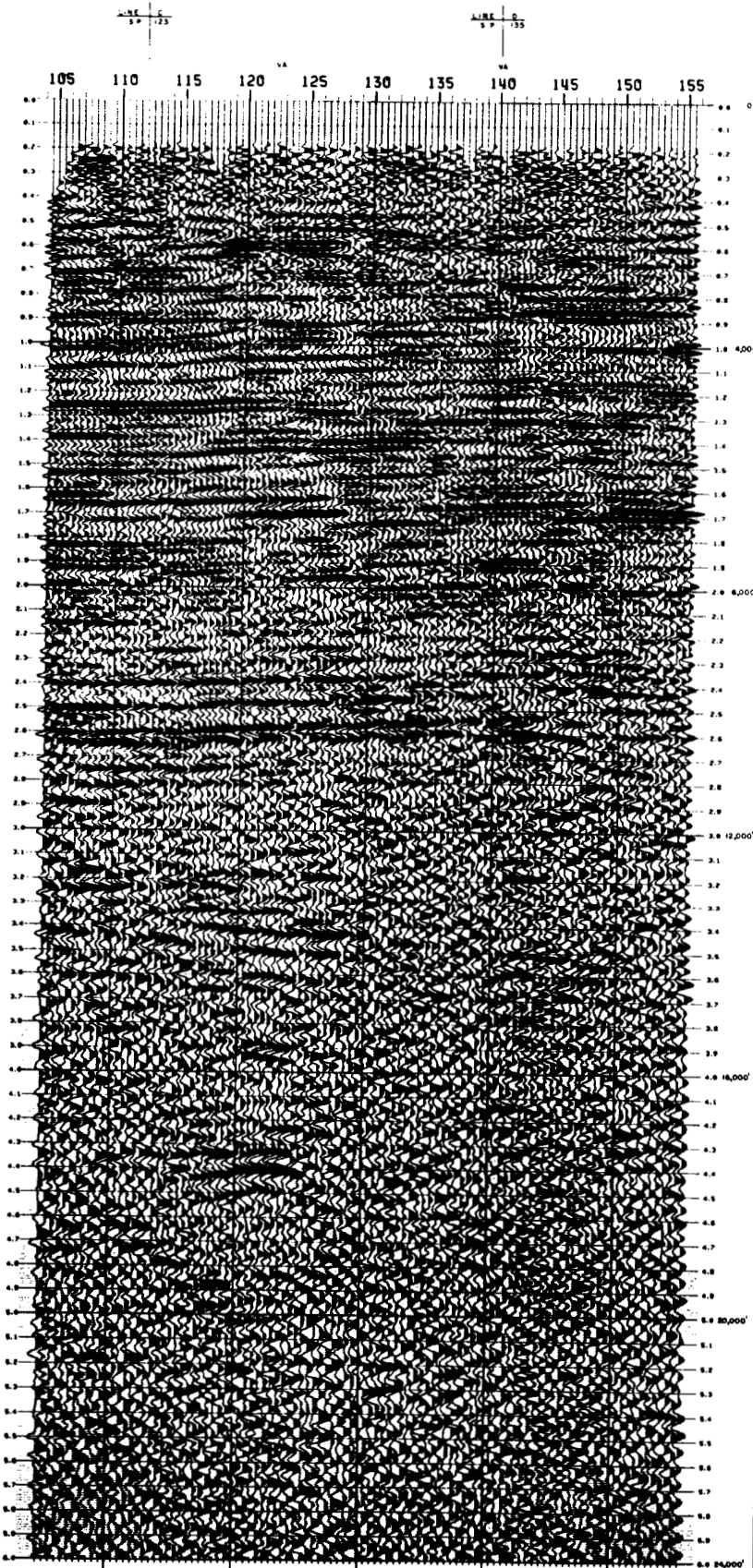
0 TRACES/INCH	5 INCHES/SECOND
CLIENT NO. 136	REEL NO. X 1330
SEPTEMBER, 1981	FOURTH, NORMAL
QUALITY CONTROLLED BY: PJD	

PROFESSIONAL GEOPHYSICS, INC.  
NEW ORLEANS, LOUISIANA

**Plate 2c**



**SOUTHEAST**



**LINE B**  
**LAFOURCHE CROSSING**

LAFOURCHE PARISH, LOUISIANA  
AND  
TERREBORE PARISH, LOUISIANA  
24-FOLD VIBROSEIS  
S.P. 135 NW S.P. 136 SE

**L. S. U.**

**RECORDING INFORMATION**

SHOT BY: PALMATH GEOPHYSICAL CORP.  
SWEEP LENGTH: 20 SEC.  
PILOT FREQUENCY: 10-40 HZ.  
GROUP INTERVAL: 330 FT.  
S.P. INTERVAL: 330 FT.  
SPREAD: 8500-990-0-890-8500 FT.  
INSTRUMENTS: 105-10 10-CHANNEL  
RECORD LENGTH: 6 SEC.  
SAMPLE RATE: 4 MS.  
DATE RECORDED: AUGUST, 1961

**PROCESSING INFORMATION**

1. DEMULTIPLY
2. COMMON DEPTH POINT GATHER  
ORIGIN: SEA LEVEL  
CORR. VELOCITY: 5000 FT./SEC.
3. DECONVOLUTION: 200 MS. GAINWISH  
TAPERED WINDOW: 1.150-3.000 SEC.
4. FILTER: 10/12-30/42 HZ.
5. VELOCITY ANALYSIS  
CONSTANT VELOCITY STACK
6. NORMAL MOVEOUT CORRECTIONS
7. FLUTE
8. AUTOMATIC RESIDUAL STATICS  
1) TRACE PILOT  
WINDOW: 0.800-3.000 SEC.
9. STACK
10. FILTER: 10/12-30/42 HZ.
11. REC: 500 MS. WINDOW
12. DEPTH CONVERSION

**VELOCITY FUNCTION**

TIME	VELOCITY
0.000	5500
0.550	6000
1.000	6375
1.300	6700
1.625	7000
2.000	7400
2.550	7800
3.150	8250
3.700	8600
4.350	8950
5.000	9700

**PHOTOGRAPHY**

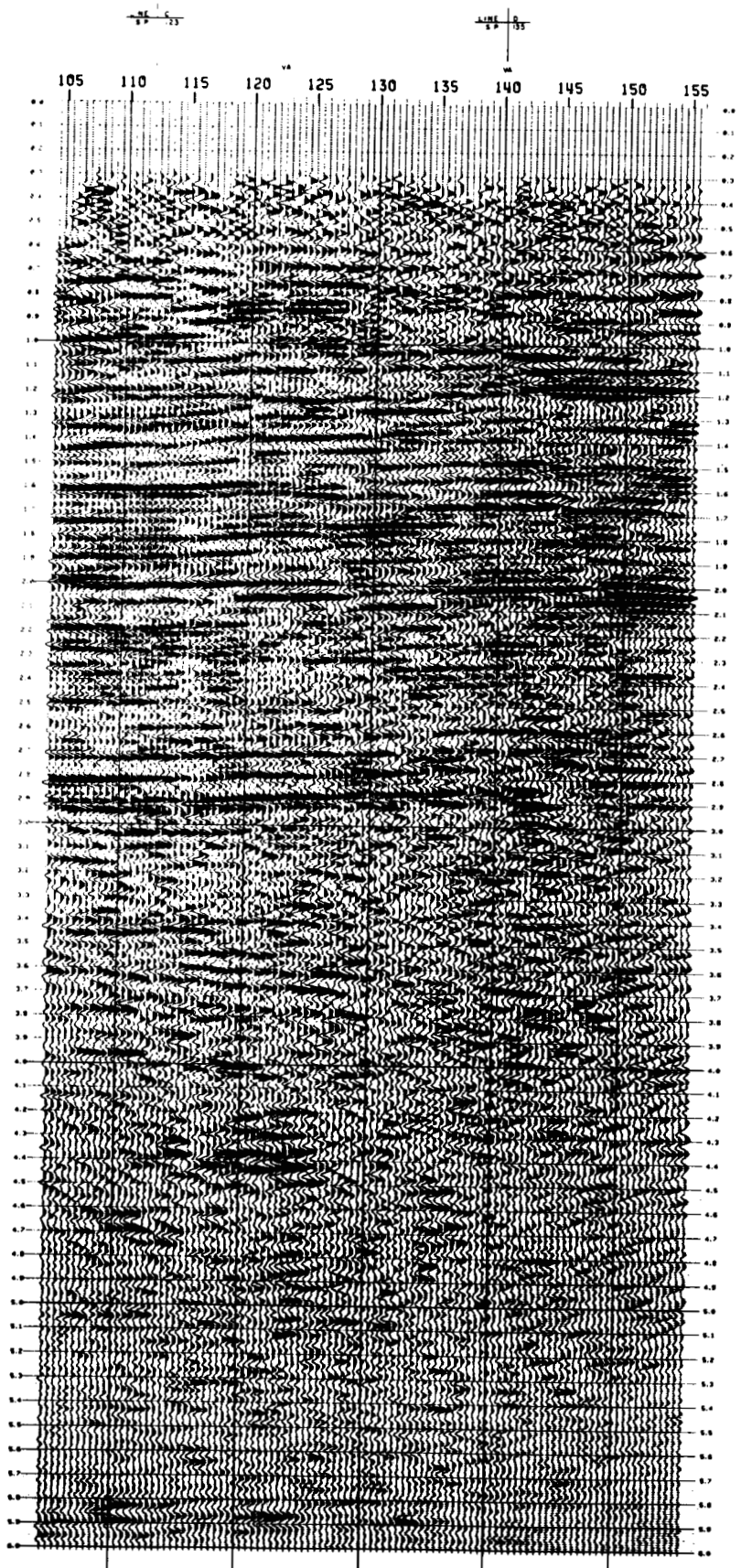
9 TRACES/INCH      5 INCHES/SECOND  
CLIENT NO. 136      REEL NO. 7 1/2  
SEPTEMBER, 1961      POLARITY: NORMAL  
QUALITY CONTROLLED BY: R.J.

**PROFESSIONAL GEOPHYSICS, INC.**  
NEW ORLEANS, LOUISIANA

**Plate 2d**



**SOUTHEAST**



**LINE B  
LAFORCHE CROSSING**

LAFORCHE PARISH, LOUISIANA  
TERREBOINE PARISH, LOUISIANA  
24-FOLD VIBROSEIS  
S.P. 104 W S.P. 156 SE

**L.S.U.**

**RECORDING INFORMATION**

SHOT BY: PALMCO GEOPHYSICAL CORP.  
SHEEP LENGTH: 20 SEC.  
PILOT FREQUENCY: 10-40 HZ.  
GROUP INTERVAL: 300 FT.  
S.P. INTERVAL: 300 FT.  
SPREAD: 8000-9000-0-9000-8500 FT.  
INSTRUMENTS: PDS-10 48-CHANNEL  
RECORD LENGTH: 8 SEC.  
SAMPLE RATE: 4 MS.  
DATE RECORDED: AUGUST, 1981

**PROCESSING INFORMATION**

1. DEMULTIPLIES
2. COMMON DEPTH POINT GATHER  
DITRA: SEA LEVEL  
CORR. VELOCITY: 5500 FT./SEC.  
3. DECONVOLUTION: 200 MS. OPERATOR  
TAPERED WINDOW: 1.150-3.000 SEC.
4. FILTER: 10-12-40-80 HZ.
5. VELOCITY ANALYSIS  
CONSTANT VELOCITY STACK
6. NORMAL MOVEOUT CORRECTIONS
7. MUTE
8. AUTOMATIC RESIDUAL STATICS  
11. TRACE PILOT  
WINDOW: 0.800-3.000 SEC.
9. STACK
10. FILTER: 10-12-40-80 HZ.
11. NDC: 500 MS. WINDOW
12. WAVE EQUATION MIGRATION

**VELOCITY FUNCTIONS**

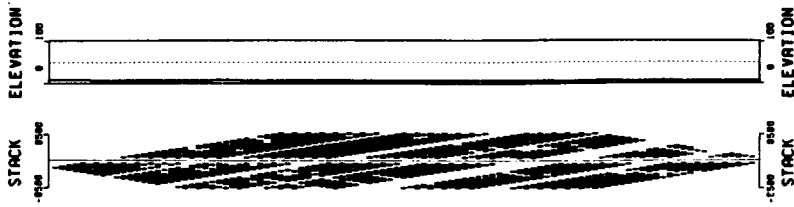
SP 123	SP 140		
TIME	VELOCITY	TIME	VELOCITY
0.000	8500	0.000	5500
0.700	6950	0.700	6050
1.250	6650	1.250	6350
1.400	6600	1.300	6300
1.750	7100	1.400	6650
2.025	7400	1.750	6950
2.300	7700	2.050	7250
2.750	8000	2.600	7700
3.050	8450	3.200	8150
4.000	8900	4.200	8600
6.000	9500	6.000	9500

**PHOTOGRAPHY**

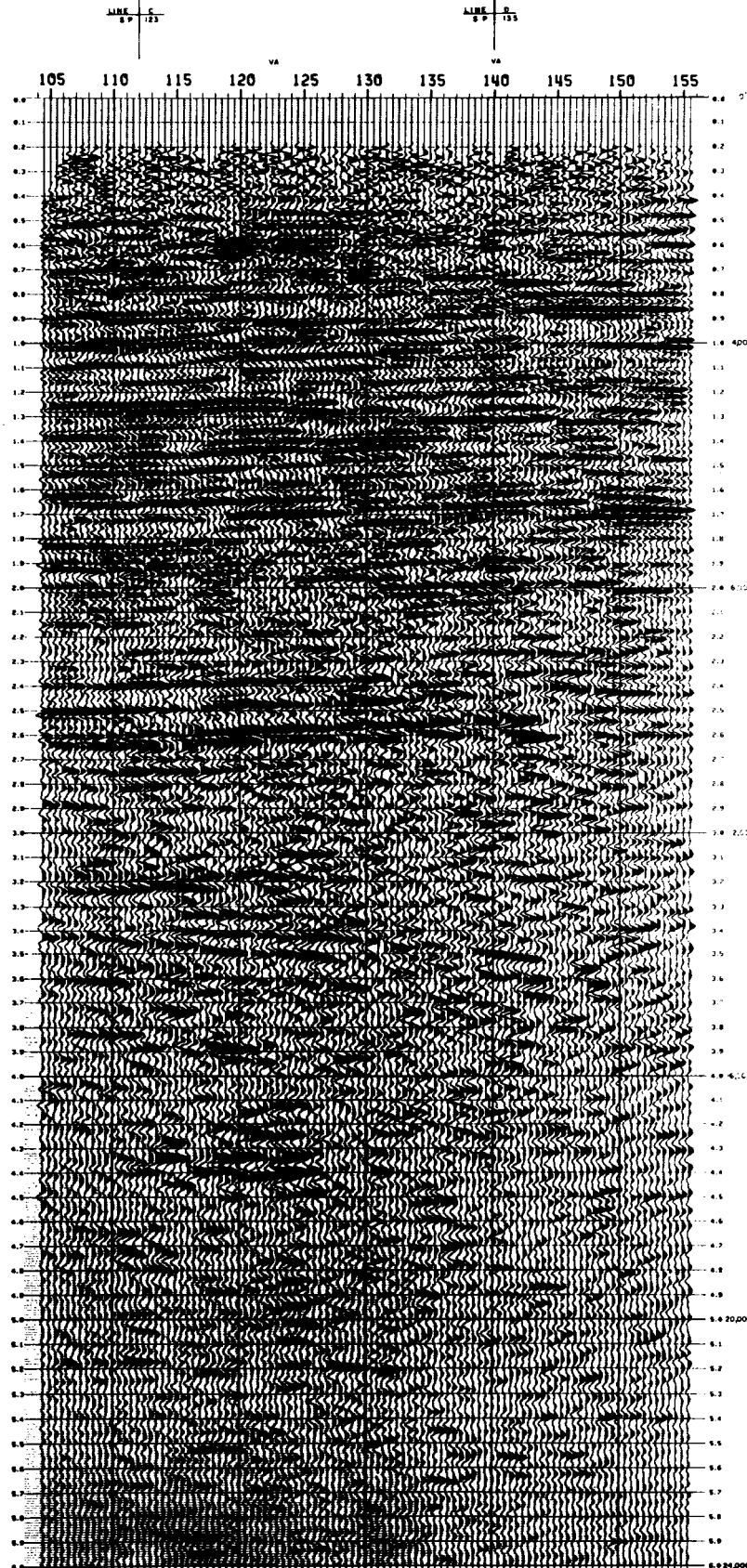
8 TRACES/INCH 5 INCHES/SECOND  
CLIENT NO. 136 REEL NO. A 1359  
SEPTEMBER, 1981 PALMCO, INC.  
QUALITY CONTROLLED BY: RJD

**PROFESSIONAL GEOPHYSICS, INC.**  
NEW ORLEANS, LOUISIANA





SOUTHEAST



**LINE B**  
**LAFORCHE CROSSING**

LAFORCHE PARISH, LOUISIANA  
 AND  
 TERREBOONE PARISH, LOUISIANA  
 24-FOLD VIBROSEIS  
 S.P. 124 NW  
 S.P. 126 SE

**L.S.U.**

**RECORDING INFORMATION**

SHOT BY: PALGREN GEOPHYSICAL CORP.  
 SHEET LENGTH: 20 SEC.  
 PLOT FREQUENCY: 10-NO. REZ.  
 GROUP INTERVAL: 330 FT.  
 S.P. INTERVAL: 330 FT.  
 SPREAD: 8500-1900-900-8500 FT.  
 INSTRUMENTS: NIS-10 48-CANNEL  
 RECORD LENGTH: 6 SEC.  
 SAMPLE RATE: 4 MS.  
 DATE RECORDED: AUGUST, 1981

**PROCESSING INFORMATION**

1. DENALTIPEX
2. COMMON SEATH POINT GATHER  
 DATA: SEA LEVEL  
 CORR. VELOCITY: 5000 FT./SEC.
3. DECONVOLUTION: 200 MS. OPERATOR  
 TAPERED WINDOW: 1.150-3.000 SEC.
4. FILTER: 10/12-40/42 HZ.
5. VELOCITY ANALYSIS  
 CONSTANT VELOCITY STACK
6. NORM. MOVEOUT CORRECTIONS
7. MUTE
8. AUTOMATIC RESIDUAL STATICS  
 11. TRACE PLOT  
 WINDOW: 0.500-3.000 SEC.
9. STACK
10. FILTER: 10/12-30/40 HZ.
11. AGC: 500 MS. WINDOW
12. WAVE EQUATION MIGRATION
13. DEPTH CONVERSION

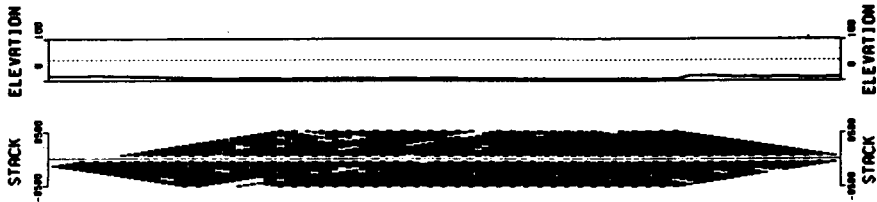
**VELOCITY FUNCTION**

TIME	VELOCITY
0.000	5500
0.500	6000
1.000	6375
1.500	6700
2.000	7000
2.500	7300
3.000	7600
3.500	7900
4.000	8250
4.500	8600
5.000	8950
5.500	9300

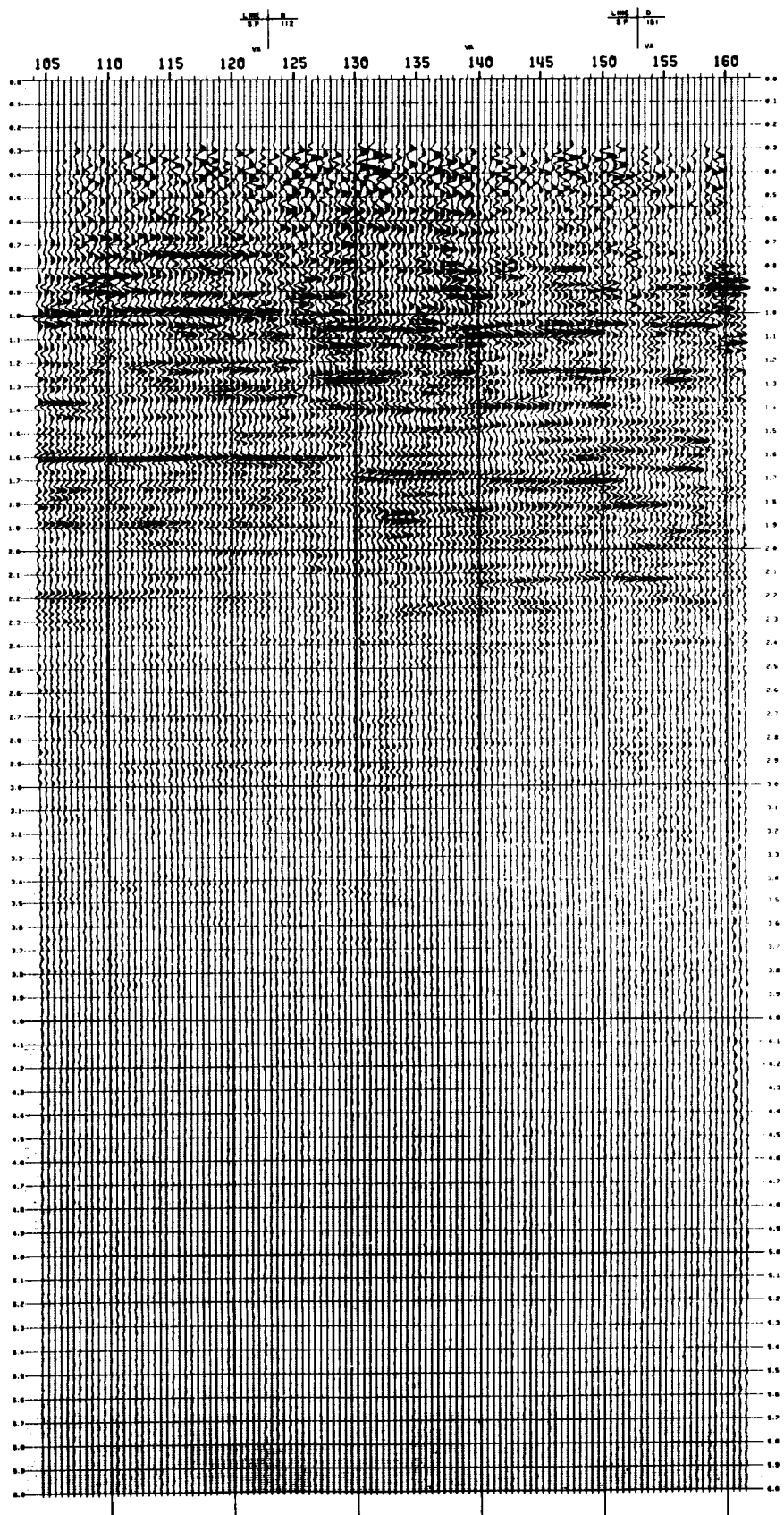
**PHOTOGRAPHY**

4. TRACES/INCH: 5 INCHES/SECOND  
 CLIENT NO.: 130 REEL NO.: X-2723  
 DATE: 1981, 08/01 POLARITY: NORMAL  
 QUALITY CONTROLLED BY: RJD

**PROFESSIONAL GEOPHYSICS, INC.**  
 NEW ORLEANS, LOUISIANA



115g



**LINE C**  
**LAFOURCHE CROSSING**

LAFOURCHE PARISH, LOUISIANA  
TERREBOONE PARISH, LOUISIANA  
24-FOLD VIBROSEIS  
S.P. 100' W. S.P. 102 SE

**L. S. U.**

**RECORDING INFORMATION**

SHOT BY: PALADIN GEOPHYSICAL, INC.  
SHEEP LENGTH: 20 SEC.  
PILOT FREQUENCY: 10-40 HZ.  
GROUP INTERVAL: 330 FT.  
S.P. INTERVAL: 330 FT.  
SPREAD: 9500-9900-9900-9500 FT.  
INSTRUMENTS: RES-10 40-CANAL  
RECORD LENGTH: 6 SEC.  
SAMPLE RATE: 4 MS.  
DATE RECORDED: AUGUST, 1981

**PROCESSING INFORMATION**

1. DEMULTIPLY
2. COMMON DEPTH POINT GATHER  
OPTIMAL SEA LEVEL
3. DECONVOLUTION: 200 MS. OPERATOR  
TAPERED WINDOW: 1.150-3.000 SEC.
4. FILTER: 10/12-30/40 HZ.
5. VELOCITY ANALYSIS  
CONSTANT VELOCITY STACK
6. NORMAL MOVEOUT CORRECTIONS
7. MUTE
8. AUTOMATIC RESIDUAL STATICS  
1/2 TRACE PICK  
WINDOW: 0.600-3.000 SEC.
9. STACK
10. FILTER: 10/12-30/40 HZ.

**VELOCITY FUNCTIONS**

SP 123		SP 138	
TIME	VELOCITY	TIME	VELOCITY
0.000	5500	0.000	5500
0.125	6275	0.625	6350
1.000	6500	1.100	6650
1.200	6650	1.400	6850
1.500	6950	1.800	7050
1.700	7250	2.250	8150
2.275	7550	2.700	8450
2.500	7850	3.200	8750
3.150	8100	3.900	9200
4.400	9050	6.000	9850
6.000	9900		

SP 153	
TIME	VELOCITY
0.000	5500
0.350	6050
1.050	6350
1.400	6650
1.800	7100
2.150	7550
2.400	7850
2.850	8150
3.850	8600
6.000	9800

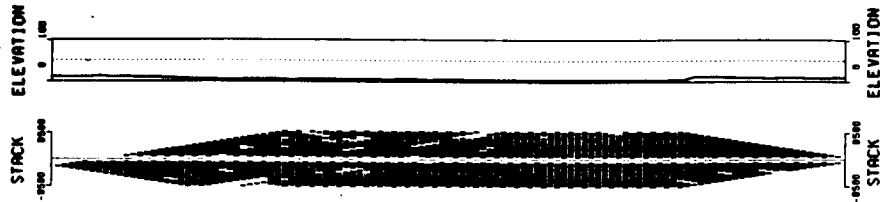
**PHOTOGRAPHY**

4 INCHES/INCH      5 INCHES/SECOND  
CLIENT NO. 136      REEL NO. 3 1895  
SEPTEMBER, 1981      POLARITY: NORMAL  
QUALITY CONTROLLED BY: RJD

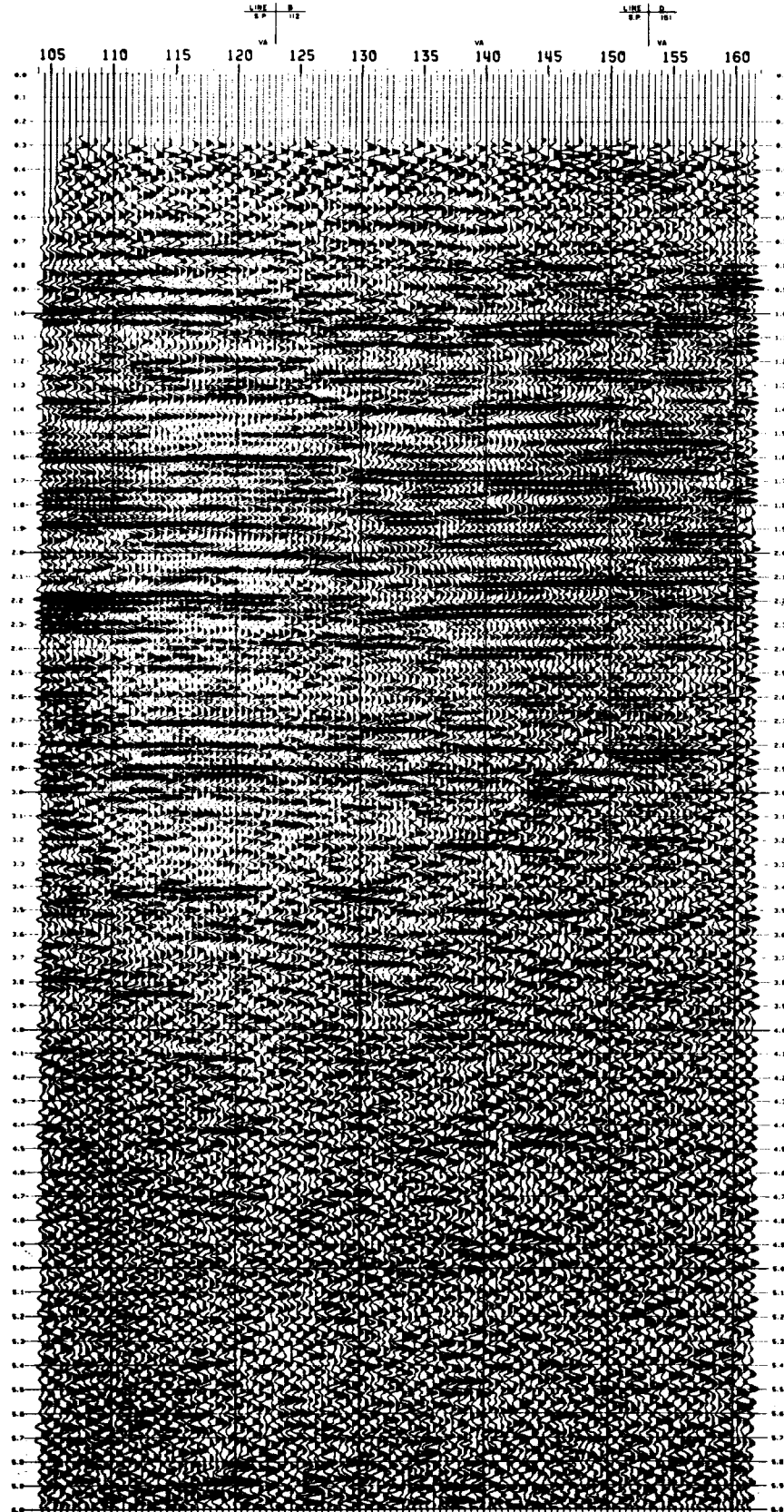
**PROFESSIONAL GEOPHYSICS, INC.**  
NEW ORLEANS, LOUISIANA

**Plate 3a**





SOUTHEAST



**LINE C  
LAFOURCHE CROSSING**

LAFOURCHE PARISH, LOUISIANA  
INC.  
TERREBOONE PARISH, LOUISIANA  
20 FOLD VIBROSEIS  
S.P. 10N 4W S.P. 150 SE

**L.S.U.**

**RECORDING INFORMATION**

SHOT BY: PALADIN GEOPHYSICAL CORP.  
SHEEP LENGTH: 20 SEC.  
PILOT FREQUENCY: 10-40 HZ.  
GROUP INTERVAL: 330 FT.  
S.P. INTERVAL: 330 FT.  
SPREAD: 8500-9900-9900-9900 FT.  
INSTRUMENTS: RES-10 48-CANAL  
RECORD LENGTH: 6 SEC.  
SAMPLE RATE: 4 MS.  
DATE RECORDED: AUGUST, 1981

**PROCESSING INFORMATION**

1. DEMULTIPLIER
2. COMMON DEPTH POINT GATHER  
DATA: SEA LEVEL  
CORR. VELOCITY: 8500 FT./SEC.
3. DECONVOLUTION: 200 MS. OPERATOR  
TAPERED WINDOW: 1.150-3.800 SEC.
4. FILTER: 10/12-40/40 HZ.
5. VELOCITY ANALYSIS  
COMMON VELOCITY STACK
6. NORMAL MOVEMENT CORRECTIONS
7. MUTE
8. AUTOMATIC RESIDUAL STATICS  
1) TRACE PILOT  
WINDOW: 0.600-3.600 SEC.
9. STACK  
WINDOW: 0.600-3.600 SEC.
10. FILTER: 10/12-36/40 HZ.
11. ACC: 500 MS. WINDOW

**VELOCITY FUNCTIONS**

SP 123		SP 135	
TIME	VELOCITY	TIME	VELOCITY
0.000	8500	0.000	8500
0.750	8275	0.625	8350
1.000	8500	1.100	8650
1.200	8650	1.400	8950
1.500	8900	1.800	9250
1.750	9250	2.250	9150
2.075	9500	2.700	9450
2.400	9800	3.200	8750
3.150	8300	3.900	8200
4.000	8050	6.000	8950
6.000	8900		

SP 153	
TIME	VELOCITY
0.000	8500
0.650	8650
1.050	8350
1.450	8650
1.800	9100
2.150	9500
2.400	9850
2.850	8150
3.850	8600
6.000	8900

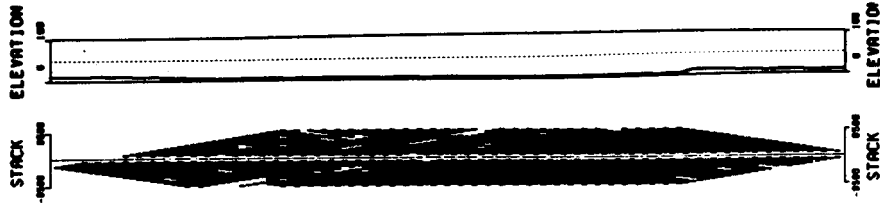
**PHOTOGRAPHY**

8 TRACES/INCH      5 INCHES/SECOND  
CLIENT NO: 136      REEL NO: A 1126  
DATE: 8/1981      POLARITY: NORMAL  
QUALITY CONTROLLED BY: RJD

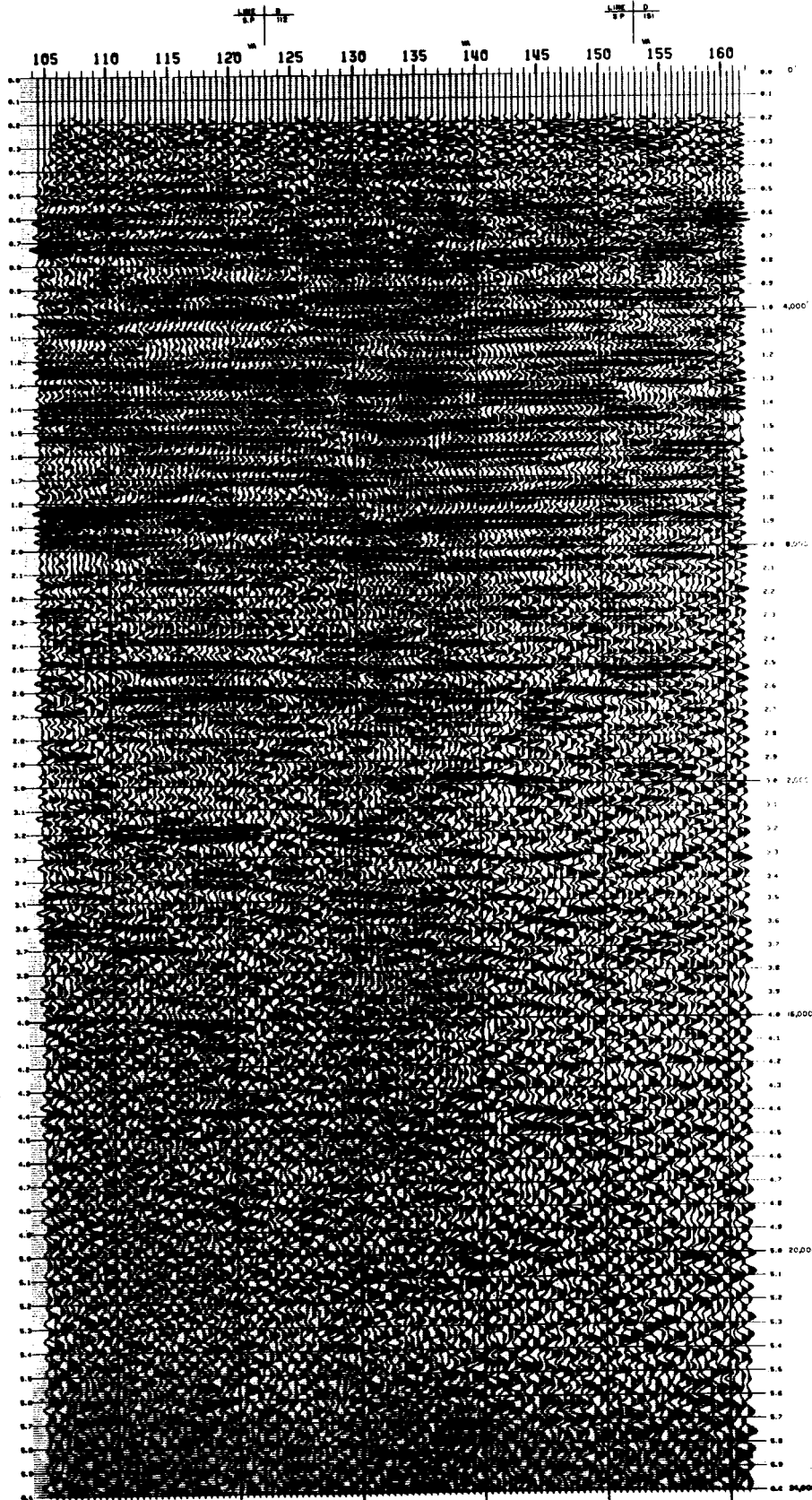
**PROFESSIONAL GEOPHYSICS, INC.**  
NEW ORLEANS, LOUISIANA



**Plate 3c**



SOUTHEAST



**LINE C**  
**LAFOURCHE CROSSING**

LAFOURCHE PARISH, LOUISIANA  
 AND  
 TERREBOONE PARISH, LOUISIANA  
 2 1/2 MILES E OF VERDEGIS  
 S.P. 10N M S.P. 182 SE

**L.S.U.**

**RECORDING INFORMATION**

SHOT BY: PALDIN GEOPHYSICAL CORP.  
 SHEEP LENGTH: 20 SEC.  
 PILOT FREQUENCY: 18-40 HZ.  
 GROUP INTERVAL: 330 FT.  
 S.P. INTERVAL: 530 FT.  
 SPREAD: 1000-1000-0-1000-1000 FT.  
 INSTRUMENTS: MS-10 16-CHANNEL  
 RECORD LENGTH: 6 SEC.  
 SAMPLE RATE: 4 HZ.  
 DATE RECORDED: AUGUST, 1981

**PROCESSING INFORMATION**

1. DEMULTIPLIER
2. COMMON DEPTH POINT GATHER  
 DATUM: SEA LEVEL  
 CORR. VELOCITY: 5000 FT./SEC.
3. DECONVOLUTION: 200 MS. OPERATOR  
 HARKER WINDOW: 1150-3.000 SEC.
4. FILTER: 10/12-60/42 HZ.
5. VELOCITY ANALYSIS  
 CONSTANT VELOCITY STACK
6. NORMAL MOVEOUT CORRECTIONS
7. MUTE
8. AUTOMATIC WIGGLER STATICS  
 1) TRACE PILOT  
 WINDOW: 0.000-3.000 SEC.
9. STACK
10. FILTER: 10/12-36/30 HZ.
11. AGC: 500 MS. WINDOW
12. DEPTH CONVERSION

**VELOCITY FUNCTION**

TIME	VELOCITY
0.000	5000
0.500	6000
1.000	6375
1.500	6750
2.000	7000
2.500	7200
3.000	7350
3.500	7500
4.000	7600
4.500	7700
5.000	7700

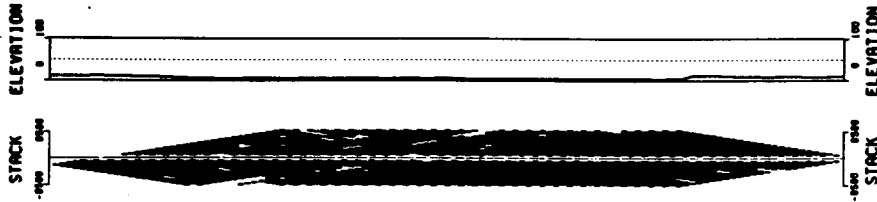
**PHOTOGRAPHY**

9 TRACES/INCH 5 INCHES/SECOND  
 CLIENT NO. 136 REEL NO. K 1893  
 SEPTEMBER, 1981 POLARITY: NORMAL  
 QUALITY CONTROLLED BY: RJD

PROFESSIONAL GEOPHYSICS, INC.  
 NEW ORLEANS, LOUISIANA

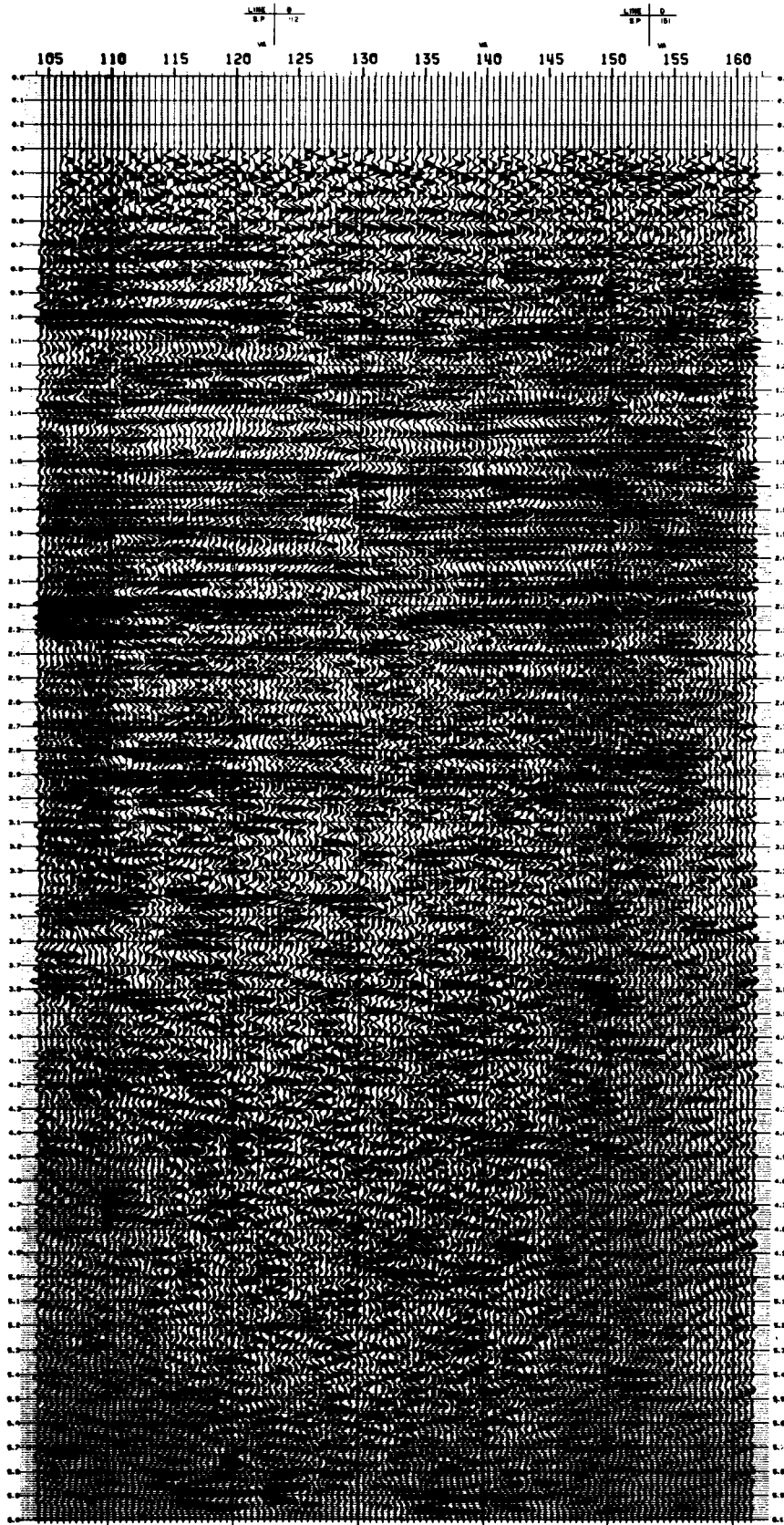


**Plate 3d**



115k

**SOUTHEAST**



**LINE C**  
**LAFORCHE CROSSING**

LAFORCHE PARISH, LOUISIANA  
AND  
TERREBORE PARISH, LOUISIANA  
7N-FIELD VIBROSEIS  
S.P. 124 NE S.P. 152 SE

**L.S.U.**

**RECORDING INFORMATION**

SHOT BY: PALGEM GEOPHYSICAL CORP.  
SWEEP LENGTH: 20 SEC.  
PILOT FREQUENCY: 10-40 Hz.  
GROUP INTERVAL: 300 FT.  
S.P. INTERVAL: 300 FT.  
SPREAD: 800-800-0-800-800 FT.  
INSTRUMENTS: VES-10 40-CHANNEL  
RECORD LENGTH: 6 SEC.  
SAMPLE RATE: 4 Hz.  
DATE RECORDED: AUGUST, 1991

**PROCESSING INFORMATION**

1. DEMULTIPLY
2. COMMON DEPTH POINT OTHER  
DATA: SEA LEVEL  
CORR. VELOCITY: 8000 FT./SEC.
3. DECONVOLUTION: 200 MS. OPERATOR  
TAPERED WINDOW: 1.100-3.000 SEC.
4. FILTER: 10/12-80/60 Hz.
5. VELOCITY ANALYSIS  
CONSTANT VELOCITY STACK  
8. NORMAL MOVEOUT CORRECTIONS
7. MUTE
8. AUTOMATIC RESIDUAL STATICS  
11. TRACE PILOT  
WINDOW: 0.800-3.000 SEC.
9. STACK
10. FILTER: 10/12-30/40 Hz.
11. AGC: 800 MS. WINDOW
12. NWC EQUATION ALIGNMENT

**VELOCITY FUNCTIONS**

SP 125		SP 130	
TIME	VELOCITY	TIME	VELOCITY
0.000	8000	0.000	8000
0.725	6275	0.625	6300
1.000	6000	1.100	6000
1.200	6000	1.400	6000
1.600	6000	1.800	7000
1.700	7000	2.200	6100
2.275	7000	2.700	6400
2.800	7000	3.200	6700
3.100	6000	3.600	6200
4.400	6000	6.000	6000
6.000	6000		

SP 155	
TIME	VELOCITY
0.000	8000
0.800	6000
1.000	6300
1.400	6000
1.800	7100
2.100	7000
2.400	7000
2.800	6150
3.800	6000
6.000	6000

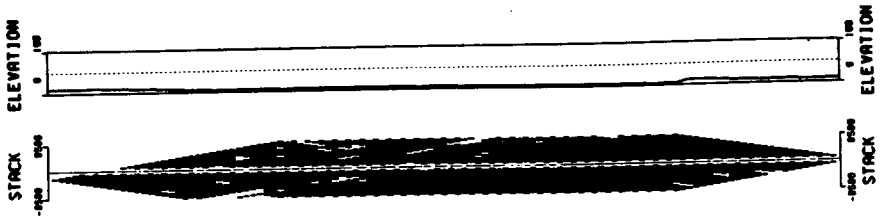
**PHOTOGRAPHY**

8 TRACES/INCH      5 INCHES/SECOND  
CLIENT NO. 138      REEL NO. 2-2100  
SEPTEMBER, 1991      POLARITY: NORMAL  
QUALITY CONTROLLED BY: P.J.D.

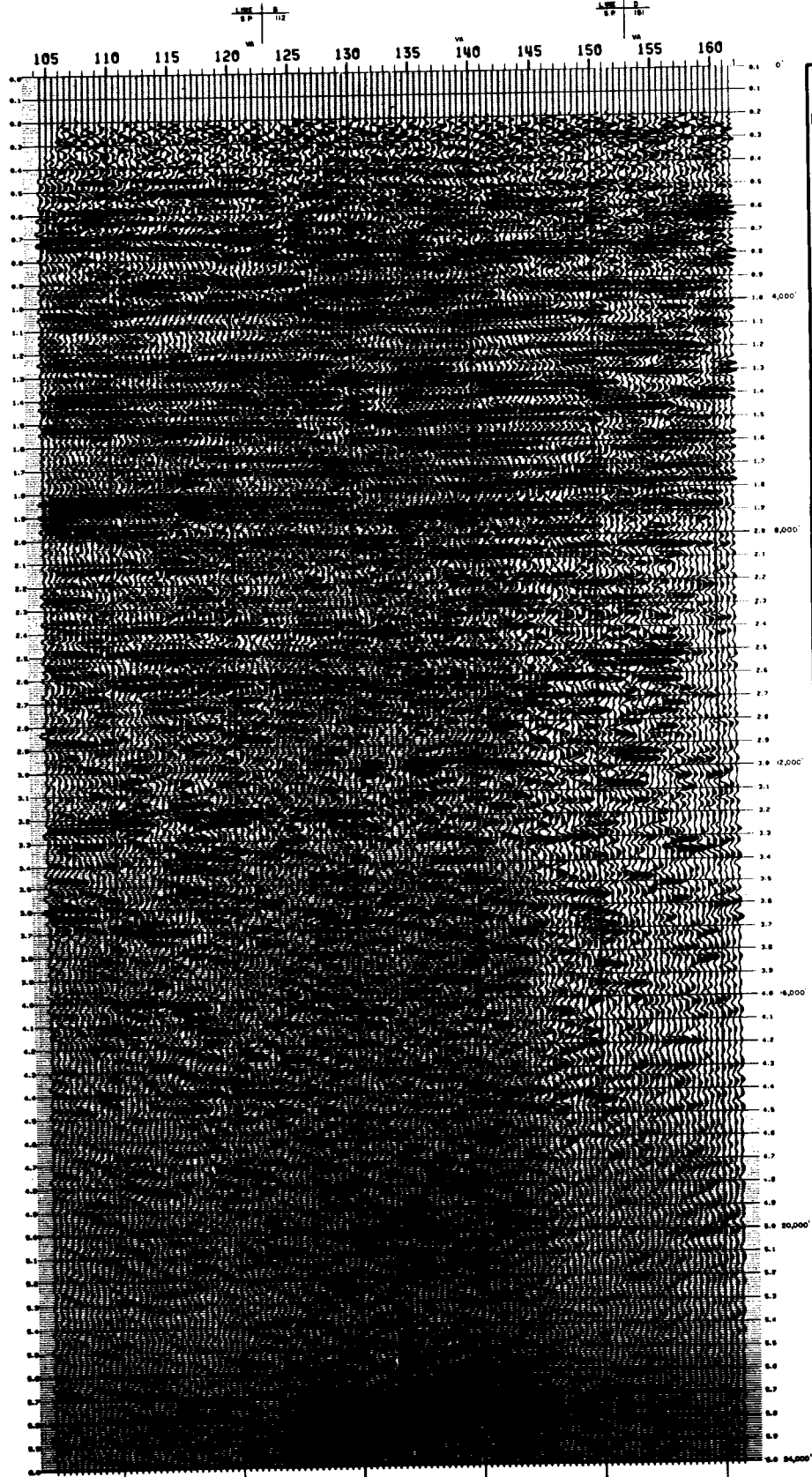
**PROFESSIONAL GEOPHYSICS, INC.**  
NEW ORLEANS, LOUISIANA



**Plate 3e**



SOUTHEAST



**LINE C  
LAFOURCHE CROSSING**

LAFOURCHE PARISH, LOUISIANA  
 AND  
 TERREBOONE PARISH, LOUISIANA  
 2N-FOLD VIBROSETS  
 S.P. 104 NS S.P. 152 SE

**L.S.U.**

**RECORDING INFORMATION**

SHOT BY: PALMOUTH GEOPHYSICAL CORP.  
 SHEEP LENGTH: 20 SEC.  
 PULSAR FREQUENCY: 10-40 HZ.  
 GROUP INTERVAL: 330 FT.  
 S.P. INTERVAL: 330 FT.  
 SPREAD: 6000-300-0-300-6000 FT.  
 INSTRUMENTS: 405-10 40-CHANNEL  
 RECORD LENGTH: 6 SEC.  
 SAMPLE RATE: 4 MS  
 DATE RECORDED: AUGUST, 1961

**PROCESSING INFORMATION**

1. DEMULTIPLY
2. COMMON DEPTH POINT GATHER  
 ORIGIN: SEA LEVEL  
 CORR. VELOCITY: 5000 FT./SEC.
3. DECONVOLUTION: 200 MS. OPERATOR  
 TAPERED WINDOW: 1.150-3.800 SEC.
4. FILTER: 10/12-40/42 HZ.
5. VELOCITY ANALYSIS  
 CONSTANT VELOCITY STACK
6. NORMAL MOVEOUT CORRECTIONS
7. MUTE
8. AUTOMATIC RESIDUAL STATISTICS  
 1) TRACE PULSAR WINDOW: 0.600-3.600 SEC.
9. STACK
10. FILTER: 10/12-36/40 HZ.  
 1) AGE: 500 MS. WINDOW
12. WAVE EQUATION MIGRATION
13. DEPTH CONVERSION

**VELOCITY FUNCTION**

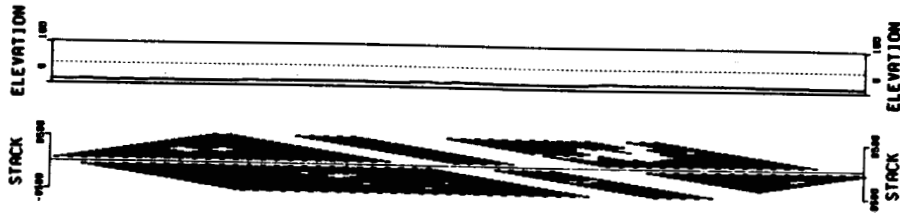
TIME	VELOCITY
0.000	5500
0.550	6000
1.000	6375
1.500	6750
1.625	7000
2.000	7400
2.500	7800
3.150	8250
3.700	8600
4.700	8950
6.000	9700

**PHOTOGRAPH**

8 TRACES/INCH 5 INCHES/SECOND  
 CLIENT NO. 136 REEL NO. X 1337  
 SEPTEMBER, 1961 PALMOUTH, NORMAL  
 QUALITY CONTROLLED BY P.J.D.

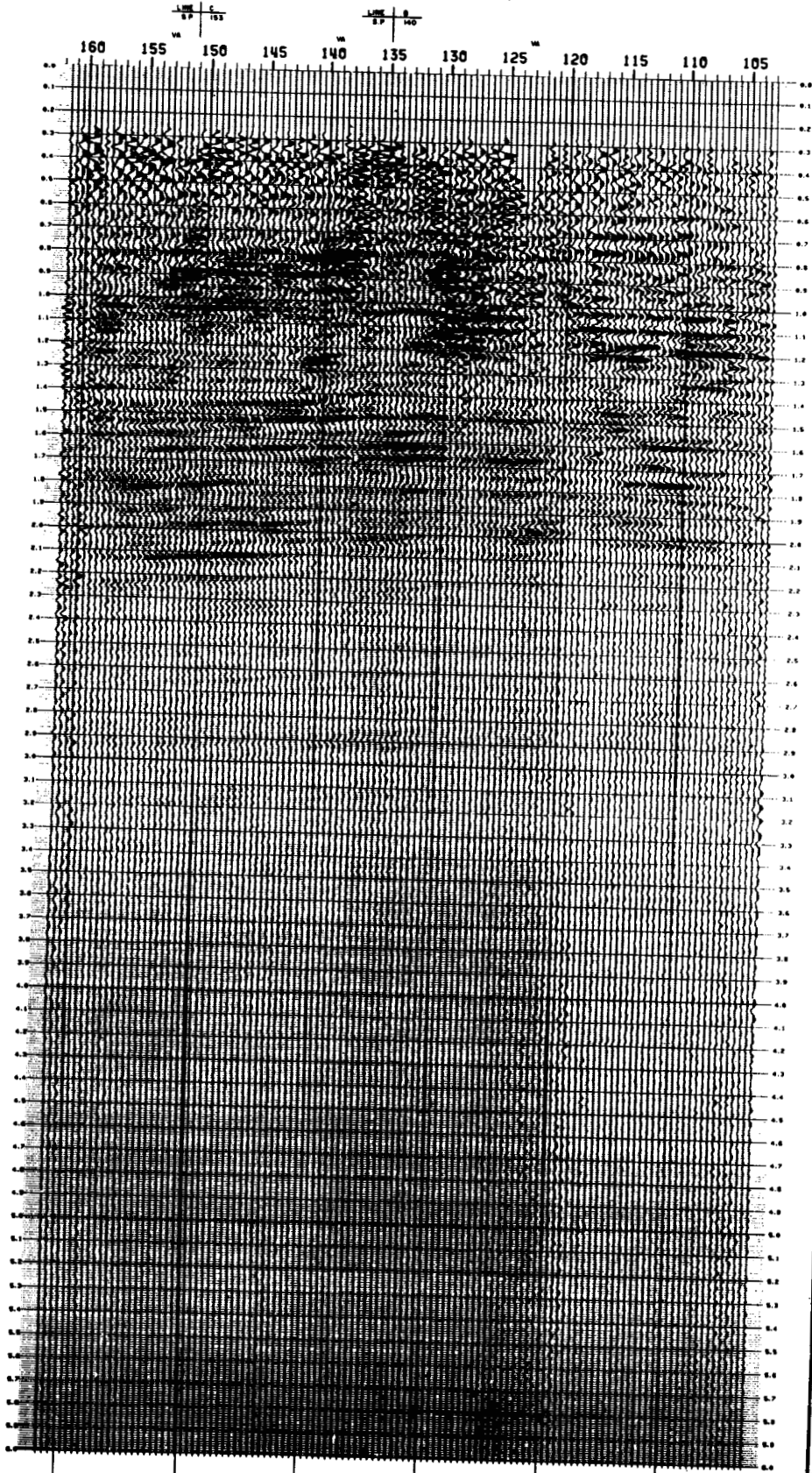
PROFESSIONAL GEOPHYSICS, INC.  
 NEW ORLEANS, LOUISIANA





115m

NORTHEAST



**LINE D**  
**LAFORCHE CROSSING**

LAFORCHE PARISH, LOUISIANA  
 AND  
 TERREBONE PARISH, LOUISIANA  
 24-FOLD VIBROSEIS  
 S.P. 102 SW S.P. 103 NE

**L.S.U.**

**RECORDING INFORMATION**

SHOT BY: POLARON GEOPHYSICAL CORP.  
 SHEEP LENGTH: 30 SEC.  
 PILOT FREQUENCY: 10-40 HZ.  
 GROUP INTERVAL: 330 FT.  
 S.P. INTERVAL: 330 FT.  
 SPREAD: 8500-990-0-990-8500 FT.  
 INSTRUMENTS: NIS-10 48-CHANNEL  
 RECORD LENGTH: 6 SEC.  
 SAMPLE RATE: 4 MS.  
 DATE RECORDED: AUGUST, 1981

**PROCESSING INFORMATION**

1. DEMULTIPLIER
2. COMMON DEPTH POINT GATHER  
 DRIFT: SEA LEVEL  
 COMP. VELOCITY: 5500 FT./SEC.
3. DECONVOLUTION: 200 MS. OPERATOR  
 TAPERED WINDOW: 1.150-3.000 SEC.
4. FILTER: 10/12-10/42 HZ.
5. VELOCITY ANALYSIS  
 CONSTANT VELOCITY STACK
6. NORMAL MOVEOUT CORRECTIONS
7. MUTE
8. AUTOMATIC RESIDUAL STATICS  
 11 TRACE PILOT  
 WINDOW: 0.600-3.000 SEC.
9. STACK
10. FILTER: 10/12-36/40 HZ.

**VELOCITY FUNCTION**

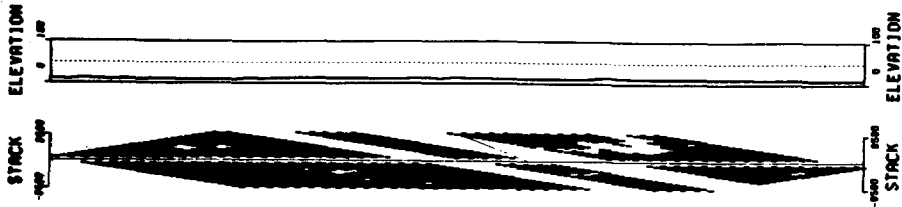
TIME	VELOCITY
0.000	5500
0.000	6000
1.250	6000
1.500	6950
1.800	7250
2.050	7400
2.375	7700
2.800	8300
3.450	8750
4.100	9075
6.000	9000

**PHOTOGRAPHY**

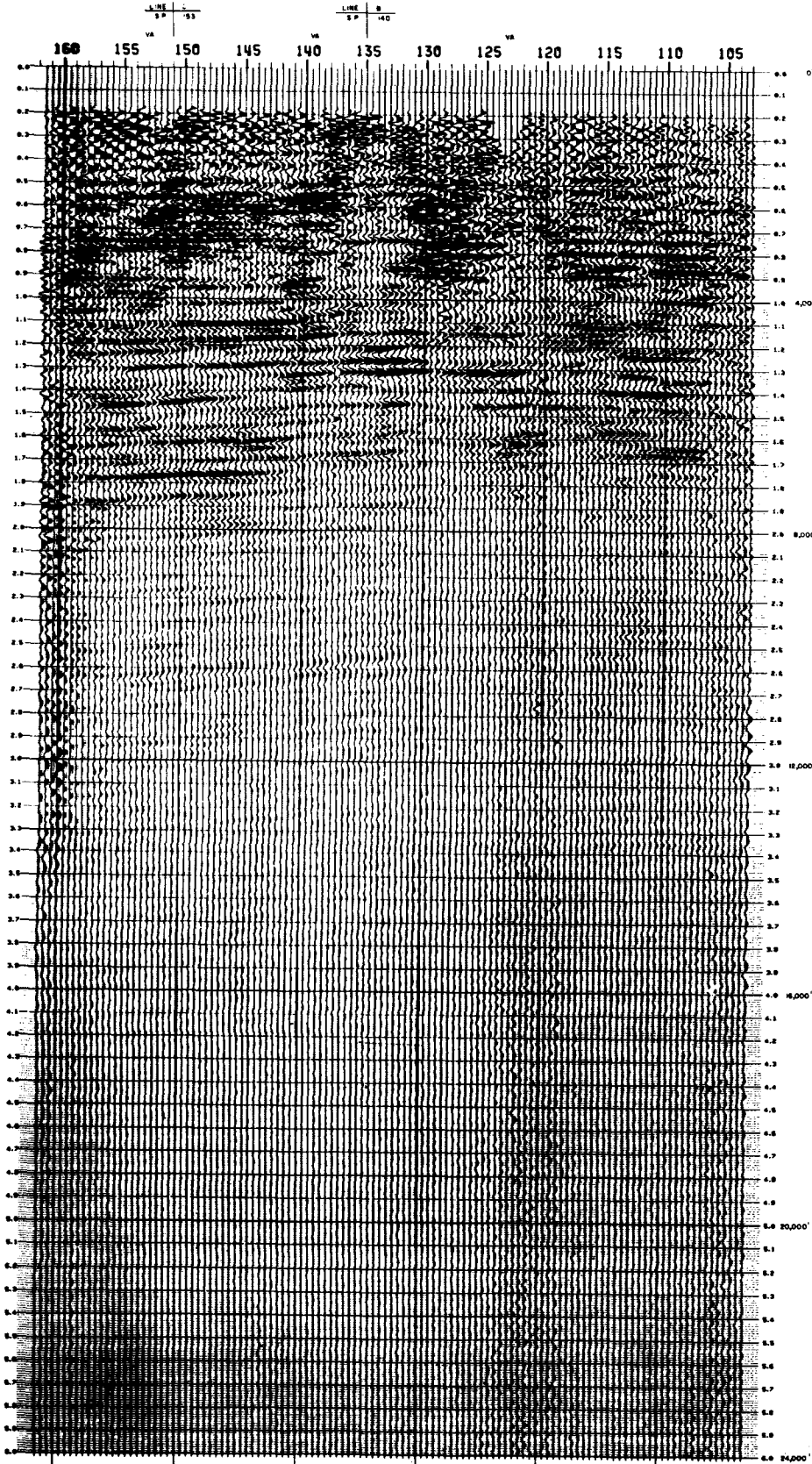
8 FRAMES-INCH      5 INCHES-SECOND  
 CLIENT NO. 136      REEL NO. 3 2350  
 SEPTEMBER, 1981      POLARITY: NORMAL  
 QUALITY CONTROLLED BY: RJD

**PROFESSIONAL GEOPHYSICS, INC.**  
 NEW ORLEANS, LOUISIANA





NORTHEAST



**LINE D**  
**LAFORCHE CROSSING**

LAFORCHE PARISH, LOUISIANA  
AND  
TERREBORE PARISH, LOUISIANA  
2N-PALO VIBROREIS  
S.P. 162 SH S.P. 163 ME  
**L.S.U.**

**RECORDING INFORMATION**

SHOT BY: PROFESSIONAL GEOPHYSICAL CORP.  
SWEEP LENGTH: 20 SEC.  
PILOT FREQUENCY: 10-40 HZ.  
GROUP INTERVAL: 330 FT.  
S.P. INTERVAL: 330 FT.  
SPREAD: 6500-680-0-680-6500 FT.  
INSTRUMENTS: VIB-16 40-COMPAK  
RECORD LENGTH: 6 SEC.  
SAMPLE RATE: 4 MS.  
DATE RECORDED: AUGUST, 1991

**PROCESSING INFORMATION**

1. DEMULTIPLY
2. CORRECT DEPTH POINT GATHER  
DATA: SEA LEVEL  
CORR. VELOCITY: 8000 FT./SEC.
3. DECONVOLUTION: 200 MS. OPERATOR  
TIMPARED WINDOW: 1.150-3.000 SEC.
4. FILTER: 10/12-30/VA HZ.
5. VELOCITY ANALYSIS  
CONSTANT VELOCITY STACK
6. NORMAL MOVEOUT CORRECTIONS
7. MUTE
8. AUTOMATIC RESIDUAL STATISTICS  
10 TRACE PILOT  
WINDOW: 0.800-3.000 SEC.
9. STACK
10. FILTER: 10/12-30/VA HZ.
11. DEPTH CONVERSION

**VELOCITY FUNCTION**

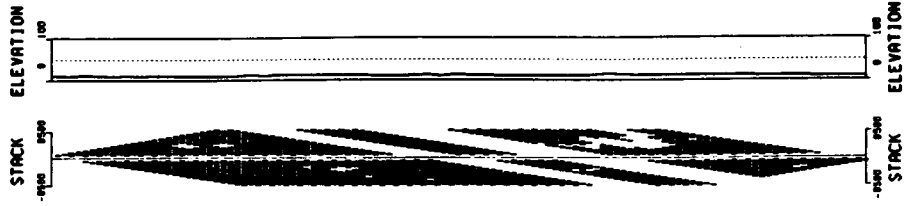
TIME	VELOCITY
0.000	5000
0.500	6000
1.000	6375
1.500	6700
1.875	7000
2.000	7400
2.500	7800
3.100	8200
3.700	8600
4.300	8950
5.000	9700

**PHOTOGRAPHY**

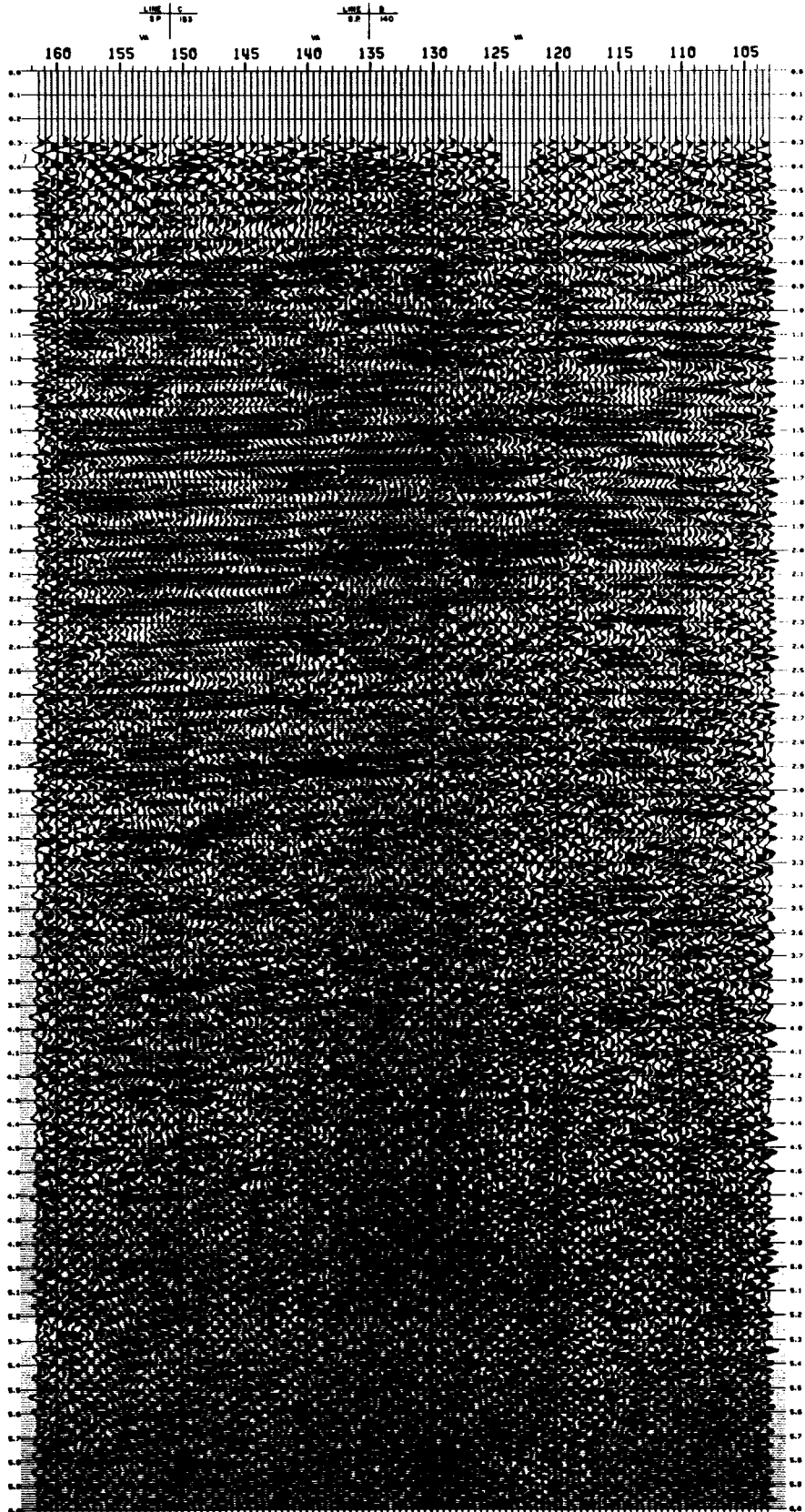
4 TRACES/INCH      5 INCHES/SECOND  
CLIENT NO. 138      REEL NO. P-1795  
SEPTEMBER, 1991      POLARITY: NORMAL  
QUALITY CONTROLLED BY: RJD

**PROFESSIONAL GEOPHYSICS, INC.**  
NEW ORLEANS, LOUISIANA

**Plate 4b**



NORTHEAST



**LINE D**  
**LAFORCHE CROSSING**

LAFORCHE PARISH, LOUISIANA  
AND  
TERREBOUNE PARISH, LOUISIANA  
24-FOLD VIBROSEIS  
S.P. 162 SW S.P. 105 NE

**L.S.U.**

**RECORDING INFORMATION**

SHOT BY: PALMUM GEOPHYSICAL CORP.  
SHEET LENGTH: 20 SEC.  
PILOT FREQUENCY: 10-40 HZ.  
GROUP INTERVAL: 330 FT.  
S.P. INTERVAL: 330 FT.  
SPREAD: 9500-990-0-990-9500 FT.  
INSTRUMENTS: 105-10 40-CHANNEL  
RECORD LENGTH: 6 SEC.  
SAMPLE RATE: 4 MS.  
DATE RECORDED: AUGUST, 1981

**PROCESSING INFORMATION**

1. DEMULTIPLY
2. COMMON DEPTH POINT GATHER  
DATA: SEA LEVEL  
CORP. VELOCITY: 5000 FT./SEC.
3. DECONVOLUTION: 200 MS. OPERATOR  
TAPERED WINDOW: 1.150-3.000 SEC.
4. FILTER: 10/12-80/12 HZ.
5. VELOCITY ANALYSIS  
CONSTANT VELOCITY STACK
6. NORMAL MOVEOUT CORRECTIONS
7. MUTE
8. AUTOMATIC RESIDUAL STATICS  
1) TRACE PILOT  
WINDOW: 0.000-3.000 SEC.
9. STACK
10. FILTER: 10/12-30/10 HZ.
11. REC: 500 MS. WINDOW

**VELOCITY FUNCTION**

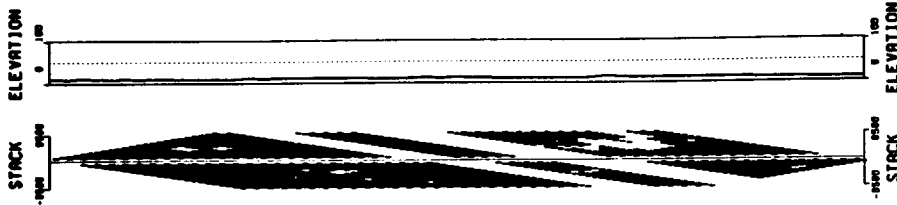
TIME	VELOCITY
0.000	5500
0.500	6050
1.250	6800
1.500	6950
1.800	7250
2.050	7600
2.375	7700
2.900	8300
3.450	8750
4.100	9050
5.000	9800

**PHOTOGRAPHY**

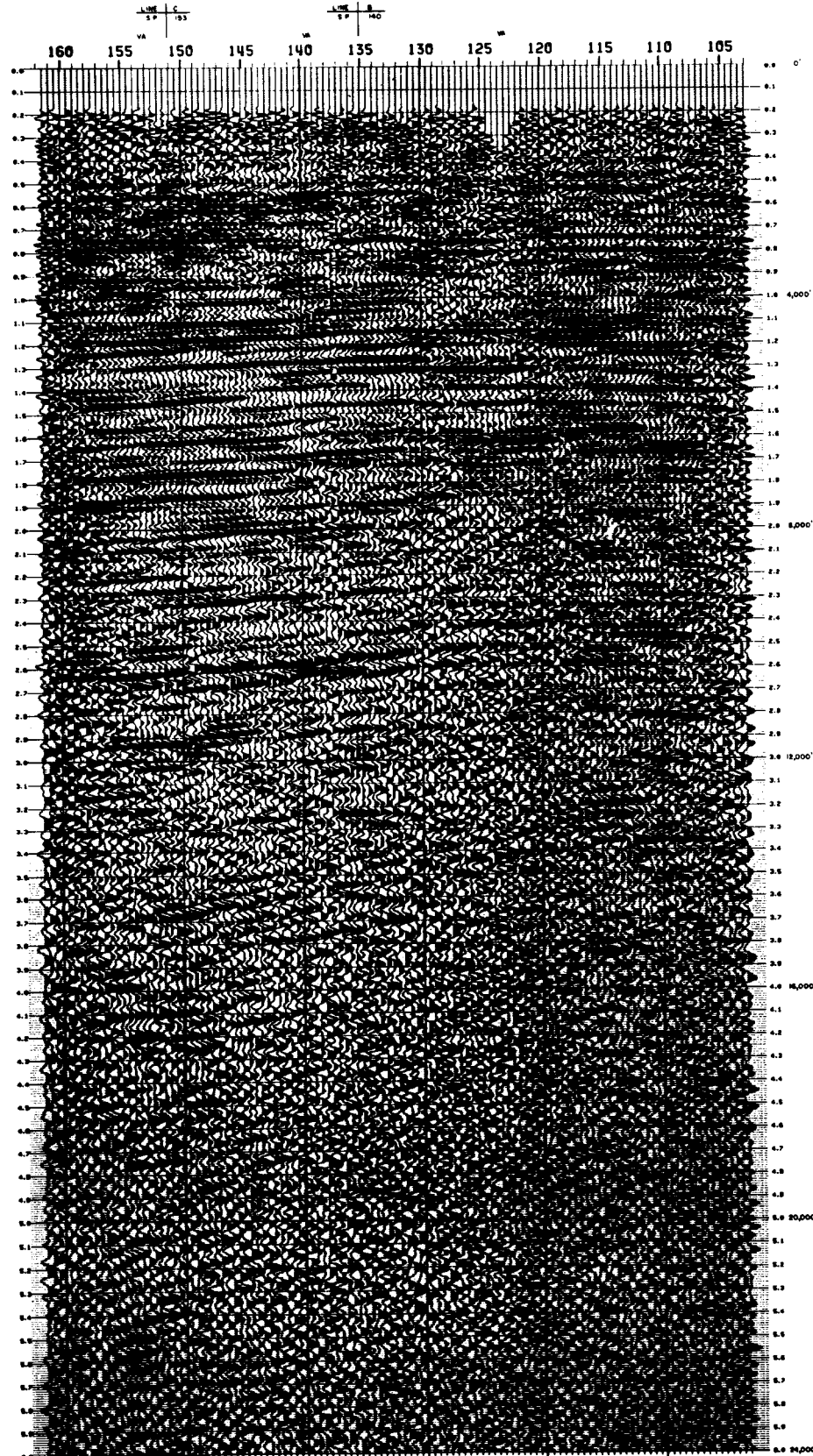
8 TRACES/INCH      5 INCHES/SECOND  
CLIENT NO. 136      REEL NO. R 1800  
SEPTEMBER, 1981      POLARITY: NORMAL  
QUALITY CONTROLLED BY: R.D.

**PROFESSIONAL GEOPHYSICS, INC.**  
NEW ORLEANS, LOUISIANA

**Plate 4c**



NORTHEAST



**LINE D**  
**LAFORCHE CROSSING**

LAFORCHE PARISH, LOUISIANA  
AND  
TERREBORE PARISH, LOUISIANA  
24-FOLD VIBROSEIS  
S.P. 182 SH S.P. 103 NE

**L.S.U.**

**RECORDING INFORMATION**

SHOT BY: PALMCOIN GEOPHYSICAL CORP.  
SHOT LENGTH: 20 SEC.  
PILOT FREQUENCY: 10-40 HZ.  
GROUP INTERVAL: 330 FT.  
S.P. INTERVAL: 330 FT.  
SPREAD: 6000-1800-0-1800-6000 FT.  
INSTRUMENTS: MDS-10 48-CHANNEL  
RECORD LENGTH: 6 SEC.  
SAMPLE RATE: 4 MS  
DATE RECORDED: AUGUST, 1981

**PROCESSING INFORMATION**

1. DEMULTIPLIER
2. COMMON DEPTH POINT GATHER  
DATA: SEA LEVEL  
CORR. VELOCITY: 5500 FT./SEC.
3. DECONVOLUTION: 200 MS. OPERATION  
TIMBER HINCH: 1.150-3.800 SEC.
4. FILTER: 10/12-40/42 HZ.
5. VELOCITY ANALYSIS  
CONSTANT VELOCITY STACK
6. NORMAL MOVEOUT CORRECTIONS
7. MUTI
8. AUTOMATIC RESIDUAL STATICS  
11 TRACE PILOT  
MINIMUM: 0.600-3.800 SEC.
9. STACK
10. FILTER: 10/12-36/40 HZ.
11. HCC: 500 MS; HINCH
12. DEPTH CORRECTION

**VELOCITY FUNCTION**

TIME	VELOCITY
0.000	5000
0.950	6000
1.000	6375
1.300	6700
1.625	7000
2.000	7400
2.950	7800
3.150	8250
3.700	8600
4.350	8950
6.000	9700

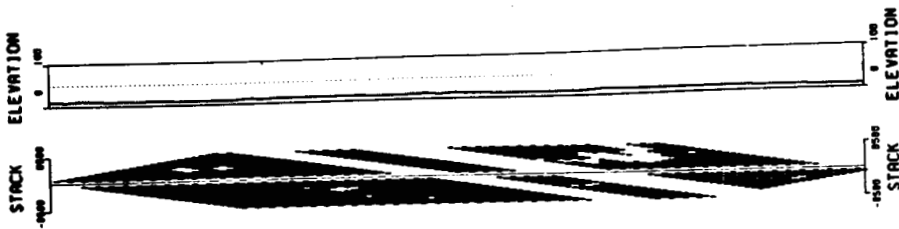
**PHOTOGRAPHY**

6 TRACES/INCH      5 INCHES/SECOND  
CLIENT NO. 136      REEL NO. 1281  
SEPTEMBER, 1981      POLARITY: NORMAL  
QUALITY CONTROLLED BY: RJD

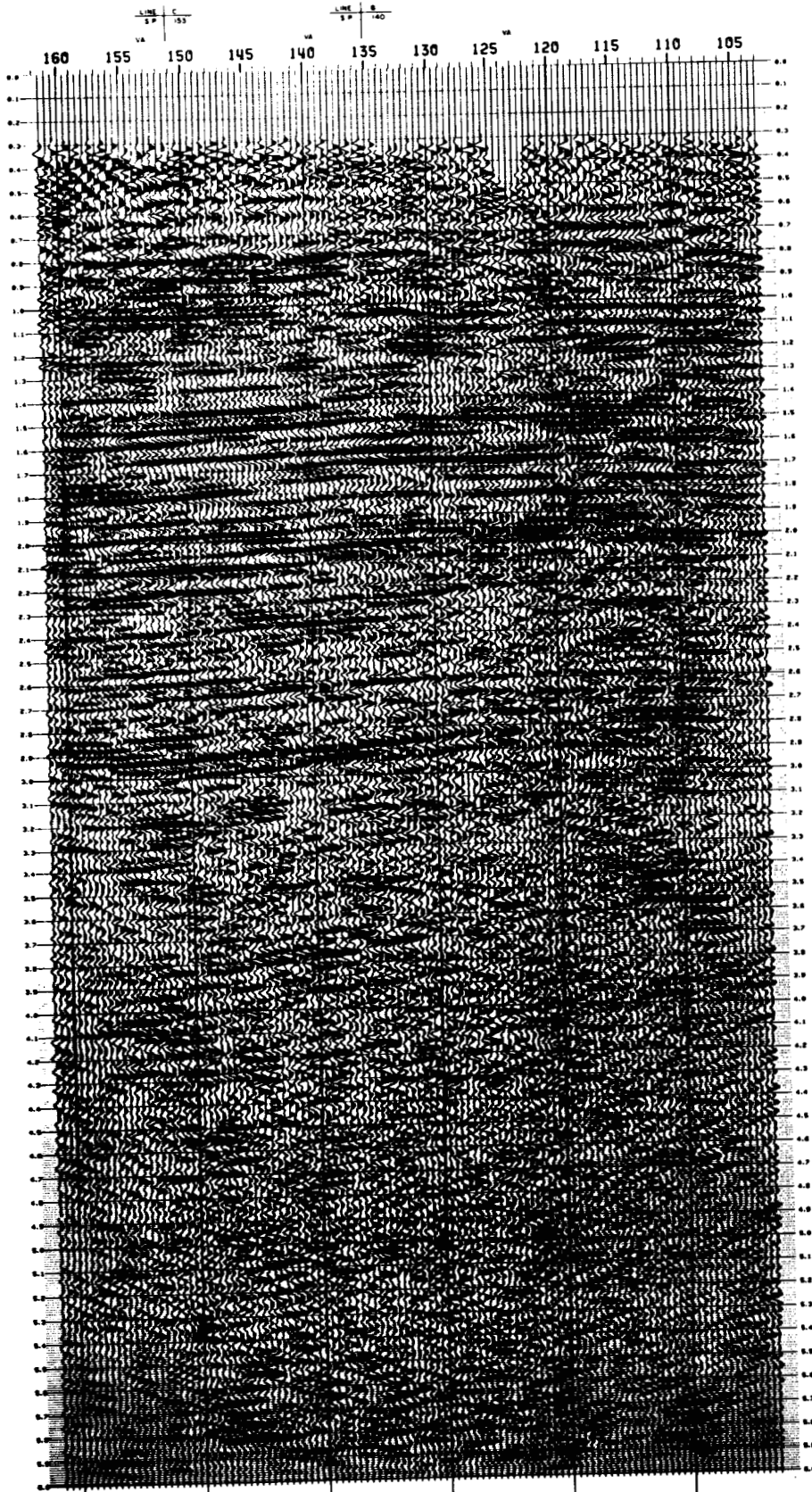
**PROFESSIONAL GEOPHYSICS, INC.**  
NEW ORLEANS, LOUISIANA



**Plate 4d**



NORTHEAST



LINE D  
LAFOURCHE CROSSING

LAFOURCHE PARISH, LOUISIANA  
AND  
TERREBOUNE PARISH, LOUISIANA  
24-FOLD VIBROSEIS  
S.P. 162 SW S.P. 105 NE

L.S.U.

RECORDING INFORMATION

SHOT BY: PALMCOIN GEOPHYSICAL CORP.  
SHOOT LENGTH: 20 SEC.  
PULSITY FREQUENCY: 10-40 HZ.  
GROUP INTERVAL: 330 FT.  
S.P. INTERVAL: 330 FT.  
SPREAD: 8000-9000-0-800-9000 FT.  
INSTRUMENTS: MDS-10 48-CANAL  
RECORD LENGTH: 6 SEC.  
SAMPLE RATE: 4 MS.  
DATE RECORDED: AUGUST, 1981

PROCESSING INFORMATION

1. REMULTIPLIER
2. COMMON DEPTH POINT GATHER  
ORIGIN: SEA LEVEL  
CORR. VELOCITY: 5000 FT./SEC.
3. DECONVOLUTION: 200 MS. OPERATOR  
FILTERED MINIMAL: 1.750-3.000 SEC.
4. FILTER: 10/12-45/42 HZ.
5. VELOCITY ANALYSIS  
CONSTANT VELOCITY STACK
6. NORMAL MOMENT CORRECTIONS
7. NOTE
8. AUTOMATIC RESIDUAL STATISTICS  
a) TRACE PLOT  
RANGE: 0.000-3.000 SEC.
9. STACK
10. FILTER: 10/12-30/40 HZ.
11. REC.: 500 MS. W/NOISE
12. WAVE EQUATION MIGRATION

VELOCITY FUNCTION

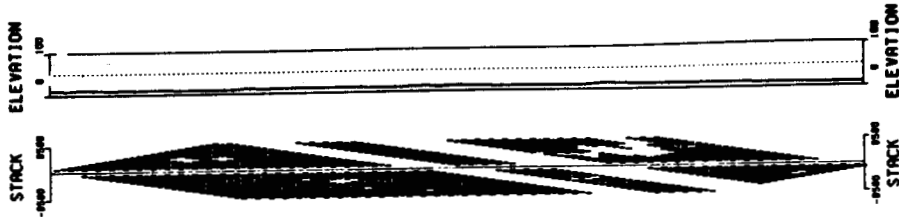
TIME	VELOCITY
0.000	5000
0.800	8050
1.200	8000
1.500	6950
1.800	7250
2.000	7000
2.375	7700
2.800	8300
3.400	8750
4.100	8500
5.000	8000

PHOTOGRAPH

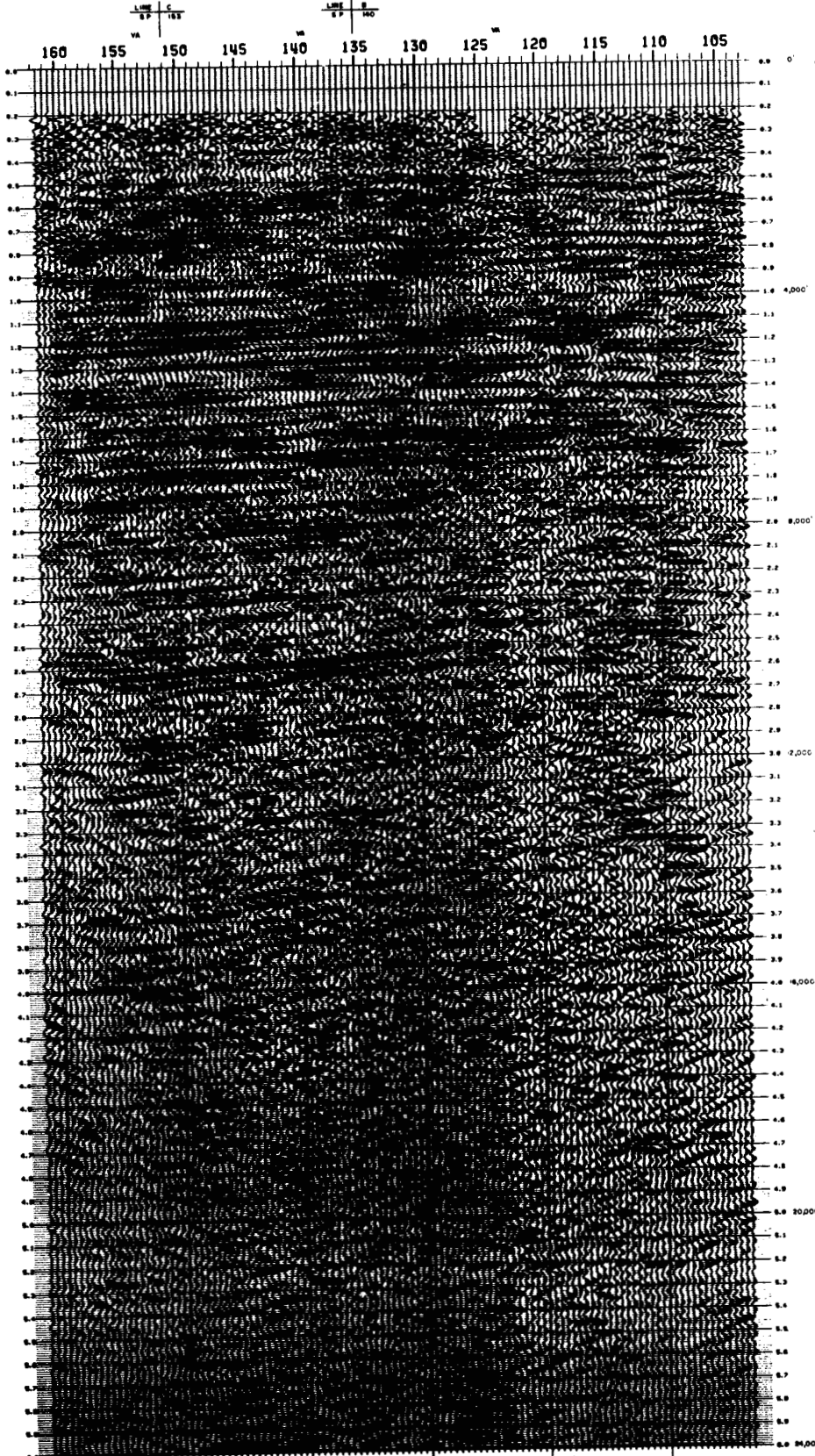
8 TRACES/INCH 5 INCHES/SECOND  
CLIENT NO. 136 REEL NO. P 2140  
DEPTH/TRACE: 100 POLARITY: NORMAL  
QUALITY CONTROLLED BY: RJD

PROFESSIONAL GEOPHYSICS, INC.  
NEW ORLEANS, LOUISIANA





NORTHEAST



**LINE D  
LAFORCHE CROSSING**

LAFORCHE PARISH, LOUISIANA  
 TERREBOINE PARISH, LOUISIANA  
 24-FOLD VIBROSEIS  
 S.P. 152 SW S.P. 103 NE

**L. S. U.**

**RECORDING INFORMATION**

SHOT BY: PALDIN GEOPHYSICAL CORP.  
 SWEEP LENGTH: 20 SEC.  
 PILOT FREQUENCY: 10-40 HZ.  
 GROUP INTERVAL: 350 FT.  
 S.P. INTERVAL: 350 FT.  
 SPREAD: 8500-8800-0-8800-8500 FT.  
 INSTRUMENTS: RDS-10 40-COMMEL  
 RECORD LENGTH: 6 SEC.  
 SAMPLE RATE: 4 MS.  
 DATE RECORDED: AUGUST, 1981

**PROCESSING INFORMATION**

1. DEMULTIPLIER
2. COMMON DEPTH POINT GATHER  
 ORIGIN: SEA LEVEL  
 CORR. VELOCITY: 9500 FT./SEC.
3. DECONVOLUTION: 200 MS. OPERATOR  
 TAPERED WINDOW: 1-150-3,000 SEC.
4. FILTER: 10/12-36/40 HZ.
5. VELOCITY ANALYSIS  
 CONSTANT VELOCITY STACK  
 NORMAL MOVEOUT CORRECTIONS
6. AUTOMATIC RESIDUAL STACKS  
 1) TRACE PILOT  
 WINDOW: 0.000-3,000 SEC.
7. MUTE
8. STACK
9. FILTER: 10/12-36/40 HZ.
10. AGC: 500 MS. WINDOW
11. WAVE EQUATION MIGRATION
12. DEPTH CONVERSION

**VELOCITY FUNCTION**

TIME	VELOCITY
0.000	5500
0.550	6000
1.000	6375
1.500	6700
1.625	7000
2.000	7200
2.500	7500
3.150	8070
3.700	8600
4.200	9000
6.000	9700

**PHOTOGRAPHY**

8 TRACES/INCH      5 INCHES/SECOND  
 CLIENT NO. 136      REEL NO. P 1347  
 SEPTEMBER, 1981      POLARITY: NORMAL  
 QUALITY CONTROLLED BY: RJD

**PROFESSIONAL GEOPHYSICS, INC.**  
 NEW ORLEANS, LOUISIANA



**Plate 4f**

GEOPRESSURE AND DIAGENETIC MODIFICATIONS OF  
POROSITY IN THE LIRETTE FIELD AREA, TERREBONNE  
PARISH, LOUISIANA

Leigh Anne Flournoy and Ray E. Ferrell, Jr.

ABSTRACT

A study of temperature, pressure, and salinity distribution in the Lirette Field reveals important information concerning the effects of the hydrodynamic regime of sandstone diagenesis. The Lirette Field is a large domal structure related to deep-seated salt (approximately 20,000 feet), bounded to the north and south by major growth faults. Isothermal surfaces in the Lirette Field closely follow the structure. Isotherms commonly drop in down-thrown fault blocks. Along fault leakage zones, temperatures increase. Pressure distribution in the Lirette Field is primarily related to structure and the presence of a sufficient shale to sand ratio. Formation water salinities are lower (50,000 ppm) for wells that have been "flushed" by geopressured waters.

Sandstone diagenesis in the Lirette Field is complex and there are significant lateral and vertical variations. The relative sequence of diagenetic events in Lirette sands is as follows: (1) spherulitic calcite cement, probably formed at or near the sediment-water interface; (2) authigenic chlorite rims and platelets, which help to preserve primary porosity; (3) quartz and feldspar overgrowths, uncommon; (4) ferroan calcite cement; (5) dissolution of carbonate and formation of secondary porosity; and (6) authigenic kaolinite cement, which reduces porosity along fluid escape routes. Late stage kaolinite cement is more extensively developed in flushed zones near faults.

## INTRODUCTION

Geopressures have been recognized for almost thirty years in the Gulf Coast. As play an important role in the search for hydrocarbons, an understanding of their distribution and origin is vital in the petroleum industry. Jones (1977) and many other authors have related the abnormally high fluid pressures to temperature and salinity anomalies, clay mineral diagenesis, growth faulting, hydrocarbon occurrences, kerogen maturation, and the development of secondary porosity in sandstone reservoirs. Mumme and Ferrell (1979) demonstrated how a detailed analysis of structure, geopressure, salinity, and temperature could be used in the Houma-Hollywood field to identify the potential routes of fluid escape from the geopressured zone to hydro pressured reservoirs.

This study used similar methods to trace potential routes of fluid escape in the Lirette Field of South Louisiana. In addition, we tried to explain how sandstone porosities and the general diagenetic sequence have been modified by the migrating fluids. It will demonstrate that probable migration paths probably can be established and flushing may reduce porosity by creation conditions favorable for the precipitation of kaolinite.

## LOCATION AND GEOLOGIC SETTING

The Lirette field is located in the coastal marshes of Terrebonne Parish, Louisiana (T19S, R19E) approximately 42 miles (6 km) southwest of New Orleans (Fig. 1). Lirette lies between the Montegut Field to the north and the Bay Baptiste field to the south. Some of the gas and condensate-producing zones are at depths greater than 10,000 feet below sea level. The field is approximately four miles west of the Tenneco Fee "N" No. 1 well, which was to be evaluated as a geothermal-geopressure-dissolved methane producer (Braden and Goode, 1979). The sediments encountered in the study area are predominantly from the inner and middle neritic sand-shale facies and the lowermost portions of the fluvio-deltiac facies. They were deposited on the fringe of the subsiding "Terrebonne Trough" during the Miocene (Limes and Stipes, 1959). A type log (after Silvernail, 1967) reveals the character of these deposits and the important depth-stratigraphic zones and micropaleontological marker zones. Bigererina A is encountered at 6,142 feet. Texturalia articulata (L) and Bigenerina 2 correlate with the 8,400 foot sand and the 10,250 foot sand, respectively. Textularia stapperi (W) is encountered at approximately 13,000 feet.

## METHODOLOGY

Data derived from geophysical well logs were used to construct the maps and salinity profiles described in this report. The methods employed to interpret the electric logs are the same as those reported by Mumme and Ferrell (1979). About 90 well logs from the locations indicated on Figure 1 were studied, 53 of them were from wells that were more locations indicated by the numbered dots in Figure 7. Representative sands were selected and about 75 were thin sectioned and analyzed

to develop the diagenetic sequence of alteration. Special attention was devoted to the analysis of samples from Wells 17 and 22.

#### STRUCTURE

The general domal structure of the Lirette Field area is illustrated in Figure 3, a structural contour map drawn on the top of the 11,500 foot sand. There is 300-350 feet of closure on the elongate structure and it is bounded by faults on the north (Fault X) and south (Fault Z) as well as a smaller one (Fault Y), which bisects the top of the main structural high. A smaller domal closure is associated with an antithetical fault in the northwestern corner of the area. The main faults have southerly dips between 55° and 65°. Fault X has a throw of approximately 1,100 feet at the 11,500 foot sand. The faults are probably part of the Golden Meadow Fault Zone of Murray (1957), and all structures are controlled by a deep-seated salt dome. Much of the movement along the fault was contemporaneous with sedimentation. Thorsen (1963) notes that a younger period of faulting (Bigenerina 2) which was superimposed on activity during Textularia W, responsible for the unusually high amounts of subsidence.

#### OCCURRENCE OF GEOPRESSURE

The top of the hard geopressure zone is defined as the depth where the 0.7 psi/ft fluid pressure gradient is first encountered. The configuration of this surface in the Lirette Field is illustrated in Figure 4. Hard geopressure is present at depths generally greater than 11,000 to 12,800 feet below sea level. In the northern and southern parts of the field shallow occurrences of hard geopressure generally correspond to structural highs. However, the principle structural high is a depressed area where hard pressure occurs at depths of approximately 12,000 feet.

There is also a northwesterly trending trough in the top of the zone extending from section 34 to section 23. The east-west elongation of the top of the hard geopressure in the vicinity of Fault Z suggests that this fault may be a more effective barrier to the migration of geopressured fluids than Faults Z and Y.

The transitional zone from fluid pressure gradients of 0.5 psi/ft to the hard geopressured zone is difficult to map in this area because sands are relatively more abundant near the top of the geopressured zone. In some areas the transition may occur within 200-300 feet, while in other areas the higher gradients are encountered in as much as 2,000 feet.

#### TEMPERATURE DISTRIBUTION

The main structural high generally corresponds to an area (Fig 5) where the 200°F isothermal surface occurs at the shallowest depth. Smaller areas of closure about highs in the isothermal surface appear to cluster near faults. Some straddle the fault while others do not. The former are interpreted as indicative of zones where the faults are leaking geopressured fluids. Areas of deepest occurrence of the 200°F isotherm are in sections 32 and 53.

#### SALINITY DISTRIBUTION

Salinity profiles in selected wells provide ways to assess the relative degree of fluid movement and flushing associated with geopressured zones. In Well 22 (Fig. 6), the salinity increases with increasing depth and then freshens markedly as the hard geopressured zone is approached. In Well 17 (Fig. 6), the formation water salinities are generally lower and the abrupt changes and increases with depth are not as evident. The sands in the latter well probably experienced a

greater degree of flushing than those in well 22.

#### FLUID ESCAPE ROUTES

Salinity profiles like those illustrated above and temperature distribution maps combined with structural interpretations are very useful in defining potential routes of fluid escape from the geopressed zone. Three areas of proposed leakage along the faults in the Lirette Field are illustrated in Figure 7. Only small portions of Faults X and Z appear to have been active, while Fault Y appears to have leaked along a major segment of its length. Well 17 is within a zone of leakage and Well 22 is about a mile from one. Within the formations the fluids may have migrated in the direction of the structural highs as indicated by the arrows.

#### SANDSTONE DIAGENESIS AND POROSITY

Middle and Upper Miocene sandstones in the Lirette Field are primarily subarkoses, with arkoses, lithic subarkoses, and lithic arkoses also present. Quartz is the most abundant framework grain, but feldspars and/or volcanic rock fragments may comprise as much as one third of the rock. Clay minerals are commonly present as an orthomatrix. Carbonates and clay minerals are the most common secondary mineral constituents and cements. The general diagenetic sequence has produced major changes in the composition of the rocks and their porosities (Flournoy, 1980).

The diagenetic sequence observed in the Lirette Field sandstone ranges from an early episode of spherulitic calcite cementation that may have occurred very near the surface to the formation of an authigenic kaolinite cement at depths in excess of 10,000 feet. The relative timing of the events can be summarized as follows:

1. Spherulitic calcite cement (early)
2. Authigenic chlorite rims and platelets
3. Quartz and feldspar overgrowths
4. Calcite cement
  - a. Low iron (?) grain replacement and fracture fill
  - b. Very high iron pore-fill and replacement
  - c. Decreased iron pore-fill
5. Dissolution
6. Authigenic kaolinite cement (late)

Loucks et al. (1977), Boles and Franks (1979) and others have described similar diagenetic episodes in other Gulf Coast sandstones. The general pattern emerging has a significant influence on the development and preservation of secondary porosity. The last two episodes are particularly important in the study area.

Dissolution and kaolinite precipitation are volumetrically the most significant late diagenetic events and exert considerable influence on the porosities found in the Lirette Field sandstones. A comparison of porosities measured in the sands in two wells (Fig. 8) illustrates the relationship. There are no obvious changes in the porosity as a function of depth, but there are considerable differences between the wells. Dissolution has been partially responsible for creating porosities that average approximately 30 percent in Well 22. In Well 17, the potential porosity is closer to 20 percent. Authigenic kaolinite is more abundant in Well 17, especially in those samples with the lowest porosities, and the mineral effectively clogs the interstitial spaces, thus reducing the effective porosity. The greater amount of fluid escape from the geopressed zone near Well 17 is assumed to be

responsible for the larger quantity of kaolinite developed there. In general, the last stage of diagenetic alteration of the sandstones is best developed in those areas nearest the zones of greatest fluid movement and flushing.

## CONCLUSIONS

A detailed study of the temperature, pressure gradients, formation water salinity distributions, and structure in the Lirette field reveals important information concerning the occurrence of geopressures in a small area and the potential effects of this hydrodynamic regime on sandstone diagenesis. Fluid leakage up fault zones creates temperature and salinity anomalies and promotes kaolinitization.

Kaolinitization is the latest stage in the diagenetic sequence revealed by a petrographic analysis of the sandstones. Diagenesis begins with a spherulitic calcite cement. Authigenic chlorite rims and platelets are followed by quartz and feldspar overgrowths and later stages of calcite cementation (with variable iron contents). Dissolution generally follows these various stages of cementation and then kaolinite forms in the enlarged pores. Kaolinite development is greatest potential leakage and transmission of geopressured fluids.

## REFERENCES CITED

- Boles, J.R., and Franks, S.G., 1979, Clay Diagenesis in Wilcox sandstones of southwest Texas: implications of smectite diagenesis on sandstone cementation: Jour. Sed. Pet., vol. 49, no. 1, pp. 55-70.
- Braden, M.W., and Goode, O.N., 1979, Testing of geopressured Miocene sands for the dissolved methane resource in the Tenneco Fee "N" no. 1 Well. Preprint, presented at Fourth U.S. Geopressured/Geothermal Energy Conference, Austin, Texas 19p
- Flournoy, L.A., 1980, Diagenesis of Middle Miocene Sands in the Geopressure Zone of Lirette Field, Terrebonne Parish, Louisiana. M.S. Thesis, Louisiana State University, Baton Rouge, Louisiana, 20p
- Jones, P.H., 1977, Geopressured Geothermal Energy, Chapter 11, Frontier Areas and Exploration TEchniques, In Geology of Alternate Energy Resources, ed. by M.C. Campbell, Houston Geological Society, pp. 215-250.
- Limes, L.L., and Stipe, J.C., 1959, Occurrence of Miocene oil in south Louisiana: Trans. Gulf Coast Assoc. Geol. Soc., vol. IX, pp. 77-90.
- Loucks, R.G., Bebout, D.G., and Galloway, W.E., 1977, Relationship of porosity formation and preservation to sandstone consolidation history-Gulf Coast lower Tertiary Frio Formation: Trans. Gulf Coast Assoc. Geol. Soc., vol. XXIV, pp. 109-120.
- Mumme, S.T., and Ferrell, R.E., 1979, Geopressure in the Houma and Hollywood Fields, Louisiana, Trans. Gulf Coast Assoc. Geol. Soc., vol. XXIX, pp. 321-327.
- Silvernail, J.D. , 1967, Lirette field, Terrebonne Parish, Louisiana, in Oil and Gas fields of Southeast Louisiana, vol.2, New Orleans Geol. Soc., pp. 109-117.

## FIGURE CAPTIONS

- Figure 1. Location of Lirette Field in South Louisiana and the approximate position of wells studied. For details of sample locations and well names refer to Flournoy (1980)
- Figure 2. Type log for the Lirette Field, Humble Oil and Refining, H.J. Ellender No. 6, sec 32T19S, R19E (after Silvernail, 1967). The units encountered range in age from Middle to Upper Miocene.
- Figure 3. Structure contour map on the top of the 11,500 foot sand illustration the nature of the domal uplift and the positions of major faults.
- Figure 4. Depth to top of the hard geopressure zone, fluid pressure gradient of 0.7 psi/ft. Same horizontal scale as Figure 3.
- Figure 5. Configuration of the 200°F (93C) isothermal surface in the Lirette Field area. Same horizontal scale as Figure 3. Faults are mapped at their intersection with the 200° surface.
- Figure 6. Formation water salinity profiles for Wells 17 and 22. The formations in #17 have apparently experienced leakage along Fault Y while those in #22 have had minimal or no leakage.
- Figure 7. Proposed routes of fluidescape. Stipled areas indicate zones of leakage along faults and the arrows suggest migration paths towards structural highs. The numbered dots refer to locations of wells from which conventional cores were available.
- Figure 8. Porosity of Lirette sandstones do not vary as a function of depth. Well 17 sandstones are more extensively flushed than those of Well 22. Pores enlarged by dissolution have been plugged by authigenic kaolinite in #17 but remain open in #22.

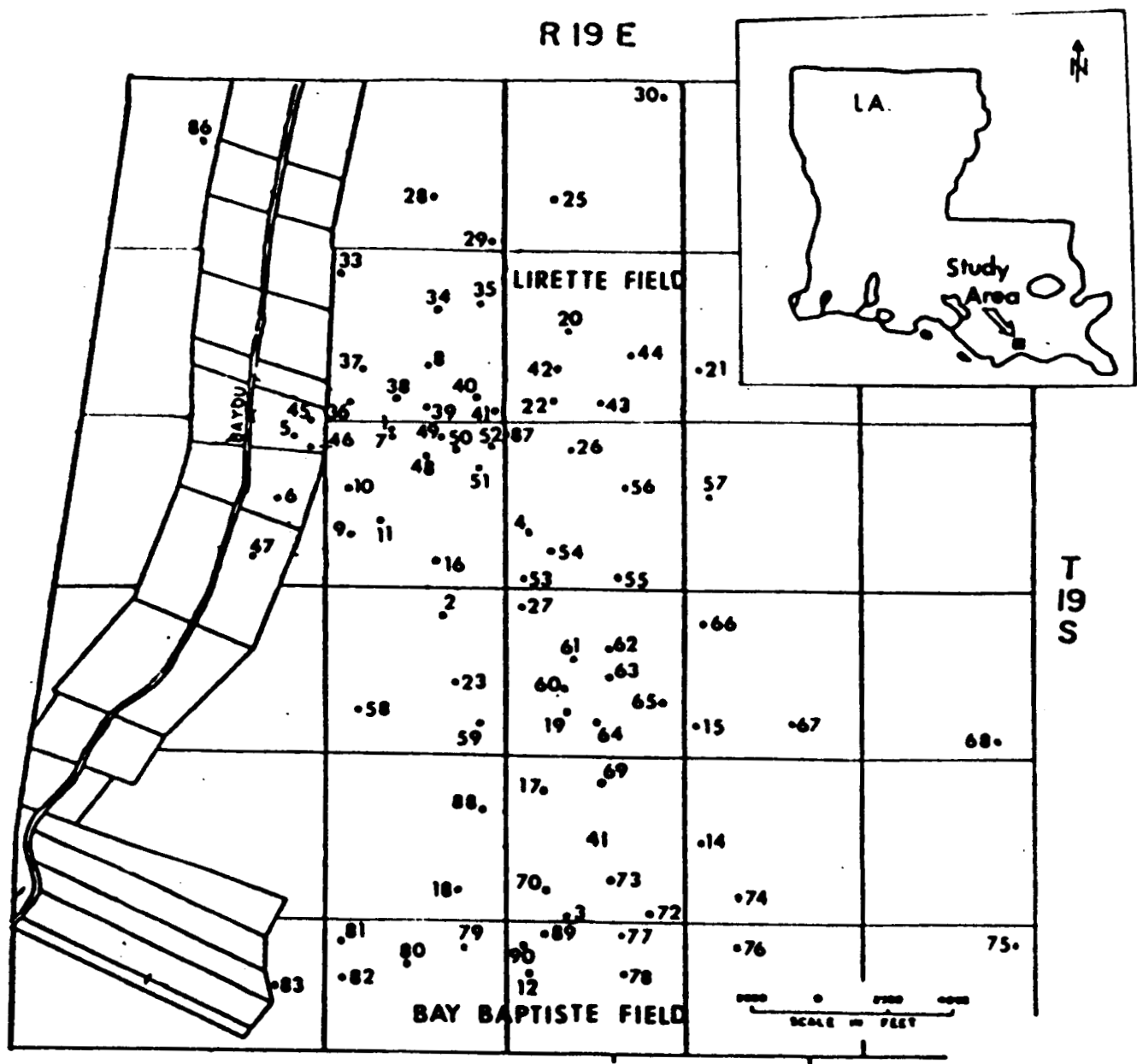


Figure 1.

# TYPE LOG

LIRETTE FIELD

MUMBLE OBR  
ELLENDER NO 6

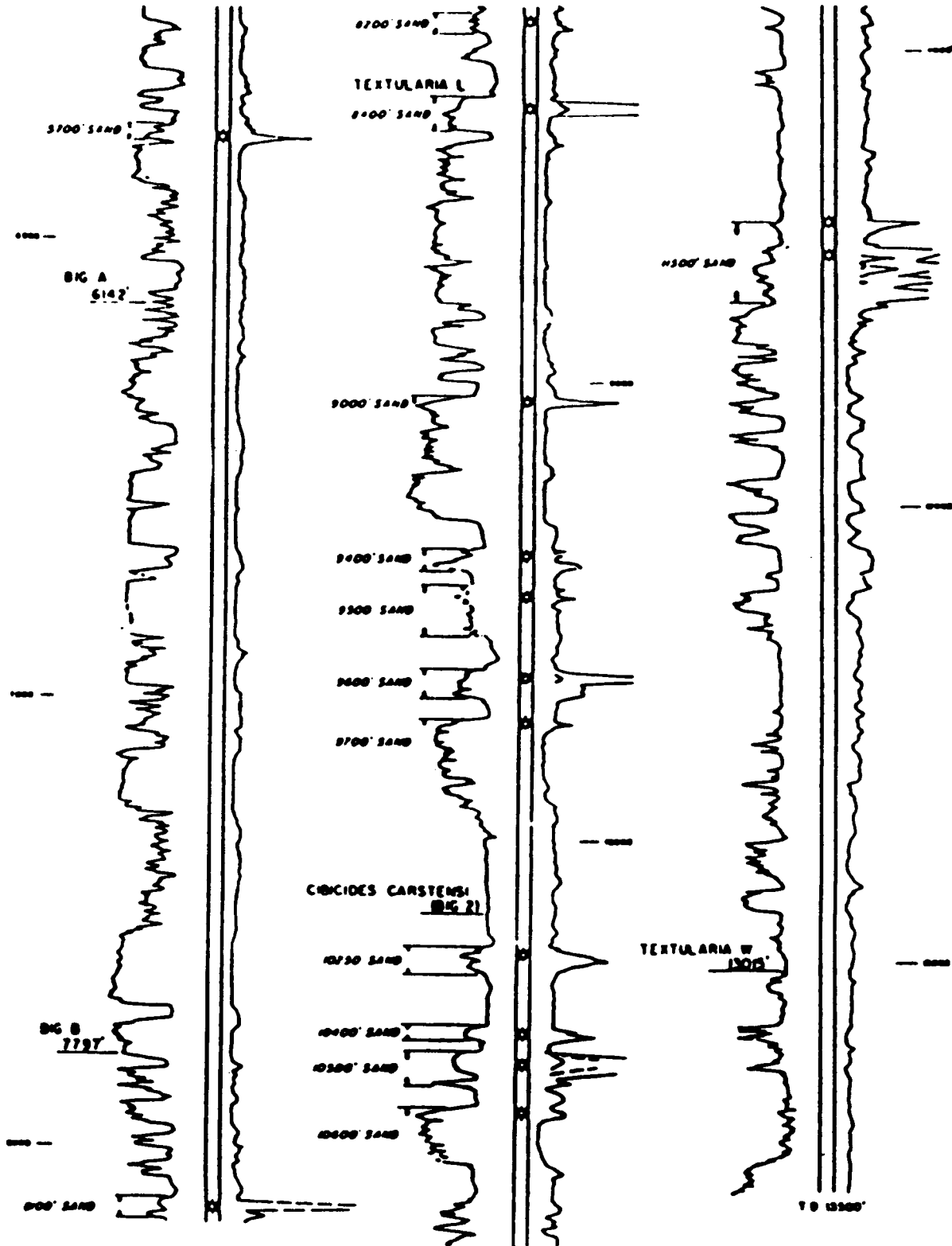


Figure 2.

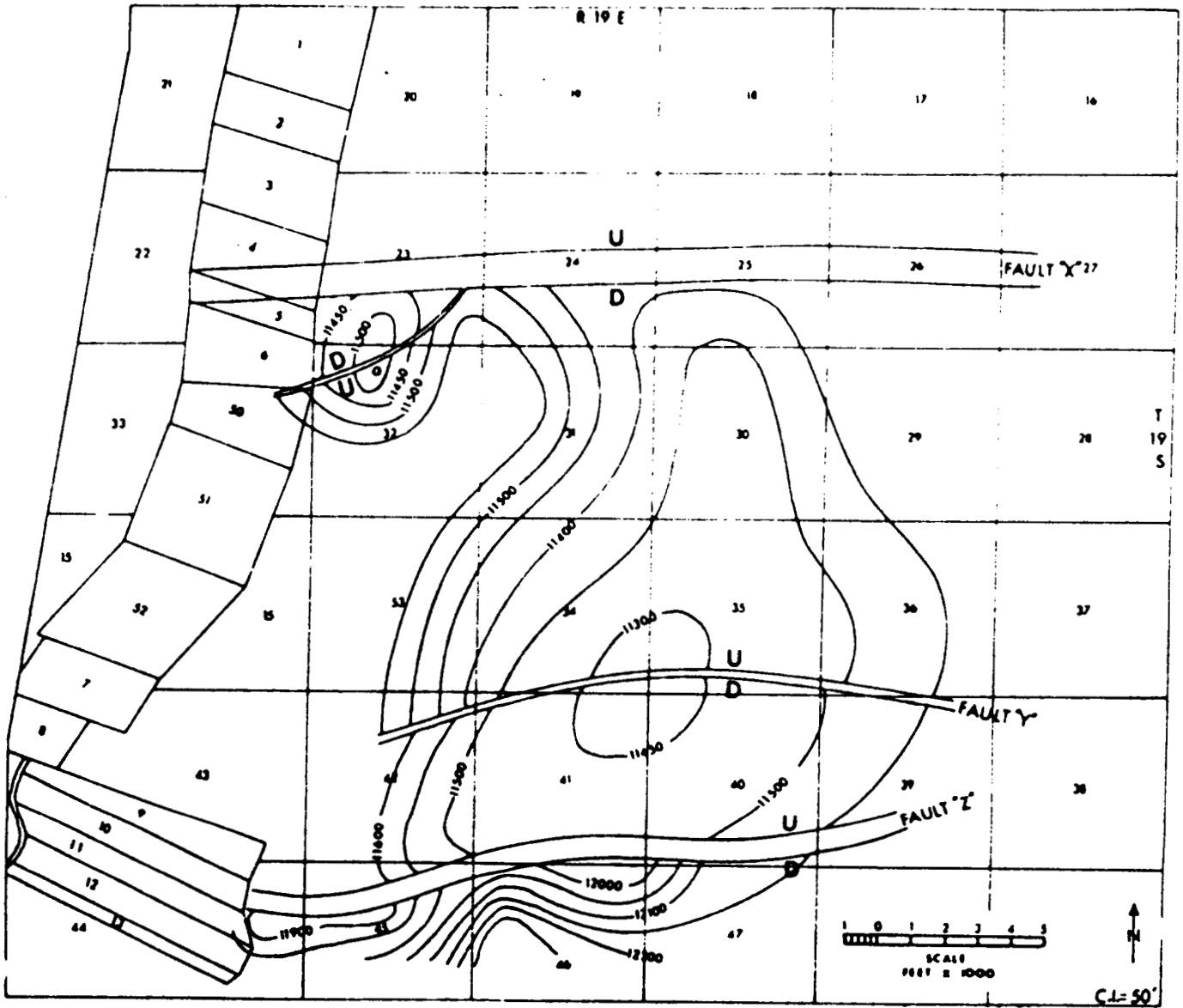


Figure 3.

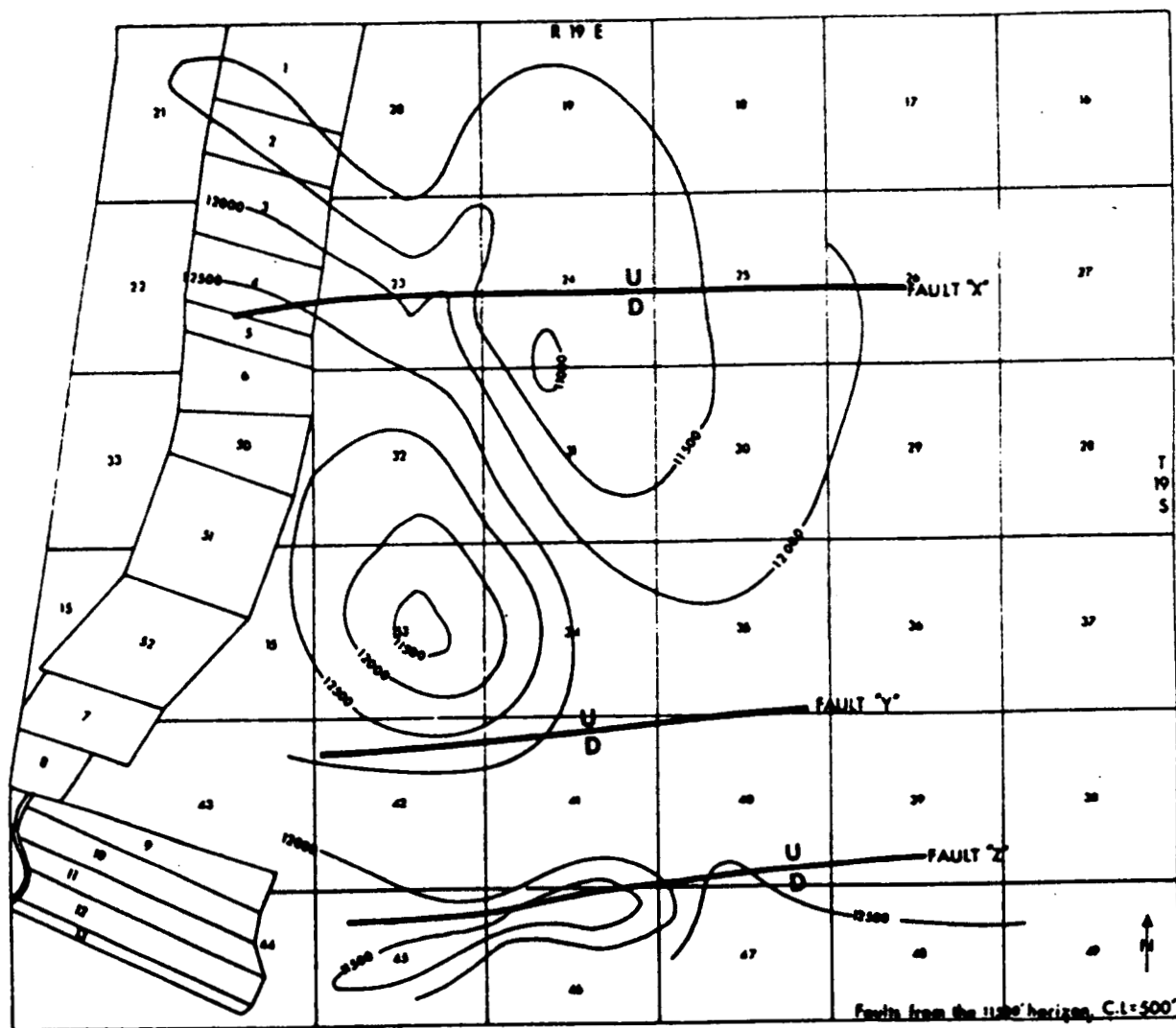


Figure 4.

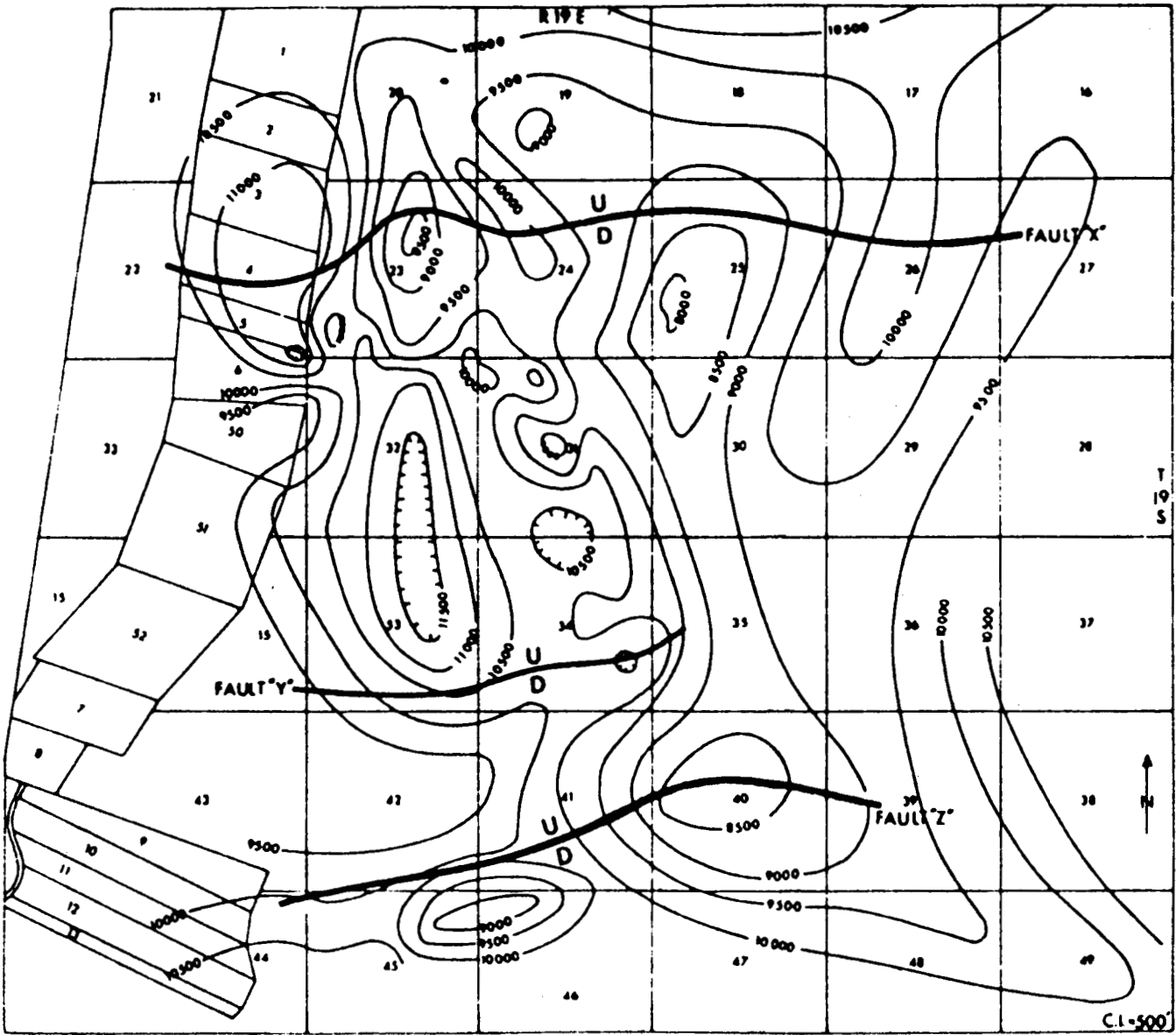


Figure 5.

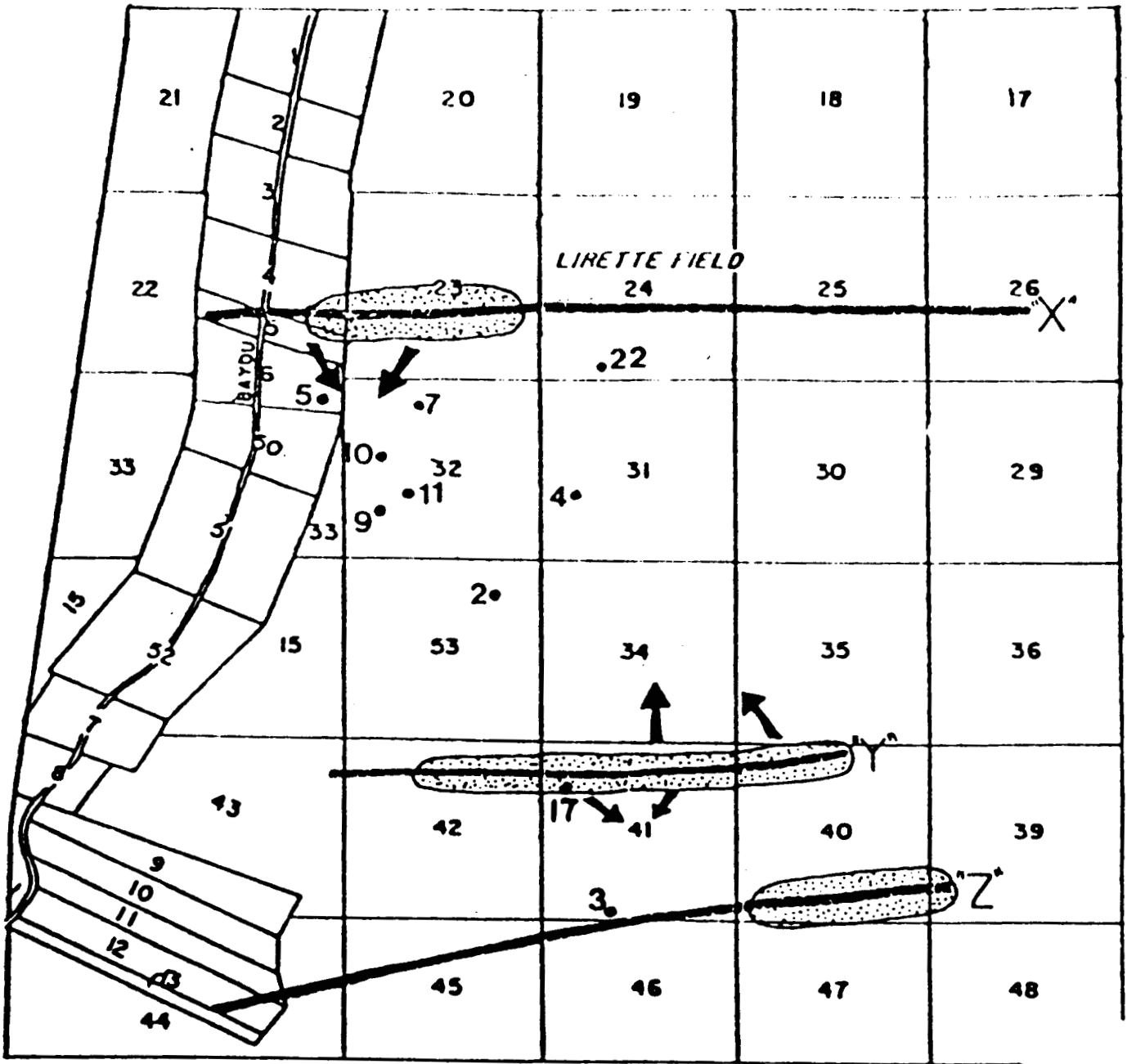


Figure 6.

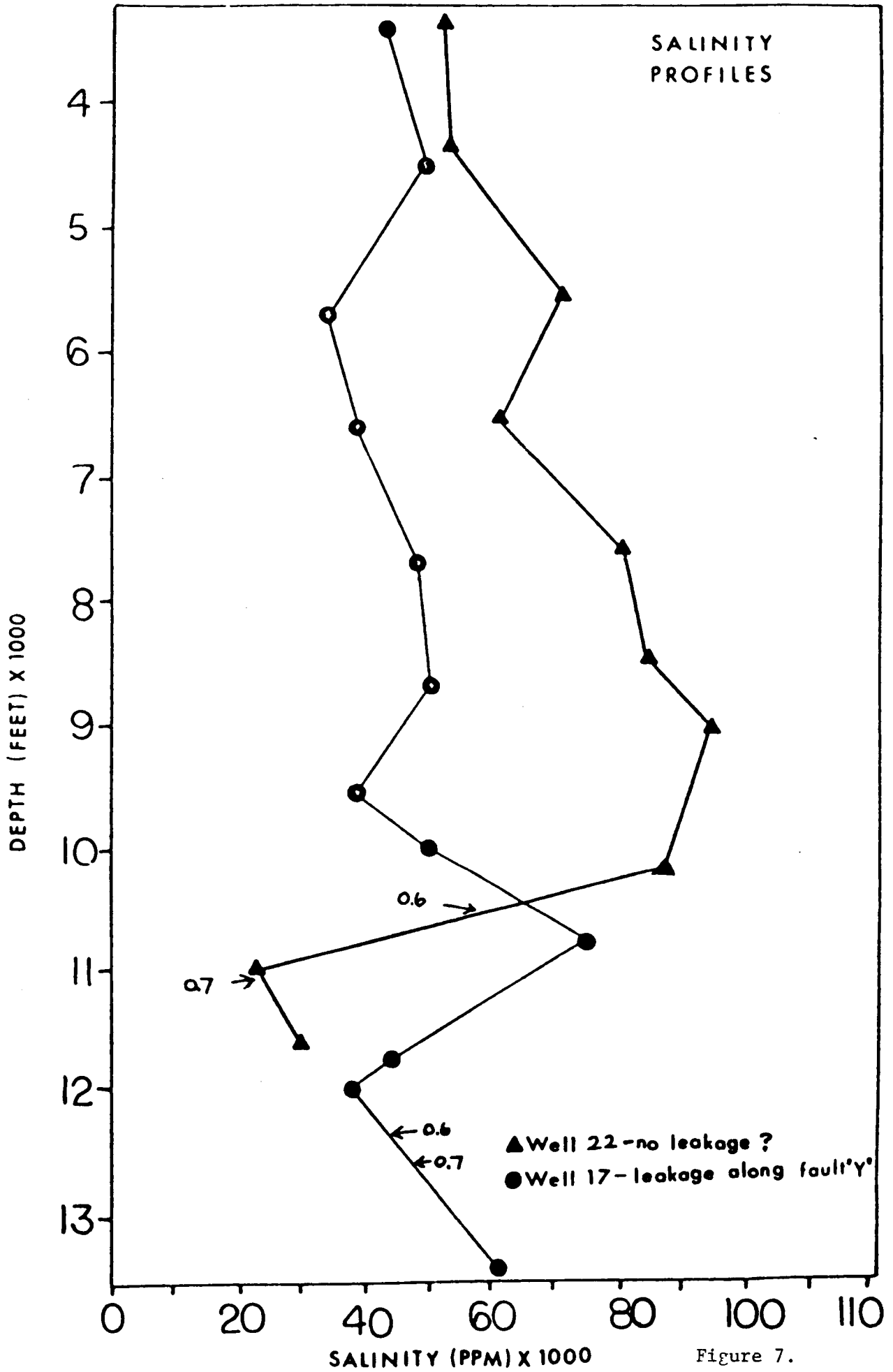


Figure 7.

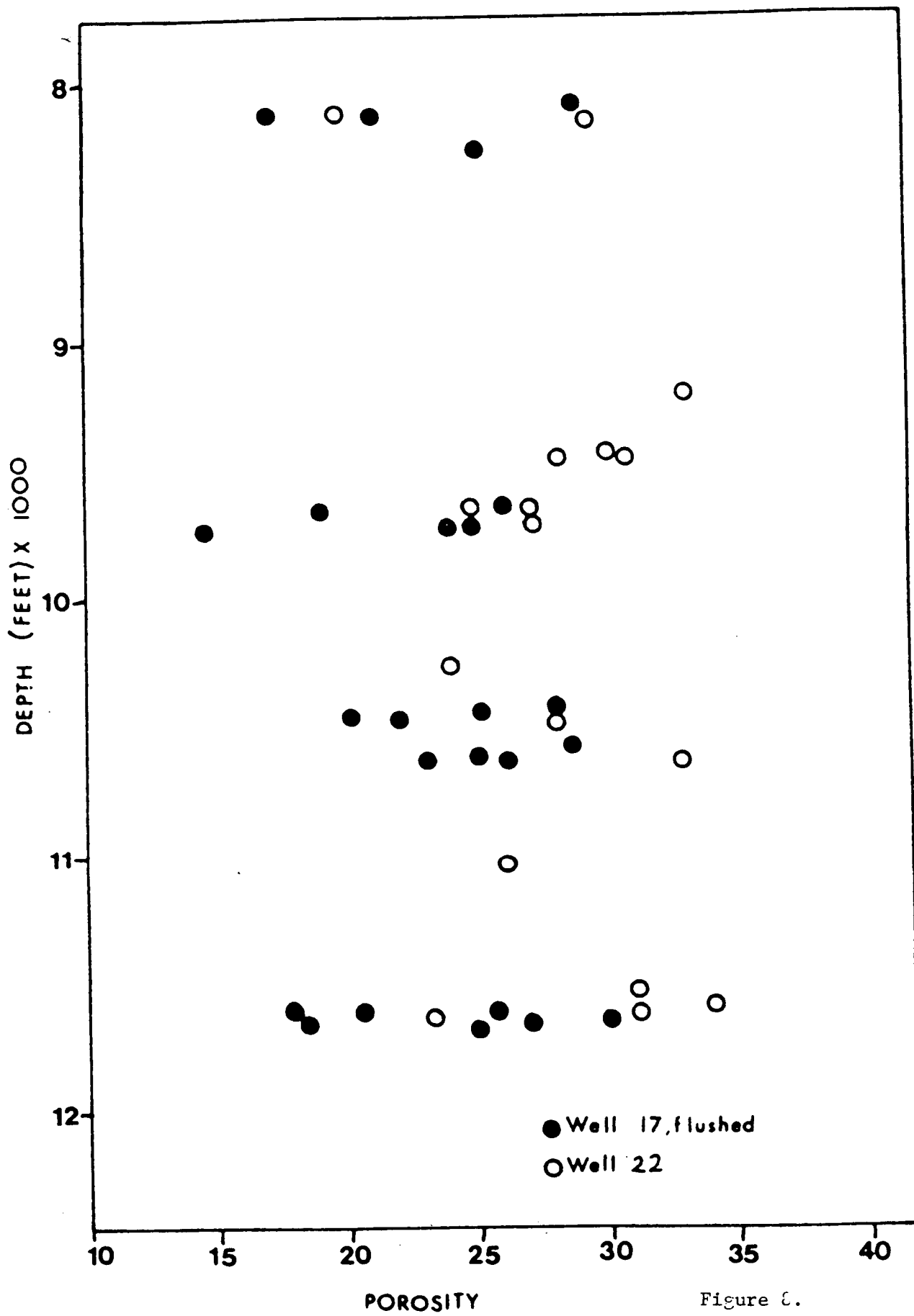


Figure 8.

APPLICATION OF COMPUTER PROSPECTING TO  
GEOPRESSURED, GEOTHERMAL, GAS-BEARING-  
GROUND-WATER RESOURCES OF LOUISIANA

by

Donald H. Kupfer

The purpose of the sub-project under Donald H. Kupfer's supervision was to determine the extent that the computer can be used to manipulate data already available in storage, and to add new data to that storage. Can the available data on the pressure, temperature, and percent sand from more than 5,000 wells in southern Louisiana be used to locate potential areas of geopressured geothermal reserves that have not been recognized by conventional studies? The sub-project studies are incomplete, but it still seems advantageous to continue this approach. A second part of the sub-project, to set up a program to incorporate into the data bank new data as they are acquired, has been less successful.

It was decided to develop a variety of routines and associated programs, and to try them all out on one area for comparison. Once the desired programs were perfected and the appropriate parameters selected, the package could then be used on the whole data bank. The program is still in the first stage. The area used (Fig. 1) was the east half of the New Orleans Two-Degree Topographic Map (USGS, Scale 1:250,000). The data were sorted to include the 1,947 wells lying within this New Orleans East (NOE) quadrangle, and within 1/4 degree outside of it (Fig. 2). All maps were originally produced at 1:250,000 scale, but they have been photographically reduced for this report to 1:500,000. The actual NOE wells (Fig. 3) are shown at the same scale (1:500,000) as the other

maps of the area (Figs. 4 to 26); this will allow the viewer to see the location of the control available.

Twelve computer programs have been developed, and they have been used to produce more than 90 computer maps and 20 cross-sections, examples of which are illustrated in this report.

#### PREVIOUS WORK

##### Clendata File

A previous study by Hawkins and others (1977) developed CLENDATA, a data base of 5,964 wells distributed uniformly over the southern half of Louisiana. Each well-file consisted of 1 to 30 cased images giving information on location, drilling depth, mud weight used for each run, bottom hole temperature of that run, and the percent of sand in all of the deep sand zones that were more than 20 feet thick. These data were then used to produce a series of computer-drawn maps of six, two-degree quadrangles covering all of southern Louisiana. The project used the SYMAP program developed by H. T. Fisher at Northwestern and Harvard Universities. Maps were prepared showing the distribution of mud weight and net sand for 2,000-foot depth intervals from 10,000 feet to 18,000 feet (6 quadrangles, 2 titles, 4 intervals = 48 maps). In addition four summary maps were prepared of the whole area.

The above maps were made by the then available routines, which gave a quick overview of the data. For several months thereafter Kupfer worked with these maps trying to analyze them geologically, locate trends, develop composite maps, and display the data in various hand-drawn formats. Hand-drawn contours were superposed over the favorable net-sand areas, and composite maps were drawn. It became apparent that the basic data were too crude to warrant this type of

intensive study, and the project was temporarily shelved. Both the data bank and the basic programs to display the data needed to be improved first.

#### Robert Hixon's Study

Robert L. Hixon (M.S., LSU, Dec 1979) used the early CLENDATA programs (Hawkins, and others, 1977) to select an area for further study in southeastern Lafourche Parish, Louisiana. The area was chosen because it appeared to have increased temperatures and pressures at moderate depths and ample net sand for storage. In addition, there was the large, unexplored Lafourche Basin in the center of the area, which seemed to have geothermal potential. Apparently it does not. The program, however, was useful in developing the following:

1. Areas on the net-sand thickness maps with abnormally thick quantities of sand are, in general, unfavorable for retaining geopressures. Thick sands generally indicate accumulation in the deltaic-plain complex at the inner edge of the continental shelf. Geopressures are generally associated with sediments of the middle to outer neritic facies, where thicker clay sequences are present to confine the pressures.

2. It was hoped that trend-surface maps could be used to determine the geothermal potential of the Lafourche Basin, but this could not be done. (a) Only a few well logs were available south of the basin. (b) There was not enough time, within the restrictions of a master's thesis, to do the studies properly. (c) The fragmentary evidence obtained suggested that Lafourche Basin was too sandy within the depths of economic interest.

3. Most of the shallow geothermal "highs" in Hixon's study area appeared to be relatively small and associated with salt domes.
4. The CLENDATA file contained many errors that needed to be corrected before the data could be used successfully.

In order to make his studies, Hixon had to develop programs to search and display his data (Appendix 1). Special steps had to be used to eliminate or correct erroneous values in the CLENDATA file. This took much too much of his time, but his programs became the foundation for the current study. Several programs have since been modified and improved. The first maps produced under the present sub-project (for example, Table 1, Set L) used his programs, and although these later had to be re-done, for several reasons, the experience gained through working with them proved invaluable.

#### Glen Gatenby's Study

Following a suggestion by Paul H. Jones in 1978, Glen Gatenby (M.S., LSU 1979) constructed two closely spaced NNE-SSW geologic sections across southern Louisiana, just east of New Orleans. They showed (Gatenby, 1980) the distribution of faults, pressure, temperature, and salinity with respect to the sedimentary facies. Gatenby used these sections to determine the paths of migration of hot, relatively fresh, geopressured waters as they moved upward into the hydro pressured regime. Several release paths were established, and all were associated with known petroleum fields as predicted by Jones. Most were associated with salt domes and/or large grabens. Possibly the most significant contribution by Gatenby was to establish that the easiest upward relief of pressure is most likely to occur at the intersections of major faults; at these places, temperatures and pressures are abnormally high and salinities abnormally low.

## Thermal Studies on Salt Domes

John Lopez, an undergraduate at LSU, did a special study in 1975 on the influence of the Plumb Bob salt dome on temperature distribution. He confirmed that temperatures rise toward the salt stock, but he discovered that they drop immediately over the salt only to rise again within the salt. He concluded:

"This indicates that the salt is actually the normal temperature and it just the strata over the salt which are warmer. This seems to eliminate the salt as a source of heat and led me to the idea that warm, deep water was being forced up."

But he went on to note that the salt was hotter in the holes that penetrated salt, and so "the salt is also a heat source."

Stuart Oden (M.S., LSU, Dec. 1979) made a much more detailed study of the thermal anomaly around the Weeks Island salt dome and found a similar situation. He showed that the temperature in the uplifted sedimentary rocks of the salt dome in each aquifer is about the same as the normal temperature within that aquifer in the areas where it is not uplifted. He concluded that the salt stock did not contribute any significant heat, but rather the hot water had moved up the aquifer.

Hixon and Gatenby, as noted previously, found geopressure release to cause thermal anomalies around the salt domes.

In summary, the thermal anomaly around salt domes is probably caused by several things, including release of geothermal heat, ground-water circulation, and the thermal conductivity of the salt.

## PROGRAMS AND MAPS

Ares (NOE)

A one-degree quadrangle, the east half of the New Orleans

two-degree topographic map (Fig. 1), was chosen as the best area in which to perfect the mapping techniques. To improve accuracy at the edge of the map, all the wells in the surrounding 15 minutes of latitude and longitude (Fig. 2) were also included in the contouring programs, but only the wells and contours within the New Orleans East (NOE) quadrangle are shown on the maps (Fig. 3). Before the decision to use the New Orleans East quadrangle eight maps were made of the New Orleans West Quadrangle using The Hixon programs. (See Table 1, set L)

#### Programming

The original programs (Hawkins and others, 1977) used to produce computer maps were essentially canned programs that displayed the available data: mud weights and net sand changes with depth. This was done in horizontal slices 2.000 feet thick vertically, and this proved to be so thick that essential details were lost. Thus one of the early objectives of the current study was to improve these computer programs and give them greater accuracy and versatility. As indicated, Hixon, working under Kupfer's direction, made the first attempts in this direction (Appendix 1). He also extracted the temperature data from CLENDATA and made them available. Data were also manipulated to give the depth to a desired mud weight or temperature, rather than to try to average the mud weight or temperature over a thick horizontal slice.

The computer programs designed for the present sub-project (Appendix 2) were designed to improve the data already available in CLENDATA, make the programs more versatile, extrapolate the known data by predetermined amounts, and to prepare simple cross-sections. After repeating some of the maps produced in the first study, and making new ones for comparison, other variations were developed. Programs were

developed to determine "gradients", the changes in pressure and temperature with depth, and to plot maps showing mud weight or temperature at various depths, and to make maps of the depth to a particular mud weight or temperature. Trend-surface maps and residual maps were also used to see if they would accentuate interesting details. It was decided that percent-sand maps, at various degrees of slope reflecting regional dip, should emphasize patterns of sedimentary deposition. A program, not yet activated, would develop weighted combinations of the values from various maps to be displayed on a single map. For example, a single map could display both temperature and pressure highs. The computer was also used to construct geologic sections; after a few false starts with available cross-section programs, it was decided to adapt a mapping program to making cross=sections.

The final step of the sub-project should be a geologic evaluation of the maps and sections to determine which are most usable. Because the earlier steps have not been completed, this final stage has not been reached.

Table 1 is a listing of most of the maps (a total of about 50) and sections (a total of about 20) that have been produced thus far as a result of this program. They are on file and available at the Department of Geology at Louisiana State University. These maps were produced at a scale of four inches to the mile (1:250,000). Selected maps from this list have been reduced in size (1:500,000) and are presented in this report. The Varian maps were not made not reproduced at the 1:250,000 scale, but only at the 1:500,000 scale. Table one only includes the best maps, which number about 100, including

20 sections. Due to variations in photoreduction, all scales are approximate.

#### Mapping Routines

Under the Hawkins study (1977), most maps were made using the SYMAP computer mapping program, a program that contours data on computer or plotter printouts. A new program, Surface II (Sampson, 1975), was acquired by the L.S.U. Department of Geology about the time of the start of the present program. It was thought to be more versatile, as it could also give Varian-plotted contour maps. Thus for nearly two years all work was designed to use this program. even though it was not yet fully operational. It was assumed it would become fully operational eventually, and that it would give better maps.

The new SURFACE II program was found to contain many problems, the most discouraging of which was that the option to print the basic data points on the output map could not be made to operate. Thus on SURFACE II maps, unlike SYMAP maps, the user has no idea of the location of the wells that supplied the data. This is a very serious objection, as a trained observer can immediately spot valid trends from false trends on a SYMAP plot, but not on a SURFACE II plot. Compare, for example, Figures 9 and 10. All of the most recent maps have been produced by the SYMAP program.

Printer maps, of the type reproduced in this report, were quickly and inexpensively produced and were very adequate for preliminary studies. Slightly slower are the maps plotted on the Varian Plotter, an electrostatic plotter that can produce maps similar to those made on a flat-bed, pen-type plotter, but at much greater speed and far less cost. (See Figs. 11, 14, and 19 for examples). It can also produce perspective block diagrams (Fig. 15), but these appear to have little value. Recent software changes will allow the Varian maps to be made at the scale of 1:250,000, but as yet none have been made at this large

scale.

The best maps are those produced on a flatbed plotter. These can be produced at any scale, on any base map (including, for example, USGS topographic base maps), and with any number of contour intervals. They are very legible and capable of large reduction in scale for publication.

In an attempt to visualize the data in the third dimension, a series of cross-sections were constructed. All wells in a north-south strip, 0.05 wide, were combined onto one display in which their latitude was used to give horizontal position, and their depth to an observation was used for the vertical dimension. The lines connecting similar observations were then drawn by hand. Anomalous data (local readings distinctly above or below the norm) were generally noted. In several cases composites of several adjacent sections were compiled (by hand). The sections were particularly useful in determining regional dip, a function also accomplished by trend maps. Trend maps, however, are of little value for data on net sands, and the net-sand sections are the most valuable.

Because of the preliminary nature of the present project, most of the maps were produced as printer-maps and a representative few are reproduced here. In a final report, most maps should be of Varian-type, and a few of the most important should be made on the flat-bed plotter.

#### Programs

The Hixon program (Appendix 1) manipulates CLEANDATA to give

mud-interval maps, and it can be used to determine temperatures at a given depth, or the depth to a given temperature. The programs are inflexible. Some maps in files B, F, and K used these programs.

MUDTREND (App. 2, File A) determines the pressure gradient with increasing depth from the weight of mud used to drill a particular interval. The degree of extrapolation beyond total depth can be specified. The gradient is then used to determine the depth to any selected mud weight, or the mud weight at any selected horizon. The printout can be made to indicate the location of bad values. A temporary tapefile can be used to produce maps or sections by SYMAP, SURFACE II, or similar programs. Use of this program has indicated many uncorrected errors in the CLEANDATA file. The present this program makes no provision for legitimate decreases in mud weight with depth; once spurious data are eliminated, this option must be added. MUDSAND (App. 2, File B) is a simple variant of MDS NDSAL (Hixon) that calculates the maximum mud weight in a vertical interval, rather than the average mud weight. This program has been superceded by the more accurate MUDTREND program.

PERSAND App. 2, File C) calculates the percent of sand in the small sand-intervals identified in CLEANDATA on the sand cards and plots the value at the average depth for that interval. The printout also gives the thickness of the interval so that thicker intervals can be identified and, if desired, given a greater weighting. This program has proved very useful in plotting cross-sections showing the distribution of sand units, but the full potential has not yet been adequately tested.

DIPSAND (App. 2, File D) calculates the average or maximum mud weight

over a selected sloping interval, and the total net sand for that interval. The slope and width of the interval can be specified to approximate that of the regional dip, if known. If not, several approximations can be made, and regional dip determined by trial and error. Sand distribution patterns plotted at regional dip should help to identify stream patterns, beach ridges, and similar features. As with PERSAND, the potential of this program has not been tested. TEMPDHK is a program under preparation that will calculate the temperature gradient in a more refined manner than TEMFILE (Hixon) and with greater versatility. The degree of extrapolation beyond the bottom of the hole can be varied, and the type of extrapolation can be changed according to the depth zone (hydropressure, transition, or geopressure). The print out will indicate the location of potential errors. The data can be used to produce better temperature maps of both the depth-to and temperature-at types.

The above programs deal with pressure (as approximated by mud weight), temperature, and lithology (net sand). The fourth important parameter, salinity, has not yet been developed.

#### Problems

As with any computer project, this sub-project has had its share of hardware and software problems. Most of these were caused by using sub-standard equipment or programs on a make-shift basis because "better" equipment or programs were expected "immediately".

As previously noted, we decided at the start of the sub-project to use the SURFACE II Program to produce maps, even though this program was not yet fully operational. The program has the potential of being very versatile, and someday it will be a far more advanced system than the

older SYMAP program. However, the software changes have not arrived, and in the last two months of the project we had to reproduce as many of the maps as possible on the older, but highly functional, SYMAP program.

#### MUD WEIGHT

The weight of the mud used while drilling a well is controlled so that it approximates the fluid pressure at the depth being drilled. Marked natural variations, such as a decrease in pressure with depth, are controlled by installing casing in the hole to contain the overlying pressures. Because it is both uneconomical and dangerous to allow pressure and mud weight to get out of balance, mud weight can generally be used as a reliable estimate of fluid pressure, which is much less commonly measured. Fluid pressure measurements were not available to the present study.

Two types of mud weight maps were produced: interval maps (Table 1B, and Figs. 4-8) and depth-to maps (Table 1CD, and Figs. 9-15). Maps of mud weight at a particular horizon were not produced, but the program to make these maps was developed (MUDTREND, App. 2, File A). MAXMUD interval maps (Figs. 5 and 8) are an approximation of the same observation. Regional cross-sections (Table 1E and Fig. 16) will be of little help until the spurious data in the original data bank are eliminated. Trend and residual maps (Table 1D and Fig. 12) show little and are given a low priority for further investigation.

#### Interval Maps

Interval maps showing the average mud weight in a 2,000-foot vertical interval (such as Figs. 4, 5, and 7) were developed for the whole of south Louisiana by Hawkins and others (1977). These maps were easy to produce without developing new programs and gave a rough picture

of pressure distribution. Kupfer's early study of these maps (early hand-drawn studies, since abandoned) indicated several interesting trends subparallel to the regional coastline, but the 2,000-foot interval proved to be too thick for detailed interpretation. In the present study several variants were tried, for example, use of a smaller vertical interval of 100-feet (Fig. 6) and also use of a half-pound contour interval.

The transition from "normal" pressure, that is, wells in which the fluid pressure is about that of the hydrostatic head for that depth, to "geopressured" well is probable best indicated by about 14 to 15 pound muds. Thus on a typical interval map, the areas with higher mud weights are highlighted by hand-drawn contours (Figs. 4-8).

An easy-to-do source variation of this program (MUDSAND App. 2B), gives the maximum mud weight found in the interval (compare Figs. 4 and 7 with Figs. 5 and 8). The MAXMUD maps for a given interval are approximations of the maps showing the mud weight at the base of the same interval. When the latter maps are produced (they have not been yet), they will be more exact. But if, as sometimes happens, lower pressures are encountered under a geopressured sand, and the well is cased and then a lower mud weight used, the latter maps might not reflect the higher-pressured sand.

In all, 13 mud-interval maps were made (Table 1B), including two Varian maps. As all were made at an early stage in the project, and all used the SURFACE II mapping routine, no well locations are shown. Without these, and because it was expected they would be available later, it was not considered worthwhile to make detailed analyses of these maps. This project was suspended pending software improvements, and it

has not been resumed.

#### DEPTH-TO-MAPS

The first significant program to be developed, MUDTREND, gives maps showing the depth to a given mud weight. Weights of 11 to 20 pounds were tried, and at various contour intervals (500 to 1,500 feet). They were reproduced by the SURFACE II, SYMAP, and Varian plotter routines. In all, more than 50 maps were produced, 37 of which were saved (Table 1C 1D), and 7 are illustrated here (Figs. 9-15).

For plots showing contour lines, the 500-foot contour interval gives a good feel of the area (Varian plots, Figs. 11 and 14), but this small interval made the printer-maps too cluttered and hard to read. The 15-pound mud weight maps were chosen for experimentation (Table 1D) as these were felt to give maximum information on the critical "transition" zone from non-geopressured to hard geopressure; 13 maps were made, including the trend and residual maps.

In general, the "depth-to" mud weight maps have been highly successful. The SYMAP maps, although less elegant than the SURFACE II maps, allow one to see where the data comes from (compare Figs. 9 and 10). There is not sufficient well control to make the maps to the higher mud weights worthwhile (Fig. 13, even though The Varian plots (Figs. 14-15) appear otherwise.

These recently produced maps have not been examined in detail, but when produced on the Varian plotter, at a large scale and with a small contour interval, they should prove to be most interesting. This will be especially true when they are compared to the net-sand cross-sections described later.

#### Trend Maps

Trend maps are statistical maps that generalize data according to

certain mathematical equations. The resulting trend surfaces are theoretical surfaces that approximate the given data. For example, a first-order trend map gives the average regional dip of the data. For Gulf Coast examples, this is generally a Gulfward dipping surface sloping southward at about 100 to 200 feet per mile ( $1^\circ - 2^\circ$ ). Residual maps made from the trend maps show how much the actual data deviates from the trend surface. Residuals from a first-order trend surface show the local "high" and "low". Higher and higher trends come nearer and nearer to approximation the actual surface being contoured, and the residuals define smaller and smaller anomalous areas.

Trend surface maps of the 15-pound mud weight (Table 1D, maps 9-13) show regional strike of  $N 89^\circ W$ , and a southward dip of 50 feet per mile. Higher order trends show very little variation from that but generally indicate that the northeastern area of the New Orleans East quadrangle has slightly higher pressures at shallow depth. Maximum slopes are 125 feet per mile (Fig. 12). Because the trend maps so nearly approximate horizontal surfaces, the residual maps derived from these (not produced here) were close approximations to the normal contour map for 15-pound mud weight (Fig. 11).

Trend and residual maps can be generated on various size map areas, ranging from the whole of southern Louisiana to an extremely small local area. The present work suggest that the regional maps would have little significance. Trend maps of  $\frac{1}{2}^\circ$  to  $1^\circ$  areas of the first and fourth order might have some meaning, especially if compared with adjacent quadrangles; residuals from these will e of little help. Detailed maps of smaller areas, such as areas of about 15 x 15 minutes, selected as a result of previous  $1^\circ$  studies, might have considerably greater

significance. These more detailed studies must await completion of the present program.

### Sections

Four cross-sections were prepared to show mud weight (Table 1E). Each north-south section consists of the well data from a 0.05 wide strip on longitudes 90.0, 90.3, 90.6 and 91.0 degrees. The two end members are reproduced (Fig. 16) to show extremes of regional slope. The western section at 91° Longitude appears to be relatively flat (15 feet per mile southward slope). It shows far more local variation between adjacent wells than from the northernmost to southernmost wells. In contrast, the eastern section at 90° longitude appears to show a pronounced regional dip to the south of about  $1\frac{1}{2}^\circ$ , which is in rather good agreement with the eastern side of the fourth-order trend map on the 15-pound mud weight (Fig. 12).

In summary, a series of trend maps of about the 4th or 5th order probably will be more useful and more reliable than an equal number of sections to give the regional slope of the equal-pressure surfaces. When adjacent quadrangles are mapped, comparison of these trend surfaces from area to area might prove interesting and informative.

### TEMPERATURE

The second parameter of direct interest in a geopressured-geothermal investigation is temperature. More specifically, in what areas are the temperatures abnormally high for any specific depth? For these studies, the observed bottomhole temperature (F°) of the mud, as recorded on the electric log, are corrected according to Table 2. In the new program, TEMPDHK, the formula at the base of the table will be used. These temperatures are assumed to

approximate the temperature of the fluid in the rock at that depth.

Using these corrected temperatures, 21 maps have been preserved in the LSU files (Table 1): 5 maps of temperature at a given depth (see F and L), 9 of depth to a given temperature (G and L), and 7 of temperature as seen in cross-section (H).

### "Highs"

Once the temperature gradient for a drill hole has been established by Hixon's TEMPFIL program, or the yet-to-be-completed TEMPCHK program, the temperature at any given-depth can be estimated for each hole and an isotherm map constructed for that depth. The hottest areas on such a map are temperature highs. Likewise, maps can be constructed showing the "depth-to" any desired temperature, and the shallowest depths on a depth-to map are also temperature highs: Needless to say, these "highs" are of the greatest interest in a search for a potential geopressured-geothermal reserve. Likewise, if they correspond with a mud-weight high as shown by the maps of the previous section, the potential is greatly increased. This, one goal of the present program, not yet accomplished, is to produce maps showing the location of these combined highs.

However, the places where high temperatures and high pressures have already been penetrated by drill holes are already known. The purpose of the present program is to seek trends or "highs" that are not known. The minimum temperature that is of interest at the present time for any commercial application is 200°F, but some programs require temperatures of 240° to 260°F and even hotter if possible.

CLEANDATA is incomplete for data shallower than 10,000 feet, thus the 10,000 foot "given-depth" maps are the shallowest that are usable,

and the temperatures at that depth are generally less than 160°F. "Given-depth" maps greater than about 15,000 feet have too few data points to be of great accuracy, and it is generally below these depths that temperatures reach 240-260°F. Thus the best available maps are those of temperatures at 10,000 to 15,000 feet, and these give temperatures that are generally too low to be of interest.

Likewise, the accurate "depth-to" maps are on the 180° to 220° temperature horizons, and the maps on higher temperatures are considerably less accurate. Thus the best given-depth and depth-to maps clearly show temperature "high", but these highs are at too low a temperature to be of commercial interest. Their importance lies in the fact these near-surface "high" probable reflect highs of greater temperature at greater depths. Thus, as an exploration tool, a "high" on the depth-to-180°F. map will very be over a similar high for 240°F.

#### Given-depth Maps

Four "given-depth" maps had been produced for the west half of the USGS New Orleans two-degree quadrangle (Table 1L), but only one (Fig. 17) for the east half (NOE). This one was at 10,000 feet and for a contour interval of 10°F.

Further given-depth maps await program TEMPDHK, correction of the CLEANDATA file, and software improvements.<sup>2</sup>

#### Depth-to Maps

Nine "depth-to" maps are in the current L.S.U. file (Table 1G, but the Varian map of the 300°F isothermal surface is too deep to be considered reliable. No SYMAP maps have been made, so the distribution of the data points is not clear. The 200°F map shows depths as shallow as about 7,000 feet (clearly an extrapolation as no data are available that shallow) and extends to 13,000 feet. The 250°F maps (Figs. 18 and

19) extends the available data to their limits; the range of depths is from 8,500 to 17,000 feet. Interpretation awaits better data, an improved program, and plots showing the data points.

#### Sections

Seven north-south temperature cross-sections were constructed, including two that extended outside of the NOE quadrangle (Table 1W). This exhibit actually includes 37 different diagrams, reproductions, and trend analyses. Six principal sections were constructed at  $0.2^\circ$  intervals, each from a band  $0.05^\circ$  wide. The sections are at longitudes  $90.0^\circ$ ,  $90.2^\circ$ ,  $90.4^\circ$ ,  $90.6^\circ$ ,  $90.8^\circ$ , and  $91.0^\circ$ , and three of these are summarized in Figure 20 at a reduced scale.

Isothermal profiles at  $20^\circ$  intervals were sketched onto each section and anomalous values were circled. The numbers of Figure 20 are a code of temperatures: 5 =  $180 - 200^\circ\text{F}$ , 6 =  $200 - 220^\circ\text{F}$ , etc. The circled values represent natural anomalies and bad data.

The data below  $220^\circ\text{F}$  are very scattered and unreliable (Fig. 20). Only the  $180^\circ\text{F}$  profile can be carried continuously across the whole NOE quadrangle with any confidence. These sections suggest that accurate maps can be constructed on the  $180^\circ$ ,  $200^\circ$ , and  $220^\circ$  isothermal surfaces. These maps can then be used to obtain trends, and continuity of trends, which can then be used to predict the deeper trends and higher temperatures.

The profiles from the six sections were separated by temperature and combined on a single section, one for each temperature (Fig. 21). A composite of all profiles was also made (not reproduced). For each temperature, several straight-line dip-trends were drawn; a high trend, a low trend, a trend encompassing the majority of the data points, and

one or two "average" trends. Dip trends ranged from 5 to 15 feet per mile, but the overall trend (Fig. 22, straight lines) shows a regional dip of 12 feet per mile ( $1/8^\circ$ ) and a gradient of  $1^\circ$  increase per 65 feet of depth ( $1.6^\circ\text{F}$  per 100 feet). The accepted regional gradient is about  $1^\circ$  to  $1\frac{1}{2}^\circ$  per 100 feet of depth.

Once the regional dip-trends of the thermal surfaces have been established, [g.21], they can be transferred to the individual sections (Fig. 22), and the thermal highs noted. Thus at latitude 29.45 north and longitude 90.8 west (Fig. 22, left of center) a strong thermal high is present. If the interpretation shown is correct, the thermal high may be disappearing with depth, and the profiles of the  $280^\circ$  and  $300^\circ$  are nearly flat. (Note that the control is very scant and the interpretation may be incorrect, or only partially correct).

It is quite possible that the same information could have been obtained from trend and residual maps of these same isothermal surfaces, in which case this would give three-dimensional control. For most people the cross-section is easier to visualize.

As yet, no trend and residual maps have been prepared on the temperature data, so it is not known how these eye-estimates will compare with computer-generated data. Estimates of regional gradients, both horizontal and vertical, will be very valuable in analyzing the temperature data for abnormalities.

#### NET SAND

A geopressured-geothermal anomaly in shale is impermeable, non-economic, and therefore not a resource. The heat, pressure, and accompanying methane gas cannot be extracted. Thus to get a large recovery of energy, a large, permeable sand reservoir is necessary. In

the Hawkins study (1977), we made the mistake of assuming that a map showing high net sand combined with high pressure was a good target. The Hixon thesis of 1979 disproved this hypothesis. Thick sand is generally part of the near-shore sand facies, and it is not geopressured. The sands must be trapped within thick shale bodies.

The main purpose of the present net sand study was to find a way to display the net sand that would indicate trapped sand bodies. To do this the regional depositional pattern must be determined (Fig. 28).

The interval maps of the Hawkins study (1977) have been refined (smaller intervals, better data, (Fig.. 23). The main emphasis, however, has been on producing maps that showed the net sand contained in southward sloping units that might reflect the regional dip. The first sloping interval maps used  $1\frac{1}{2}$  a value taken from commercially available regional maps. Slopes of  $1^\circ$  and  $2^\circ$  were also tried. None were very successful at showing regional drainage patterns or beach trends of the type shown in Figure 28.

Meanwhile the program to draw geologic sections was developed, and as a result of these studies the regional dip was [at first], approximated at  $1.13^\circ$ . Three interval maps were made at this interval (Figs. 25-27). Later calculations suggest that  $1.2^\circ$  might be better, but no maps have been made. The present depth-interval of 1,000 feet is probably much too thick, and thinner intervals must be tried.

In short, the net sand study is the most difficult part of the exploration program but probably will be the most rewarding if it can be made to work. It may show which of the "highs" indicated by the combined temperature-pressure program will be commercial.

### Horizontal Interval Maps

Interval maps of 2,000 feet were produced in the Hawkins program (1977). The present program produced five maps at 1,000-foot intervals (Table 11) and because of lack of time no variations from this were attempted. Maps 1 and 2 of Group 1 (Table 1) compare the SURFACE II and SYMAP programs. The four SYMAP maps cover the 1,000-foot intervals from 10,000 to 14,000 feet (Fig. 23 is an example). As sloping interval maps are clearly superior, there is no reason to produce any more horizontal-interval maps, at least not at these thicknesses.

### Sloping Interval Maps

Twelve sloping interval maps have been produced (Table I J): three by SURFACE II and the others by SYMAP. Three depth intervals were chosen, each 1,000 feet apart (5,000, 6,000, and 7,000 feet for the top of the interval). The upper depth is set for the northernmost wells, which are 15 minutes north of the NOE quadrangle, that is, at  $30.25^\circ$  Latitude. Table 3 summarizes the depth data for the top of the interval at various depths and slopes. Typical depths are shown for the north, middle, and south edge of the NOE quadrangle for each interval. Slopes of  $1^\circ$ ,  $1.13^\circ$ ,  $1.5^\circ$ , and  $2^\circ$  have been tried. Those at  $1.13^\circ$ , which probably are nearest to the regional dip, have been reproduced here (Figs. 25, 26, and 27).

A quick examination of the maps suggests vague northerly sand trends that might represent stream channels, and other more westerly trends that might be beach ridges. However the interval of 1,000 feet is probably too thick to distinguish these features. Smaller intervals must be tried.

### Trends

Two trends and two residual maps were run (Table II, maps 6 to 9),

but nothing significant appeared. The trend maps (1st. and 3rd.) indicated a flat surface with dips of less than 1 and 2 feet per mile respectively, and the residual maps merely mimicked the highs on the original interval maps (the lows were suppressed).

It is unlikely that trend maps will be of much help in the study of net sands.

### Sections

To construct net-sand and cross-sections, the PERSAND program was used to identify and label the sand intervals. The percent of sand within the interval was plotted at the mid point. Clay intervals were also plotted. The first section was  $0.05^\circ$  wide, but this was not wide enough to give sufficient data. Four sections were then plotted at  $0.1^\circ$  widths at longitudes  $90.0^\circ$ ,  $90.2^\circ$ , and  $90.4^\circ$  (Table 1 K). It was then decided to weight the interval by the formula  $W = (I/10) \times (P-10)$ , where  $W$  is the weighting factor,  $I$  is the interval thickness, and  $P$  is the percent sand in the interval. This formula gives a greater weight-value to the thicker intervals, and it virtually eliminates the thin intervals and those with a low percent sand. This formula was applied to longitudes  $90.4^\circ$ ,  $90.6^\circ$ , and  $90.8^\circ$  (Table 1 K).

Figures 29 and 30 compare the weighted and unweighted intervals. The solid lines of these figures are attempts to align the thicker sand bodies to determine their regional dip. Note that in the south the dips range from about  $1^\circ$  at the surface to about  $2^\circ$  at depth.

Neither the weighted nor unweighted sections are entirely adequate, and a better cross-section program will have to be devised. The sections must be drawn at a larger scale, and the top and bottom of the intervals indicated. It remains to be seen if these improvements will

give the regional dip and thus help locate trapped-sand bodies.

#### CONCLUSIONS

The present phase of the computer-map subproject has emphasized programs, software, and preliminary maps. The maps produced so far are neither accurate nor technically correct, and thus not suitable for geological evaluation.

Once the data bank has been corrected and updated, and the pressure and temperature gradients within each drill hole established, then the best maps will probably be the "depth-to" maps and their associated trends maps. For mud weight, emphasis should be on the 14, 15, and 16 pound surfaces; for temperatures emphasis should be on the 180°, 200°, and 220° surfaces.

Next, a comparison of temperature and pressure highs needs to be made. This can be done visually, or by a "weighting" program. The temperature times a weighting factor can be added to, or multiplied by, the pressure times it's weighting factor. These weighted values can then be plotted and contoured.

If salinity is brought into the program, it can be treated in a manner similar to temperature and pressure, but geological relationships between salinity and geopressure are more complex.

The best way to treat the net-sand data will be by a combination of geological cross-sections and sloping-interval net-sand maps. Trend maps are not likely to be significant.

## References

- Coleman, J. M., and Wright, L. D., 1975. (In) Deltas, Models for Exploration: Editor: M. B. Broussard. Houston Geological Society.
- Fisher, H. T., 1968, Synagraphic Computer Mapping. A program developed at Purdue and Northwestern Universities and currently administered by Harvard University, Cambridge, Mass. (Version 5/20).
- Gatenby, G. M., 1980, Exploration ramification of subsurface fluid migrations in the Lake Borne -- Valentine area of southeastern Louisiana: Transactions of the Gulf Coast Geological Societies, 30, pp. 91-104.
- Hawkins, M. F., 1977, Project Director of : Investigations of the Geopressure Energy Resource of Southern Louisiana: ERDA Contract No. EY-76-S-05-4889, Petroleum Engr. Dept., La. State Univ. 4-15-77.
- Sampson, R. J., 1975, Surface II Graphics System: Series of Spatial Analysis, Kansas Geological Survey, Lawrence, Kansas.

## Table 1. Computer-Produced Maps

October 1980

Original maps are at scale 1: 250,000; all are computer printout maps except as noted. A copy of each of these maps is on file at Department of Geology, Louisiana State University. Maps were produced to test computer programs and program parameters and are not considered to be accurate.

CI = Contour Interval      S = SYMAP map      # = Pounds  
 K = 1000 feet              II = SURFACE II map      VBD = Varian  
 block-diagram

\*Map reproduced in this report at reduced scale, figure number in parenthesis

A. Index Maps \*1 USGS published topographic map, New Orleans 2°-sheet,  
 CI = 25 ft.

(Fig 1).

\*2 Location of all wells used in study area, including perimeter, II.

(Fig. 2).

\*3 Location of all wells within the New Orleans East (NOE) quad., II,

(Fig. 3).

4 Location of wells for mud weight program, II, poor data: same as  
 D-4.

## B. Mudweight - Interval Maps

(Average or maximum mud weight for 1K or 2K intervals; CI =  $\frac{1}{2}$ , 1, 2#)

1 10-12 K, CI = 1#, II Some hand-drawn outlines

2	11-12 K	1#	II Some outlining
*3	12-13 K	1#	II (Fig. 6)
4	13-14 K	1#	
5	13-14 K	1#	Varian
*6	10-12 K	1#	II(Fig. 4)
*7	10-12 K	1#	II Maximum mud weight (Fig. 5)
8	10-12 K	½#	II Maximum mud weight
*9	12-14 K	1#	II(Fig. 7)
10	12-14 K	½#	II
11	12-14 K	1#	II Maximum mud weight (Fig. 8)
12	12-14 K	½#	II Maximum mud weight

## C. Mudweight -- Depth-to Maps

(Depth [ft.] to a given mud weight; various patterns used)

1. 11# CI = 500 ft. Varian
2. 12# 500 II
3. 12# 1000 II
4. 12# 500 Varian
5. Same VBD VBD
6. 13# 500 Varian
7. Same VBD Varian
8. 13# 1000 II
9. 13# 1500 II
10. 14# 500 Varian
11. Same VBD
12. 14# 1000 II
13. 14# 1000 Varian
14. 14# 1500 II
15. 15# See Section "D" for all 15-pound mud weight maps.
- \*16. 16# 1000 II (Fig. 13)
- \*17. 17# 500 Varian (Fig. 14)
- \*18. Same VBD VBD (Fig. 15)
19. 18# 500 Varian
20. Same VBD VBD
21. 19# 500 Varian
22. Same VBD VBD
23. 20# 500 Varian
24. Same VBD VBD

## D. Mud weight -- Depth to 15#

(Including trend and residual maps)

- |      |        |      |  |
|------|--------|------|--|
| 1.   | Symap  | 500  | C. L.  |
| *2.  | Symap  | 1000 | (Fig. 10)  |
| 3.   | S-II   | 1000 | Zero and negative data eliminated                                |
| 4.   | S-II   | 1000 | Plot of data points for D-3-- Filed at A-4                       |
| 5.   | S-II   | 1000 | Same as D-3 but contours indexed differently<br>(Fig. 9)         |
| 6.   | S-II   | 1000 | Solid-print pattern, only data from 7,000 to<br>20,000 ft. used. |
| **7. | Varian | 1000 | (Fig. 11)  |
| 8.   | S-II   | 1500 |  |
| 9.   | Symap  |      | First-order trend map; regional dip south of 54 ft./mi.          |
| 10.  | Symap  |      | Third-order trend  |
| *11. | Symap  |      | Fourth-order trend (Fig. 12)                                     |
| 12.  | Symap  |      | Third-order residuals (CI-4000 to +1000; almost same as<br>D-1   |
| 13.  | Symap  |      | Third-order residuals (-1000 to +1000; too detailed)             |

## E. Mud weight -- Cross-sections

(E-1 to E-4 are raw data; E-5 to E-8 are with hand drawn trend lines. North-south sections combine data from 0.5° width of longitude. Section made using SYMAP.)

1. 90.00 to 90.05 longitude.
2. 90.03      90.35      "
3. 90.60      90.65      "
4. 90.95 to 91.00      "
- \*5. 90.00      90.05      "
6. 90.30      90.05      "
7. 90.60      90.65      "
- \*8. 90.95      91.00      "

## F. Temperature at given depth

- \*1. Temp. at 10,000 ft. depth, C. I. = 10° F, II. (Fig. 17)
- 2. A for similar temperature maps, b for New Orleans West; See Section L.

## G. Depth to given temperature

(All at 500-foot contour intervals)

- 1. 200° F    II depths: 6,900 to 13,000 ft.
- 2. 200°    Varian (just New Orleans East)
- 3. 200°    Varian (with border area also)
- 4. 200°    VBD (messed up)
- \*5. 250°    II depths: 8,500 to 17,000 ft. (Fig. 18)
- \*6. 250°    Varian (Fig. 19)
- 7. 250°    VBD (still poor)
- 8. 300°    Varian
- 9. 300°    VBD

### H. Temperature - Sections

(Bottom-hole temperatures, °F, plotted vertically on north-south sections of 0.05° width. For each number: B is the computer-produced section, A is hand-marked to show trends, and C is a xerox reduction for compilation. All use the SYMAP program.)

- |      |  |                    |                              |
|------|--|--------------------|------------------------------|
| 1.   | 29.0 to 30.2 Lat.                        | 89.5 to 89.6 Long. | A, B, C                      |
| 2.   | 29.0 to 30.0                             | 90.0 to 90.5       | A and C                      |
| 3.   | "  | 90.2 90.25         | A, B, C                      |
| 4.   | "  | 90.4 90.45         | A, B, C                      |
| 5.   | "  | 90.6 90.65         | A, B, C                      |
| *6.  | "  | 90.8 90.85         | A and C (Base for<br>Fig.22) |
| 7.   | 29.0 to 30.15                            | 90.95 91.00        | A and C                      |
| *8.  | Composite of H-2, H-4, and H-6 (3 Figs.) |                    | 2 sizes (Fig. 20)            |
| *9.  | 180°F lines from H-6 (3 Figs.)           |                    | A and Unmarked (Fig.21)      |
| *10. | 200                                      |                    | A and Unmarked (Fig. 21)     |
| *11. | 220                                      |                    | A and Unmarked (Fig. 21)     |
| *12. | Composite of trends from H-8 to H-11     |                    | A summary of H-14(Fig.21)    |
| 13.  | Composite of H-9, H-10, and H-11         |                    |                              |
| 14.  | Composite of H-13 with trends.           |                    |                              |

NOTE that sections 8-14 are not computer-produced, but hand-drawn interpretations.

## I. Net Sand - Interval maps

(Thousand-foot intervals, upper surface horizontal)

1.	10K to 11K (feet)	Flat S-II	S-II C.I. = 50 feet of sand
2.	10	11	Symap 50
3.	11	12	Symap 50
*4.	12	13	Symap 50 (Fig. 23)
5.	13	14	Symap 50
6.	12K to 13K (feet)	CI = 5%	Symap 1st Order trend
7.	Same		1rd Order residual
*8.	Same		3rd Order trend (Fig.24)
9.	Same		3rd Order residual

## J. Net Sand - Sloping Intervals

(Intervals with upper surface sloping at various degrees, intervals are 1,000 feet thick vertically. Intervals start ) on north) at 30.25 Lat. with tops at 5,000, 6,000, or 7,000 feet. The elevation of the top is thus deeper than that at the north edge of map.)

1.	1° of southward dip	Symap (2 copied)	Upper (5-6K) interval
*2.	1.13°	S-II	Upper " (Fig. 25)
4.	1½°	S-11	Upper "
6.	1°	Symap	Mid (6-7K)
*7.	1.13°	Symap	Mid " (Fig. 26)
8.	1½	Symap	Mid (6-7K)
9.	1½	S-II	Mid "
10.	2	Symap	Mid "
**11.	1.13	Symap	Lower (7-8K), (Fig.27)
12.	1½	S-II	Lower

## K. Percent Sand Cross-sections

(the percent of sand in a discrete interval is plotted in the middle of the interval, the figure  $\times 10 = \%$ ; the weighted sections gives greater weight to thicker intervals with a higher percent of sand in the interval (on scale of eleven); Symap plots; North-south sections from  $29.0^\circ$  to  $30.0^\circ$  latitude.)

1.  $90.00^\circ$  to  $90.05^\circ$  Longitude, Non-weighted, C.I. = 10%
2.  $90.00^\circ$      $90.00^\circ$                     Non-weighted, C.I. = 10%
- \*3.  $90.2^\circ$      $90.3^\circ$                     Non-weighted, C.I. = 10% (Fig. 29)
- \*4.  $90.2^\circ$      $90.3^\circ$                     Weighted in eleven units (Fig. 30)
5.  $90.4^\circ$      $90.5^\circ$                     Non-weighted, C.I. = 10%
6.  $90.4^\circ$      $90.5^\circ$                     Weighted
7.  $90.6^\circ$      $90.7^\circ$                     Weighted
8.  $90.8^\circ$      $90.9^\circ$                     Weighted
9. 1st Order Trend on weighted data; no trend observed.
10. 3rd Order Trend on weighted data; trend not significant.



## MUD WEIGHT ILLUSTRATIONS

## Figure

4. Average mud weight used between 10,000 to 12,000 feet depth (10-12K) or a 2,000-foot thick interval (2,000 ft); contour interval based on one pound increase per gallon (CI = 1#), and solid contour lines start with a 12 pound mud weight (CL 12#).  
This:
  4. Average mud weight, 10-12 K (2,000 ft), CI = 1#, CL = 12#
  5. Average mud weight, 10-12 K (2,000 ft), CI = 1#, CL = 14#
  6. Average mud weight, 12-13 K (1,000 ft), CI = 1#, CL = 14#
  7. Average mud weight, 12-14 K (2,000 ft), CI = 1#, CL = 13#
  8. Maximum mud weight, 12-14 K (2,000 ft), CI = 1#, CL = 15#
  9. Depth to 15# mud weight, Surface II map, CI = 1,000 feet.
  10. Depth to 15# mid weight, SYMAP map, CI = 1,000 feet.
  11. Depth to 15# mud weight, Varian plot, CI = 1,000 feet.  
10,000 feet (highs) are shaded; H=High.
  12. Depth to 15# mud weight, 4th-order trend-surface, CI = 500 feet.
  13. Depth to 16# mud weight, Surface II map, CI = 1,000 feet, CL = variable.
  14. Depth to 17# mud weight, Varian plot, CI = 500 feet, highs hachured.
  15. Three dimensional block diagram of Fig. 14 as seen from southeast.

## NET SAND AND IT'S DISTRIBUTION

## Figure

23. Net sand in a 1,000-foot-thick, vertical interval from 12-13 K; CI = 50 feet of sand, SYMAP; areas of greater than 30% sand are hand
24. Net sand; third-order residual on Fig. 23 (12-13 K), CI = 5% SYMAP
25. Net sand in a 1,000-foot-thick sloping interval, CI = 50 ft., SYMAP. The top of the interval slopes southward at  $1.13^\circ$ ; elevation at the north edge of quadrangle is about 6,800 feet and at the south edge is about 14,000 feet (see Table 3).
26. Net sand, 1,000-foot interval, sloping  $1.13^\circ$  from 7,800 to 15,000 feet.
27. Net sand, 1,000-foot interval sloping  $1.13^\circ$  from 8,800 to 16,000 feet.
28. Typical distribution patterns of net sands in a modern delta, after Coleman & Wright (1975). This diagram indicates the types of patterns that interval net sand maps if the interval is kept small enough.
29. Distribution of percent sand (figure  $\times 10$  = percentage), north-south section, strip  $0.1^\circ$  wide ( $90.2^\circ$ - $90.3^\circ$  Long.); trends hand-drawn.
30. Weighted distribution of sand, from L - Low, through 1-9, to \* and H = High; weighted to thicker intervals, north-south section, strip  $0.1^\circ$  wide ( $90.2^\circ$ - $90.3^\circ$  long.); trends hand-drawn.

Table 2. TEMPERATURE CORRECTION

The temperature correction (T) in degrees Fahrenheit to be added to the observed bottom-hole temperature (F°) for each thousand feet of depth (D). Modified from formula by Amer. Assoc. Geol. Comm. on "Geothermal Study of North American (1971).

<u>D</u>	<u>T</u>	<u>D</u>	<u>T</u>	<u>D</u>	<u>T</u>	<u>D</u>	<u>T</u>
1	3.2	6	22.5	11	32.7	16	27.3
2	7.5	7	25.4	12	33.1	17	23.7
3	11.6	8	28.0	13	32.8	18	19.3
4	15.5	9	30.1	14	31.7	19	13.8
5	19.1	10	31.7	15	29.9	20	7.3

$$T=0.008819 d^3+0.02143 d^2 - 4.375 D+1.108$$

Table 3, ELEVATIONS of the Top Surface in feet  
 below sea level for sloping intervals. The BE (base elevation)  
 is set at 30.25° latitude. Numbers in the table give the elevation  
 for North (30°), Mid (29½°) and South (29°) positions on the map.

SLOPE	<u>1.0°</u>	<u>1.13°</u>	<u>1.2°</u>	<u>1.5°</u>	<u>2.0°</u>
BE = Zero (Accurate)					
North	1587	1796	1907	2385	3181
Mid	4768	5390	5723	7155	9542
South	7949	8983	9539	11925	15902
BE = Zero (Highly rounded)					
North	1500	2000	2000	2500	3000
Mid	5000	5500	6000	7000	9500
South	8000	9000	9500	12000	16000
BE = 5000					
North	6600	6800	6900	7400	8200
Mid	9750	10400	10700	12150	14500
South	12950	14000	14550	16900	20900
BE = 6000					
North	7600	7800	79008	8400	9200
Mid	10800	11400	11700	13200	15500
South	14000	15000	15500	17900	21900
BE = 7000					
North	8600	8800	8900	9400	10200
Mid	11800	12400	12700	14200	16600
South	15000	16000	16500	18900	22900

## APPENDIX I.

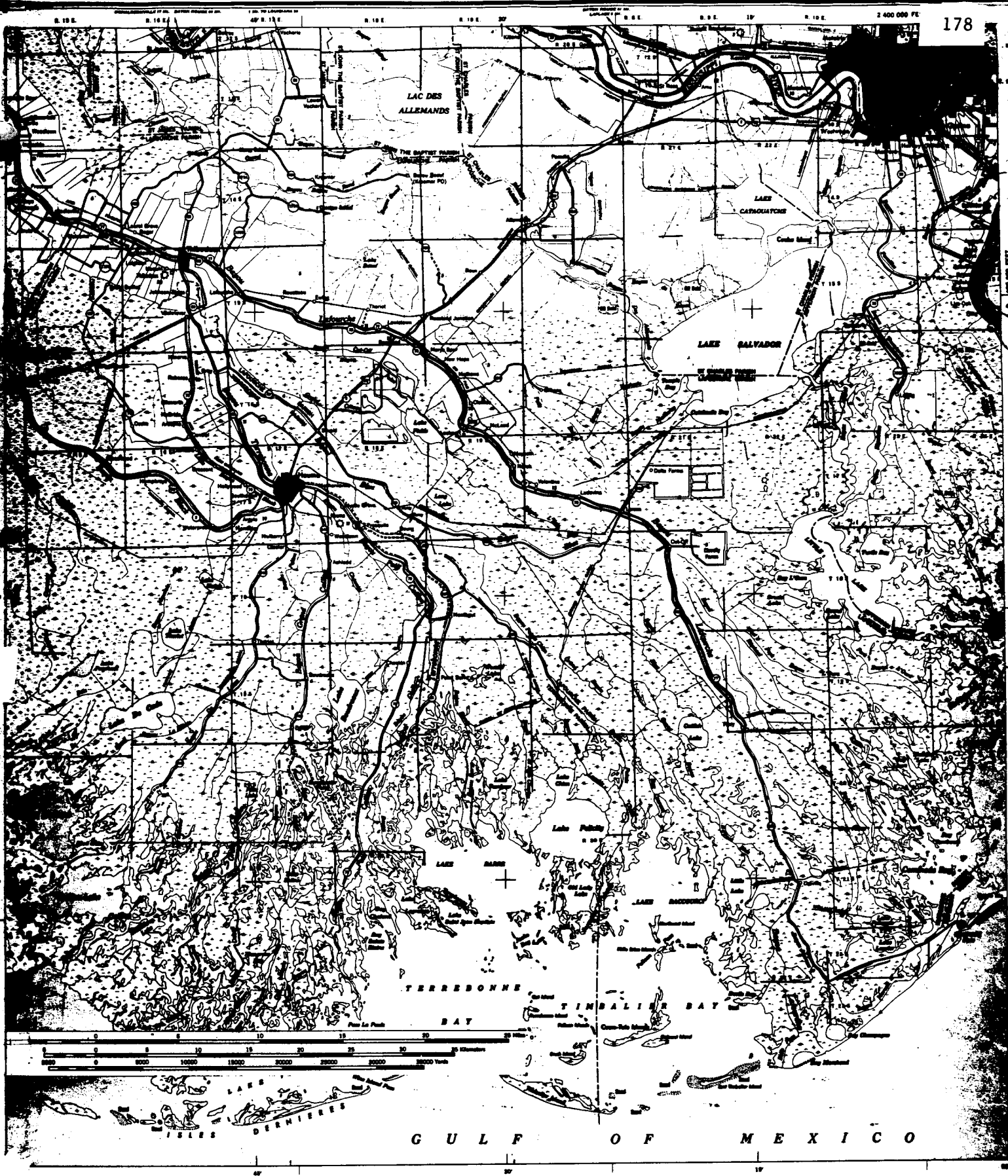
## Programs Produced by R. L. Hixon

- A. LISTWELL selects wells for a specific area from the CLEANDATA file.
- B. MDSNDSAL calculates the average mud weight and the cumulative sand thickness for given vertical intervals.
- C. TEMPFILE determines the temperature gradient with depth, for corrected drill-hole temperature.
- D. LISTGRAD selects data for a specific area from TEMPFILE.
- E. ISOTHERM calculates depth to a specific temperature.
- F. TMPONHRZ calculates the temperature at a given depth.
- G. CASSIE calculates the salinity of selected sands from mud resistivity and SP\_data on well log.
- H. SALINRMF is similar to CASSIE, but uses mud filtrate resistivity to calculate the salinity.

## APPENDIX 2

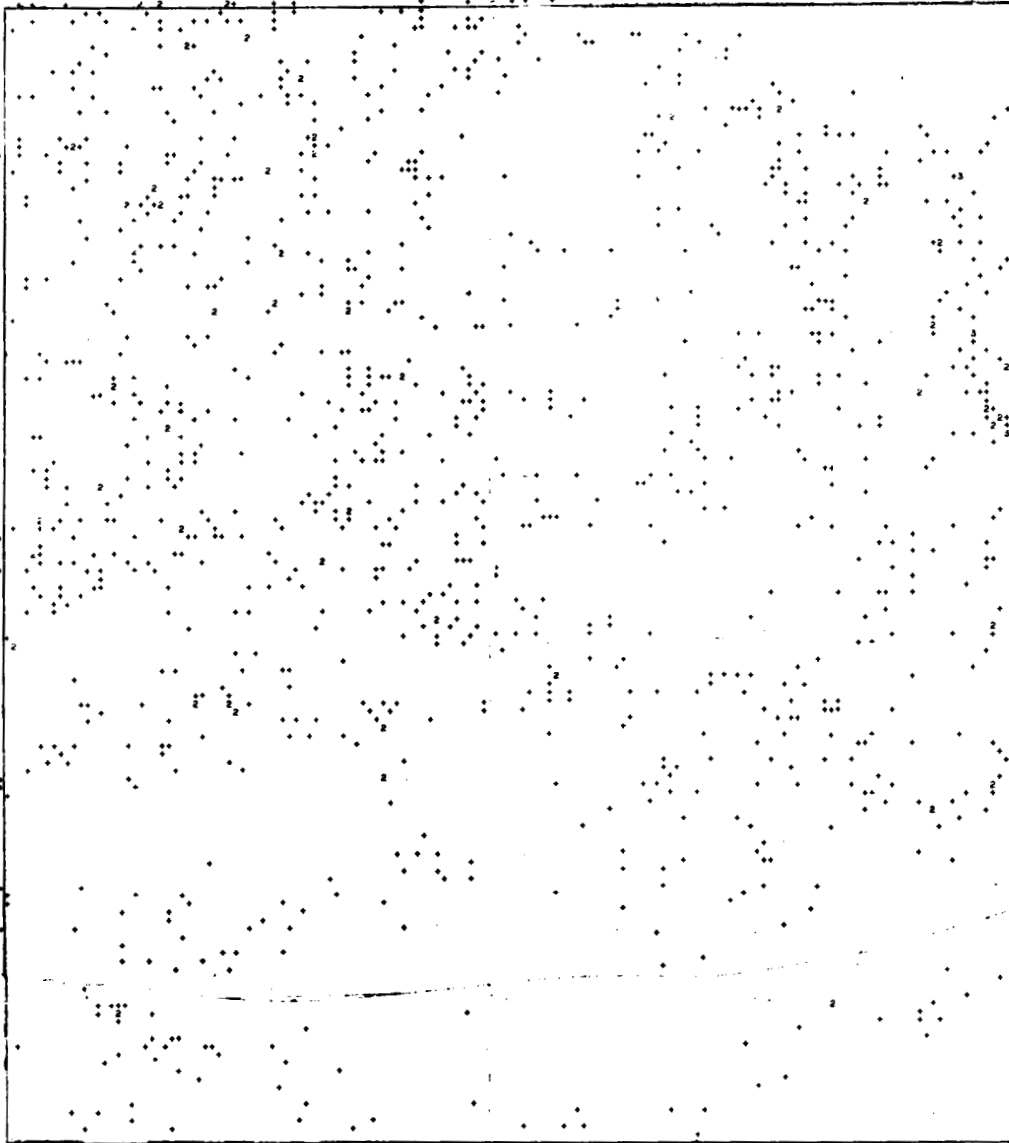
Program by D. H. Kupfer and K. C. Meade

- A. MUDTREND, a program to determine the approximate pressure gradient with increasing depth for each drillhole; the angle of slope of the gradient, used for extrapolation, changes within the transition and geopressured zones. The program can be used to calculate depth to a certain mud weight or mud weight at a given depth.
- B. MUDSAND, a variant of MDSNDSAL to calculate the average or maximum mud weight and the net sand within four vertical intervals.
- C. PERSAND, calculates the percent sand in a small intervals of mixed lithology, and plots it at the average depth of that interval; useful in making cross-section.
- D. DIPSAND, calculates the average mud weight, or the total net sand, for a south-sloping interval of 1,000 vertical feet; the slope given should appropriate regional dip.
- E. TEMPDHK, program in preparation to calculate temperature gradient, correcting obvious errors, and extrapolating readings according to depth zone (hydropressure, transition, or geopressured).



1. Base map of New Orleans East (NOE) quadrangle, from U.S. Geological Survey topographic map originally published at a scale of this and all the following maps is about :500,000 (8 mi./inch).

2

LOCATION OF WELLS IN EAST HALF NEW ORLEANS QUAD,  
INCLUDING PERIMETER

2. Location of all control wells used in study of NOE quadrangle, including those in the adjacent 15-minute-wide perimeter area. Rectangle is NOE quadrangle of Figures 1 and 3. Note that this map is not at scale of the other maps.

# LOCATION OF WELLS IN EAST HALF, NEW ORLEANS QUAD

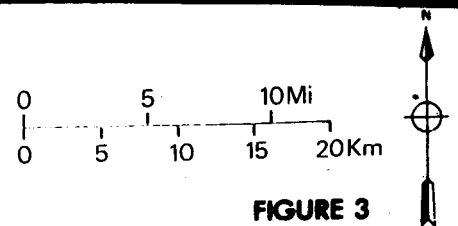
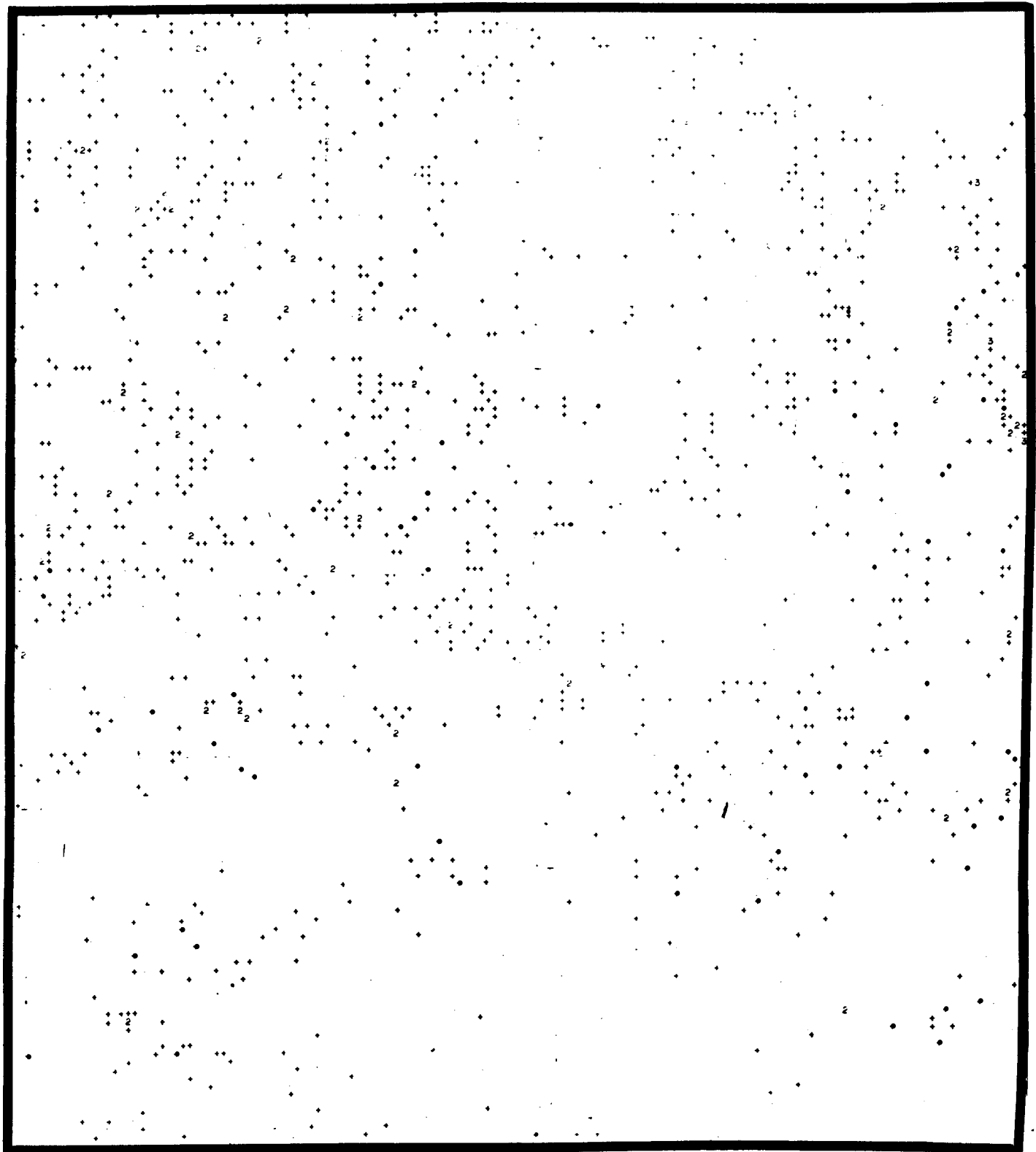


**FIGURE 3**

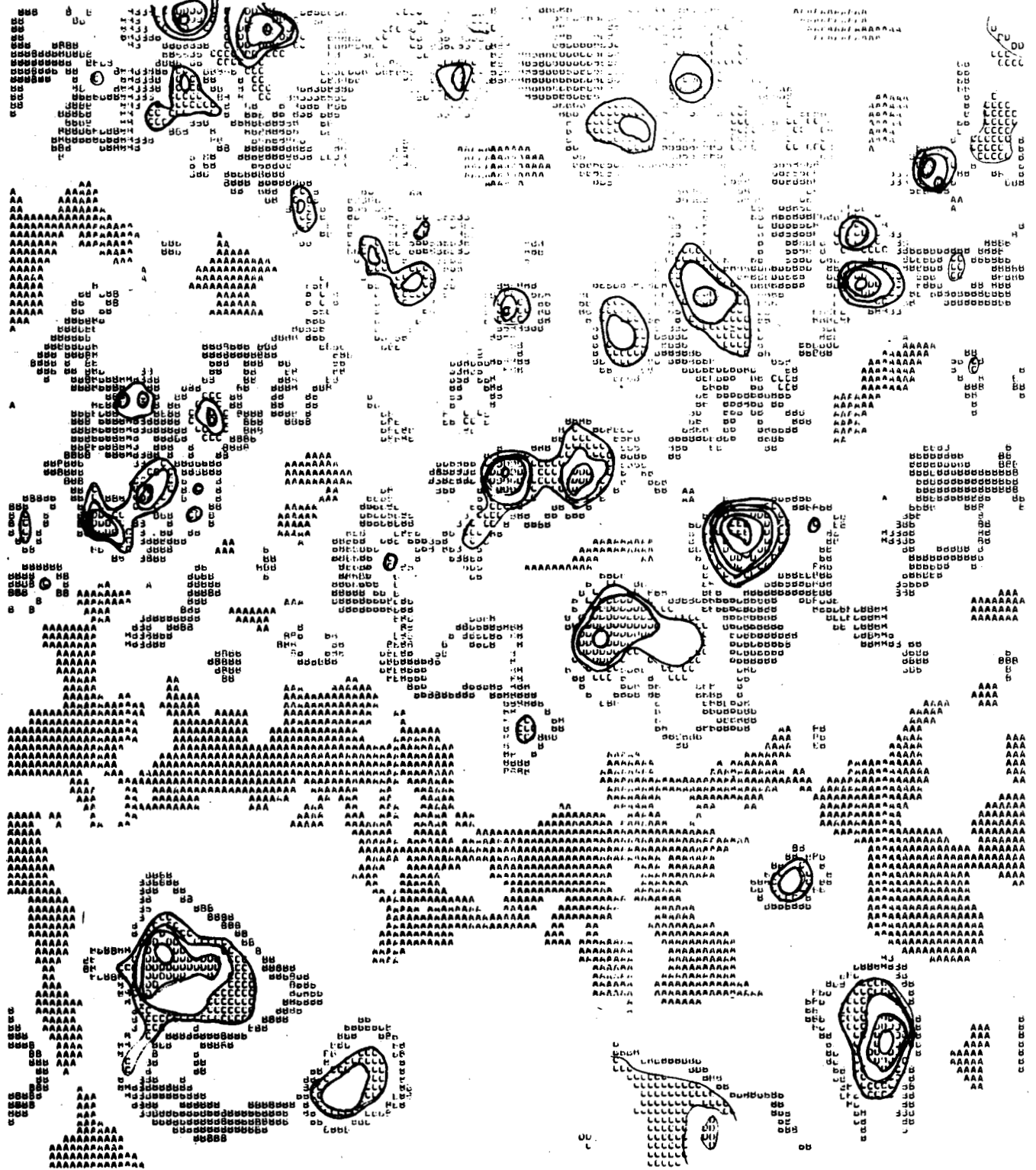
3. Location of control wells within NOE quadrangle. The numbers indicate that 2 (or 3) wells are too close together to be plotted separately.

### AVERAGE MUDWEIGHT BETWEEN 10,000 - 12,000 FEET



4. Average mud weight used between 10,000 to 12,000 feet depth (10-12K), a 2,000-foot thick interval (2,000 ft); contour interval based on one pound increase per gallon (CI = 1#), and solid contour lines start with a pound mud weight (CL 12#). Thus:

# MAXIMUM MUDWEIGHT BETWEEN 10,000 - 12,000 FEET



Mudweight (ppg)

CCCCC	14
DDDDD	15
EEEE	16
FFFF	17
GGGG	18

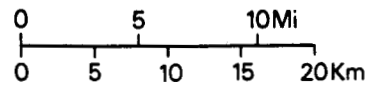
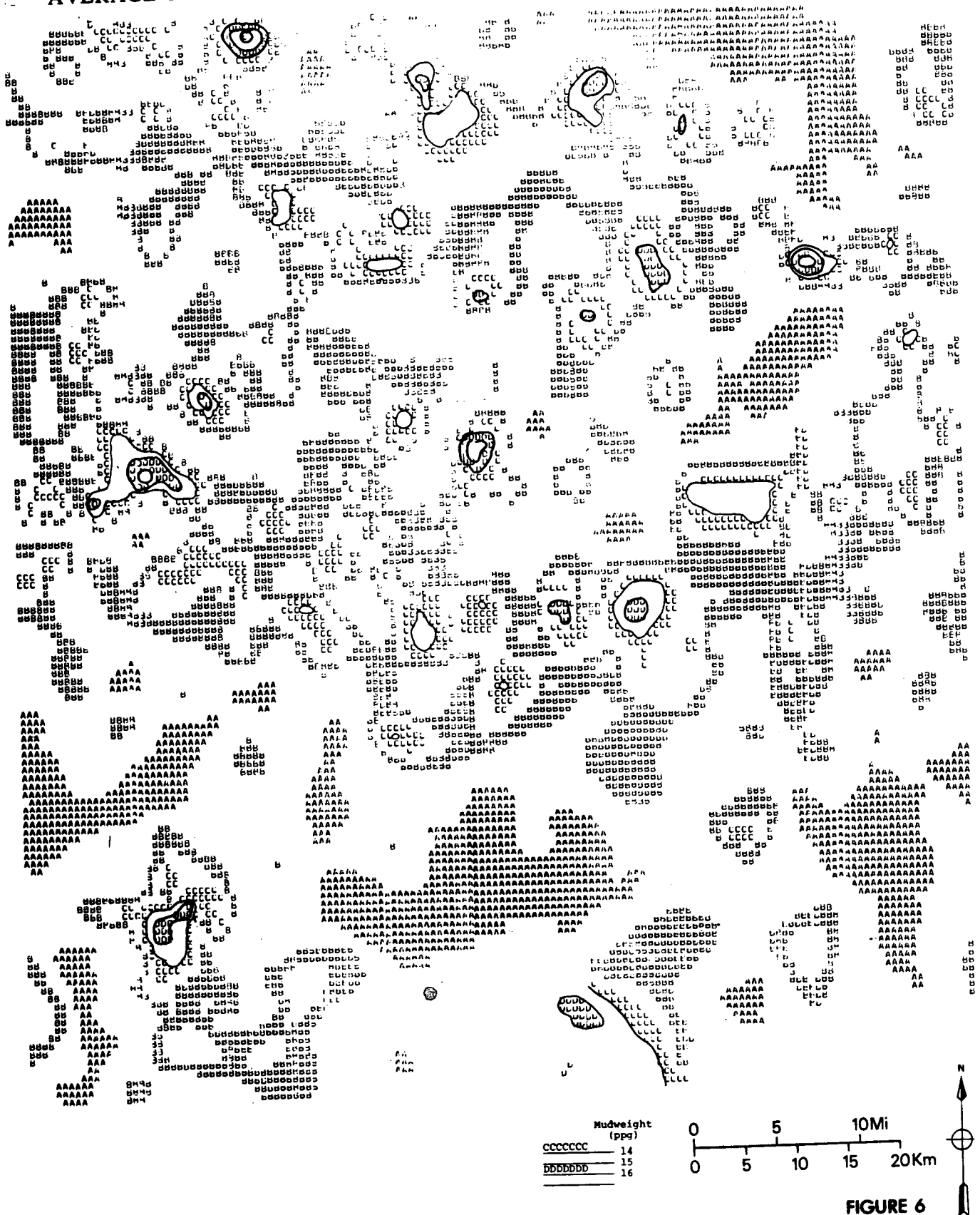


FIGURE 5

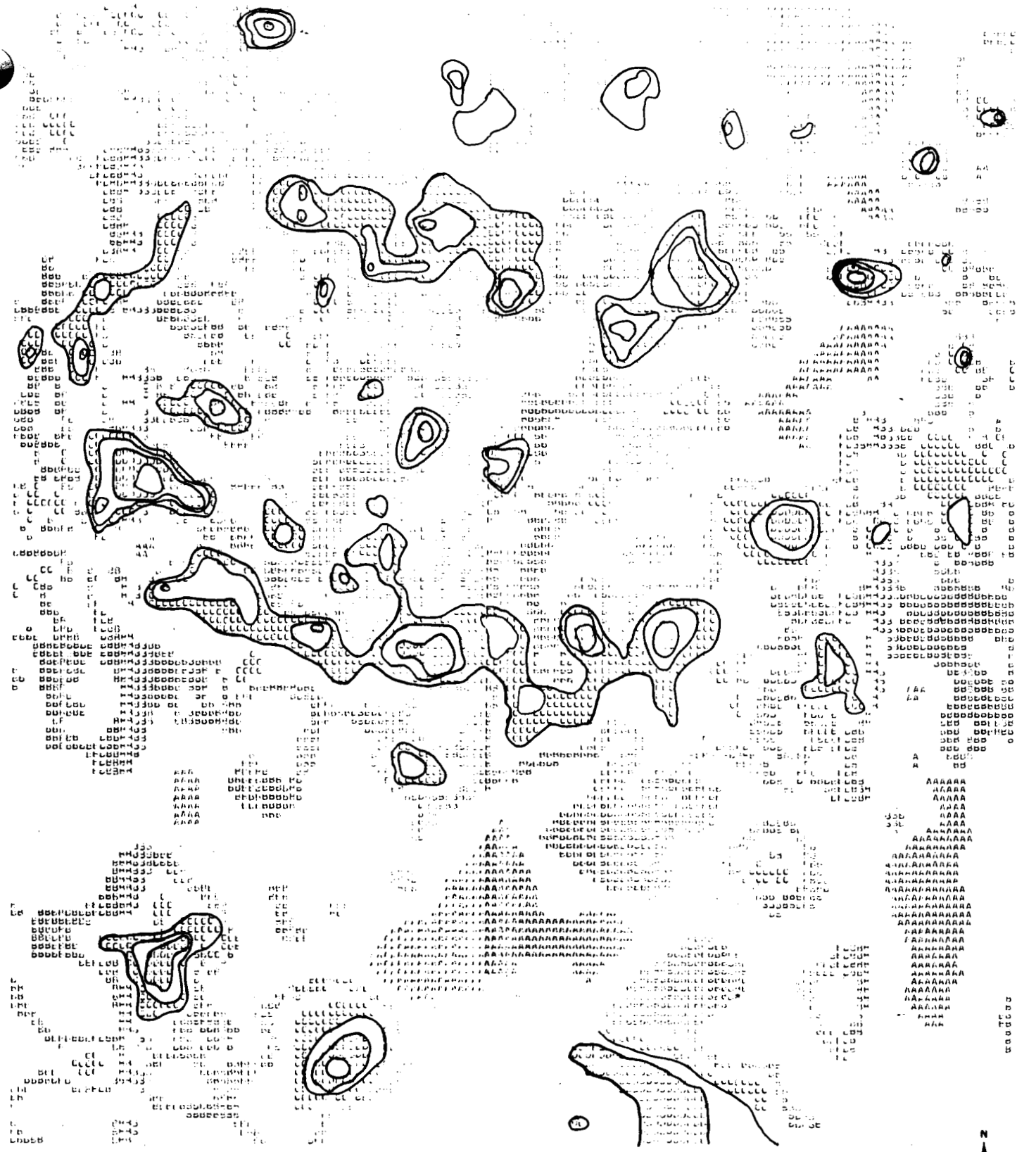
5. Maximum mud weight, 10-12K (2,000ft), CI = 1#, CL = 14#.

# AVERAGE MUDWEIGHT BETWEEN 12,000 - 13,000 FEET



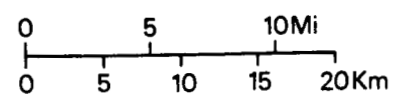
6. Average mud weight, 12-13K (1,000 ft), CI = 1#, CL = 14#.

# 7 AVERAGE MUDWEIGHT BETWEEN 12,000 - 14,000 FEET



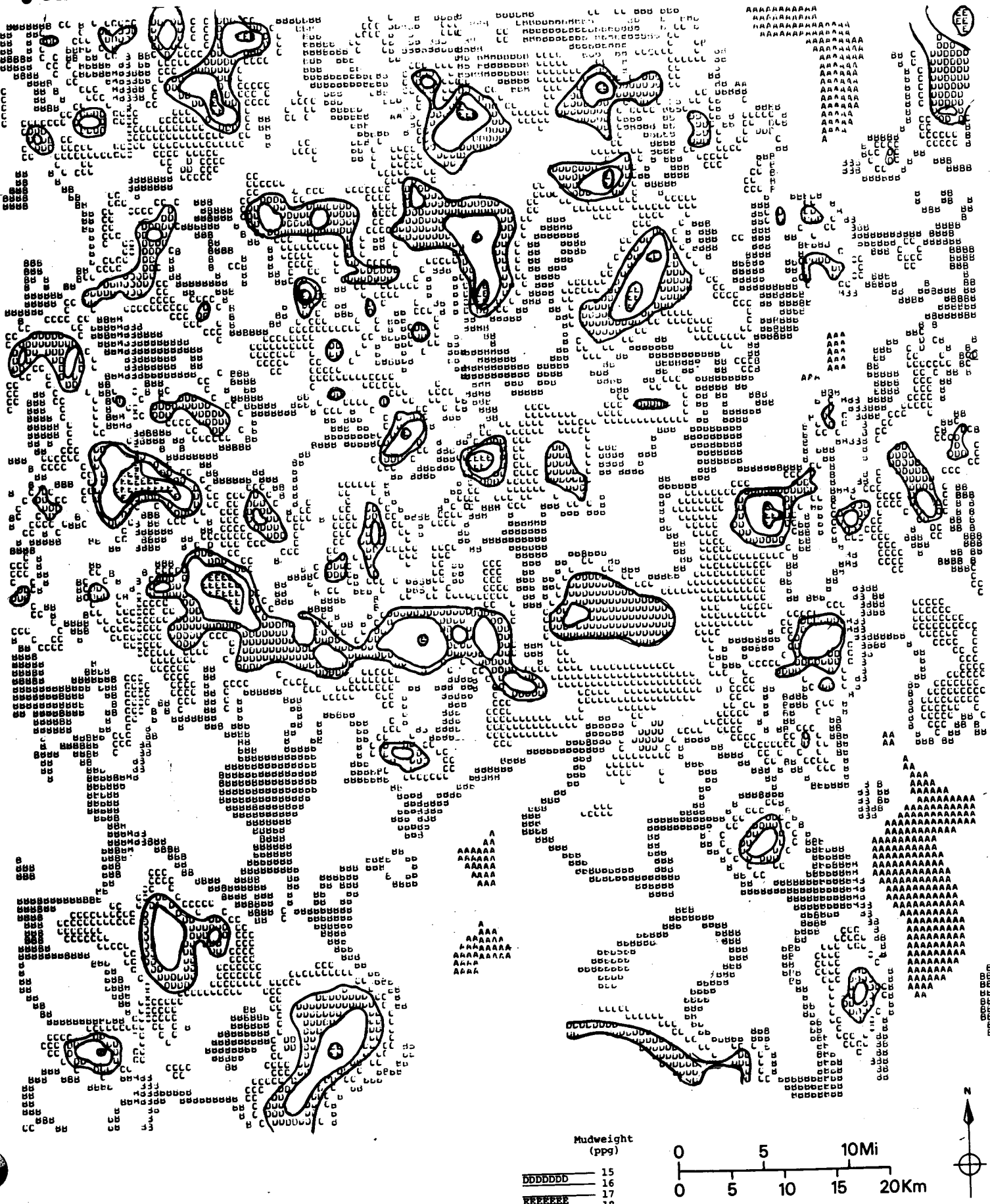
Mudweight (ppg)

CCCCCCC	13
DDDDDDD	15
EEEEEEE	18

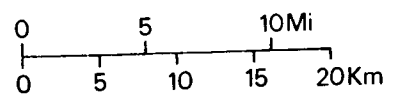
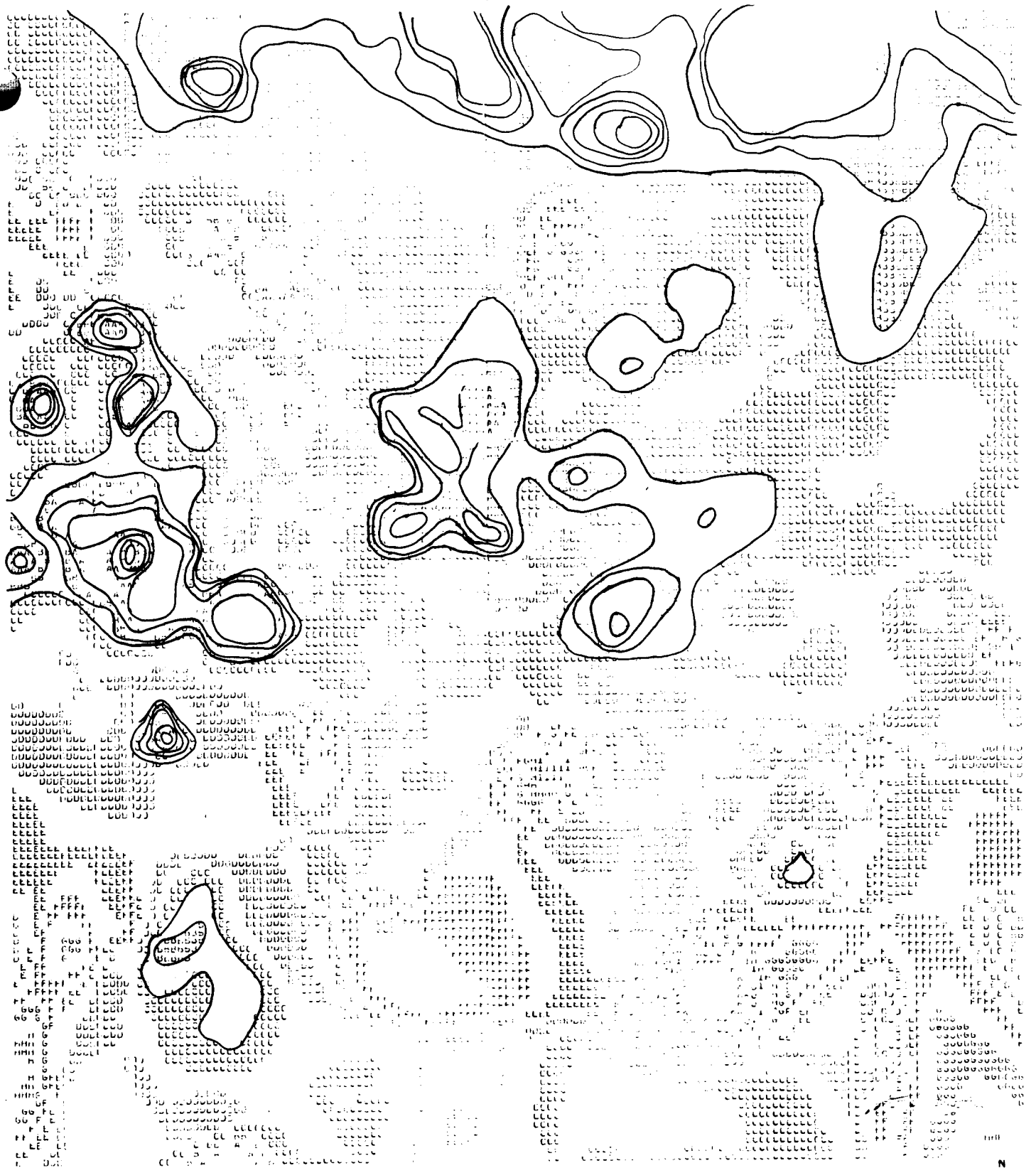


7. Average mud weight, 12-14K (2,000 ft.), CI = 1#, CL = 13#.

# 8 MAXIMUM MUDWEIGHT BETWEEN 12,000 - 14,000 FEET

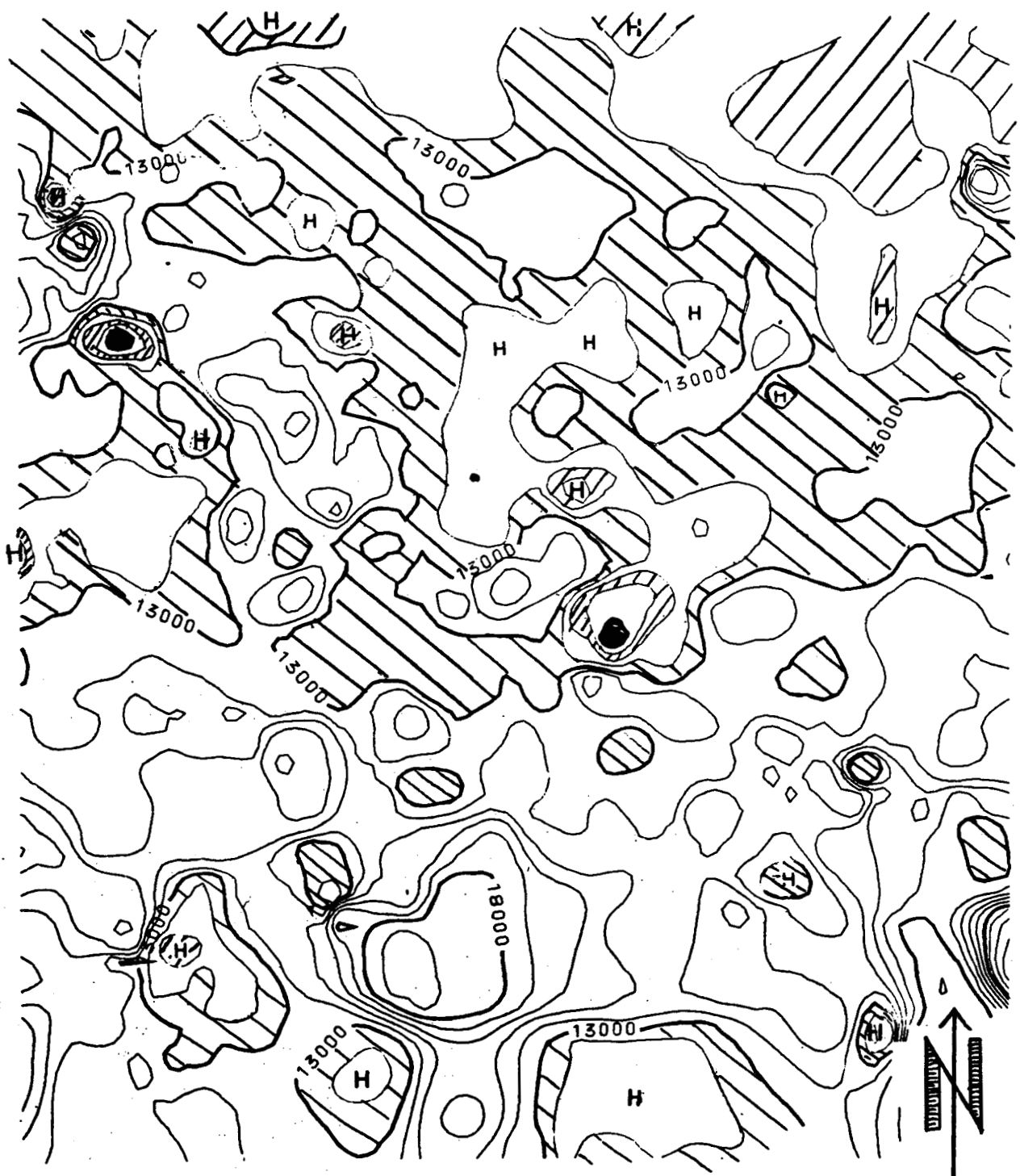


8. Maximum mud weight, 12-14D (2,000 ft.), CI = 1#, CL = 15#.



9. Depth to 15# mud weight, Surface II map, CI = 1,000 feet.





11 DEPTH TO 15 POUND MUDWEIGHT, EAST HALF, N.O.  
DATE 9/16/80

FIGURE 11

11. Depth to 15# mud weight, Varian plot, CI = 1,000 feet; area above 10,000 feet (highs) are shaded, H = High.

DEPTH TO 15 POUND MUDWEIGHT (4TH ORDER TREND)

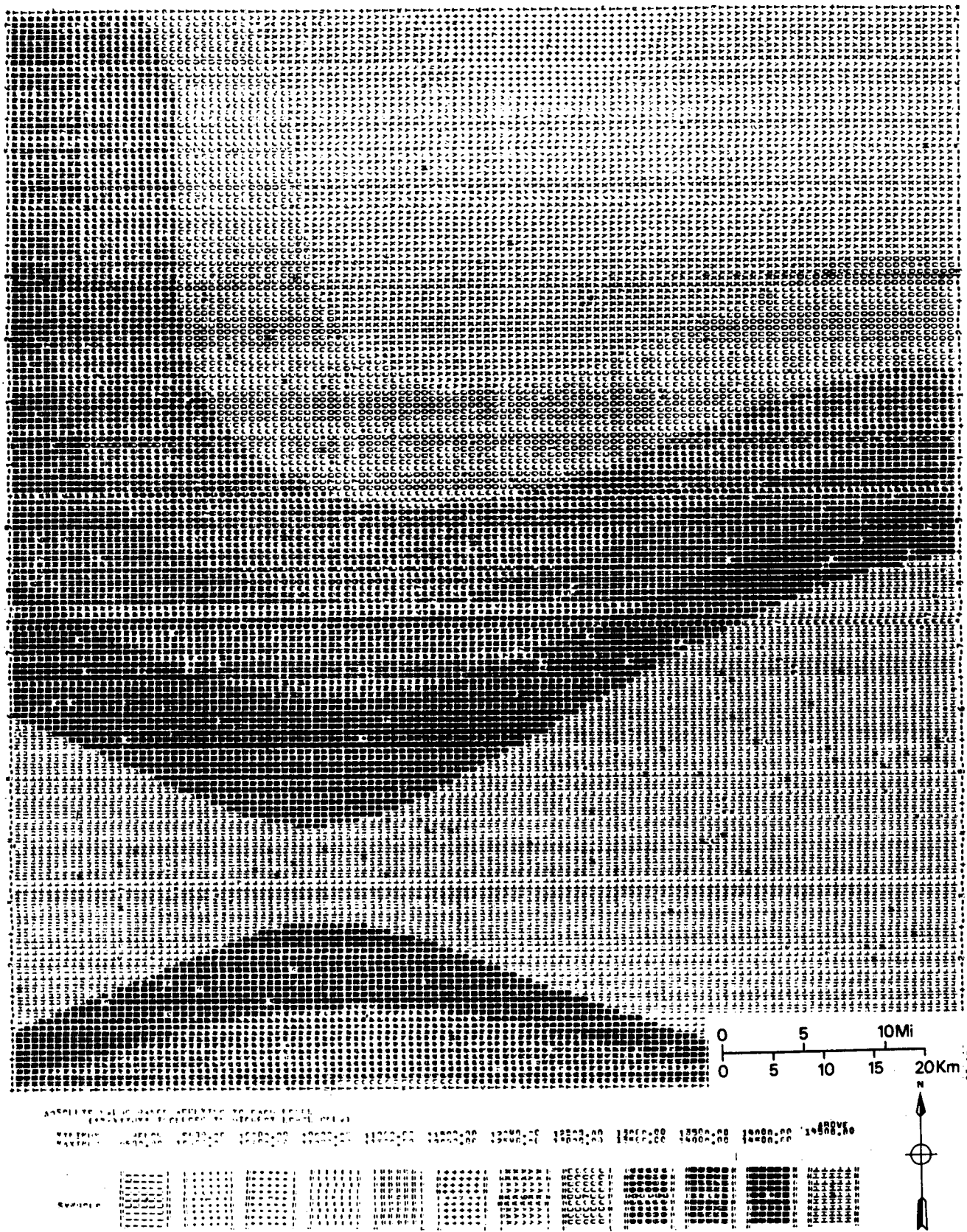
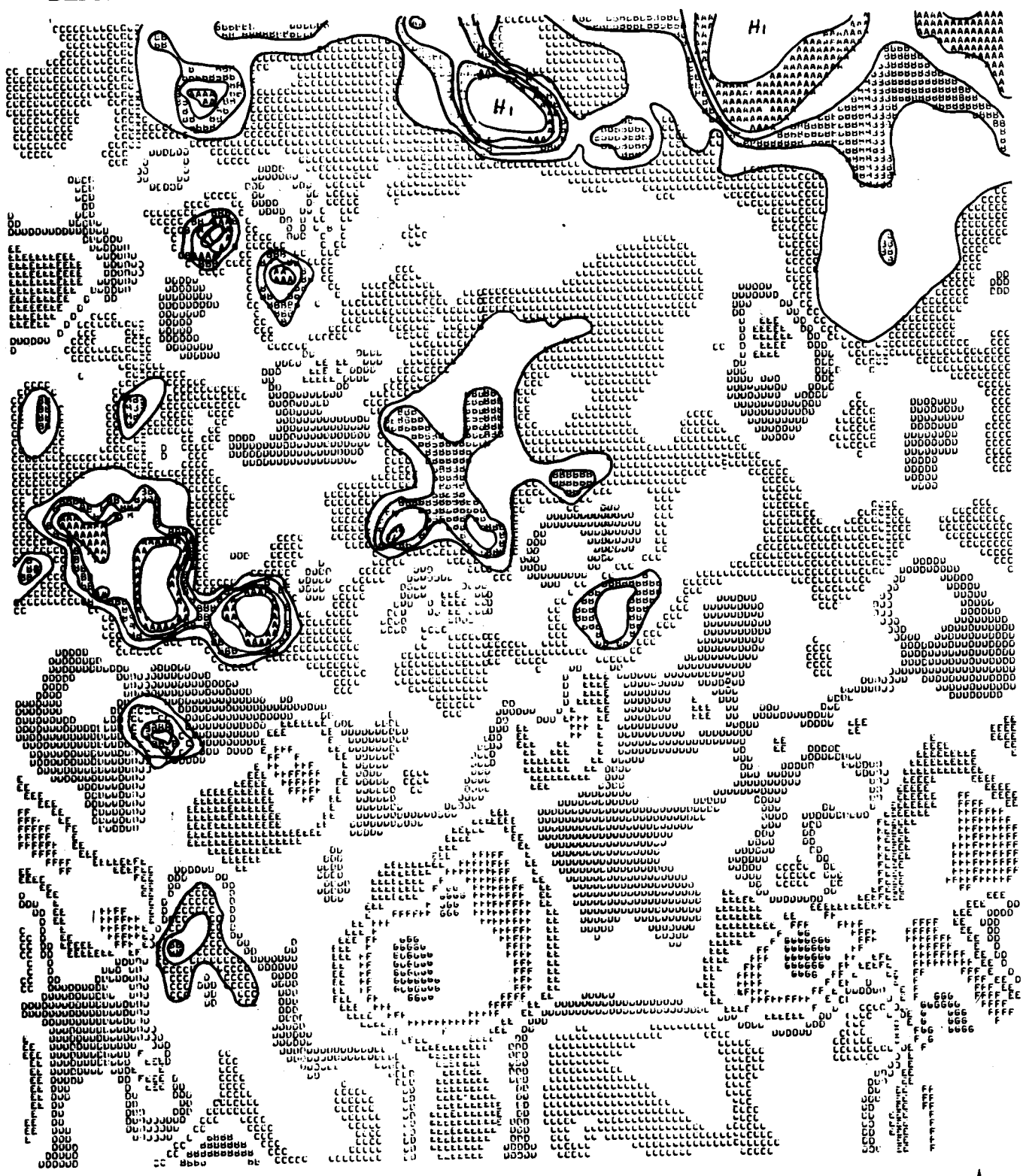


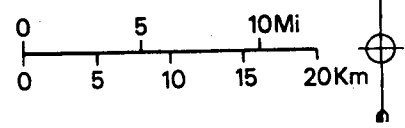
FIGURE 12

12. Depth to 15# mud weight, 4th-order trend-surface, CI = 500 feet.

# DEPTH TO 16 POUND MUDWEIGHT



Character	Depth (ft)
AAAAAA	8,000
BBBBBB	9,000
CCCCCC	10,000
DDDDDD	11,000
EEEEEE	12,000
FFFFFF	13,000



13. Depth to 16# mud weight, Surface II map, CI = 1,000 feet, CL = variable.

14 DEPTH TO 17 POUND MUDWEIGHT

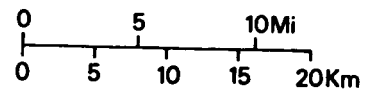
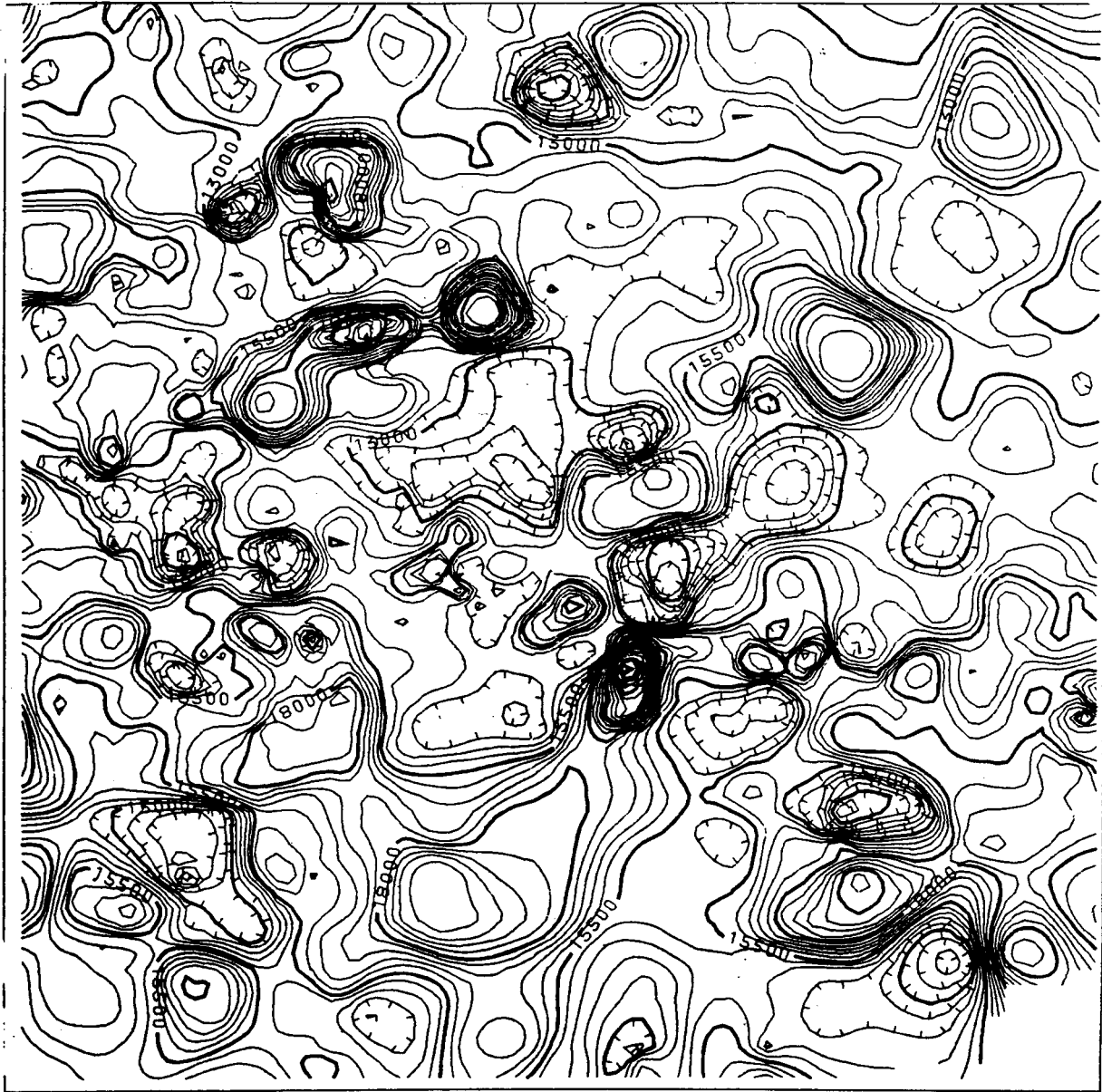


FIGURE 14

14. Depth to 17# mud weight, Varian plot, CI = 500 feet, highs hachured.

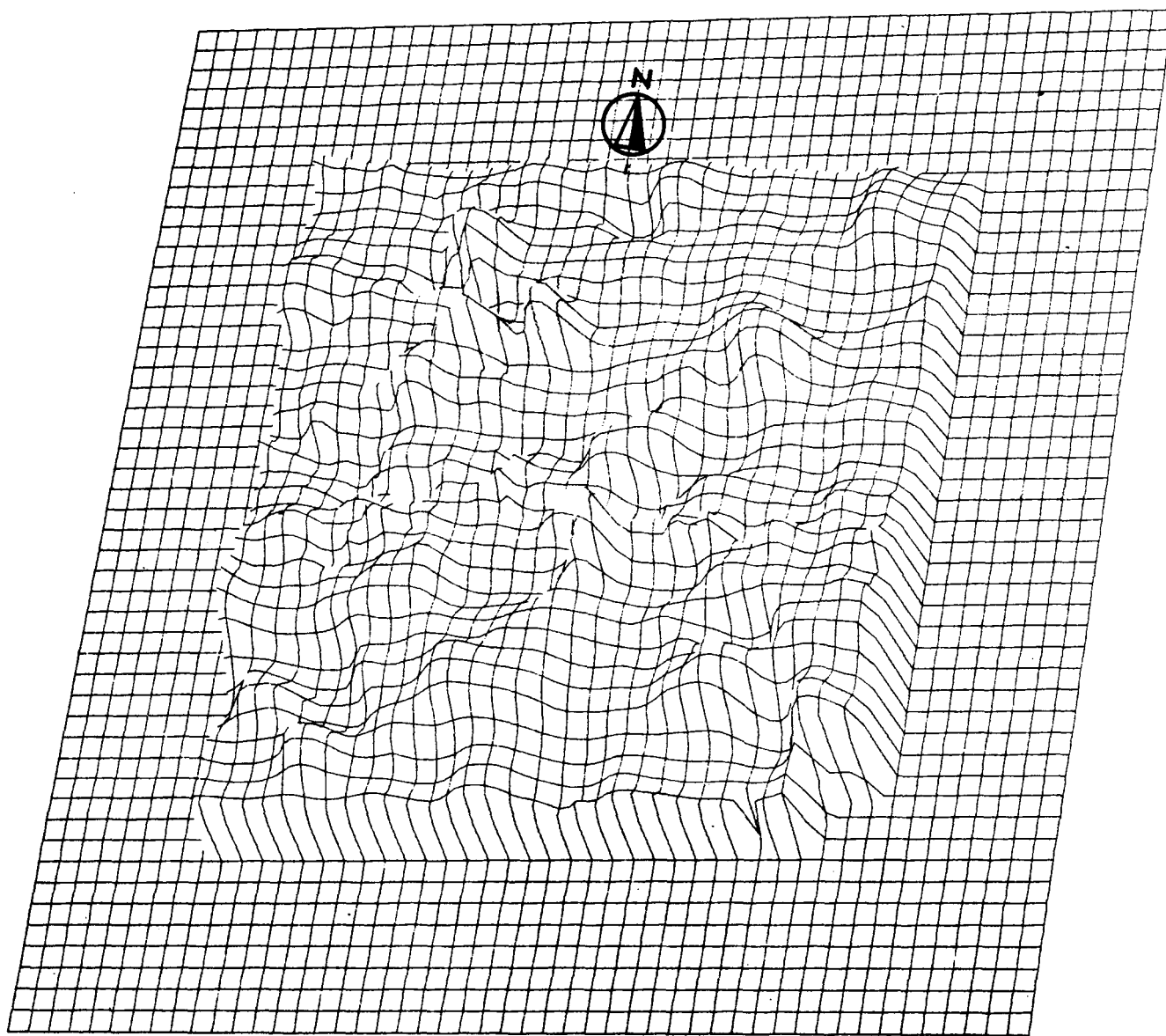


FIGURE 15

15. Three dimensional block diagram of Fig. 14 as seen from southeast.

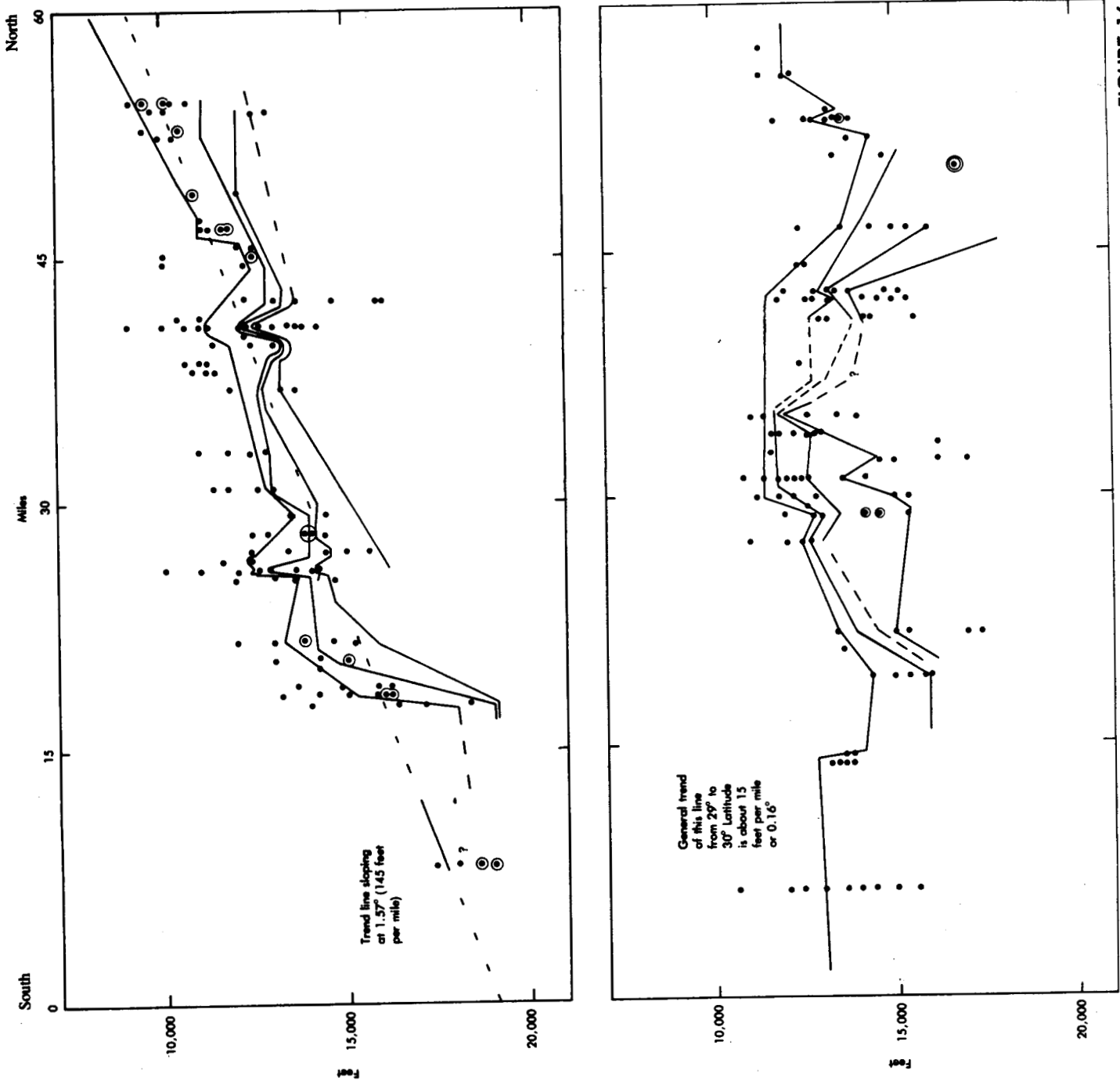


FIGURE 16

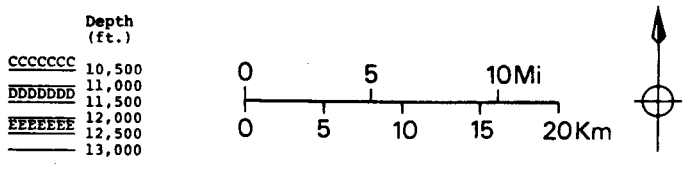
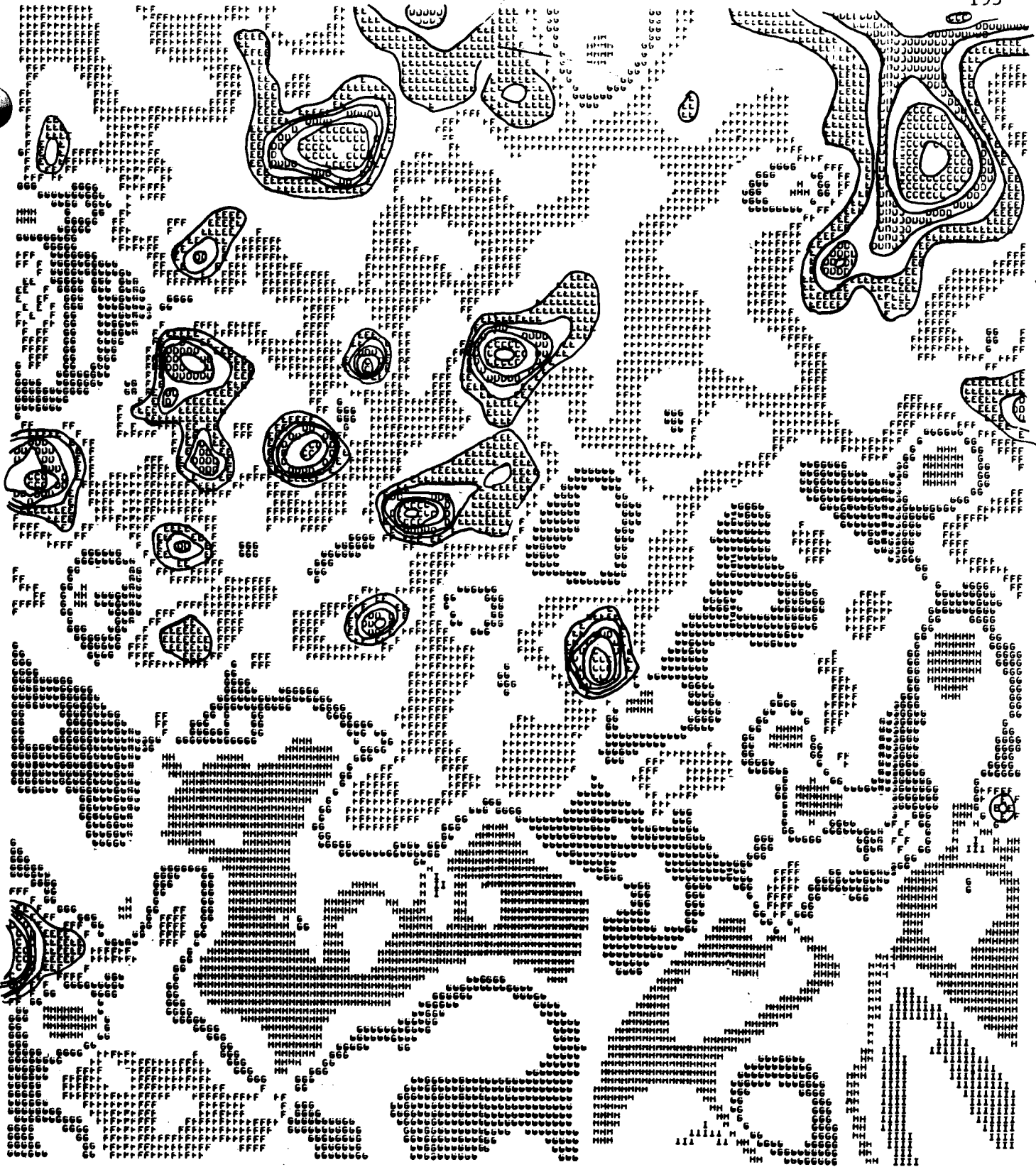
16. Mud weight distribution in north-south cross-sections across NOE Quadrangle, with hand-drawn profile lines; a=East side, B=West side. Mud weights range by half-pound intervals, from L=below 12#, by half-pound intervals, through 5 = 14#-14½#, \* 16 ½#-17#, to H = over 17#. Profiles are drawn on 13#, 14 ½#, 16#, and 17#.

TEMPERATURE (°F) AT 10,000 FEET



FIGURE 17

17. Temperatures at 10,000 feet, CI = 10°F, "highs" hand-contoured.



18. Depth (ft.) to 250°F, CI = 500 ft., SURFACE-II map, "highs" hand-contoured.

19. Depth (ft.) to 250°F, CI - 500 ft., Varian plot, "highs" hachured.  
Map includes perimeter area and is not to standard scale.

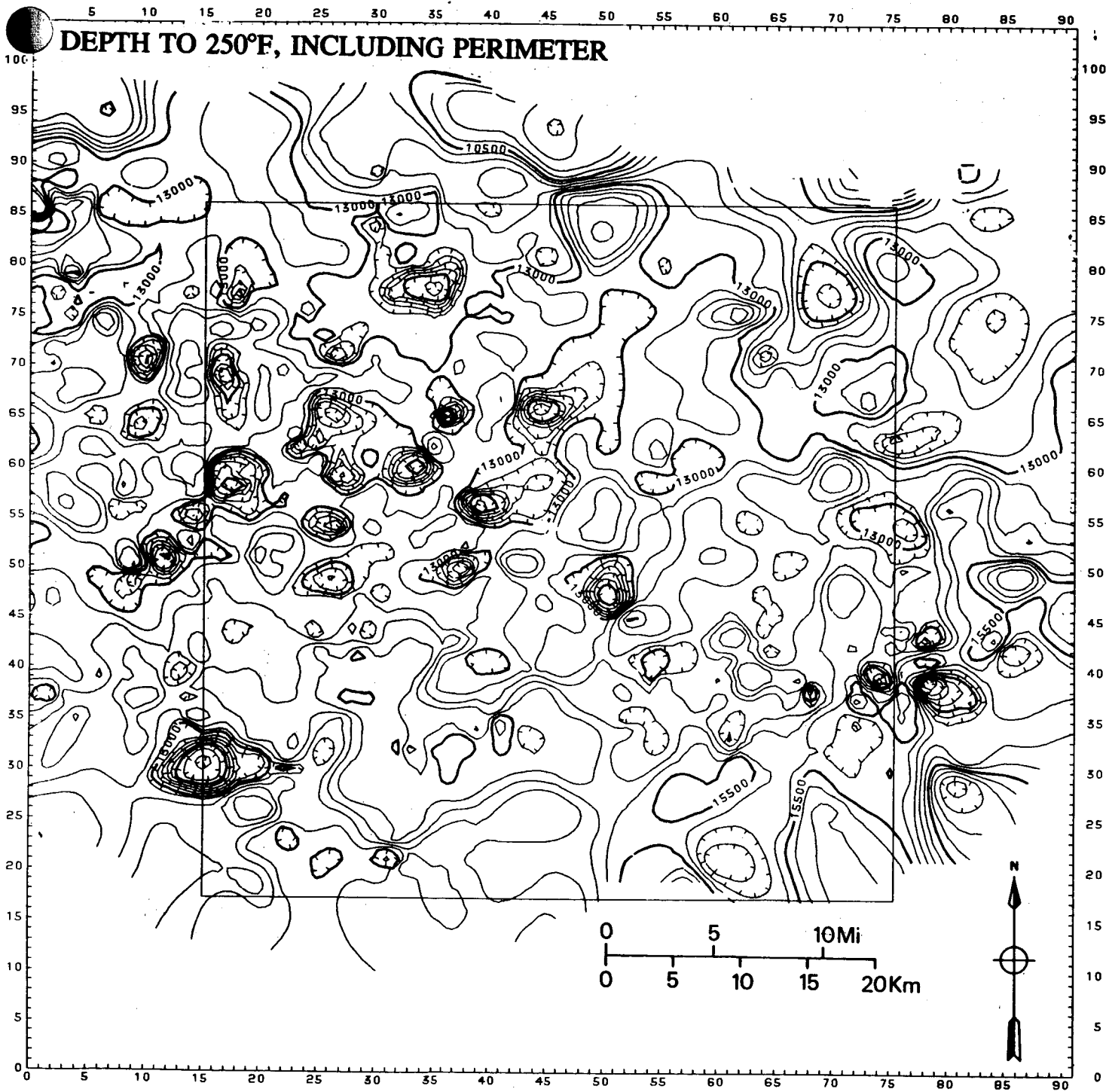


FIGURE 19

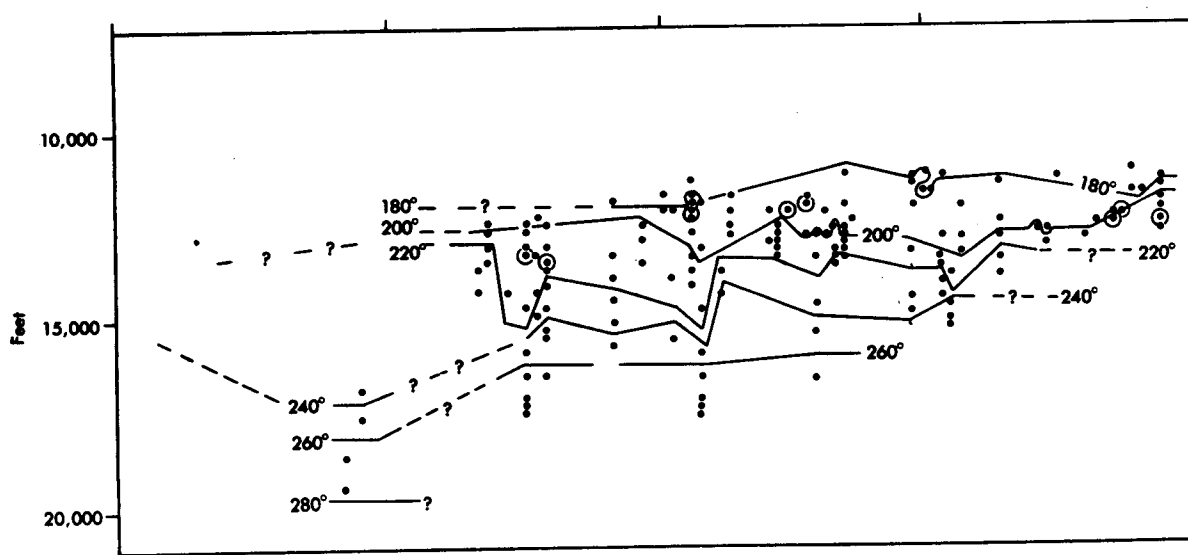
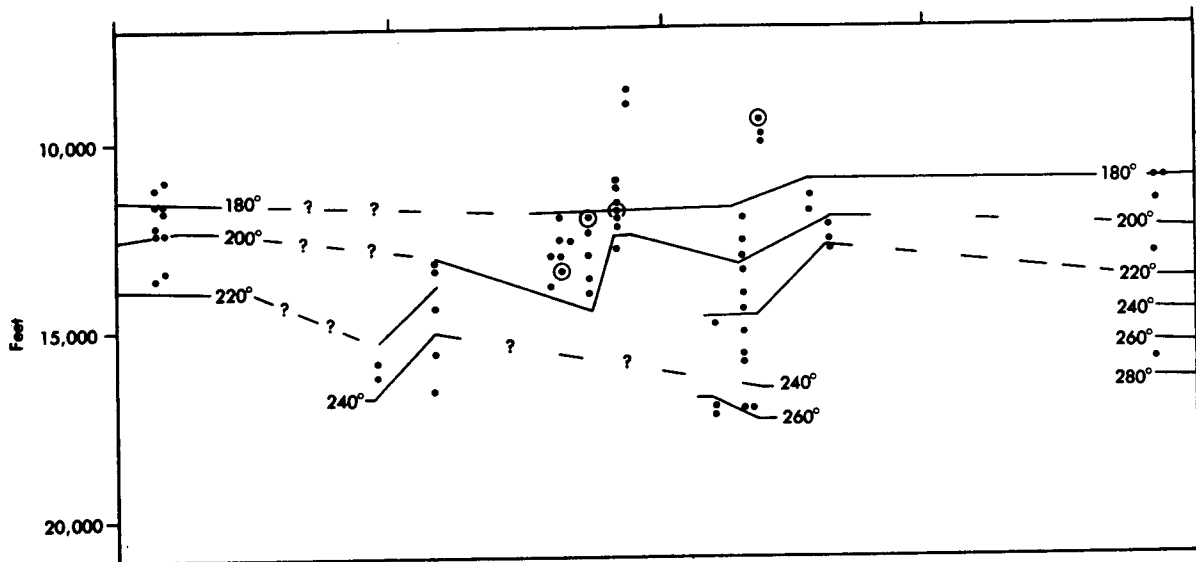
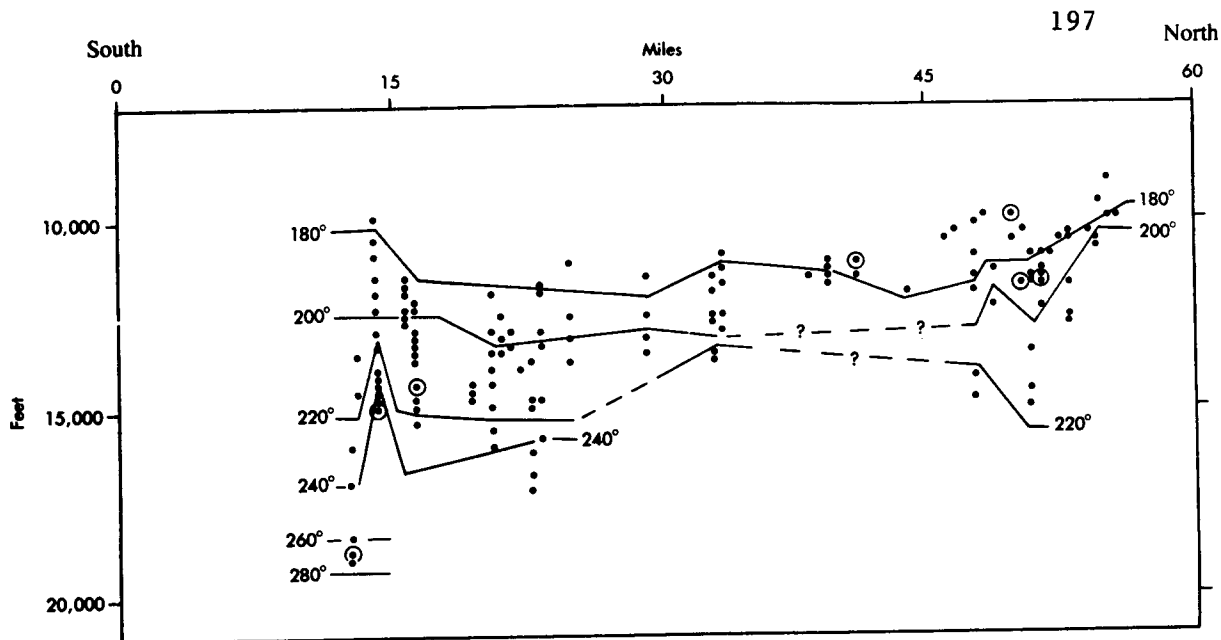


FIGURE 20

20. Temperature distribution in cross-sections across NOE quadrangle, with hand-drawn profile line. Data from wells in a strip 0.05° wide; 4 = 160°-180°F, 5 = 180°-200°F, \* = 280°-300°F. A. Longitude 90.0°; B. Longitude 90.4°; C. Longitude 90.8°.

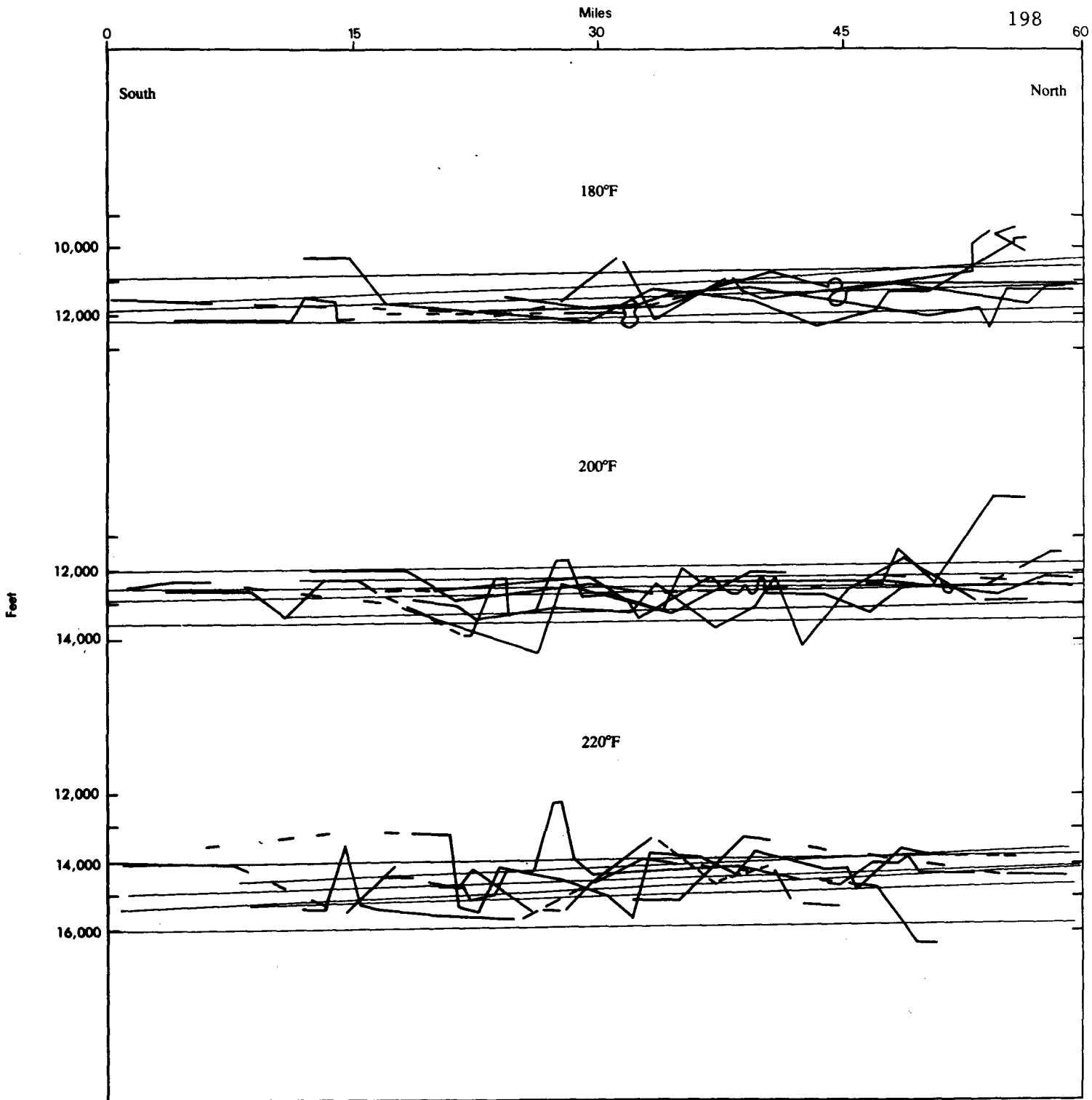


FIGURE 21

21. Composite temperature cross-sections. A. Summary of hand-drawn trend lines (from Fig. 20, and others) for 180°F, 200°F, and 220°F. B. Summary, all trends, all sections; temperature gradient of 1.6°/ 100 feet of depth and regional slope of 12 feet per mile to south.

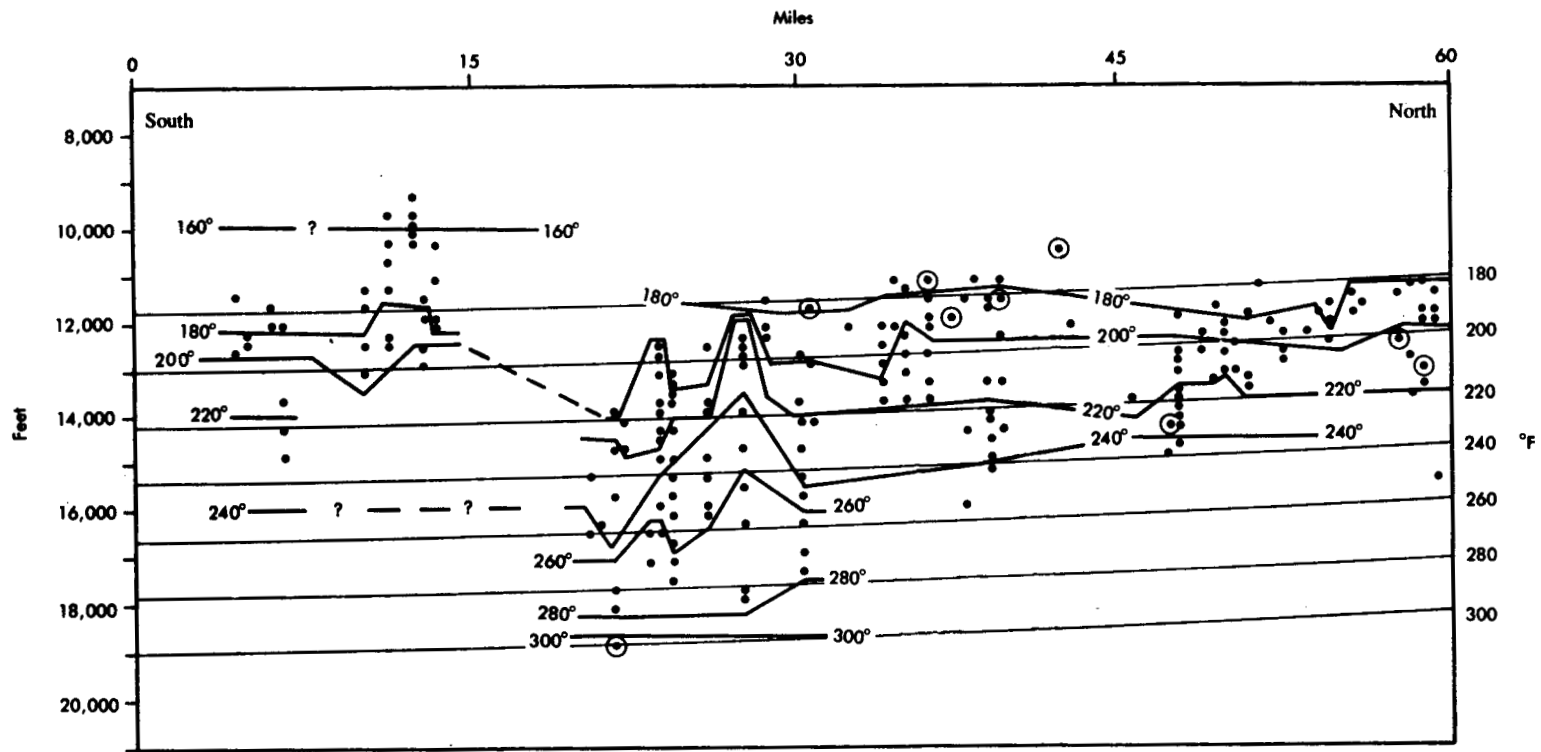


FIGURE 22

22. Regional temperature slopes (straight lines, from Fig. 21) superposed on profiles from one section. Thermal highs are shaded.

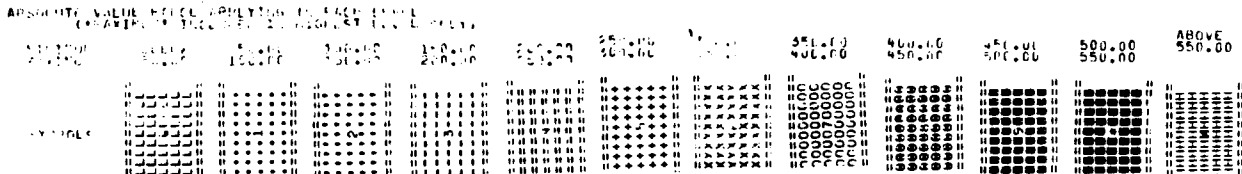
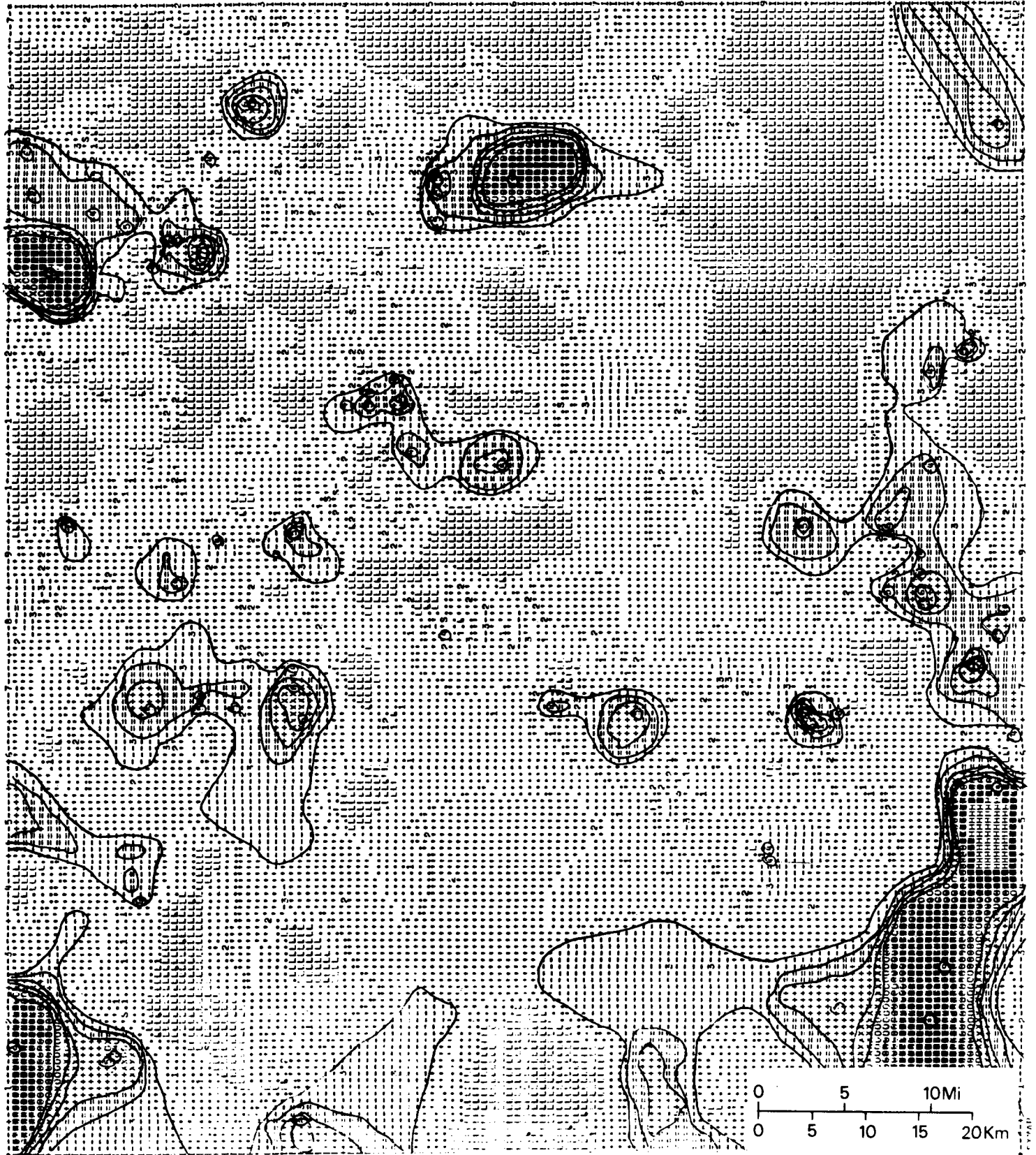
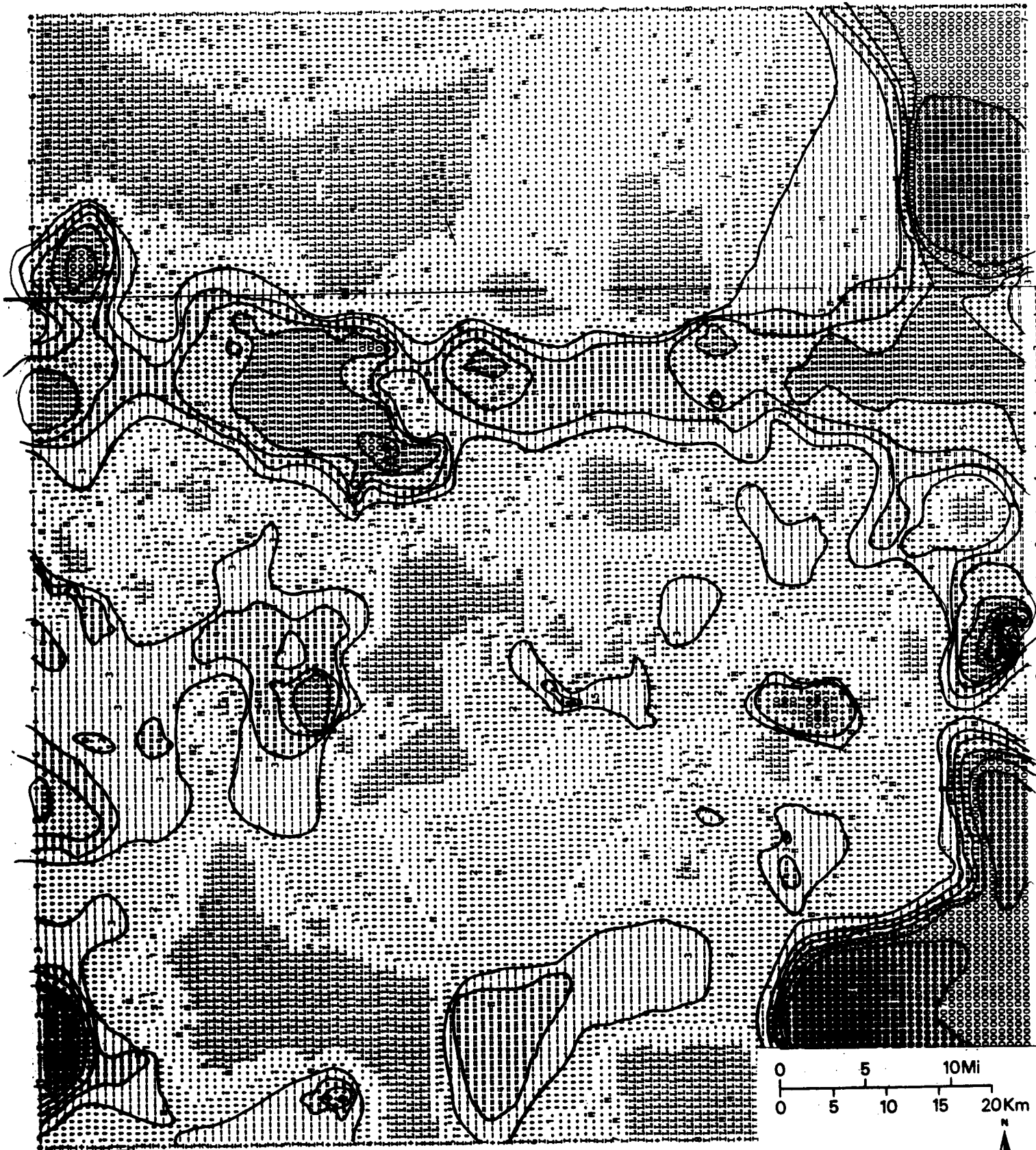


FIGURE 23

23. Net sand in a 1,000-foot-thick, vertical interval from 12-13 K; CI = 50 feet of sand. SYMAP: areas of greater than 30% sand are hand

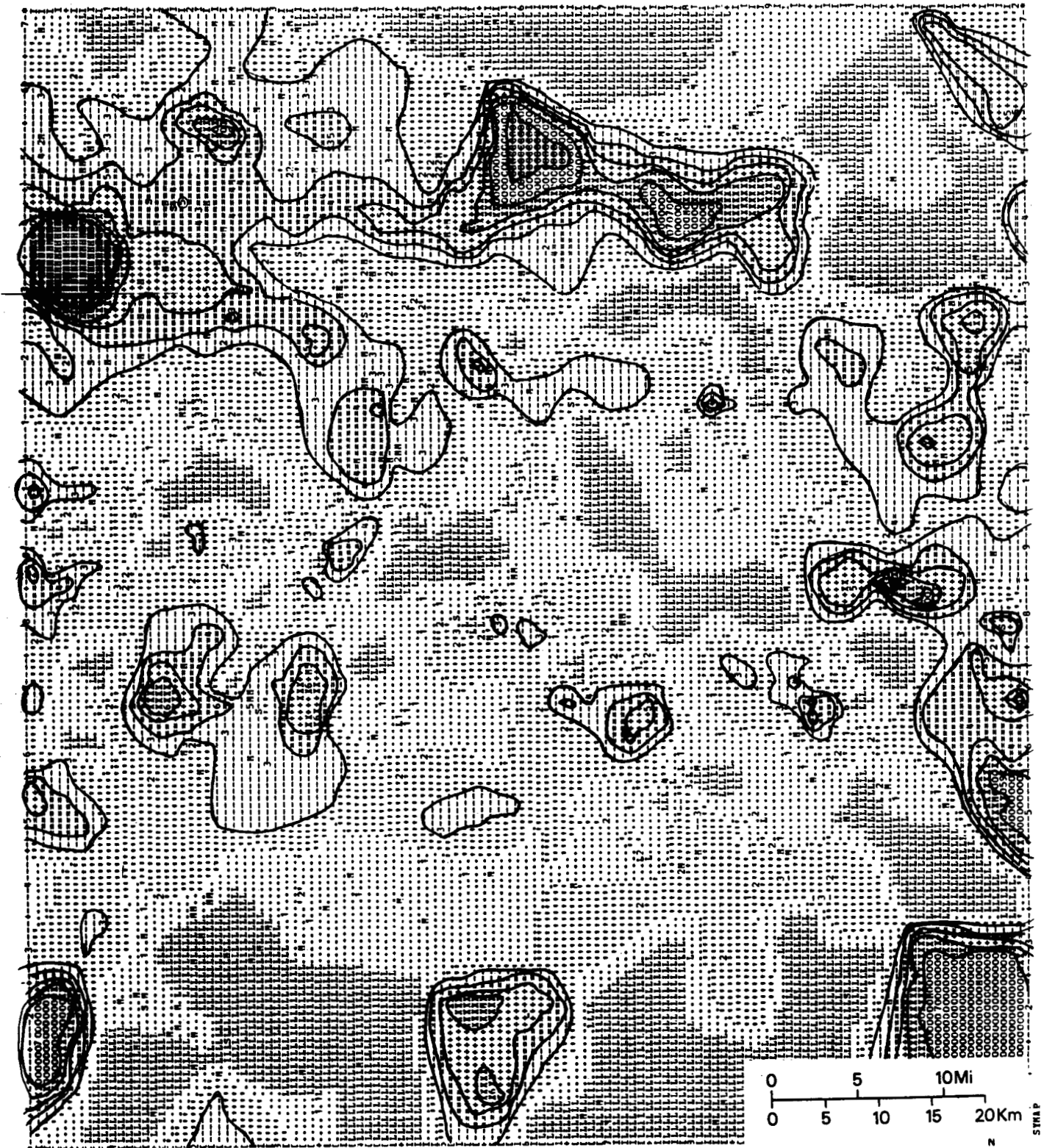




ABSOLUTE VALUE RANGE APPLYING TO EACH LEVEL  
 ('MAXIMUM' INCLUDED IN HIGHEST LEVEL ONLY)

MINIMUM	MAXIMUM	BELOW	50.00	100.00	150.00	200.00	250.00	300.00	350.00	400.00	450.00	500.00	550.00	600.00	ABOVE
		50.00	100.00	150.00	200.00	250.00	300.00	350.00	400.00	450.00	500.00	550.00	600.00	650.00	658.90
SYMBOLS		[Symbol]													

25. Net sand in a 1,000-foot-thick sloping interval, CI = 50 ft., SYMAP. The top of the interval slopes southward at 1.13

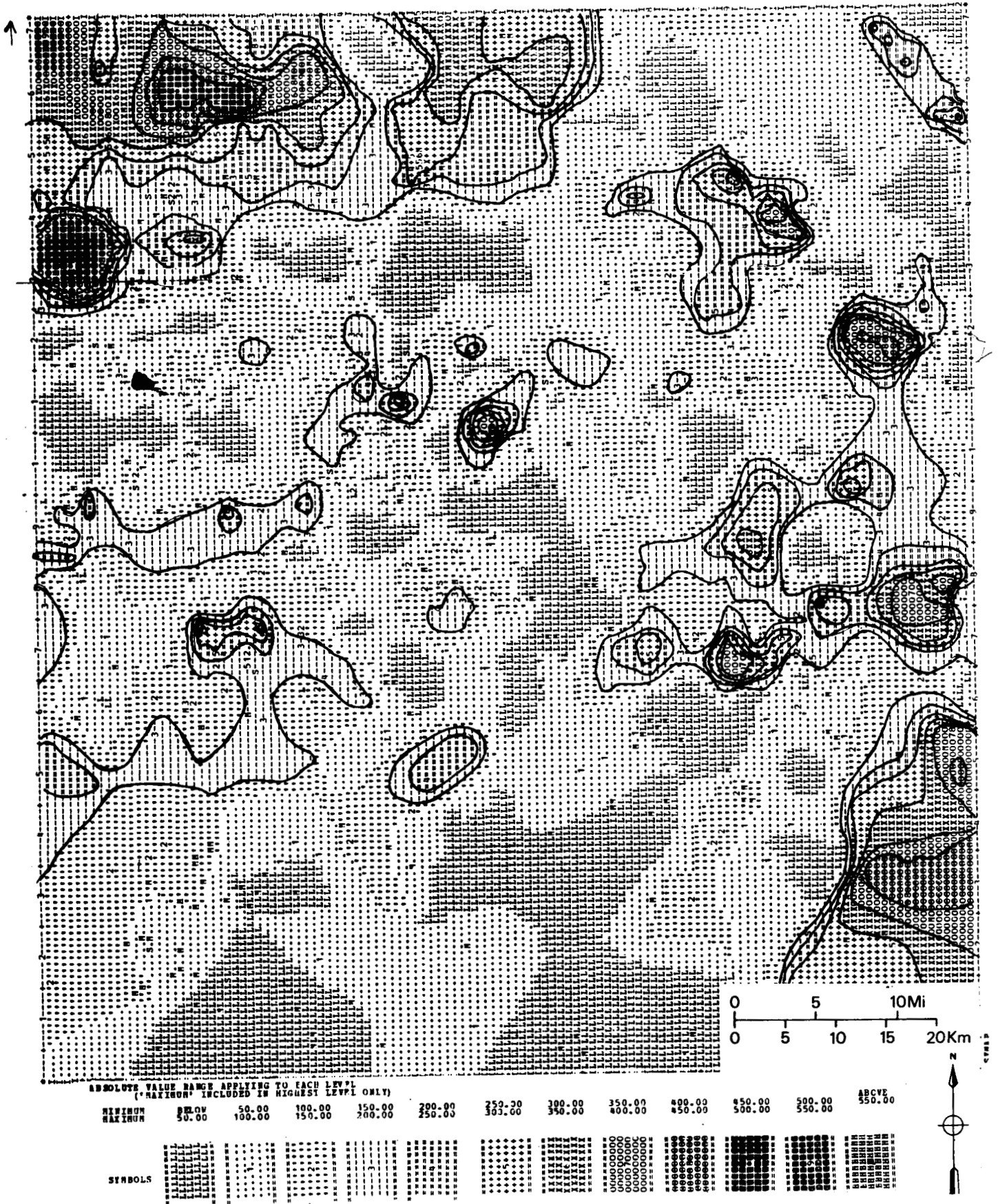


ABSOLUTE VALUE RANGE APPLYING TO EACH LEVEL ONLY  
(\*MAXIMUM\* INCLUDED IN HIGHEST LEVEL ONLY)

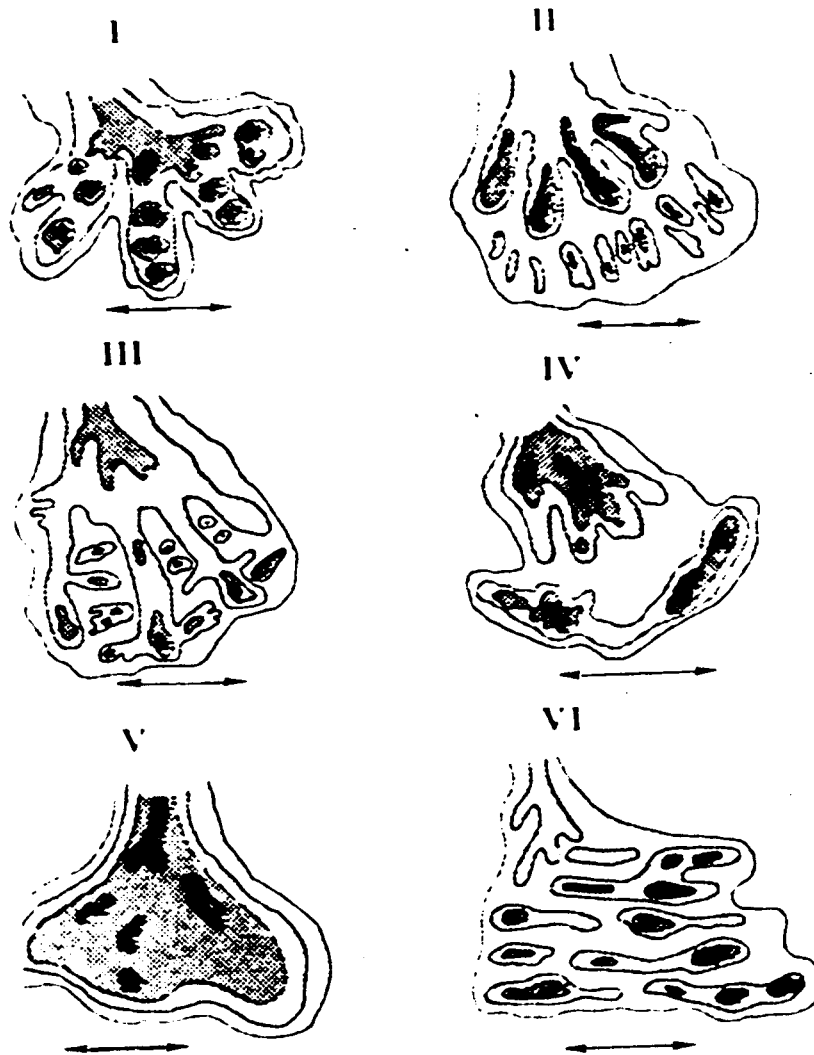
MINIMUM MAXIMUM	BELOW 50.00	100.00	150.00	200.00	250.00	300.00	350.00	400.00	450.00	500.00	550.00	ABOVE 550.00
SYMBOLS	[Symbol]	[Symbol]	[Symbol]	[Symbol]	[Symbol]	[Symbol]	[Symbol]	[Symbol]	[Symbol]	[Symbol]	[Symbol]	[Symbol]



26. Net sand, 1000-foot interval, sloping 1.13° from 7,800 to 15,000 feet.

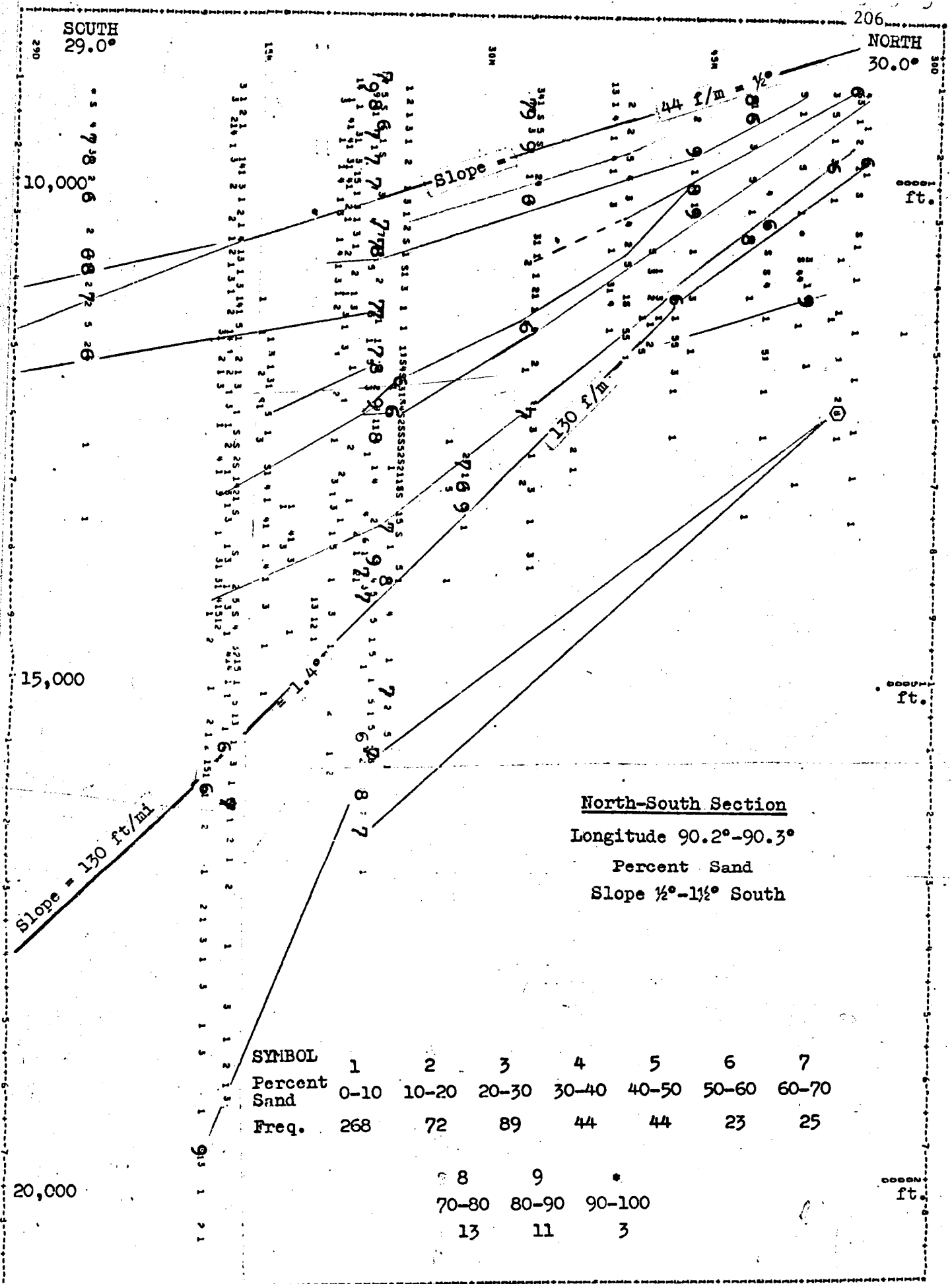


27. Net sand, 1,000-foot interval, sloping 1.13° from 8,800 to 16,000 feet.

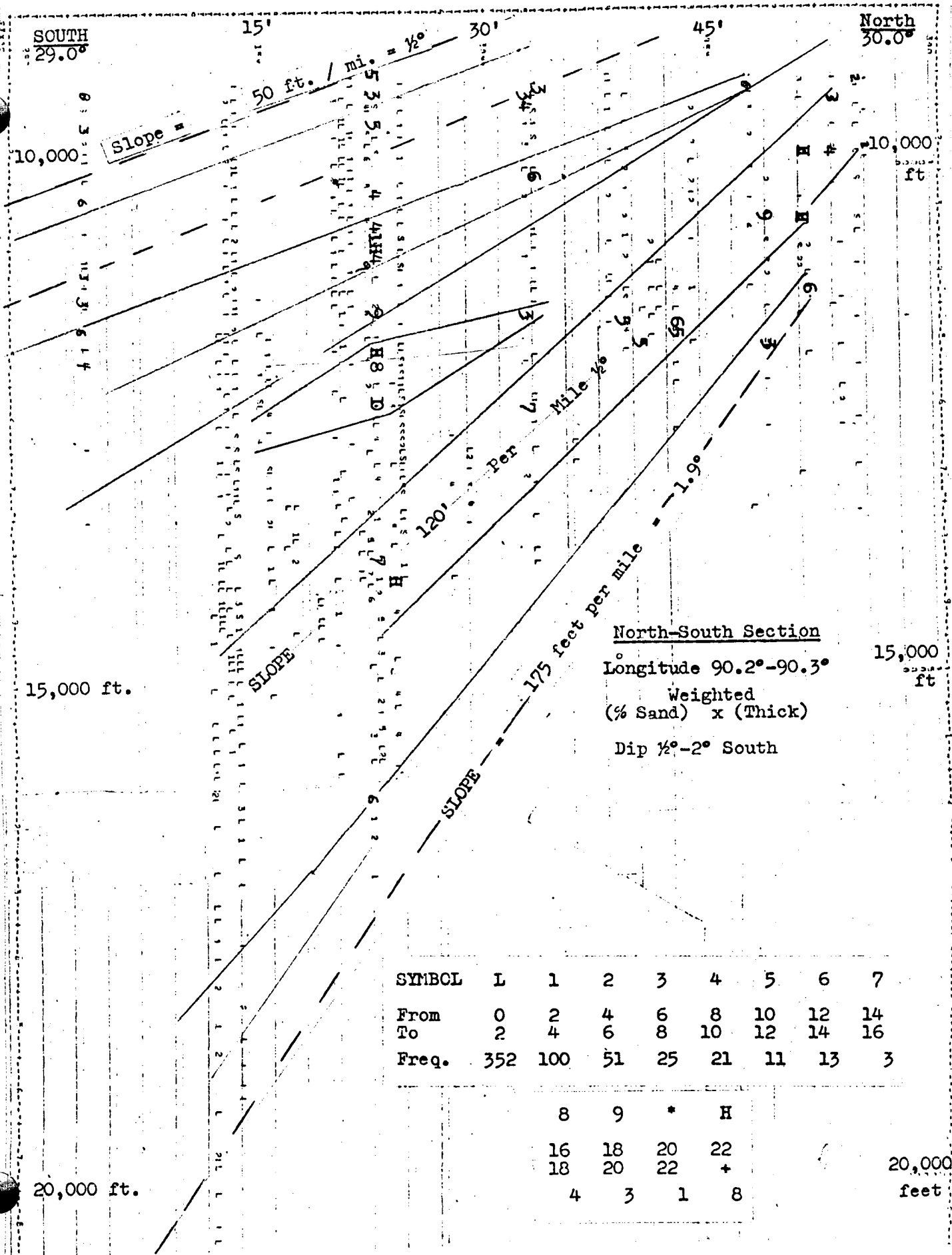


NET SAND DISTRIBUTION IN MODERN DELTAS

28. Typical distribution patterns of net sands in a modern delta, after Coleman & Wright (1975). This diagram indicates the types of patterns that might be recognized in sloping-interval net sand maps if the interval is kept small enough.



29. Distribution of percent sand (figure x 10 = %), north-south section, strip 0.1° wide (90.2°-90.3° long.); trends hand-drawn.



North-South Section  
 Longitude 90.2°-90.3°  
 Weighted  
 (% Sand) x (Thick)  
 Dip 1/2°-2° South

SYMBOL	L	1	2	3	4	5	6	7
From	0	2	4	6	8	10	12	14
To	2	4	6	8	10	12	14	16
Freq.	352	100	51	25	21	11	13	3
		8	9	*	H			
		16	18	20	22			
		18	20	22	+			
		4	3	1	8			

30. Weighted distribution of sand, from L=Low, through 1 to 9, to \* and H = High; weighted to thicker intervals, north-south sections, strip 0.1° wide (90.±-90.3° Long.); trends hand-drawn.

APPENDIX 1

Programs Produced by R. L. Hixon

APPENDIX 1

Programs Produced by R. L. Hixon

208

```

//LISTWELL JOB (1J05,F3H20,1,5,5000,....),*BOB HIXON*
//SLIUP          T250J
//              PLEASE INTERPRET, THANKS
//              EXLC FORTGCLG,PARM,FUNT=*MAP*,TIML=3
//FONT,SYSTN DD *
C
C      GEOPRESSED-GEOTHERMAL PROJECT
C
C      *LISTWELL* LISTS THE WELL DATA, FROM THE *CLENDATA* FILE ON
C      MAGNETIC TAPE, FOR A DESIRED AREA, * PROGRAMMER: ROBERT L. HIXON *
C      L.S.U., BATON ROUGE, LOUISIANA * 1978
C
C      INTEGER X,Z,R
C      DIMENSION X(3),Z(5)
C      R=0
C      READ-IN DATA FROM THE PARAMETER CARD---
C      READ(5,*,END=1999)XLA,XLN,YLA,YLN
C      READ-IN DATA FROM TAPE---
C      999 READ(8,10,END=2999)X
C      10 FORMAT(110,6A4,3(A1,A4),A1,2A4,2A2,15,6I2,15,13,15,A1,2I2,3X)
C      DECIMALIZE THE LATITUDE AND LONGITUDE---
C      DLAT=X(20)+FLCAT(X(21))/60.0+FLCAT(X(22))/3600
C      DLONG=X(23)+FLUAT(X(24))/60.0+FLOAT(X(25))/3600
C      IF (DLAT.LE.XLA.AND.DLONG.LE.XLN).AND.(DLAT.GE.YLA.AND.DLONG.
C      GE.YLN)GO TO 47
C      JJ=X(30)
C      IF(JJ.EQ.0)GO TO 7
C      DO 7 I=1,JJ
C      READ(8,17,END=3999)IDUM
C      17 FORMAT(10,94X)
C      7 CONTINUE
C      II=X(31)
C      IF(II.EQ.0)GO TO 999
C      DO 8 J=1,II
C      READ(8,18,END=4999)IDUM
C      18 FORMAT(10,94X)
C      8 CONTINUE
C      GO TO 999
C      47 CONTINUE
C      MER=1
C      WRITE(6,20)(X(I),I=1,31),R
C      20 FORMAT(1X,110,5A4,4(A4,A1),2A4,2A2,15,6I2/5X,'C',15,13,15,A1,2I2,
C      C13)
C      WRITE(7,1)(X(I),I=1,31),R
C      1 FORMAT(110,5A4,4(A4,A1),2A4,2A2,15,6I2/5X,'C',15,13,15,A1,2I2,
C      C13)
C      JJ=X(30)
C      IF(JJ.EQ.0)GO TO 99
C      DO 99 M=1,JJ
C      READ(3,22,END=5999)I1,A1,I2,A2,I3,I4
C      22 FORMAT(10,F5.1,15,F5.2,15,A1,73X)
C      WRITE(6,77)I1,A1,I2,A2,I3,I4
C      77 FORMAT(1X,10,F5.1,15,F5.2,15,A1,73X)
C      WRITE(7,2)I1,A1,I2,A2,I3,I4
C      2 FORMAT(10,F5.1,15,F5.2,15,A1,53X)
C      99 CONTINUE
C      II=X(31)
C      IF(II.EQ.0)GO TO 999
C      DO 109 N=1,II
C      READ(8,23,END=6999)Z
C      23 FORMAT(10,3I5,A1,70X)
C      WRITE(6,24)Z
C      24 FORMAT(1X,10,3I5,A1,70X)
C      WRITE(7,3)Z
C      3 FORMAT(10,3I5,A1,50X)
C      109 CONTINUE
C      GO TO 999
C      1999 STOP 100
C      2999 STOP 200
C      3999 STOP 300
C      4999 STOP 400
C      5999 STOP 500
C      6999 STOP 600
C      END)
//GD,FT08F001 DD DSN=CLENDATA,UNIT=TAPE,DISP=(OLD,KEEP),
//VCL=DSN=12500,LABCL=(2,SL),DCB=(RECFM=FB,LRECL=100,BLKSIZE=2000)
//GD,SYSTN DD *
C      THE FOLLOWING PARAMETER CARD LISTS THE EXTREME LATITUDE AND
C      LONGITUDE OF THE UPPER LEFT-HAND CORNER AND THE LOWER RIGHT-HAND
C      CORNER OF A RECTANGULAR GEOGRAPHICAL AREA.
C      29.50 50.00 28.75 06.75
//
//

```

```

//MDSNDAL JOB (1J09,8J820,1,5,1000,.,.,0),*BOU MIXCN-
//MESSAGE PLEASE INTERPRET MY CARDS
// EXEC NATFIV
//SYSIN DD *
$JCB          RUN=FREE,PAGES=10,TIME=20
C
C   *MDSNDAL* CALCULATES THE AVERAGE MUD WEIGHTS AND THE CUMULATIVE
C   SANDS FOR FOUR GIVEN INTERVALS: 10 TO 12, 12 TO 14, 14 TO 16,
C   AND 16 TO 18 THOUSAND FOOT INTERVALS.
C   *MDSNDAL* ALSO PREPARES AND STRUCTURES THE DATA FOR INPUT INTO
C   A PROGRAM THAT WILL CALCULATE THE AVERAGE SALINITIES
C   (THE DATA IS PUNCHED-OUT ON CARDS).
C
C   TWO OF THE THREE WRITE STATEMENTS MAY BE LEFT OUT WHEN OBTAINING
C   THE THIRD TYPE OF DATA. OTHERWISE ALL OF THE CARDS WILL BE
C   INTERSPERSED WITH ONE ANOTHER.
C
C   *MDSNDAL* USES THE ORIGINAL DATA FROM THE *CLENDDATA* FILE
C   ON MAGNETIC TAPE. THIS PROGRAM ALSO ALLOWS YOU TO SELECT
C   A SPECIFIC AREA OF INTEREST BY PLACING THE EXTREME
C   COORDINATES ON THE PARAMETER CARD.
C
C   THIS PROGRAM IS SET-UP TO READ THE *CLENDDATA* INFORMATION FROM
C   CARDS ONLY. THE JOB CONTROL CARDS AND THE READ STATEMENTS WOULD
C   HAVE TO BE ALTERED TO READ FROM THE ORIGINAL TAPE.
C
C   PROGRAMMER: ROBERT L. MIXCN * L.S.U. * 1978 *
C
C   INTEGER X,R,L,M,DEPTH,TEMP,SUMSND,THN,TOPSND,BUTSND,SP
C   REAL MWT
C   DIMENSION X(31),DEPTH(30),MWT(30),TEMP(30),RM(30),TRM(30),
C   CTOPSND(75),BUTSND(75),NTSND(75),SP(75),MOTV(75),AVGMAT(4),
C   CSUMSND(4),I(75)
C   DATA X,DLPTH,TEMP,THN,TOPSND,BUTSND,NTSND,SP,SUMSND/425*0/
C   DATA RM,MWT,AVGMAT/64*0./
C   LLL=0
C   IJK=1000
C   READ(5,4,END=1999)XLA,XLB,YLA,YLE
C   999 READ(5,10,END=2999)X
C   1J FURMAT(11J,5A4,4(1A4,A1),2A4,2A2,15,6I2/6X,15,13,15,A1,2I2,3X)
C   DLAT=X(20)+FLUAT(X(21))/60.0*FLCAT(X(22))/3600
C   DLONG=X(23)+FLUAT(X(24))/60.0*FLCAT(X(25))/3600
C   IF((DLAT.LE.XLA.AND.DLONG.LE.XLB).AND.(DLAT.GE.YLA.AND.DLONG.
C   GE.YLE))GO TO 47
C   JJ=X(30)
C   IF(JJ.EQ.0)GO TO 8888
C   DO 7 IJR=1,JJ
C   READ(5,17,END=3999)IDUM
C   17 FURMAT(16,74X)
C   7 CONTINUE
C   8888 CONTINUE
C   II=X(31)
C   IF(II.EQ.0)GO TO 999
C   DO 8 J=1,II
C   READ(5,18,END=4999)IDUM
C   18 FURMAT(16,74X)
C   8 CONTINUE
C   GO TO 999
C   47 CONTINUE
C   JJ=X(30)
C   IF(JJ.EQ.0)GO TO 999
C   DO 9 M=1,JJ
C   READ(5,22,END=5999)DEPTH(M),MWT(M),TEMP(M),THN(M),MOTV(M)
C   22 FURMAT(16,F5.1,15,F5.2,15,A1)
C   99 CONTINUE
C   AVERAGE MUD WEIGHTS FOR 10 TO 12, 12 TO 14, 14 TO 16, AND 16 TO
C   18 THOUSAND FOOT INTERVALS:---
C   LL=8000
C   KK=10000
C   DO 64 K=1,4
C   LL=LL+2000
C   KK=KK+2000
C   AVGMAT(K)=0.00
C   HNN=0.00
C   SUMUD=0.00
C   DO 68 PM=1,JJ
C   IF(MWT(M).EQ.0.0)GO TO 88
C   IF(MWT(M).LT.3.0)MWT(M)=MWT(M)*10.0
C   IF(DLPTH(MM).LT.LL)GO TO 88
C   IF(DEPTH(MM).GE.LL.AND.DEPTH(MM).LT.KK)GO TO 93
C   GO TO 894
C   93 CONTINUE
C   SUMUD=SUMUD+MWT(M)
C   HNN=HNN+1.0
C   AVGMAT(K)=SUMUD/HNN
C   88 CONTINUE
C   894 CONTINUE
C   II=X(31)
C   IF(II.EQ.0)GO TO 9994
C   CUMULATIVE SAND CALCULATIONS:---
C   DO 109 MNK=1,II
C   READ(5,23,FDC=6999)TCPSND(MNK),BUTSND(MNK),NTSND(MNK),
C   CSP(MNK),I(MNK)
C   23 FURMAT(16,15,15,15,A1)
C   109 CONTINUE
C   KK=10000
C   LL=8000
C   DO 14 NN=1,4
C   LL=LL+2000
C   KK=KK+2000
C   SUMSND(NN)=0.00
C   PRUPOR=0.0
C   N=0
C   *Insert: IXZY=II+1
C   IF(N.EQ.IXZY) GO TO 94
C   DO 110 N=1,35
C   IF(N.LU.II)GO TO 94
C   PROPORTIONS USED IN DETERMINING HOW MUCH SAND IS WITHIN THE
C   INTERVAL IN THE CASE WHERE A SAND OVERLAPS THE BOUNDARIES IN
C   SOME WAY:---
C   IF(TOPSND(N).GT.LL.CR.BOTSND(N))LE.KK)GO TO 94
C   IF(NTSND(N).GT.2000.OR.NTSND(N).EQ.0)GO TO 110
C   IF(TOPSND(N).LT.LL.AND.BOTSND(N).LT.LL)GO TO 110
C   IF(TOPSND(N).GE.KK.AND.BOTSND(N).GE.KK)GO TO 110
C   IF(TOPSND(N).LT.LL.AND.BOTSND(N).GE.KK)GO TO 293
C   IF(TOPSND(N).GE.LL.AND.BOTSND(N).LT.KK)GO TO 111
C   IF(TOPSND(N).LT.LL)GO TO 291
C   PRUPOR=(KK-TCPSND(N))/((BUTSND(N)-TOPSND(N))+1.0)
C   SUMSND(NN)=SUMSND(NN)+(PRUPOR*NTSND(N))
C   GO TO 110
C   293 CONTINUE

```

```

293 CONTINUE
PROPOR=(KK-LL)/((BOTSND(N)-TOPSND(N))*1.0)
SUMSND(NN)=SUMSND(NN)+(PROPOR*NTSND(N))
GO TO 110
291 CONTINUE
PROPOR=(BOTSND(N)-LL)/((BOTSND(N)-TOPSND(N))*1.0)
SUMSND(NN)=SUMSND(NN)+(PROPOR*NTSND(N))
GO TO 110
111 CONTINUE
SUMSND(NN)=SUMSND(NN)+NTSND(N)
110 CONTINUE
94 CONTINUE
9994 CONTINUE
IF(11.07.0)GO TO 1112
SUMSND(1)=0
SUMSND(2)=0
SUMSND(3)=0
SUMSND(4)=0
1112 CONTINUE
LLL=LLL+1
MOMIZ=50.50-DLUNG
VEMT=DLAT-28.75
YCOORD=VERT*6.007
XCOWD=MOMIZ*6.047
S1=SUMSND(1)
S2=SUMSND(2)
S3=SUMSND(3)
S4=SUMSND(4)
WRITE(6,54)XCOWD,YCOORD,AVGMWT(1),AVGMWT(2),AVGMWT(3),AVGMWT(4),
CS1,S2,S3,S4,X(1),DLAT,DLONG,LLL
54 FORMAT(1X,2F7.3,4F5.1,4F5.0,110,2F7.3,5X,14)
C WRITE STATEMENT FOR THE AVERAGE MUD WEIGHTS:---
WRITE(7,2223)XCOWD,YCOORD,AVGMWT(1),AVGMWT(2),AVGMWT(3),
CAVGMWT(4),X(1),LLL
2223 FORMAT(2F7.3,1X,4F5.1,110,15,30X)
C WRITE STATEMENT FOR THE CUMULATIVE SANDS:---
WRITE(7,3333)XCOWD,YCOORD,S1,S2,S3,S4,X(1),LLL
3333 FORMAT(2F7.3,1X,4F5.0,110,15,30X)
C BEGINNING OF THE SALINITY SECTION OF THE PROGRAM:---
IF(JJ.LE.1)GO TO 449
KLM=0
ITHIND=0
DO 434 R=2,JJ
KLM=K-1
IF(DEPTH(R).LE.0.CR.DEPTH(R).GT.30000)GO TO 434
IF(DEPTH(KLM).LE.0.UR.DEPTH(KLM).GT.30000)GO TO 434
IF(MWT(R).LE.0.CR.MWT(R).GT.29.0)GO TO 434
IF(TEMP(R).LE.0.UR.TEMP(KLM).LE.0)GO TO 434
IF(TEMP(R).GT.500.UR.TEMP(KLM).GT.500)GO TO 434
IF(KN(R).LE.0.UR.KN(R).GT.4.0)GO TO 434
IF(11.EC.0)GO TO 449
DO 436 ITHIND=1,11
IJK=IJK+1
IF(TOPSND(ITHIND).EQ.0.UR.BOTSND(ITHIND).EQ.0)GO TO 436
IF(NTSND(ITHIND).GT.2000.UR.ATSND(ITHIND).EQ.0)GO TO 436
IF(SP(ITHIND).GT.300.UR.SP(ITHIND).LE.0)GO TO 436
IF(TOPSND(ITHIND).LT.DEPTH(KLM))GO TO 436
IF(TOPSND(ITHIND).GE.DEPTH(R))GO TO 434
DINTSU=(BOTSND(ITHIND)-TOPSND(ITHIND)-NTSND(ITHIND))/2
TOPAG=TOPSND(ITHIND)+DINTSU
BOTAG=BOTSND(ITHIND)-DINTSU
TTUP=TEMP(KLM)
TUCI=TEMP(R)
UTOP=DEPTH(KLM)
UBOT=DEPTH(R)
CKSP=SP(ITHIND)*(-1.0)
C WRITE STATEMENT FOR THE SALINITY DECK:---
WRITE(6,321)X(15),X(31),TOPAG,BOTAG,JJ,MDTY(R),MWT(R),
CKM(R),TTUP,TUCI,UTOP,UBOT,OKSP,IJK,XCOWD,YCOORD,X(1)
321 FORMAT(1X,4,14,2F10.1,12,A4,F5.1,F5.2,2F5.1,2F10.3,F5.0,
CSX,14,2F10.3,110)
C WRITE STATEMENT FOR THE SALINITY DECK:---
WRITE(7,222)X(15),X(31),TOPAG,BOTAG,JJ,MDTY(R),MWT(R),
CKM(R),TTUP,TUCI,UTOP,UBOT,OKSP
222 FORMAT(A4,14,2F10.1,12,A4,F5.1,F5.2,2F5.1,2F10.0,F5.0,1X)
436 CONTINUE
434 CONTINUE
GO TO 999
1999 STOP 100
2599 STOP 200
5999 STOP 500
3999 STOP 300
4554 STOP 400
6999 STOP 600
END
SENTRY
C PARAMETER CARD FOR LOCATING A CERTAIN AREA (EXTREME COORDINATES
C AS DESCRIBED IN THE OTHER PROGRAMS SUCH AS 'ISOTHERM':---
29.50 90.50 28.75 89.75
**
//

```

```
//TEMPFILE JOB (1304,83820,1,5,1000,.,.,0),*BOB NIXON*
//SETUP TSCMAT(2) ***** PLEASE INTERPRET
//STPI EXLC FONTCLG.TIME=30,REGION=25&K
//FONT.SYSIN DD *
```

BOB00030

```
GEOPRESSURED-GEOTHERMAL PROJECT
```

BOB00070  
BOB00050  
BOB00060

```
*TEMPFILE* CORRECTS THE RUN TEMPERATURES FOR COOLING DUE TO THE
MUD CIRCULATION IN THE BOREHOLE. *TEMPFILE* ALSO CALCULATES THE
TEMPERATURE GRADIENTS BETWEEN THE RUN DEPTHS AND DECMILIZES THE
LATITUDE AND LONGITUDE COORDINATES.
THE LOCATION OF THE WELL IS SORTED ACCORDING TO THE LATITUDE AND
EACH WELL IS ASSIGNED A CONSECUTIVE NUMBER FOR EASY
IDENTIFICATION. * PROGRAMMER: RUBERT L. NIXON * U.S.U. * 1978 *
```

BOB00130  
BOB00160  
BOB00170  
BOB00180  
BOB00190

```
STEP 1 EDITS THE CLENDATA TAPE, CORRECTS FOR THE EQUILIBRIUM
TEMPERATURE, AND CALCULATES THE GRADIENTS FOR EACH RUN.
STEP 1 ALSO CHANGES CERTAIN INTEGER VALUES INTO REAL VARIABLES.
```

BOB00200  
BOB00210  
BOB00220

```
530 DIMENSION DEPTH(30),WT(30),TEMP(30)
READ(5,4,END=999)WELL,DEPTH,LA1,LA2,LA3,L01,L02,L03,MDEPTH,
CMTFMP,NLOG,NL
4 FORMAT(110,52X,15,612/6X,15,13,6X,12,12,3X)
```

BOB00240

```
DEPU=0.0
```

```
TEMPO=72.0
```

```
CHANGE TOTAL DEPTH TO REAL
```

```
TD=DEPTH
```

```
IF THESE ARE SECOND RECORDS (A GEOPRESSURED WELL),
```

```
GO DIRECTLY TO THEM.
```

```
IF (NLOG.GT.0) GO TO 20
```

```
CHANGE THE NON-GEOPRESSURED DATA INTO REAL NUMBERS:
```

```
DEPTH(I)=MDEPTH
```

```
TEMP(I)=MTEMP
```

```
GET THE GRADIENT FOR THE NON-GEOPRESSURED DATA:
```

```
Z=(DEPTH(I)-DEPU)
```

```
IF (Z.EQ.0.0) GO TO 500
```

```
IF (TEMP(I).EQ.0.0) GO TO 500
```

```
IF (DEPTH(I).GT.0.0.AND.DEPTH(I).LE.1000.0)TEMP(I)=TEMP(I)+2.0
```

```
IF (DEPTH(I).GT.1000.0.AND.DEPTH(I).LE.2000.0)TEMP(I)=TEMP(I)+6.0
```

```
IF (DEPTH(I).GT.2000.0.AND.DEPTH(I).LE.3000.0)TEMP(I)=TEMP(I)+10.0
```

```
IF (DEPTH(I).GT.3000.0.AND.DEPTH(I).LE.4000.0)TEMP(I)=TEMP(I)+14.0
```

```
IF (DEPTH(I).GT.4000.0.AND.DEPTH(I).LE.5000.0)TEMP(I)=TEMP(I)+17.8
```

```
IF (DEPTH(I).GT.5000.0.AND.DEPTH(I).LE.6000.0)TEMP(I)=TEMP(I)+21.3
```

```
IF (DEPTH(I).GT.6000.0.AND.DEPTH(I).LE.7000.0)TEMP(I)=TEMP(I)+24.5
```

```
IF (DEPTH(I).GT.7000.0.AND.DEPTH(I).LE.8000.0)TEMP(I)=TEMP(I)+27.0
```

```
IF (DEPTH(I).GT.8000.0.AND.DEPTH(I).LE.9000.0)TEMP(I)=TEMP(I)+29.1
```

```
IF (DEPTH(I).GT.9000.0.AND.DEPTH(I).LE.10000.0)
```

```
CTEMP(I)=TEMP(I)+30.7
```

```
IF (DEPTH(I).GT.10000.0.AND.DEPTH(I).LE.11000.0)
```

```
CTEMP(I)=TEMP(I)+32.1
```

```
IF (DEPTH(I).GT.11000.0.AND.DEPTH(I).LE.12000.0)
```

```
CTEMP(I)=TEMP(I)+33.0
```

```
IF (DEPTH(I).GT.12000.0.AND.DEPTH(I).LE.13000.0)
```

```
CTEMP(I)=TEMP(I)+33.0
```

```
IF (DEPTH(I).GT.13000.0.AND.DEPTH(I).LE.14000.0)
```

```
CTEMP(I)=TEMP(I)+32.8
```

```
IF (DEPTH(I).GT.14000.0.AND.DEPTH(I).LE.15000.0)
```

```
CTEMP(I)=TEMP(I)+31.8
```

```
IF (DEPTH(I).GT.15000.0.AND.DEPTH(I).LE.16000.0)
```

```
CTEMP(I)=TEMP(I)+29.9
```

```
IF (DEPTH(I).GT.16000.0.AND.DEPTH(I).LE.17000.0)
```

```
CTEMP(I)=TEMP(I)+27.2
```

```
IF (DEPTH(I).GT.17000.0.AND.DEPTH(I).LE.18000.0)
```

```
CTEMP(I)=TEMP(I)+23.4
```

```
IF (DEPTH(I).GT.18000.0.AND.DEPTH(I).LE.19000.0)
```

```
CTEMP(I)=TEMP(I)+19.0
```

```
IF (DEPTH(I).GT.19000.0.AND.DEPTH(I).LE.20000.0)
```

```
CTEMP(I)=TEMP(I)+17.3
```

```
IF (DEPTH(I).GT.20000.0.AND.DEPTH(I).LE.21000.0)
```

```
CTEMP(I)=TEMP(I)+6.0
```

```
GRAD=(TEMP(I)-TEMPO)/(DEPTH(I)-DEPU)
```

```
WT(I)=10.0
```

```
NLOG=1
```

```
WRITE(6,10)WELL,TD,LA1,LA2,LA3,L01,L02,L03,NLOG,NL
```

```
DEPTH(I),WT(I),TEMP(I),GRAD
```

```
10 FORMAT(110,F10.2,6I3,2I3,11X,/,F10.2,F5.1,F10.2,F9.3,21X)
```

```
GO TO 500
```

```
20 CONTINUE
```

```
JLOG=0
```

```
DO 100 J=1,NLOG
```

```
READ(5,2,END=1449)KDEPTH,XBT,KTEMP
```

```
2 FORMAT(10,F5.1,15,64X)
```

```
CHANGE TO REAL
```

```
DEPTH(J)=KDEPTH
```

```
TEMP(J)=KTEMP
```

```
IF (DEPTH(J).EQ.0.0)GO TO 100
```

```
Y=(DEPTH(J)-DEPU)
```

```
IF (Y.EQ.0.0)GO TO 100
```

```
IF (TEMP(J).EQ.0.0)GO TO 100
```

```
JLOG=JLOG+1
```

```
DEPTH(JLOG)=DEPTH(J)
```

```
WT(JLOG)=WT
```

```
TEMP(JLOG)=TEMP(J)
```

```
DEPU=DEPTH(J)
```

```
100 CONTINUE
```

BOB00380  
BOB00390  
BOB00400  
BOB00410  
BOB00420  
BOB00430  
BOB00440  
BOB00450  
BOB00460  
BOB00470  
BOB00480  
BOB00490  
BOB00500  
BOB00510  
BOB00520  
BOB00530  
BOB00540  
BOB00550  
BOB00560  
BOB00570  
BOB00580  
BOB00590  
BOB00600  
BOB00610  
BOB00620  
BOB00630  
BOB00640  
BOB00650  
BOB00660  
BOB00670  
BOB00680  
BOB00690  
BOB00700  
BOB00710  
BOB00720  
BOB00730  
BOB00740  
BOB00750  
BOB00760  
BOB00770  
BOB00780  
BOB00790  
BOB00820  
BOB00830  
BOB00840  
BOB00850  
BOB00860  
BOB00870  
BOB00880  
BOB00890  
BOB00900  
BOB00910  
BOB00920  
BOB00930  
BOB00940  
BOB00950

## TEMPFILE (Page 2)

```

100 CONTINUE
IF (JLOG.EQ.0) GO TO 200
DEPU=0.0
TEMPO=72.0
WRITE (8,12) IWELL,TD,LA1,LA2,LA3,LO1,LO2,LO3,JLOG,NL
12 FORMAT(110,F10.2,6I3,2I3,11X)
DO 200 J=1,JLOG
IF (DEPTH(J).GT.0.0.AND.DEPTH(J).LE.1000.0) TEMP(J)=TEMP(J)+2.0
IF (DEPTH(J).GT.1000.0.AND.DEPTH(J).LE.2000.0) TEMP(J)=TEMP(J)+6.0
IF (DEPTH(J).GT.2000.0.AND.DEPTH(J).LE.3000.0) TEMP(J)=TEMP(J)+10.0
IF (DEPTH(J).GT.3000.0.AND.DEPTH(J).LE.4000.0) TEMP(J)=TEMP(J)+14.0
IF (DEPTH(J).GT.4000.0.AND.DEPTH(J).LE.5000.0) TEMP(J)=TEMP(J)+17.8
IF (DEPTH(J).GT.5000.0.AND.DEPTH(J).LE.6000.0) TEMP(J)=TEMP(J)+21.3
IF (DEPTH(J).GT.6000.0.AND.DEPTH(J).LE.7000.0) TEMP(J)=TEMP(J)+24.5
IF (DEPTH(J).GT.7000.0.AND.DEPTH(J).LE.8000.0) TEMP(J)=TEMP(J)+27.0
IF (DEPTH(J).GT.8000.0.AND.DEPTH(J).LE.9000.0) TEMP(J)=TEMP(J)+29.1
IF (DEPTH(J).GT.9000.0.AND.DEPTH(J).LE.10000.0)
CTEMP(J)=TEMP(J)+30.7
IF (DEPTH(J).GT.10000.0.AND.DEPTH(J).LE.11000.0)
CTEMP(J)=TEMP(J)+32.1
IF (DEPTH(J).GT.11000.0.AND.DEPTH(J).LE.12000.0)
CTEMP(J)=TEMP(J)+33.0
IF (DEPTH(J).GT.12000.0.AND.DEPTH(J).LE.13000.0)
CTEMP(J)=TEMP(J)+33.0
IF (DEPTH(J).GT.13000.0.AND.DEPTH(J).LE.14000.0)
CTEMP(J)=TEMP(J)+32.0
IF (DEPTH(J).GT.14000.0.AND.DEPTH(J).LE.15000.0)
CTEMP(J)=TEMP(J)+31.8
IF (DEPTH(J).GT.15000.0.AND.DEPTH(J).LE.16000.0)
CTEMP(J)=TEMP(J)+29.9
IF (DEPTH(J).GT.16000.0.AND.DEPTH(J).LE.17000.0)
CTEMP(J)=TEMP(J)+27.2
IF (DEPTH(J).GT.17000.0.AND.DEPTH(J).LE.18000.0)
CTEMP(J)=TEMP(J)+23.4
IF (DEPTH(J).GT.18000.0.AND.DEPTH(J).LE.19000.0)
CTEMP(J)=TEMP(J)+18.8
IF (DEPTH(J).GT.19000.0.AND.DEPTH(J).LE.20000.0)
CTEMP(J)=TEMP(J)+17.5
IF (DEPTH(J).GT.20000.0.AND.DEPTH(J).LE.21000.0)
CTEMP(J)=TEMP(J)+0.0
GRAD=(TEMP(J)-TEMPU)/(DEPTH(J)-DEPU)
WRITE (8,14) DEPTH(J),TEMP(J),GRAD
14 FORMAT(F10.2,F10.1,F10.2,F9.3,21X)
C RESSETTING THE VALUES FOR THE NEXT CALCULATION
TEMPO=TEMP(J)
DEPO=DEPTH(J)
200 CONTINUE
IF (NL.EQ.0) GO TO 500
DO 60 J=1,NL
DUMMY VARIABLE TO OMIT THE THIRD RECORD
READ (5,3) END=2999)IDLM
3 FORMAT(16,16X,5HX)
60 CONTINUE
GO TO 500
999 STOP 100
1999 STOP 200
2999 STOP 300
END
//GO.FT08F001 DD DSN=TEMP2,UNIT=SCRATCH,SPACE=(550,(7200,100),RLSE),
// DCB=(LRECL=55,DLK=1,ZL=550,RECFM=FB),DISP=(NEW,PASS)
//GC.SYSIN DD *
//GO.DELTE DD DSN=LLG0SET,DISP=(OLD,DELETE)
//STP2 EXEC FORTGCLG,TIME=30,REGICN=256K
//PORT.SYSIN DD *
C STEP 2 TAKES THE 55 BLCK RECCDS FROM STEP 1 AND PLACES ALL THE
C RECORDS INTO ONE SINGLE RECORD FORM IN PREPARATION FOR SORTING.

```

80800940  
80800950  
80800970  
80800990  
80801000  
80801010  
80801020  
80801030  
80801040  
80801050  
80801060  
80801070  
80801080  
80801090  
80801100  
80801110  
80801120  
80801130  
80801140  
80801150  
80801160  
80801170  
80801180  
80801190  
80801200  
80801210  
80801220  
80801230  
80801240  
80801250  
80801260  
80801270  
80801280  
80801290  
80801300  
80801310  
80801320  
80801330  
80801340  
80801350  
80801360  
80801370  
80801380  
80801390  
80801400  
80801410  
80801420  
80801450  
80801460  
80801470  
80801480  
80801490  
80801500  
80801540  
80801550  
80801510  
80801570  
80801580  
80801590

```

C STEP 2 TAKES THE 55 HLCK RECCRDS FROM STEP 1 AND PLACES ALL THE
C RECORDS UNTO ONE SINGLE RECORD FORM IN PREPARATION FOR SORTING.
C
NN=0
LL=U
LOGICAL*1 OUT(1265)
5 READ(8,10,END=99)(OUT(I),I=1,55),NLOG
10 FORMAT(55A1,T3V,13)
NN=NN+1
DO 20 I=1,NLOG
  J=I*55+1
  K=J+54
  HEAD(8,11)(OUT(L),L=J,K)
11 FORMAT(55A1)
  LL=LL+1
20 CONTINUE
  WRITE(9,30)OUT
30 FORMAT(2J(55A1))
  GO TO 5
99 STOP
  END
//
//GO.FT08F001 DD DSN=TEMP2,DISP=(OLD,DELETE)
//GO.FT09F001 DD DSN=NEW,UNIT=TAPE,VOL=(,RETAIN),
//DCB=(LRECL=1265,BLKSIZE=1265,RECFM=FB),DISP=(NEW,PASS)
//GO.DELETE DD DSN=666USLT,DISP=(OLD,DELETE)
//STEP EXEC SORTD,TIME=30,REGICN=256K
//* THREE IS THE SORT-MERGE ROUTINE---IBM PACKAGE
//SORTK01 DD SPACE=(TRK,(400)),CCNTIG),UNIT=SCRATCH
//SORTK02 DD SPACE=(TRK,(400)),CCNTIG),UNIT=SCRATCH
//SORTK03 DD SPACE=(TRK,(400)),CCNTIG),UNIT=SCRATCH
//SORTK04 DD SPACE=(TRK,(250)),CCNTIG),UNIT=SCRATCH
//SORTK05 DD SPACE=(TRK,(250)),CCNTIG),UNIT=SCRATCH
//SORTK06 DD SPACE=(TRK,(250)),CCNTIG),UNIT=SCRATCH
//SORTIN DD DSN=NEW,DISP=(OLD,DELETE),
//DCH=(RECFM=FB,LRECL=1265,BLKSIZE=1265),UNIT=TAPE
//SORTOUT DD DSN=TEMPJ,UNIT=TAPE,DISP=(NEW,PASS),
//DCB=(LRECL=1265,BLKSIZE=1265,RECFM=FB),VOL=(,RETAIN)
//SYSIN DD *
  SORT FIELDS=(22,8,CH,D,31,8,CH,D),SIZE=E73000
//STEP EXEC SORTCLG,TIME=30,REGICN=256K
//FORT,SYN IN DD *
C STEP 4 TAKES THE DATA FROM THE SORT AND BREAKS UP THE SINGLE
C RECORD INTO 55 ULOGS FORMAT AS IT WAS IN THE BEGINNING OF STEP 2.
C
LL=0
NN=0
LOGICAL*1 CUT(1265)
5 HEAD(9,15,END=99)(OUT,NLOG
15 FORMAT(23(55A1),T3V,13)
  WRITE(4,25)(OUT(I),I=1,55)
25 FORMAT(55A1)
  NN=NN+1
  DO 35 I=1,NLOG
    J=I*55+1
    K=J+54
    WRITE(4,25)(OUT(L),L=J,K)
  LL=LL+1
35 CONTINUE
  GO TO 5
19 STOP
  END
//
//GO.FT09F001 DD DSN=TEMPJ,DISP=(OLD,DELETE)
//GO.FT04F001 DD DSN=TEMP1,UNIT=SCRATCH,DISP=(NEW,PASS),
//DCB=(LRECL=55,BLKSIZE=55,RECFM=FB),SPACE=(150,(7200,100),RLST)
//GO.DELETE DD DSN=666USLT,DISP=(OLD,DELETE)
//STEP EXEC SORTCLG,PARM=FORT=MAP,TIME=30,REGIIN=256K
//FORT,SYN IN DD *
C STEP 5 GIVES EACH WELL IN OUR STUDY AN L.S.U. NUMBER, AND
C ULLICALIZES THE LATITUDE AND LONGITUDE COORDINATES.
C
K=0
77 HEAD(4,17,END=3999)(WELL,TD,LA1,LA2,LA3,LC1,LC2,LUJ,NLOG,NL
17 FORMAT(110,F10.2,6I3,2I3,11X)
  DLAT=LA1+FLOAT(LA2)/60.0+FLCAT(LA3)/3600
  DLONG=LO1+FLUAT(LU2)/60.0+FLOAT(LU3)/3600
  K=K+1
  LSUND=K
  WRITE(6,6)LSUND,WELL,TD,DLAT,DLONG,NLOG,NL
6 FORMAT(1X,14,110,F10.2,2F7.3,2I3,11X)
  WRITE(7,56)LSUND,WELL,TD,DLAT,DLONG,NLOG,NL
56 FORMAT(14,110,F10.2,2F7.3,2I3,11X)
  DO 65 J=1,NLOG
  READ(4,10,END=9999)DEPTH,WT,TEMP,GRAD
16 FORMAT(F10.2,F5.1,F10.2,F9.3,2I1X)
  WRITE(6,1)DEPTH,WT,TEMP,GRAD
1 FORMAT(1X,15X,F10.2,F5.1,F10.2,F9.3,6X)
  WRITE(7,30)DEPTH,WT,TEMP,GRAD
39 FORMAT(15X,F10.2,F5.1,F10.2,F9.3,6X)
65 CONTINUE
  GO TO 77
3999 STOP 400
4000 STOP 500
  END
//GO.FT04F001 DD DSN=TEMP1,DISP=(OLD,DELETE)
//
//

```

BOB01580  
 BOB01590  
 BOB01600  
 BOB01610  
 BOB01620  
 BOB01630  
 BOB01640  
 BOB01650  
 BOB01660  
 BOB01690  
 BOB01700  
 BOB01710  
 BOB01720  
 BOB01730  
 BOB01740  
 BOB01760  
 BOB01770  
 BOB01780  
 BOB01790  
 BOB01800  
 BOB01810  
 BOB01820  
 BOB01830  
 BOB01840  
 BOB01850  
  
 BOB01870  
 BOB01880  
 BOB01890  
 BOB01900  
 BOB01910  
 BOB01920  
 BOB01930  
 BOB01940  
 BOB01950  
 BOB01960  
 BOB01970  
 BOB01980  
  
 BOB02010  
 BOB02020  
 BOB02030  
 BOB02040  
 BOB02050  
 BOB02060  
 BOB02070  
 BOB02080  
 BOB02090  
 BOB02100  
 BOB02110  
 BOB02120  
 BOB02150  
 BOB02160  
 BOB02170  
 BOB02180  
 BOB02190  
 BOB02210  
 BOB02220  
 BOB02230  
 BOB02240  
 BOB02250  
 BOB02260  
 BOB02270  
 BOB02280  
  
 BOB02300  
 BOB02310  
 BOB02320  
 BOB02330  
 BOB02340  
 BOB02350  
  
 BOB02360  
 BOB02370  
 BOB02380  
 BOB02390  
 BOB02400  
  
 BOB02430  
 BOB02440  
 BOB02450  
  
 BOB02470  
 BOB02480  
 BOB02490  
 BOB02500  
 BOB02510  
 BOB02520  
 BOB02540  
 BOB02530

```

//LISTGHAD JOB (100.1009.1.5..2000..0)*83820 BCC MIXON*
//*SLTOP T1058.MUNCH-W PLEASE RUN AFTER TEMPPFILE.THANKS
// EXEC FORTUCLD.FARM.FCAT=*MAP*.TIME=3
//FCAT.SYSIN DD *
C
C *LISTGHAD* ACCESSES THE RESULTING DATA FROM 'TEMPPFILE' AND ALLOWS
C YOU TO GET A LISTING FOR A PARTICULAR GEOGRAPHICAL AREA.
C THE EXTREME COORDINATES OF A RECTANGULAR AREA (UPPER LEFT-HAND
C CORNER AND LOWER RIGHT-CORNER) ARE PUNCHED ONTO A PARAMETER
C CARD NEAR THE END OF THE PROGRAM.
C * PROGRAMMER: ROBERT L. MIXON * L.S.U. * 1970 *
C
      N=0
      READ(5,*,END=1999)XLA,XLN,YLA,YLN
595 READ(8,10,END=2999)LSUNC,INELL,TC,CLAT,DLONG,NLOG,NL
      DO 10 I=1,N
10  FORMAT(14,110,F10.2,2F7.3,2I3,11X)
      IF ((DLAT,LL,XLA,AND,DLONG,LE,XLN),AND,(DLAT,GF,YLA,AND,DLONG,
      CCE,YLN))GO TO 17
      DO 7 I=1,NLOG
      READ(8,17,END=3999)IDUM
17  FORMAT(10,49X)
      7 CONTINUE
      GO TO 999
47  CONTINUE
      N=N+1
      READ(8,45)LSUNC,INELL,TD,LLAT,DLONG,NLOG,NL,N
45  FORMAT(11X,14,110,F10.2,2F7.3,2I3,5X,15,20X)
      WRITE(9,32)LSUNC,INELL,TC,CLAT,DLONG,NLOG,NL,N
32  FORMAT(14,110,F10.2,2F7.3,2I3,5X,15,20X)
      DO 99 M=1,NLOG
      READ(8,22,END=4999)DEPTH,WT,TEMP,GNAC
22  FORMAT(15X,F10.2,F5.1,F10.2,F9.3,0A)
      WRITE(6,41)DEPTH,WT,TEMP,GNAC
41  FORMAT(15X,F10.2,F5.1,F10.2,F9.3,11X)
      WRITE(5,59)DEPTH,WT,TEMP,GNAC
59  FORMAT(15X,F10.2,F5.1,F10.2,F9.3,11X)
      99 CONTINUE
      GO TO 999
1999 STOP 100
2999 STOP 200
3999 STOP 300
4999 STOP 400
      END
//GO.F100F001 DD DSN=TEMPPFILE,UNIT=TAPE,DISP=(OLD,KLCPI),
// VLLSRL=TIGEL,LABELL=(1,5L),CC=(RECFM=FB,LHCLL=55,BLKSIZE=500)
//GO.F100F001 DD DSN=LOGRAD,UNIT=SCATCH,DISP=(,DELETE),
// SPACE=(2000,(10,10),RLSE)
//
// DCB=(RECFM=FB,LRECL=100,BLKSIZE=2000)
//GO.SYSIN DD *
C COORDINATE PARAMETER (ARC:---
      29.50 50.50 28.75 89.75
//
//

```



```

//CASSIE JOB (1305,03820,2,2,900,2481,.,.48),*MCH HIXON*
//*MCHL PUNCH LOGICAL PLEASE INTERPRET
// EXEC FORTGLG.MIGIUNE=150K
//FCN1.SYSPRINT DD EJMNY
//FOUT.SYSIN DD *
C THIS PROGRAM USES THE MUD RESISTIVITY AND THE SPONTANEOUS
C POTENTIAL FROM THE ELECTRIC LOG TO CALCULATE THE APPROXIMATE
C SALINITY FOR CLAY SANDS THAT ARE GREATER THAN TWENTY FEET IN THICKNESS.
C NM DLCK
C PROGRAM SP5AL 0040
DIMENSION MC(2),YTAU(34),XTAB(34),YITAB(6,34),XITAU(6,34), 0050
1 TAMP(6),MS75(34),SAL(34) 0060
DATA SYM1,SYM2,SYM3/J.,A.,2./
TEMP(1)=75. 0070
TEMP(2)=100. 0080
TEMP(3)=150. 0090
TEMP(4)=200. 0100
TEMP(5)=300. 0110
TEMP(6)=400. 0120
HEAD 1000,MS75(1),SAL(1),I=1,34) 0130
1000 FURMAT (2F10.3) 0140
DO 1020 J=1,34 0150
HEAD 1010, YITAB(1,J),XITAB(1,J),J=1,2) 0160
HEAD 1010, YITAB(1,J),XITAB(1,J),J=3,34) 0170
1010 FURMAT (2F10.3) 0180
1020 CONTINUE 0190
PRINT 5 0200
5 FURMAT (1H1,1X,'WELL NO.',6X,'DEPTH',4X,'THICK',2X,'MUD WT',2X,'TEM
1P',2X,'CCR TEMP',2X,'SAL PPM',4X,'PSI',7X,'LOG',JX,'MUD',JX,'SP',
25X,'HWE',7X,'HW',6X,'PGN',///) 0210
10 HEAD 12,MC(1),MC(2),DTAO,DDAC,RUN, TYFL,XMB,MH,DHT1,DHT2, 0240
10H01,MH02,SP 0250
11 CONTINUE 0260
12 FURMAT (2A4,2F10.0,12,A4,F5.1,F5.2,2F5.0,2F10.0,F5.0) 0270
IF (MC(2)-0.1325,32.15 0280
C COMPUTE MIDPOINT OF ACUIFER 0290
15 DMAG=(D0AU-DTAU)/2.+DTAU 0300
C COMPUTE FORMATION TEMPERATURE 0310
DHT2C=DHT2-P.819*DHD2*3.*1.E-12-2.143*DHD2*2.*1.E-8+.375*BHD2*
11.E-03-1.010
DHT1C=DHT1-P.819*DHD1*3.*1.E-12-2.143*DHD1*2.*1.E-8+.375*BHD1*
11.E-03-1.010
DMAD=(DHT2C-DHT1C)/(DHD2-DHD1)
FTE=(DMAD-DHD1)*GRAD+DHT1C
LEFT
C USE CHART GEN-9 TO OBTAIN KM AT FORMATION TEMPERATURE (HFT) 0360
R75=(KM*(DHT2+7.0))/82. 0370
0380
C DETERMINE RESISTANCE OF MUD FILTRATE (RMF) 0390
IF (XMB=10.)J0=20,20 0400
IF (XMB=16.)J0=40,40,30 0410
20 RMF=.75*RFT 0420
30 RMF=.75*RFT 0430
GO TO 100 0440
40 CONTINUE 0450
44 IF (XMB=11.)J0=46,46,55 0460
46 RMF1=(.4342944819*ALOG(HFT)-.07679)/.94155 0470
RMF2=(.4342944819*ALOG(HFT)-.13630)/.94624 0480
DXM=XMB-10. 0490
RMF1=EXP(RMF1/.4342944) 0500
RMF2=EXP(RMF2/.4342944) 0510
RMF=(RMF2-RMF1)*DXM+RMF1 0520
GO TO 100 0530
55 IF (XMB=12.)J0=56,56,65 0540
56 RMF1=(.4342944819*ALOG(HFT)-.15280)/.95545 0550
RMF2=(.4342944819*ALOG(HFT)-.22531)/.95545 0560
DXM=XMB-11. 0570
GO TO 47 0580
65 IF (XMB=13.)J0=66,66,75 0590
66 RMF1=(.4342944819*ALOG(HFT)-.22531)/.95545 0600
RMF2=(.4342944819*ALOG(HFT)-.30103)/.95545 0610
DXM=XMB-12. 0620
GO TO 47 0630
75 IF (XMB=14.)J0=76,76,85 0640
76 RMF1=(.4342944819*ALOG(HFT)-.30103)/.95545 0650
RMF2=(.4342944819*ALOG(HFT)-.36680)/.95545 0660
DXM=XMB-13. 0670
GO TO 47 0680
85 IF (XMB=15.)J0=86,86,95 0690
86 RMF1=(.4342944819*ALOG(HFT)-.36680)/.95545 0700
RMF2=(.4342944819*ALOG(HFT)-.39794)/.95545 0710
DXM=(XMB-14.)/2. 0720
GO TO 47 0730
100 CONTINUE 0740
C DETERMINE EQUIVALENT RESISTANCE OF MUD FILTRATE (HMF) 0750
104 IF (FT=100.)J0=106,106,110 0760
106 J=1 0770
GO TO 130 0780
110 IF (FT=150.)J1=112,112,115 0790
112 J=2 0800
GO TO 130 0810
115 IF (FT=200.)J1=118,118,120 0820
118 J=3 0830
GO TO 130 0840
120 IF (FT=300.)J1=122,122,125 0850
122 J=4 0860
GO TO 130 0870
125 IF (FT=400.)J1=126,126,128 0880
126 J=5 0890
GO TO 130 0900
128 J=6 0910
130 CONTINUE 0920
R75=(HMF*(FT+7.))/82. 0930
IF (R75=0.)J2=20,102,102 0940
102 HMF=.85*HMF 0950
GO TO 4000 0960
2020 DO 133 I=1,34 0970
YTAU(I)=YITAB(J,I) 0980
XITAU(I)=XITAB(J,I) 0990
133 CONTINUE 1000
DO 135 K=1,34 1010
IF (HMF-YTAU(K))140,140,135 1020
135 CONTINUE 1030
140 RMF1=AGRN(RMF,YTAD(K-2),XTAD(K-2)) 1040
145 DO 148 I=1,34 1050
YTAU(I)=YITAB(J+1,I) 1060
XITAU(I)=XITAB(J+1,I) 1070
DO 147 K=1,34 1080
IF (HMF-YTAU(K))150,150,147 1090
147 CONTINUE

```

CASSIE (Continued)

```

147 CONTINUE
150 RMF2=AGHAN(RMF,YTAU(K-2),XTAB(K-2))
    GRAU=(RMF2-RMF1)/(1LMP(J+1)-TEMP(J))
    RMFE=RMF1*(FT-TEMP(J))*GRAU
4000 CONTINUE
C USE CHART SP-1 TO FIND (RMF)/(RWIE)
    IF(FT-100.1155,155.160
155 RAT1=-(.74036750.)*SP
    RAT2=-(.9542470.)*SP
    T1=50.
    T2=100.
    GO TO 190
160 IF(FT-150.1162,162.165
162 RAT1=-(.9542470.)*SP
    T1=100.
    RAT2=-(.1/80.)*SP
    T2=150.
    GO TO 190
165 IF(FT-200.1167,167.170
167 RAT1=-(.1/80.)*SP
    T1=150.
    RAT2=-(.01291/70.)*SP
    T2=200.
    GO TO 190
170 IF(FT-250.1172,172.175
172 RAT1=-(.01291/70.)*SP
    T1=200.
    RAT2=-(.127875/120.)*SP
    T2=250.
    GO TO 190
175 IF(FT-300.1177,177.180
177 RAT1=-(.127875/120.)*SP
    T1=250.
    RAT2=-(.1/100.)*SP
    T2=300.
    GO TO 190
180 IF(FT-350.1182,182.185
182 RAT1=-(.1/100.)*SP
    T1=300.
    T2=350.
    RAT2=-(.65321/70.)*SP
    GO TO 190
185 RAT1=-(.65321/70.)*SP
    T1=350.
    RAT2=-(.41497/160.)*SP
    T2=400.
190 CONTINUE
    RAT1=EXP(RAT1/.4342544)
    RAT2=EXP(RAT2/.4342544)
    IF(SP)195,200,205
200 HAT=1.0
    GO TO 206
195 GRAD=(RAT2-RAT1)/50.
    RAT=(FT-T1)*GRAU+HAT
    GO TO 200
205 GRAD=(RAT1-HAT2)/50.
    RAT=-GRAD*(FT-T1)+RAT1
206 CONTINUE
C CALCULATE THE EQUIVALENT RESISTANCE OF THE WATER-(RWIE)
    RWE=RMFE/HAT
C USE CHART SP-2 TO DETERMINE RESISTANCE OF THE WATER -RW
    DO 1320 I=1,34
    YTAU(I)=YITAU(J,I)
    XTAU(I)=XITAU(J,I)
1330 CONTINUE
    CD 210 K=1,34
    IF(RWE-XTAD(K))215,215,210
210 CONTINUE
215 RWI=AGHAN(RWE,XTAU(K-2),YTAU(K-2))
220 DO 230 I=1,30
    YTAB(I)=YITAB(J+1,I)
230 XTAB(I)=XITAB(J+1,I)
    DO 240 K=1,30
    IF(RWE-XTAD(K))245,245,240
240 CONTINUE
245 RW2=AGHAN(RWE,XTAB(K-2),YTAB(K-2))
    GRAU=(RW2-RW1)/(TEMP(J+1)-TEMP(J))
    RWE=RW1*(FT-TEMP(J))*GRAU
C USE CHART GEN-4 TO DETERMINE SALINITIES
    MW75=(RW*(FT+7.0))/R2.
    DO 260 I=1,34
    IF(MW75-RS75(I))270,270,260
260 CONTINUE
270 GRAU=(RS75(1)-RS75(I-1))/(SAL(1)-SAL(I-1))
    GRAD=1./GRAD
    DSAL=(RW75-RS75(I-1))*GRAD+SAL(I-1)
    TH=DSAL*CTAU
    PGH=.052*XMW*DMAO
    PGH=.052*XMW
    FMINT 300,MC(1),MC(2),DTAG,DEAG,TH,XMW,FT,E,DSAL,P,RUN,TYFL,SP
    I,MW,RW,PGH
300 FORMAT(1X,2A4,1X,F7.0,1H-,F7.0,F5.0,3X,F5.1,1X,F6.0,3X,F6.0,3X,
    +F8.0,1X,F8.0,1X,12,1X,A4,1X,F5.0,3X,F6.2,3X,F6.2,3X,F5.3)
    DAV=(DBAO*DTAG)/2
    BR)TE(7,510)DAV,PGH,SYMI,E,SYM2,DSAL,SYM3
510 FORMAT(2F10.3,F5.0,F10.3,F5.0,F10.3,F5.0)
    GO TO 10
325 STOP
    END
FUNCTION AGRAN(D,XT,Y)
DIMENSION XT(1),Y(1),X(4)
DO 10 I=1,4
10 X(I)=D-XT(I)
13 CONTINUE
    AGRAN=-1
    1(Y(1)*X(2)*X(3)*X(4))/((X(1)-X(2))*(X(1)-X(3))*(X(1)-X(4))) +
    2(Y(2)*X(1)*X(3)*X(4))/((X(2)-X(1))*(X(2)-X(3))*(X(2)-X(4))) +
    3(Y(3)*X(1)*X(2)*X(4))/((X(3)-X(1))*(X(3)-X(2))*(X(3)-X(4))) +
    4(Y(4)*X(1)*X(2)*X(3))/((X(4)-X(1))*(X(4)-X(2))*(X(4)-X(3)))
    RETURN
    END
//GO,SYSIN CD *
    .040 250000.
    .042 200000.
    .054 150000.
    .071 100000.
    .060 100000.
    .087 60000.
    .113 60000.
    .133 50000.
    .143 40000.
    .210 30000.

```

1040  
1050  
1060  
1070  
1080  
1090  
1100  
1110  
1120  
1130  
1140  
1150  
1160  
1170  
1180  
1190  
1200  
1210  
1220  
1230  
1240  
1250  
1260  
1270  
1280  
1290  
1300  
1310  
1320  
1330  
1340  
1350  
1360  
1370  
1380  
1390  
1400  
1410  
1420  
1430  
1440  
1450  
1460  
1470  
1480  
1490  
1500  
1510  
1520  
1530  
1540  
1550  
1560  
1570  
1580  
1590  
1600  
1610  
1620  
1630  
1640  
1650  
1660  
1670  
1680  
1690  
1700  
1710  
1720  
1730  
1740  
1750  
1760  
1770  
1780  
1790  
1800  
1810  
1820  
1830  
1840  
1850  
1860  
1870  
1880  
1890  
1900  
1910  
1920  
1930  
1970  
1980  
1990  
2000  
2010  
2020  
2030  
2040  
2050  
2060  
2070  
2080  
2090  
2100  
2110  
2120

```

//SALINRMF JOB (1305,83620,2,2,900,2481,.,.48),LCH MIXCN*
//ROUTE PUNCH LOCAL PLEASE INTERPRET
// EXEC FORTGCLD,RFGLCN=150K
//FONT,SYSPRINT DD DUMMY
//FORT,SYSDIN DD *

```

0030

0040

```

C THIS PROGRAM USES THE MUD FILTRATE RESISTIVITY INSTEAD OF THE
C MUD RESISTIVITY TO CALCULATE THE SALINITY FOR AN AQUIFER.
C THE RESULTS ARE SOMEWHAT BETTER THAN WHEN USING THE MUD
C RESISTIVITY .
C RMF DLCK
C PROGRAM SPSAL
C DIMENSION MC(2),YTAB(34),XTAB(34),YITAB(6,34),XITAB(6,34),
C ITEMP(6),HS75(34),SAL(34)
C DATA SYM1,SYM2,SYM3/3.,4.,2./
C TEMP(1)=75.
C TEMP(2)=100.
C TEMP(3)=150.
C TEMP(4)=200.
C TEMP(5)=300.
C TEMP(6)=400.
1000 READ 1000,(RS75(I),SAL(I),I=1,34)
C FORMAT (2F10.3)
C DO 1020 I=1,6
C READ 1010,(YITAB(I,J),XITAB(I,J),J=1,2)
C READ 1010,(YITAB(I,J),XITAB(I,J),J=3,34)
1010 FORMAT (6F10.5)
1020 CONTINUE
C PRINT 5
C 5 FORMAT(1H,1X,'WELL NO.',6X,'DEPTH',4X,'THICK',2X,'MUD WT',2X,'TEM
C 1P',2X,'CON. TEMP',2X,'SAL PPM',4X,'PSI',1X,'LOG',3X,'MUD',3X,'SP',
C 25X,'WELL',7X,'THICK',6X,'PGM',///)
C 10 HEAD 12,MC(1),MC(2),DTAO,DEAO,RUN, TYFL,XM,RMF,BHT1,BHT2,
C 1BHD1,BHD2,SP
11 CONTINUE
C 12 FORMAT(2A4,2F10.0,12A4,F5.1,F5.2,2F5.0,2F10.0,F5.0)
C IF(MC(2)-0)325,325,15
C COMPUTE MIDPOINT OF AQUIFER
C 15 DMAU=(DBAU-DTAU)/2.+DTAU
C COMPUTE FORMATION TEMPERATURE
C BHT2C=BHT2-.219*BHD2*.3*.1E-12-2.143*BHD2*.2*.1E-8+4.375*BHD2*
C 11.E-03-1.016
C BHT1C=BHT1-.219*BHD1*.3*.1E-12-2.143*BHD1*.2*.1E-8+4.375*BHD1*
C 11.E-03-1.016
C GRAD=(BHT2C-BHT1C)/(BHD2-BHD1)
C FT=(DMAU-BHD1)*GRAD+BHT1C
C E=FT
C USE CHART GEN-9 TO OBTAIN RMF AT FORMATION TEMPERATURE (HFT)
C GO TO 100
C CONTINUE
C 100 DETERMINE EQUIVALENT RESISTANCE OF MUD FILTRATE (RMF)C
C 104 IF(FT=100.)106,106,110
C 106 J=1
C GO TO 130
C 110 IF(FT=150.)112,112,115
C 112 J=2
C GO TO 130
C 115 IF(FT=200.)118,118,120
C 118 J=3
C GO TO 130
C 120 IF(FT=300.)122,122,125
C 122 J=4
C GO TO 130
C 125 IF(FT=400.)126,126,128
C 126 J=5
C GO TO 130
C 128 J=6
C 130 CONTINUE
C R75=(RMF*(BHT2+7.))/d2.
C HFT=(RMF*(BHT2+7.))/(FT+7.)
C IF(R75=0.)12020,102,102
C 102 RMFL=.25*HFT
C GO TO 4000
2020 DO 133 I=1,34
C YTAU(I)=YITAB(J,I)
C XTAU(I)=XITAB(J,I)
133 CONTINUE
C DO 135 K=1,34
C IF(RMF-YTAU(K))140,140,135
135 CONTINUE
C RMF1=AGMAN(RMF,YTAU(K-2),XTAU(K-2))
C DO 146 I=1,34
C YTAB(I)=YITAB(J+1,I)
C XTAB(I)=XITAB(J+1,I)
C DO 147 K=1,34
C IF(RMF-YTAB(K))150,150,147
147 CONTINUE
C 150 RMF2=AGMAN(RMF,YTAB(K-2),XTAB(K-2))
C GRAD=(RMF2-RMF1)/(TLMP(J+1)-TEMP(J))
C RMFE=RMF1+(FT-TEMP(J))*GRAD
4030 CONTINUE
C USE CHART SP-1 TO FIND (RMF)E/(RM)E
C IF(FT=100.)155,155,160
C 155 RAT1=(-.74036/50.)*SP
C RAT2=(-.5424/70.)*SP
C T1=50.
C T2=100.
C GO TO 160
160 IF(FT=150.)162,162,165
C 162 RAT1=(-.5424/70.)*SP
C T1=100.
C RAT2=(-.17/80.)*SP
C T2=150.
C GO TO 170
165 IF(FT=200.)167,167,170
C 167 RAT1=(-.17/80.)*SP
C T1=150.
C RAT2=(-.21251/70.)*SP
C T2=200.
C GO TO 170
170 IF(FT=250.)172,172,175
C 172 RAT1=(-.81291/70.)*SP
C T1=200.
C RAT2=(-.127875/120.)*SP
C T2=250.
C GO TO 170
175 IF(FT=300.)177,177,180
C 177 RAT1=(-.127875/120.)*SP
C T1=250.
C RAT2=(-.17/100.)*SP
C T2=300.
C GO TO 180
180 IF(FT=350.)182,182,185
C 182 RAT1=(-.17/100.)*SP
C T1=300.
C T2=350.
C RAT2=(-.16531/70.)*SP
C GO TO 180

```

1180

```

185 RAT1=-(.65J21/70.)*SP
    T1=J50.
    RAT2=-(.41457/160.)*SP
    T2=400.
190 CONTINUE
    RAT1=LXP(RAT1/.4342544)
    RAT2=LXP(RAT2/.4342544)
    IF(S*195.200.205
200 RAT1=1.0
    GO TO 206
195 GRAU=(RAT2-RAT1)/50.
    RAT=(R1-11)*GHAD+RAT1
    GO TO 206
205 GHAD=(RAT1-RAT2)/50.
    RAT=-GHAD*(R1-11)+RAT1
206 CONTINUE
C CALCULATE THE EQUIVALENT RESISTANCE OF THE WATER - (HWE)
    HWE=RMFE/RAT
C USE CHART SP-2 TO DETERMINE RESISTANCE OF THE WATER - RW
    DO 1370 I=1,34
    YTAB(I)=YITAB(J,I)
    XTAB(I)=XITAB(J,I)
1330 CONTINUE
    DO 210 K=1,34
    IF(HWE-XTAB(K))215,215,210
210 CONTINUE
215 RW1=AGRN(HWE,XTAB(K-2),YTAB(K-2))
220 DO 230 I=1,30
    YTAB(I)=YITAB(J+1,I)
    XTAB(I)=XITAB(J+1,I)
230 DO 240 K=1,30
    IF(HWE-XTAB(K))245,245,240
240 CONTINUE
245 RW2=AGRN(HWE,XTAB(K-2),YTAB(K-2))
    GHAD=(RW2-RW1)/(TEMP(J+1)-TEMP(J))
    RW=RW1+(R1-TEMP(J))*GHAD
C USE CHART GEN-4 TO DETERMINE SALINITIES
    RW75=(RW*(R1+7.0))/82.
    DO 260 I=1,34
    IF(RW75-RS75(I))270,270,260
260 CONTINUE
270 GRAD=(RS75(I)-RS75(I-1))/(SAL(I)-SAL(I-1))
    GRAD=1./GHAD
    DSAL=(RW75-RS75(I-1))*GHAD+SAL(I-1)
    TH=DTAO-DTAD
    P=.052*XM*DMAD
    PGR=.052*XMW
    PRINT 300,MC(1),MC(2),DTAO,DBAQ,TH,XM,F1,E,DSAL,P,RUN,TYFL,SP
1370 WRITE(4,2A4,1X,F7.0,1H-,F7.0,F5.0,3X,F5.1,1X,F6.0,3X,F6.0,3X,
    *F3.0,1X,F8.0,1X,12,JX,AA,1X,F5.0,3X,F6.2,3X,F5.3)
    DAV=(DBAQ+DTAD)/2
    WRITE(7,5I10)DAV,PGR,SYM1,E,SYM2,DSAL,SYM3
510 FORMAT(2F10.3,F5.0,F10.3,F5.0,F10.3,F5.0)
    GO TO 10
325 STOP
    END
    FUNCTION AGRN(D,XT,Y)
    DIMENSION XT(1),Y(1),X(4)
    DO 10 I=1,4
10 X(I)=D-XT(I)
13 CONTINUE
    AGRN=-1
    1/(Y(1)*X(2)*X(3)*X(4))/((X(1)-X(2))*(X(1)-X(3))*(X(1)-X(4))) +
    2/(Y(2)*X(1)*X(3)*X(4))/((X(2)-X(1))*(X(2)-X(3))*(X(2)-X(4))) +
    3/(Y(3)*X(1)*X(2)*X(4))/((X(3)-X(1))*(X(3)-X(2))*(X(3)-X(4))) +
    4/(Y(4)*X(1)*X(2)*X(3))/((X(4)-X(1))*(X(4)-X(2))*(X(4)-X(3)))
    RETURN
    END

```

1190  
1200  
1210  
1220  
1230  
1240  
1250  
1260  
1270  
1280  
1290  
1300  
1310  
1320  
1330  
1340  
1350  
1360  
1370  
1380  
1390  
1400  
1410  
1420  
1430  
1440  
1450  
1460  
1470  
1480  
1490  
1500  
1510  
1520  
1530  
1540  
1550  
1560  
1570  
1580  
1590  
1600  
1610  
1620  
1630  
1640  
1650  
1660  
1670  
1680  
1690  
1700  
1710  
1720  
1730  
1740  
1750  
1760  
1770  
1780  
1790  
1800  
1810  
1820  
1830  
1840  
1850  
1860  
1870



```

0100 62 CONTINUE
0101 IF (JJ-2) 69,66,80
0102 C CHECK FOR 1.2 OR 3+ MUD RUNS
0103 66 IF (WT(2)-WT(1)) 67,69,68
0104 C IF (NEGATIVE, SET TREND) FOR 1. SAME FOR 2
0105 67 JERR=JERR+1
0106 WT(2)=WT(1)
0107 GO TO 69
0108 68 TREND(2)=(ND(2)-ND(1))/(WT(2)-WT(1))
0109 C TO SET VALUE OF TREND(1)
0110 69 IF (WT(1).LE.12.0) GO TO 71
0111 IF (WT(1).GE.16.5) GO TO 71
0112 TREND(1)=400.0
0113 GO TO 76
0114 71 TREND(1)=4000.0
0115 GO TO 76
0116 76 IF (WT(2).EQ.WT(1)) TREND(2)=TREND(1)
0117 GO TO 100
0118 C THREE MUD MUDS
0119 80 IF (WT(1).LE.12.0) GO TO 81
0120 IF (WT(1).GE.16.5) GO TO 81
0121 TREND(1)=400.0
0122 GO TO 82
0123 81 TREND(1)=4000.0
0124 82 DO 98 M=2, JJ
0125 IF (WT(M)-WT(M-1)) 92,90,91
0126 C IF ERROR, GO TO 92
0127 90 TREND(M)=TREND(M-1)
0128 GO TO 98
0129 91 TREND(M)=(ND(M)-ND(M-1))/(WT(M)-WT(M-1))
0130 GO TO 98
0131 92 IF (M.EQ.JJ) GO TO 94
0132 IF (WT(M+1)-WT(M-1)) 95,94,94
0133 JERR=JERR+2
0134 WT(M)=WT(M-1)
0135 TREND(M)=TREND(M-1)
0136 GO TO 98
0137 95 IF (WT(1).GE.WT(M)) GO TO 97
0138 97 WT(1)=WT(M)
0139 C REMOVE LOW HIGH VALUE AND SLND THROUGH DO-LOOP AGAIN FOR RECHECK
0140 WT(M-1)=WT(M)
0141 JERR=JERR+3
0142 GO TO 80
0143 98 CONTINUE
0144 C V=1 IS ANOMALOUSLY HIGHER THAN NEXT TWO.
0145 100 LLL=LLL+1
0146 XCOORD=(AWL-OLDWG)*DX
0147 TCOORD=(LLAT-TSLA)*DY
0148 IF (JERR.EQ.0) GO TO 110
0149 DO 101 M=1, JJ
0150 WRITE(6,102) LLL, JERR, ND(M), WT(M), TREND(M)
0151 102 FORMAT(1A,15,F3.16,F5.1,F8.3)
0152 STOP
0153 C STEP TWO USES TRENDS TO CALCULATE DEPTHS TO MUDWETS 10, 11, .....
0154 C NO DATA IS EXTRAPOLATED DOWNWARD MORE THAN TWO JOBLIGHTS
0155 C IM=UNIT MUDWEIGHT; JK= NUMBER OF PROJECTIONS
0156 110 IM=9
0157 JK=0
0158 115 DO 150 L=1,11
0159 UMUD(L)=-999.
0160 IM=IM+1
0161 DO 145 M=1, JJ
0162 UD=WT(M)-IM
0163 IF (UD) 121,122,123
0164 123 UMUD(L)=(ND(M)-UD)*TREND(M)
0165 GO TO 150
0166 122 UMUD(L)=ND(M)
0167 GO TO 150
0168 121 IF (M.EQ.JJ) GO TO 146
0169 GO TO 145
0170 146 JK=JK+1
0171 IF (JK.GE.3) GO TO 150
0172 IF (JK.EQ.2.AND.IM.GE.18) GO TO 150
0173 UMUD(L)=ND(M)+((IM-WT(M))*TREND(M))
0174 145 CONTINUE
0175 150 CONTINUE
0176 200 WRITE(6,201) LLL, (UMUD(L), L=1,11), JK
0177 201 FORMAT(1X,14,1F8.0,15)
0178 IF (LLL.GE.50) GO TO 4999
0179 GO TO 999
0180 1999 STOP 100
0181 2999 STOP 200
0182 3999 STOP 300
0183 4999 STOP 400
0184 5999 STOP 500
0185 LNU
0186 SIGHTY
0187 89.75 91.25 28.75 30.25 60.252 68.875
0188 55

```

```

0001: //MUDSAND JOB (1029,83668,2,5*200,0029),*KUPFER*
0002: //SETUP 12500,12549-W
0003: // EXEL FORTGCLG
0004: //FORT.SYSIN DD =
0005: C
0006: C MUDSAND IS A VARIANT OF MDSNDAL AND CALCULATES AVERAGE OR
0007: C MAXIMUM MUDWEIGHTS AND NETSAND FOR FOUR INTERVALS.
0008: C MIXED PROGRAM OF 3/78 MODIFIED BY KUPFER 6/79
0009: C NO MORE THAN FOUR INTERVALS CAN BE DONE AT ONE TIME
0010: C
0011: C PARAMETER CARD:
0012: C XLLN, XLLN, YSLA, YNLA, ITOP, INTV, DX, DY, MAXMUD
0013: C
0014: C THE FIRST FOUR ITEMS GIVE THE EAST AND WEST LONGITUDE AND SOUTH
0015: C AND NORTH LATITUDE OF THE AREA TO BE USED. USF DECIMALS, NOT MINUTES
0016: C AND SECONDS
0017: C ITOP IS THE TOP OR HIGHEST ELEVATION (IN FEET) OF THE HIGHEST OF THE FOUR
0018: C INTERVALS TO BE CHECKED, (I.E. 10000)--AN INTEGER NUMBER.
0019: C INTV IS THE INTERVAL (IN FEET) BETWEEN TOP AND BASE OF AN INTERVAL
0020: C (I.E. 2000)--AN INTEGER NUMBER
0021: C THUS THE ABOVE (10000, 2000) WOULD GIVE 2000-FOOT INTERVALS FROM
0022: C MINUS 10000 TO MINUS 18000 FEET.
0023: C DX AND DY ARE THE CONVERSION FACTORS TO BE USED TO CONVERT DEGREES OF
0024: C LONGITUDE (X) AND LATITUDE (Y) INTO FEET
0025: C MAXMUD DETERMINES WHAT OPERATIONS WILL BE PERFORMED.
0026: C IF MAXMUD IS BLANK, ZERO, OR -1, PROGRAM CALCULATES THE AVERAGE
0027: C MUDWEIGHT OF THE INTERVAL, INCLUDING THAT OF THE PREVIOUS INTERVAL.
0028: C IF MAXMUD IS 1 OR 2 IT TAKES THE HIGHEST MUD IN THE INTERVAL
0029: C IF MAXMUD IS -1 OR 2, NO SAND CALCULATIONS ARE MADE.
0030: C THE PROGRAM CONSISTS OF FOUR OPERATIONS:
0031: C 1. READ 1ST RECORD AND DECIMALIZE LAT/LONG, SORT FOR AREA SOUGHT.
0032: C 2. READ 2ND RECORD (MUDDATA) AND CALCULATE AVERAGE OR MAXIMUM
0033: C WEIGHT OF MUD USED IN THE FOUR INTERVALS.
0034: C 3. READ 3RD RECORD (SANDDATA) AND CALCULATE THE TOTAL THICKNESS
0035: C OF SAND IN EACH INTERVAL
0036: C 4. WRITE OUT THE DATA ON CARDS, PRINTER, TAPE, OR DISK
0037: C
0038: C
0039: C INTEGER X,DEPTH,TLMP,TKM,TOPSND,BOTSND,SP
0040: C REAL MWT
0041: C DIMENSION A(31),DEPTH(30),MWT(30),TEMP(30),RM(30),TRM(30),
0042: C CTOPSND(75),BOTSND(75),NTSND(75),SPI(75),MDTY(75),AVGMWT(4),
0043: C (SUMSND(4),LITH(75))
0044: C DATA SETS ALL OF THE VARIABLES TO ZERO.
0045: C DATA X,DEPTH,TEMP,TRM,IUPSND,BOTSND,NTSND,SP/421*0/
0046: C DATA RM,MWT,AVGMWT,SUMSND/68*0./
0047: C DATA IL/0/
0048: C LLL IS A COUNTER FOR # OF HOLES EXAMINED
0049: C LLL=0
0050: C READ(5,*)XLLN,XLLN,YSLA,YNLA,ITOP,INTV,DX,DY,MAXMUD
0051: C READ(5,*) READS PARAMETER DATA IN FLOATING FORMAT FROM CARDS
0052: C WRITE(6,38)XLLN,XLLN,YSLA,YNLA,ITOP,INTV,DX,DY,MAXMUD
0053: C 38 FORMAT(11,*,PARAM,2X,4F7.2,2I6,2F7.3,I5)
0054: C 999 READ(10,10)END=9999IX
0055: C 10 FORMAT(110,5A4,(A4,A1)12A4,2A2,I5,6I2,I5,I3,I5,A1,2I2,3X)
0056: C INTEGER "IX" IS USED TO READ THE FIRST RECORD INTO 31 UNITS OF
0057: C INFORMATION, OF WHICH 20-25 REFER TO LAT/LONG
0058: C LAT/LONG ARE THEN DECIMALIZED
0059: C DLAT=X(20)+FLOAT(X(21))/60.0+FLOAT(X(22))/360.0
0060: C DLONG=X(23)+FLOAT(X(24))/60.0+FLOAT(X(25))/360.0
0061: C IF THE DATA ARE IN THE AREA, GO TO 47. IF NOT, THE REMAINING CARDS
0062: C ARE READ INTO A DUMMY-FILE (IDUM) AND DISCARDED, THE NEXT FILE IS
0063: C READ (999)
0064: C IF ((DLAT.LE.YNLA.AND.DLONG.LE.XLLN).AND.(DLAT.GE.YSLA.AND.DLONG.
0065: C CGE.XLLN))GO TO 47
0066: C JJ=X(30)
0067: C IF (JJ.EQ.0)GO TO 8888
0068: C DO 7 I=1,JJ
0069: C READ(10,17)END=39999IDUM
0070: C 17 FORMAT(10,94X)
0071: C 7 CONTINUE
0072: C 8888 CONTINUE
0073: C II=X(31)
0074: C IF (II.EQ.0)GO TO 999
0075: C DO 8 J=1,II
0076: C READ(10,18)END=49999IDUM
0077: C 18 FORMAT(10,94X)
0078: C 8 CONTINUE
0079: C GO TO 999
0080: C 47 CONTINUE
0081: C JJ=X(30)
0082: C IF (JJ.EQ.0)GO TO 805
0083: C JJ IS A COUNTER OF NUMBER OF CARDS IN THE MUDFILE. IF JJ = ZERO,
0084: C THEN NO SAND FILE IS PRESENT (NOW), BUT THIS MAY LATER BE CHANGED.
0085: C IDPTH=0
0086: C LHMUD=0.0
0087: C CARDS OF THE MUD FILE ARE NOW READ
0088: C DO 99 M=1,JJ
0089: C READ(10,22)END=59999IDPTH(M),MWT(M),TEMP(M),RM(M),TRM(M),
0090: C CMDTY(M)
0091: C 22 FORMAT(16,F5.1,I5,F3.2,I5,A1,73X)
0092: C 99 CONTINUE
0093: C MUDFILE IS READ AND DEPTH INTERVAL SET (AT ONE INTERVAL LOWER THAN
0094: C TU OR LL)
0095: C LL=ITOP-INTV
0096: C KK=ITOP
0097: C HMMUD=10.0
0098: C IF NO MUDWEIGHT ASSUME 10M MUD
0099: C NEXT CHECK FOR INCREASING DEPTH AND MUDWEIGHT
0100: C 721 DO 722 V=1,JJ
0101: C IF (IDPTH.GT.DEPTH(M))GO TO 351
0102: C IF (CHKMUD.GT.MWT(M))GO TO 352
0103: C IDPTH=DEPTH(M)
0104: C CHKMUD=MWT(M)
0105: C 722 CONTINUE
0106: C GO TO 365
0107: C 351 IE=1
0108: C GO TO 360
0109: C 352 IE=2
0110: C GO TO 360
0111: C ENRUK #1 = BAD DEPTH ORDER ON MUD1 #2 = DECREASING MUDWEIGHT
0112: C 360 WRITE(6,361)X(11),DLAT,DLONG,X(19),X(30),X(31),IE
0113: C 361 FORMAT(1X,110,2F8.4,1X,I5,3I3)
0114: C THE NEXT DO-LOOP COUNTS THE FOUR DEPTH INTERVALS AND CALCULATES AN AVGMWT
0115: C FOR EACH OF THE FOUR. MNN IS THE COUNTER.
0116: C 365 DO 894 K=1,4
0117: C LL=LL+INTV
0118: C KK=KK+INTV
0119: C AVGMWT(K)=10.
0120: C SUMMUD=HMMUD
0121: C MNN=1,0
0122: C

```

```

0122 C DU-LOOP TO DETERMINE THE AVERAGE MUDWEIGHT IN THE INTERVAL
0123 C SOME 12# MUDS ARE RECORDED AS 1,2 AND SO * TEN
0124 C MUDWEIGHT OF PREVIOUS INTERVAL (HMUD) HELD OVER INTO NEXT INTERVAL
0125 DO 88 MM=1,4
0126 IF (MWT(MM).EQ.0.0)MWT(MM)=10.0
0127 IF (MWT(MM).LT.3.0)MWT(MM)=MWT(MM)*10.0
0128 IF (DEPTH(MM).LT.AL) GO TO 87
0129 IF (DEPTH(MM).GE.AL.AND.DEPTH(MM).LT.AK)GO TO 93
0130 GO TO 894
0131 93 CONTINUE
0132 SUMUD=SUMUD+MWT(MM)
0133 MNN=MNN+1.0
0134 AVGMWT(K)=SUMUD/RNN
0135 87 HMUD=MWT(MM)
0136 IF (MAXMUD.GT.0)AVGMWT(K)=HMUD
0137 C PROGRAM USES MAXIMUM MUD WEIGHT NOT THE AVERAGE MUDWT
0138 88 CONTINUE
0139 894 CONTINUE
0140 GO TO 895
0141 885 IE=8
0142 DO 4 IJ=1,4
0143 AVGMWT(IJ)=-99.
0144 4 CONTINUE
0145 895 CONTINUE
0146 C START OF STEP THREE--TO CALCULATE THE FEET OF SAND IN AN INTERVAL
0147 I=X(I,2)
0148 890 IF (HMUD.EQ.0.OR.MAXMUD.EQ.1) GO TO 993
0149 IF (II.EQ.0.0) GO TO 9994
0150 DO 9 JM=1,11
0151 HEAD(10,994:END=7999)IDUM
0152 994 FORMAT(16,94X)
0153 9 CONTINUE
0154 GO TO 9994
0155 993 SUMSND(1)=0
0156 SUMSND(2)=0
0157 SUMSND(3)=0
0158 SUMSND(4)=0
0159 IF (II.EQ.0)GO TO 1112
0160 C IF NO SANDS, SUMSND SET TO -99.. NOT 7FRD
0161 DO 109 MNK=1,11
0162 READ(10,23,END=6999)TOPSND(MNK),BOTSND(MNK),NTSND(MNK),
0163 CSP(MNK),LITH(MNK)
0164 23 FORMAT(16,15,15,15,A1,78X)
0165 C SAND DATA ARE READ IN AND NUMBERED (MNK)
0166 109 CONTINUE
0167 CHKSND=0.0
0168 XL=ITOP-INTV
0169 XK=ITOP
0170 IF (TOPSND(1).GT.XK.OR.BOTSND(11).LE.(XK+4*INTV))IE=6
0171 ERROR #6 = PART OF INTERVAL MISSING
0172 C CHECK TO SEE IF NET SAND AND DEPTH HAVE INHERENT ERRORS.
0173 IDPTH=0
0174 DO 712 N=1,11
0175 IF (NTSND(N).GT.(BOTSND(N)-TOPSND(N)))GO TO 604
0176 IF (NTSND(N).GT.1000)GO TO 605
0177 IF (IDPTH.GT.TOPSND(N))GO TO 606
0178 C ERROR #4 = BAD NET SAND; #5 = DEPTH ERROR
0179 GO TO 608
0180 605 IE=4
0181 GO TO 607
0182 606 IE=5
0183 GO TO 607
0184 607 WRITE(6,362)X(1),DLAT,DLONG,X(19),X(30),X(31),IE,TOPSND(N)
0185 362 FORMAT(1X,110,2F8.4,1X,15,313,16)
0186 608 IDPTH=BOTSND(N)
0187 712 CONTINUE
0188 C NEXT OO-LOOP SETS THE INTERVAL
0189 DO 94 NN=1,4
0190 XL=XL+INTV
0191 XK=XK+INTV
0192 SUMSND(NN)=0.00
0193 C PROPR=0.0
0194 C NEXT OO-LOOP SUMS THE SAND OF THE INTERVAL
0195 DO 10 N=1,11
0196 TST=TOPSND(N)
0197 BST=BOTSND(N)
0198 SST=NTSND(N)
0199 IF (TST.LT.XL.AND.BST.LT.XL)GO TO 110
0200 IF (TST.GE.XK)GO TO 94
0201 IF (TST.LT.XL.AND.BST.GE.XK)GO TO 293
0202 IF (TST.GE.XL.AND.BST.LT.XK)GO TO 111
0203 IF (TST.LT.XL.AND.BST.LT.XK)GO TO 291
0204 C WHAT IS LEFT IS TST.GE.XL.AND.BST.GE.XK
0205 PROPR=(XK-TST)/(BST-TST)
0206 GO TO 295
0207 293 PROPR=(XK-XL)/(BST-TST)
0208 GO TO 295
0209 291 PROPR=(BST-XL)/(BST-TST)
0210 GO TO 295
0211 111 PROPR=1.0
0212 295 SUMSND(NN)=SUMSND(NN)+(PROPR*SST)
0213 110 CONTINUE
0214 94 CONTINUE
0215 GO TO 1113
0216 1112 SUMSND(1)=-99.
0217 DO 2 IJK=1,4
0218 SUMSND(IJK)=-99.
0219 2 CONTINUE
0220 C NEGATIVE 99. SUMSND=MUD OF 12# OR MORE AND NO SAND
0221 9994 CONTINUE
0222 1113 LLL=LLL+1
0223 XCOORD=(XWLN-OLONG)*DX
0224 YCOORD=(ULAT-YSLA)*DY
0225 WRITE(6,54)XCOORD,YCOORD,AVGMWT(1),AVGMWT(2),AVGMWT(3),AVGMWT(4),
0226 CSUMSND(1),SUMSND(3),SUMSND(3),SUMSND(4),X(1),DLAT,DLONG,LLL,IE
0227 54 FORMAT(1X,2F7.3,4F5.1,4F5.0,110,2F7.3,4X,14,2X,12)
0228 WRITE(9,55)IWELL,LLL,XCOORD,YCOORD,AVGMWT(1),AVGMWT(2),
0229 CAVGMWT(3),AVGMWT(4)
0230 55 FORMAT(2X,1PTM,110,14,3X,2F8.3,4F7.1)
0231 WRITE(9,56)IWELL,LLL,XCOORD,YCOORD,SUMSND(1),SUMSND(2),
0232 CSUMSND(3),SUMSND(4)
0233 56 FORMAT(2X,2PTS,110,14,3X,2F8.3,4F7.1)
0234 9995 IE=0
0235 GO TO 999
0236 2999 STOP 300
0237 3999 STOP 400
0238 4999 STOP 500
0239 5999 STOP 600
0240 6999 STOP 700
0241 7999 STOP 800
0242 END
0243 //GO F10F001 DD UNIT=TAPE,VOL=SER=T2500,DISP=OLD,
0244 // LABEL=2,DSN=CLENDATA
0245 //GO F109F001 DD DSN=NEWDIR,VOL=SER=T2549,UNIT=TAPE,LABEL=29,
0246 // DISP=(,KEEP),DCB=(LRECL=80,BLKSIZL=6400,RECFM=FB)
0247 //GO,SYSDN DD *
0248 89.75 91.25 28.75 30.25 5000 1000 60.242 68.472 0 .0197

```

```

0001 //PERSAND JOB (1029,83668,.....0)'MEADE'
0002 //SEIU
0003 // EXEC FORTGCLG
0004 C PERSAND PROGRAM CALCULATES THE PERCENT OF SAND (PS) IN AN INTERVAL (I)
0005 C AND PLOTS IT AT THE AVERAGE DEPTH OF THAT INTERVAL (AVGDP).
0006 I=INTEGER X(31),DEPTH,TEMP,?
0007 REAL WAT
0008 DATA X,DEPTH,TEMP/33.0/
0009 =0
0010 READ(5,*)XELN,XWLN,YSLA,YNLA,DX,DY,DLAT,DP
0011 WRITE(6,3)XELN,XWLN,YSLA,YNLA,DX,DY,DLAT,DP
0012 38 FORMAT('1','PARAM',1X,4F7.2,2F7.3,2F5.1)
0013 999 READ(10,10,END=2999)X
0014 10 FORMAT(10,5A4,4(A4,A1),2A4,2A2,15,6I2,15,13,15,A1,2I2,3X)
0015 DLAT=X(20)+FLOAT(X(21))/60.0+FLOAT(X(22))/3600.
0016 DLONG=X(23)+FLOAT(X(24))/60.0+FLOAT(X(25))/3600.
0017 IF(DLAT.LE.YNLA.AND.DLONG.LE.XWLN.AND.DLAT.GE.YSLA.AND.DLONG.
0018 GE.XELN) GO TO 47
0019 JJ=X(30)
0020 IF(JJ.EQ.0) GO TO 88
0021 DO 7 LL=1,JJ
0022 READ(10,17,END=3999)IDUM
0023 17 FORMAT(10,94X)
0024 7 CONTINUE
0025 88 II=X(31)
0026 IF(II.EQ.0) GO TO 999
0027 DO 8 JJ=1,II
0028 READ(10,18,END=4999)IDUM
0029 18 FORMAT(16,94X)
0030 8 CONTINUE
0031 47 JJ=X(30)
0032 DO 90 JJ=1,JJ
0033 READ(10,994,END=7999)IDUM
0034 994 FORMAT(16,94X)
0035 90 CONTINUE
0036 II=X(31)
0037 IF(II.EQ.0) GO TO 999
0038 DO 99 M=1,II
0039 99 IN=0
0040 READ(10,55)ITP,IBT,NS,SP,L
0041 55 FORMAT(10,3I5,A1)
0042 AVGDP=(ITP+IBT)/2.0
0043 BX=(DLAT-DLAT)*OT
0044 I=IHI-ITP
0045 IF(I.LE.0) GO TO 50
0046 P=FLOAT(NS)/FLOAT(I)*100.
0047 C ORKUR COOLS: 5 IS 40 % SAND IN A 100 FT INTERVAL, 6 IS 50% IN 150
0048 C 7 IS 60 % IN 200 INTERVAL
0049 IF(P.GE.40.0.AND.I.GE.100) IR=5
0050 IF(P.GE.50.0.AND.I.GE.150) IR=6
0051 IF(P.GE.60.0.AND.I.GE.200) IR=7
0052 GO TO 66
0053 50 P=-1.
0054 IR=IR+1
0055 66 WRITE(6,60)X(1),BX,AVGDP,P,I,IR
0056 60 FORMAT(11,110,F8.3,F8.1,F8.3,I5,I3)
0057 99 CONTINUE
0058 GO TO 999
0059 885 CONTINUE
0060 2999 STOP 200
0061 3999 STOP 300
0062 4999 STOP 400
0063 5999 STOP 500
0064 7999 STOP 700
0065 END
0066 //60,1999,001 DD UNIT=TAPE,VOL=SER=T2549,LABEL=28,OTSP=(,KEEP),
0067 // DSN=PERSAND,DCB=(LRECL=80,BLKSIZE=6400,RECFM=FB)
0068 90.80 90.90 29.00 30.00 60.252 68.874 30.00 400.00

```

```

0001 //DIPSAND JOB (1029,83,8,3,0018,0),MEADL
0002 //SECT (2500,1254)-
0003 //EXEC FORTGCLG
0004 //FORT.SISIN DD *
0005
0006 DIPSAND IS A VARIANT OF MUDSAND AND CALCULATES THE MUDWEIGHT AND THE NET
0007 SAND FOR FOUR SLOPING INTERVALS.
0008 NO MORE THAN FOUR INTERVALS CAN BE DONE AT ONE TIME
0009
0010 PARAMETER CARD:
0011 XELN, XWLN, YSLA, YNLA, ITOP, INTV, DX, DY, MAXMUD, DIP
0012
0013 THE FIRST FOUR ITEMS GIVE THE EAST AND WEST LONGITUDE AND SOUTH
0014 AND NORTH LATITUDE OF THE AREA TO BE USED. USE DECIMALS, NOT MINUTES
0015 AND SECONDS
0016 ITOP IS THE TOP OR HIGHEST ELEVATION (IN FEET) OF THE HIGHEST OF THE FOUR
0017 INTERVALS TO BE CHECKED, (I.E. 10000)--AN INTEGER NUMBER.
0018 INTV IS THE INTERVAL (IN FEET) BETWEEN TOP AND BASE OF AN INTERVAL
0019 (I.E. 2000)--AN INTEGER NUMBER
0020 THUS THE ABOVE (10000, 2000) WOULD GIVE 2000-FOOT INTERVALS FROM
0021 MINUS 10000 TO MINUS 18000 FEET.
0022 DX AND DY ARE THE CONVERSION FACTORS TO BE USED TO CONVERT DEGREES OF
0023 LONGITUDE (X) AND LATITUDE (Y) INTO FEET.
0024 MAXMUD DETERMINES WHAT OPERATIONS WILL BE PERFORMED.
0025 IF MAXMUD IS BLANK, ZERO, OR -1, PROGRAM CALCULATES THE AVERAGE
0026 MUDWEIGHT OF THE INTERVAL, INCLUDING THAT OF THE PREVIOUS INTERVAL.
0027 IF MAXMUD IS 1 OR 2 IT TAKES THE HIGHEST MUD IN THE INTERVAL
0028 IF MAXMUD IS -1 OR 2, NO SAND CALCULATIONS ARE MADE.
0029 DIP IS THE REGIONAL DIP OF THE AREA. IT IS USED TO CALCULATE SLOPING
0030 INTERVALS.
0031 THE PROGRAM CONSISTS OF FOUR OPERATIONS.
0032 1. READ 1ST RECORD AND DECIMALIZE LAT/LONG, SORT FOR AREA SOUGHT.
0033 2. READ 2ND RECORD (MUDDATA) AND CALCULATE AVERAGE OR MAXIMUM
0034 WEIGHT OF MUD USED IN THE FOUR INTERVALS.
0035 3. READ 3RD RECORD (SANDDATA) AND CALCULATE THE TOTAL THICKNESS
0036 OF SAND IN EACH INTERVAL.
0037 4. WRITE OUT THE DATA ON CARDS, PRINTER, TAPE, OR DISK
0038
0039
0040
0041 INTEGER X,DEPTH,TEMP,IRM,TOPSND,BOTSND,SP
0042 REAL MWT
0043 DIMENSION X(31),DEPTH(30),MWT(30),TEMP(30),RM(30),TRM(30),
0044 C TOPSND(75),BOTSND(75),NTSND(75),SP(75),MOTY(75),AVGMWT(4),
0045 C CSUMSND(4),LITH(75)
0046 DATA SETS ALL OF THE VARIABLES TO ZERO.
0047 DATA X,DEPTH,TEMP,IRM,TOPSND,BOTSND,NTSND,SP/421*0/
0048 DATA RM,MWT,AVGMWT,SUMSND/68*0./
0049 C DATA IE/0/
0050 LLL IS A COUNTER FOR # OF HOLES EXAMINED
0051 LLL=0
0052 C READ(15,*)XELN,XWLN,YSLA,YNLA,ITOP,INTV,DX,DY,MAXMUD,DIP
0053 C READ (15,*) READS PARAMETER DATA IN FLOATING FORMAT FROM CARDS
0054 WRITE(6,38)XELN,XWLN,YSLA,YNLA,ITOP,INTV,DX,DY,MAXMUD,DIP
0055 38 FORMAT('1','PARAM',2X,4F7.2,2I6,2F7.3,I3,F6.4)
0056 C ANG=TAN(DIP)*DY*5280
0057 C DD=1-USED TO LABEL DEPTH AT NORTH, MIDDLE, AND SOUTH LATITUDES.
0058 DD=YSLA-YSLA)/6
0059 DD1=YNLA-DDD*3
0060 DD3=YNLA-DDD*5
0061 DD5=YNLA-DDD*5
0062 WRITE(6,6)DD1,DD3,DD5
0063 6 FORMAT(1X,3F11.3)
0064 999 READ(10,10,END=2999)X
0065 10 FORMAT(1I10,5A4,4(A4,A1),2A4,2A2,I5,6I2,I5,I3,I5,A1,2I2,3X)
0066 C INTEGER "X" IS USED TO READ THE FIRST RECORD INTO 31 UNITS OF
0067 C INFORMATION, OF WHICH 20-25 REFER TO LAT/LONG
0068 C LAT/LONG ARE THEN DECIMALIZED
0069 DLAT=X(20)+FLOAT(X(21))/60.0+FLOAT(X(22))/3600
0070 C DLONG=X(23)+FLOAT(X(24))/60.0+FLOAT(X(25))/3600
0071 C IF THE DATA ARE IN THE AREA, GO TO 47, IF NOT, THE REMAINING CARDS
0072 C ARE READ INTO A DUMMY-FILE (IDUM) AND DISCARDED, THE NEXT FILE IS
0073 C READ (999)
0074 IF((DLAT.LL,YNLA,AND,DLONG.LE,XWLN).AND.(DLAT.GE,YSLA,AND,DLONG.
0075 C GE,XELN))GO TO 47
0076 JJ=X(30)
0077 IF(JJ.LT.0)GO TO 8888
0078 DO 7 LK=1,JJ
0079 READ(10,17,END=3999)IDUM
0080 17 FORMAT(16,94X)
0081 7 CONTINUE
0082 8888 CONTINUE
0083 II=X(31)
0084 IF(II.LT.0)GO TO 999
0085 DO 8 J=1,II
0086 READ(10,18,END=4999)IDUM
0087 18 FORMAT(16,94X)
0088 8 CONTINUE
0089 GO TO 999
0090 47 CONTINUE
0091 JJ=X(30)
0092 IF(JJ.EQ.0)GO TO 885
0093 C JJ IS A COUNTER OF NUMBER OF CARDS IN THE MUDFILE, IF JJ = ZERO,
0094 C THEN NO SAND FILE IS PRESENT (NOW), BUT THIS MAY LATER BE CHANGED.
0095 C THE SLOPING DEPTH INTERVAL IS NOW SET FOR THE PARTICULAR WELL.
0096 WJST=(YNLA-DLAT)*ANG
0097 IDPTH=0
0098 LHMUD=0.0
0099 C CARDS OF THE MUD FILE ARE NOW READ
0100 DO 99 M=1,JJ
0101 READ(10,22,END=5999)DEPTH(M),MWT(M),TEMP(M),RM(M),TRM(M),
0102 C CMOTY(M)
0103 22 FORMAT(16,F5.1,I5,F5.2,I5,A1,73X)
0104 99 CONTINUE
0105 C MUDFILE IS READ AND DEPTH INTERVAL SET (AT ONE INTERVAL LOWER THAN
0106 C TO BE USED)
0107 AL=ITOP-INTV+DIST
0108 AK=ITOP+DIST
0109 HMUD=10.0
0110 C IF NO MUDWEIGHT ASSUME 10M MUD
0111 C NEXT CHECK FOR INCREASING DEPTH AND MUDWEIGHT
0112 DO 721 M=1,JJ
0113 IF(DEPTH.GT,DEPTH(M))GO TO 351
0114 IF(CHKMUD.GT,MWT(M))GO TO 352
0115 IDPTH=DEPTH(M)
0116 CHKMUD=MWT(M)
0117 721 CONTINUE
0118 GO TO 365
0119 351 IE=1
0120 GO TO 360
0121 352 IE=2
0122 GO TO 360
0123 C ERROR #1 = BAD DEPTH ORDER ON MUD; #2 = DECREASING MUDWEIGHT
0124 C WRITE(6,361)X(1),DLAT,DLONG,X(19),X(30),X(31),IE
0125 361 FORMAT(1X,I10,2F8.4,1X,I5,3I3)
0126 C THE NEXT DO-LOOP COUNTS THE FOUR DEPTH INTERVALS AND CALCULATES AN AVGMWT
0127 C FOR EACH OF THE FOUR. RNN IS THE COUNTER.
0128 DO 894 K=1,4
0129 AL=AL+INTV
0130 AK=AK+INTV
0131 AVGMWT(K)=10.0
0132 SUMUD=HMUD
0133 RNN=1.0
0134

```

```

0133 000 DU-LOOP TO DETERMINE THE AVERAGE MUDWEIGHT IN THE INTERVAL
0134 SOME 12M MUDS ARE RECORDED AS 1.2 AND SO * TEN
0135 MUDWEIGHT OF PREVIOUS INTERVAL (MMUD) HELD OVER INTO NEXT INTERVAL
0136 DO 88 MM=1,JJ
0137 IF(MWT(MM).EQ.0.0)MWT(MM)=10.0
0138 IF(MWT(MM).LT.3.0)MWT(MM)=MWT(MM)*10.0
0139 IF(DEPTH(MM).LT.AL) GO TO 87
0140 IF(DEPTH(MM).GE.AL.AND.DEPTH(MM).LT.AK)GO TO 93
0141 GO TO 894
0142 93 CONTINUE
0143 SUMUD=SUMUD+MWT(MM)
0144 KNN=RNN+1.0
0145 AVGMWT(K)=SUMUD/RNN
0146 87 MMUD=MWT(MM)
0147 IF(MAXMUD.GT.0)AVGMWT(K)=MMUD
0148 C PROGRAM USES MAXIMUM MUD WEIGHT NOT THE AVERAGE MUOWT
0149 88 CONTINUE
0150 894 CONTINUE
0151 GO TO 895
0152 885 IE=8
0153 DO 4 IJ=1,4
0154 AVGMWT(IJ)=-99.
0155 4 CONTINUE
0156 895 CONTINUE
0157 C START OF STEP THREE--TO CALCULATE THE FEET OF SAND IN AN INTERVAL
0158 II=X(31)
0159 890 IF(MAXMUD.EQ.0.OR.MAXMUD.EQ.1) GO TO 993
0160 IF(II.EQ.0.0) GO TO 9994
0161 DO 9 JM=1,II
0162 KLAD(10,994,END=7999)IDUM
0163 994 FORMAT(16,94X)
0164 9 CONTINUE
0165 GO TO 9994
0166 993 SUMSND(1)=0
0167 SUMSND(2)=0
0168 SUMSND(3)=0
0169 SUMSND(4)=0
0170 IF(II.EQ.0)GO TO 1112
0171 C IF NO SANDS, SUMSND SET TO -99.. NOT ZERO
0172 DO 109 MJK=1,II
0173 READ(10,23,END=6999)TOPSND(MNK),BOTSND(MNK),NTSND(MNK),
0174 CSP(MNK),LITH(MNK)
0175 23 FORMAT(16,15,15,15,A1,78X)
0176 C SAND DATA ARE READ IN AND NUMBERED (MNK)
0177 109 CONTINUE
0178 CHMSND=0.0
0179 XL=ITOP-INTV+DIST
0180 AK=ITOP+DIST
0181 IF(TOPSND(1).GT.XK.OR.BOTSND(II).LE.(XK+4*INTV))IE=6
0182 C ERROR #6 = PART OF INTERVAL MISSING
0183 C CHECK TO SEE IF NET SAND AND DEPTH HAVE INHERENT ERRORS.
0184 IDPTH=0
0185 DO 712 N=1,II
0186 IF(NTSND(N).GT.(BOTSND(N)-TOPSND(N)))GO TO 607
0187 IF(INTSND(N).GT.1000)GO TO 605
0188 IF(IDPTH.GT.TOPSDND(N))GO TO 606
0189 C ERROR #4 = BAD NET SAND; #5 = DEPTH ERROR
0190 GO TO 608
0191 605 IE=4
0192 GO TO 607
0193 606 IE=5
0194 GO TO 607
0195 607 WRITE(6,362)X(1),DLAT,DLONG,X(19),X(30),X(31),IE,TOPSND(N)
0196 362 FORMAT(1X,110,2F8.4,1X,15,3I3,16)
0197 608 IDPTH=BOTSND(N)
0198 712 CONTINUE
0199 C NEXT DO-LOOP SETS THE INTERVAL
0200 DO 94 NN=1,4
0201 XL=XL+INTV
0202 AK=XK+INTV
0203 SUMSND(NN)=0.00
0204 PROPOR=0.0
0205 C NEXT DO-LOOP SUMS THE SAND OF THE INTERVAL
0206 DO 110 N=1,II
0207 TST=TOPSND(N)
0208 BST=BOTSND(N)
0209 SST=NTSND(N)
0210 IF(TST.LT.XL.AND.BST.LT.XL)GO TO 110
0211 IF(TST.GE.XK)GO TO 94
0212 IF(TST.LT.XL.AND.BST.GE.XK)GO TO 293
0213 IF(TST.GE.XL.AND.BST.LT.XK)GO TO 111
0214 IF(TST.LT.XL.AND.BST.LT.XK)GO TO 291
0215 C WHAT IS LEFT IS TST,GE,XL.AND,BST,GE,XK
0216 PROPOR=(XK-TST)/(BST-TST)
0217 GO TO 295
0218 293 PROPOR=(XK-XL)/(BST-TST)
0219 GO TO 295
0220 291 PROPOR=(BST-XL)/(BST-TST)
0221 GO TO 295
0222 111 PROPOR=1.0
0223 SUMSND(NN)=SUMSND(NN)+(PROPOR*SST)
0224 110 CONTINUE
0225 94 CONTINUE
0226 GO TO 1113
0227 1112 SUMSND(1)=-99.
0228 DO 2 IJK=1,4
0229 SUMSND(IJK)=-99.
0230 2 CONTINUE
0231 C NEGATIVE 99. SUMSND=MUD OF 12M OR MORE AND NO SAND
0232 9994 CONTINUE
0233 1113 LLL=LLL+1
0234 XCOORD=(XWLN-DLONG)*DX
0235 YCOORD=(DLAT-52.4)*DY
0236 WRITE(6,54)XCOORD,YCOORD,AVGMWT(1),AVGMWT(2),AVGMWT(3),AVGMWT(4),
0237 CSUMSND(1),SUMSND(2),SUMSND(3),SUMSND(4),X(1),DLAT,DLONG,LLL,IE
0238 54 FORMAT(1X,2F7.3,4F5.1,4F5.0,11U,2F7.3,4X,14,2X,12)
0239 WRITE(9,55)IWELL,LLL,XCOORD,YCOORD,AVGMWT(1),AVGMWT(2),
0240 CAVGMWT(3),AVGMWT(4)
0241 55 FORMAT(2X,'1PTM',110,14,3X,2F8.3,4F7.1)
0242 WRITE(9,56)IWELL,LLL,XCOORD,YCOORD,SUMSND(1),SUMSND(2),
0243 CSUMSND(3),SUMSND(4)
0244 56 FORMAT(2X,'2PTS',110,14,3X,2F8.3,4F7.1)
0245 9995 IE=0
0246 GO TO 999
0247 2999 STOP 300
0248 3999 STOP 400
0249 4999 STOP 500
0250 5999 STOP 600
0251 6999 STOP 700
0252 7999 STOP 800
0253 ENU
0254 //60,FT10F001 DD UNIT=TAPE,VOL=SER=T2500,DISP=OLD,
0255 // LABEL=2,DSN=CLNDATA
0256 //60,FI09F001 DD DSN=NEWDIRP,VOL=SER=T2549,UNIT=TAPE,LABEL=29,
0257 // DISP=(,KEEP),DCB=(LRECL=80,BLKSIZE=6400,RECFM=FB)
0258 //60,SYSDD
0259 89.75 91.25 26.75 30.25 5000 1000 60.242 6A.472 0 .0197

```

BOR02500  
BOB0251U